



Durham E-Theses

Structure - reactivity patterns in nucleophilic addition to activated aromatic compounds

Stevens, James Andrew

How to cite:

Stevens, James Andrew (1990) *Structure - reactivity patterns in nucleophilic addition to activated aromatic compounds*, Durham theses, Durham University. Available at Durham E-Theses Online: <http://etheses.dur.ac.uk/6217/>

Use policy

The full-text may be used and/or reproduced, and given to third parties in any format or medium, without prior permission or charge, for personal research or study, educational, or not-for-profit purposes provided that:

- a full bibliographic reference is made to the original source
- a [link](#) is made to the metadata record in Durham E-Theses
- the full-text is not changed in any way

The full-text must not be sold in any format or medium without the formal permission of the copyright holders.

Please consult the [full Durham E-Theses policy](#) for further details.

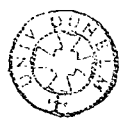
Structure – Reactivity Patterns in Nucleophilic Addition to Activated Aromatic Compounds

by

James Andrew Stevens, B.Sc. Hons. (Southampton)

A thesis submitted for the degree of Doctor of Philosophy in the
University of Durham, Department of Chemistry, 1990

The copyright of this thesis rests with the author.
No quotation from it should be published without
his prior written consent and information derived
from it should be acknowledged.



24 JUL 1991

Statement of Copyright

The copyright of this thesis rests with the author. No quotation from it should be published without his prior written consent and information derived from it should be acknowledged.

Declaration

This thesis is the result of research carried out in the Department of Chemistry at Durham University, between October 1987 and October 1990. It has not been submitted for any other degree and is the author's own work except where acknowledged by reference.

Abstract

Kinetic and equilibrium data for the reactions of some aromatic nitro-compounds with nucleophiles have been investigated using various spectrophotometric techniques (UV/visible, stopped-flow and temperature jump) and nmr spectroscopy.

Kinetic and equilibrium data are reported for the formation of 1:1 and 1:2 adducts in aqueous solutions from 1,3,5-trinitrobenzene (TNB) and 2,4,6-trinitrotoluene (TNT) with thiolate ions derived from thioglycolic acid, thiomalic acid and glutathione. The results are used to determine intrinsic reactivities, k_0 , for the thiolate ions in adduct-forming reactions at the nitro-aromatic ring. The values for the three thiolate ions are all *ca.* 5×10^4 and are considerably higher than comparable values, calculated from literature data, for the sulphite ion (500) and the hydroxide ion (10).

Kinetic and equilibrium data are reported for the reactions in water of ethanethiolate, thioglycolate and thiomalate ions with 1-X-2,4,6-trinitrobenzenes (X=H, SEt, OEt and Cl). The thiolate ions show strong kinetic preference for attack at unsubstituted ring positions. However, the isomeric 1:1 adducts have similar thermodynamic stabilities. This is in marked contrast with the corresponding reactions of alkoxides. 1:2 adducts are formed by thiolate attack at two unsubstituted ring positions. A 1:3 adduct has been identified by reaction of ethanethiolate ions with TNB and the kinetic data recorded.

^1H nmr measurements in DMSO have been used to examine the structures of intermediates and reaction products; they show the irreversible displacement of nitro groups by thiolate ions.

The initial reaction of 1-X-2,4,6-trinitrobenzenes (X=H, Cl, CH_3) in methanol with the anions of dimethylmalonate, ethylcyanoacetate and a selection of substituted phenylacetonitriles yield σ -adducts by carbanion attack at unsubstituted ring positions. With ethylcyanoacetate there was evidence for the ionisation of the remaining exocyclic hydrogen and this process is increasingly favoured as the X-substituent becomes more electron-withdrawing ($\text{Cl} > \text{H} > \text{CH}_3$). An acidity function approach is used to determine the equilibrium acidities of the substituted phenylacetonitriles in methanol. The data are well correlated with σ^- values (7 points) and the plot is used to estimate the acidities of three further phenylacetonitriles. However, the equilibrium acidity of 4-nitrophenylacetonitrile is shown to be anomalous. For the most strongly basic anions, derived from the most weakly acidic phenylacetonitriles, reaction with TNB was found to proceed at or near the diffusion controlled limit. The kinetic and equilibrium data are used to determine values of intrinsic rate constants, k_0 , for reaction at an unsubstituted position of the trinitro-aromatic ring. The values are dimethylmalonate (200), ethylcyanoacetate (200), 4-nitrophenylacetonitrile (280), 4-cyanophenylacetonitrile (10^3) and 2-cyanophenylacetonitrile (10^3).

Kinetic and equilibrium measurements are reported for the reactions of 1-X-2,4-dinitrobenzenes (X=F, Br) with hydroxide ions in 80/20 (v/v) DMSO/ H_2O . The results provide evidence for two types of steric effects: (i) increasing size of the halogen results in disruption of the planarity of the nitrogroups giving a general decrease in reactivity at both unsubstituted and halogen-substituted positions and (ii) unfavourable steric and electrostatic repulsions between entering and leaving groups.

Hydrogen exchange experiments were carried out with 1-fluoro-2,4-dinitrobenzene and OD^- in $[\text{}^2\text{H}_6]\text{-DMSO/D}_2\text{O}$. The results show that there is slightly more hydrogen exchange at the 3-position of the substituted product (the phenoxide) than there is at the 3-position of the unreacted starting material. However, these observations do not necessarily require the formation of an intermediate on the pathway to σ -adduct formation.

Publications

Some of the work in this thesis has been the subject of the following papers:

Reactions of 1-X-2,4,6-trinitrobenzenes and 1-X-2,4-dinitrobenzenes with hydroxide ions. Comparisons of the relative rates of nucleophilic attack at substituted and unsubstituted ring-positions.

J. Chem. Soc. Perkin Trans. II, 1989, 675

M.R. Crampton, A.B. Davis, C. Greenhalgh and J.A. Stevens.

Kinetic and Equilibrium Studies of the reactions of some Thiolate Ions with Trinitroaromatic Compounds: Intrinsic Reactivities.

J. Chem. Soc. Perkin Trans. II, 1989, 925

M.R. Crampton and J.A. Stevens.

Kinetic and Thermodynamic Preferences in the reactions of Thiolate ions with 1-substituted-2,4,6-trinitrobenzenes.

J. Chem. Soc. Perkin Trans. II, 1990, 1097

M.R. Crampton and J.A. Stevens.

Acknowledgements

I would like to thank my supervisor Dr M.R. Crampton for guidance, encouragement and numerous helpful discussions.

Thanks are also due to various members of staff who helped in any way — notably Dr R.S. Mathews, Dr G.M. Brooke, C. Greenhalgh, V.J. McNeilly and L.W. Lauchlan.

Finally, I would like to thank members (past and present) of my research group and Colin Greenhalgh for typing this thesis.

Contents		page
1	GENERAL INTRODUCTION	1
	Adducts from sulphur bases	9
	Adducts from carbon bases	7
	Quantitative measurement of nucleophilicity	28
	Acidity functions in basic solutions	34
	References	37
2	EXPERIMENTAL	44
	Materials	45
	Measurement techniques	47
	References	52
3	KINETIC AND EQUILIBRIUM STUDIES OF THE REACTIONS OF SOME THIOLATE IONS WITH TRINITROAROMATIC COMPOUNDS. DETERMINATION OF INTRINSIC REACTIVITIES	53
	Introduction	54
	Experimental	56
	Results and Discussion	57
	Reactions with 1,3,5-trinitrobenzene	58
	Reactions with 2,4,6-trinitrotoluene	69
	Comparisons and determination of intrinsic reactivities	78
	Appendix: Derivation of rate expressions	85
	References	87

4	KINETIC AND THERMODYNAMIC PREFERENCES IN THE REACTIONS OF THIOLATE IONS WITH 1-SUBSTITUTED-2,4,6-TRINITROBENZENES.	89
	Introduction	54
	Experimental	56
	Results and Discussion:	
	¹ H nmr measurements	96
	Kinetics and equilibria:	
	1,3,5-trinitrobenzene and ethanethiolate ions	101
	Ethylthiopicrate and ethanethiolate ions	106
	Ethylpicrate and ethanethiolate ions	108
	Ethylpicrate and thioglycolate ions	112
	Picryl chloride and thioglycolate ions	118
	Ethylpicrate and thiomalate ions	119
	Reactions of ethylpicrate and ethylthiopicrate with hydroxide ions	123
	Conclusions and Comparisons	127
	Appendix – derivation of rate expressions	132
	References	135
5	KINETIC AND EQUILIBRIUM STUDIES OF THE REACTIONS OF SOME CARBANIONS WITH TRINITROAROMATIC COMPOUNDS. DETERMINATION OF INTRINSIC REACTIVITIES.	137
	Introduction	138
	Experimental	140
	Results and Discussion:	
	Acidities of dimethylmalonate and ethylcyanoacetate	145
	Acidities of substituted phenylacetonitriles	149

Phenylnitromethane	160
Reactions with 1,3,5-trinitrobenzene	176
Reactions with picryl chloride	205
Reactions with 2,4,6-trinitrotoluene	219
Comparisons of data and determination of intrinsic reactivities	228
Appendix	
(i) derivation of rate expressions	239
(ii) sample kinetic runs	242
References	245
6 REACTIONS OF 1-X-2,4-DINITROBENZENES WITH HYDROXIDE IONS. COMPARISON OF RELATIVE RATES OF NUCLEOPHILIC ATTACK AT SUBSTITUTED AND UNSUBSTITUTED RING-POSITIONS.	248
Introduction	249
Experimental	251
Results and Discussion	252
Comparisons of data	261
Appendix	
(i) Derivation of rate expressions	263
(ii) Sample kinetic runs	266
References	268

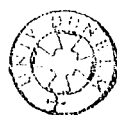
7 HYDROGEN EXCHANGE IN 1-FLUORO-2,4-DINITROBENZENE. EVIDENCE FOR INTERMEDIATES ON A PATHWAY TO σ-ADDUCT FORMATION ?	269
Introduction	270
Experimental	273
Results and Discussion	273
References	277

APPENDIX

(a) Lectures and Colloquia organised by Durham University Chemical Society.	279
(b) Research Conferences.	
(c) First Year Induction Course.	

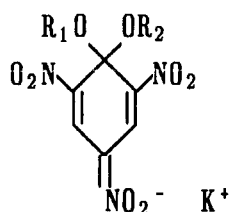
Chapter 1

General Introduction

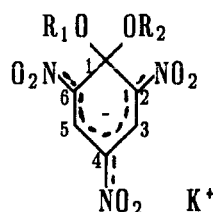


As early as 1886, Janovsky^{1,2} found that treating an acetone solution of *meta*-dinitrobenzene (*m*-DNB) with an alcohol solution of acetone gave rise to an intense violet colour. Later it was observed that the same effect resulted from the action of many alkaline solutions of ketones on *m*-DNB^{3,4}. In 1905, Lobry de Brun⁵ isolated and analysed a red crystalline material that was formed from the interaction of methanolic 1,3,5-trinitrobenzene with an equimolar amount of potassium hydroxide while other crystalline solids were reported from the reactions of alkyl picrates⁶, 2,4,6-trinitrotoluene⁷, and 2,4,6-trinitrobenzoic acid⁸ with alkoxides.

In 1900 a quinoid structure (1.1) was proposed by Jackson and Gazzolo⁹ for the coloured adducts formed from picryl ethers and potassium alkoxides.



1.1



1.2

Meisenheimer¹⁰ obtained structural evidence for 1.1 by obtaining the same product from the reactions of 2,4,6-trinitroanisole (TNA) with potassium ethoxide and from 2,4,6-trinitrophenetole (TNP) with potassium methoxide. On acidification, the product yielded roughly equimolar amounts of TNA and TNP. Further structural evidence has come from X-ray crystallography ($R_1 = R_2 = Et$ ¹¹, $R_1 = R_2 = Me$ ¹²) while ¹H nmr was first applied¹³ to the σ -adduct obtained with TNA and methoxide ($R_1 = R_2 = Me$). The more usual representation of 1.1 is that shown in 1.2 with the negative charge delocalised in the ring and over the nitro groups. These and similar compounds, obtained from a wide variety of nucleophiles and activated aromatics, are known as Meisenheimer or σ -adducts. Their formation involves delocalisation of electron density

originally associated with the nucleophile into the electron deficient aromatic with concomitant formation of a covalent bond to an aromatic ring carbon which becomes tetrahedrally coordinated⁷¹.

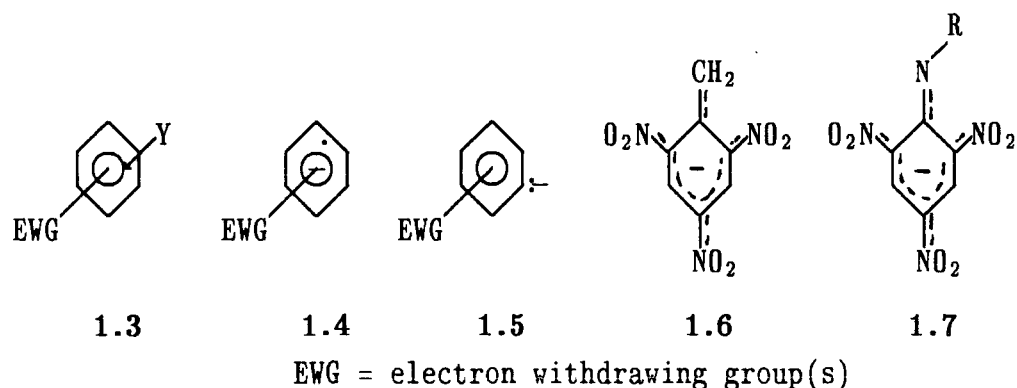
Crystal structures for the adducts 1.2 ($R_1 = R_2 = Et$) and 1.2 ($R_1 = R_2 = Me$) show^{11,12} that the C4-N bond is significantly shorter than the C2-N or C6-N bonds and that the C2-C3 and C5-C6 bonds are shorter than the other C-C bonds. This result shows that resonance contributors like 1.1 are more important than those which have a single C4-N bond. Consequently a large proportion of the negative charge will be situated on the *para*-nitro group¹⁴.

In spite of the C2-C1-C6 angle of 109° the ring is essentially planar. Ring planarity and concomitant ring strain may result from steric compression between geminal-alkoxyl and *ortho*-nitro groups¹⁴.

These latter are nearly coplanar with the ring in the adducts whereas dihedral angles of up to 62° have been observed between the ring plane and nitro-groups *ortho* to the ethoxyl group in trinitrophenetole, presumably owing to steric compression between these two functions. Release of this compression in the adduct 1.2 may be one of the reasons for the greater stability of 1,1-adducts relative to 1,3-adducts formed from alkoxides and alkyl 2,4,6-trinitrophenyl ethers¹⁴.

Besides the formation of σ -adducts there are several other possible modes of interaction of nitroaromatic compounds with bases. π -complexes 1.3 (also known as donor-acceptor or charge-transfer complexes) may form through partial transfer of electronic charge from the base. Such complexes have been observed in some non-polar solvents, possibly as intermediates on the pathway to σ -adduct formation.¹⁶ Nitroaromatic compounds may also be converted into radical anions by accepting a single electron from a base. The identification of radical anions and a determination of their concentration is made with electron-spin resonance techniques¹⁵. For example, 4-nitrotoluene¹⁸ has been observed to give a high

concentration of radical anions when dissolved in *t*-butyl alcohol containing potassium *t*-butoxide. With more activated substrates however, the formation of anionic σ -adducts becomes increasingly favoured at equilibrium relative to the formation of radical anions. Thus the concentration of the latter produced from 1,3,5-trinitrobenzene and *t*-butoxide in *t*-butyl alcohol was found to be very small¹⁹.

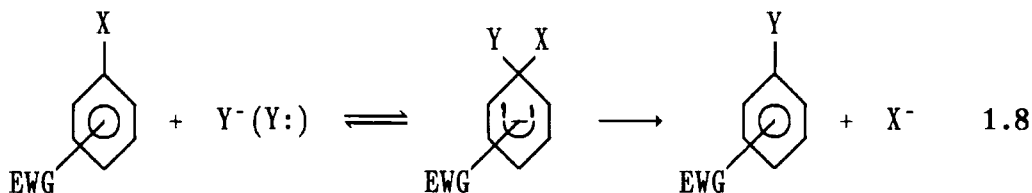


Recently there has been a proposal¹⁷ that σ -adduct formation between trinitro-activated aromatics and hydroxide ions involves several steps which may be observed spectrophotometrically. These steps are rapid formation of a π -complex followed by a single electron transfer to form a radical pair and collapse of the radical pair to give the σ -adduct. This proposal will be discussed later in the thesis.

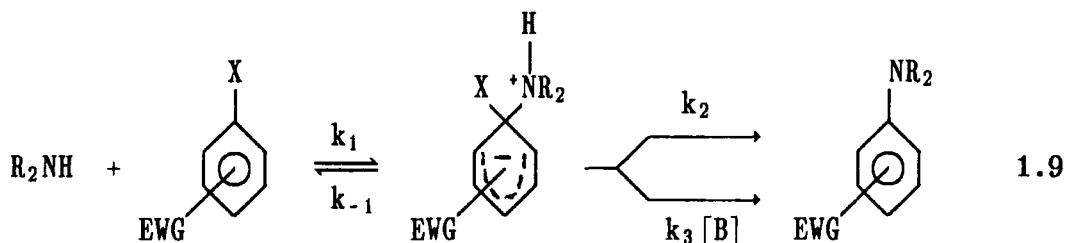
A further possibility is the abstraction of a ring hydrogen to yield aryl carbanions 1.5¹⁵. Evidence for their formation has mostly come from isotopic exchange experiments, the carbanions being formed at least as transient intermediates²⁰. Finally there is the possibility of reactions involving ring substituents. Examples include the production of anions from 2,4,6-trinitrotoluene^{21,22} (1.6) and anilines²² (1.7) and base addition to cyano-²³ and nitro-groups²⁴.

Research in the area of anionic σ -adduct has been strongly stimulated by Bunnett's proposal^{24,25} that most nucleophilic aromatic substitutions (SN_{Ar})

reactions involving activated substrates and good leaving groups proceed by a two step mechanism (1.8) involving a σ -adduct intermediate as opposed to the possibility of synchronous bond formation / bond breakage involving an S_N2 type transition state.



The likelihood of such an intermediate has been demonstrated kinetically by the observation of base catalysis in the substitution reactions of amines with nitroaromatics (equation 1.9). The key feature in these systems is the presence of a labile proton on the nitrogen atom of the postulated intermediate. Removal of the proton in a base catalysed step favours formation of product since R_2N^- is a poorer leaving group than R_2NH . Thus there is the possibility of two competing pathways, one base catalysed and the other uncatalysed. The kinetic expression



(derived using a steady state treatment for the zwitterionic intermediate) is given in 1.10 and predicts a curvilinear dependence of the second order rate constant k with $[\text{B}]$.

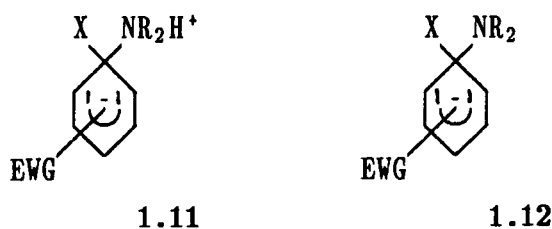
$$\frac{\text{Rate}}{[\text{ArX}] [\text{R}_2\text{NH}]} = k = \frac{k_1 k_2 + k_1 k_3 [\text{B}]}{k_{-1} + k_2 + k_3 [\text{B}]} \quad 1.10$$

There are two limiting cases

- (i) When $k_{-1} \ll k_2 + k_3[B]$ then $k = k_1$ Thus the formation of the intermediate is rate determining and base catalysis is not observed.
- (ii) When $k_{-1} \gg k_2 + k_3[B]$ the product forming processes are rate determining and base catalysis is expected.

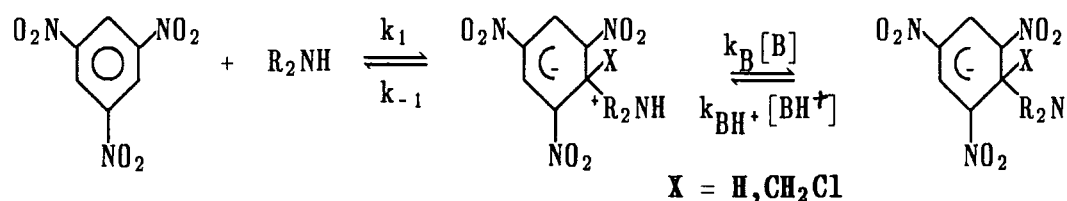
Since case (i) will be favoured when k_2 is large it follows that the poorer X is as a leaving group, the more base catalysis becomes important. This was borne out experimentally in the reactions of 1-chloro- and 1-fluoro-2,4 dinitrobenzenes with N-methylaniline²⁶. Very marked catalysis by both hydroxide and acetate was observed in the reaction of the fluoro-compound but catalysis was barely detectable in the chloro-compound. The reactions of 4-nitrophenyl phosphate²⁷ and 2,4-dinitrophenyl phenyl ether²⁸ with piperidine are catalysed by hydroxide and the rate constants show a curvilinear dependence with base concentration. However a number of systems were found for which this predicted dependence did not materialise¹⁵.

More recently, attention has been focussed on the possible mechanisms of base catalysis. Briefly, these are (i) rate limiting proton transfer^{33,34} from the zwitterionic intermediate 1.11 to base, first proposed by Bunnett²⁶ and (ii) rapid deprotonation of 1.11 followed by general acid catalysed rate limiting nucleofuge expulsion from 1.12. The former process generally applies in protic solvents, while



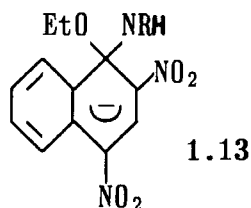
in aprotic solvents where leaving group expulsion is more difficult, the latter mechanism holds³⁰.

Base catalysis is not expected when formation of zwitterionic adducts 1.11 is rate limiting. Such is the case in the reaction of 1-fluoro-2,4-dinitrobenzene with piperidine in solvents of chloroform, acetonitrile, and nitromethane³¹. Kinetic studies made on some trinitroactivated aromatics that form stable σ -adducts with primary and secondary amines²⁹ have shown that proton transfer may be kinetically significant. Reduction in the values of k_B below those expected for

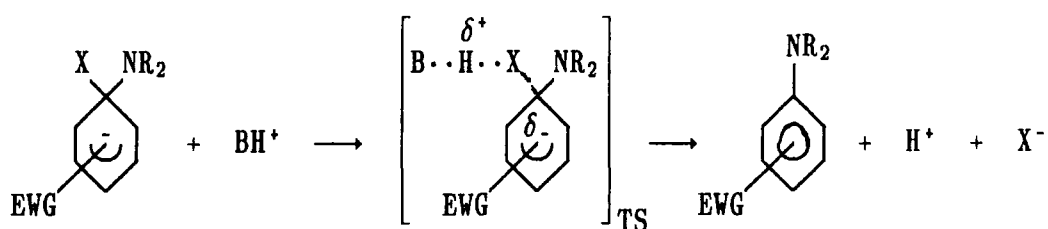
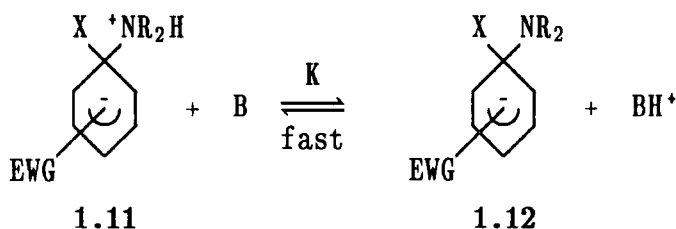
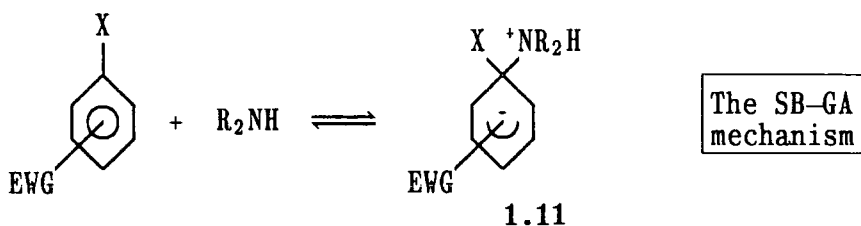


diffusion controlled reactions was attributed to steric effects which are particularly severe when the reaction involves secondary amines or when there are bulky substituents at the reaction site³⁰.

In the case of rate limiting nucleofuge expulsion, the initially formed zwitterionic intermediate 1.11 undergoes a fast equilibrium proton transfer yielding 1.12 followed by a general acid catalysed removal of the leaving group by BH^+ . It has been called the SB-GA mechanism (specific base - general acid). In a kinetic study of the reactions of 1-ethoxy-2,4-dinitronaphthalene with *n*-butylamine and *t*-butylamine in DMSO, Orvik and Bunnett were able to observe in separate steps formation of intermediates of structure 1.13 ($\text{R} = n\text{-Bu}, t\text{-Bu}$) (which were not base catalysed) and their acid catalysed conversion into substitution products. The structure of the intermediate 1.13 ($\text{R} = n\text{-Bu}$) has been confirmed by flow nmr spectroscopy³⁸. The reaction of 2,4,6-trinitroanisole with *n*-butylamine³² in DMSO has been shown to follow a similar pathway.



In the reaction of methyl-4-methoxy-3,5-dinitrobenzoate with pyrrolidine in DMSO, base catalysis is observed in the formation of the intermediate of type 1.12 but general acid catalysed expulsion of methoxide is rate limiting in the overall substitution³⁵.



Adducts from sulphur bases

It is well known that sulphur bases though having a smaller affinity for protons than oxygen bases show a greatly enhanced reactivity towards carbon. Thus a number of such bases react easily with activated aromatics to form sulphur-bonded σ -adducts as stable or transient species³⁹.

a) Sulphite

Sodium sulphite reacts reversibly with 1,3,5-trinitrobenzene to form highly coloured adducts^{9,10}. In aqueous solution both 1:1 and 1:2 adducts can be formed³⁹ and the latter has been isolated as a dark red material⁴⁰. Examination of the system by stopped-flow spectrophotometry has shown three time dependent processes⁴¹. The results have been interpreted in terms of formation of a 1:1 adduct and two isomeric *cis* and *trans* 1:2 adducts. The 1:2 adducts have very similar thermodynamic stabilities and similar though not identical UV-visible spectra⁴¹. The isomeric adducts were later characterised by proton nmr^{42,43}. For TNB in 1M aqueous sodium sulphite, Crampton found pairs of resonances at 8.6, 6.05ppm and 8.5, 5.9ppm, the high field resonances corresponding to hydrogens at sp^3 hybridised carbon atoms. Reactions of sodium sulphite with 1-X substituted trinitrobenzenes ($X = CH_3, CH_2Cl^{48}, OMe^{46}, SO_3^{44}, O^{-45}, NO_2^{50}, NH_2, NHMe, NMe_2^{39,49}$) in aqueous solution yield 1:1 and 1:2 adducts by addition of sulphite to unsubstituted ring positions. *Cis/trans* isomerism has not been observed in these 1:2 adducts, one isomer, probably *trans*, being favoured^{46,48}.

Changing the ionic strength of the medium does not appreciably affect the value of the equilibrium constant K_1 when when X is an uncharged substituent. In contrast K_1 values for charged substituents ($X = O^-, SO_3^-$) and all the K_2 values strongly increase with increasing ionic strength as expected for the reaction of multicharged species. Equilibrium data are shown in table 1.14. Values of K_1 for $X = OMe$ and $X = H$ are similar indicating that the electronic effects of these

substituents do not appear to affect the stabilities of these adducts greatly. However this effect is likely to be important in the TNT-sulphite 1:1 adduct, along with the disruption in planarity of the nitro groups caused by the CH₃ substituent. Factors such as solvation differences, steric effects and, in the case of picramide and N-methylpicramide, hydrogen bonding of amino protons to the adjacent nitro groups will all play a major role in determining adduct stability⁶³.

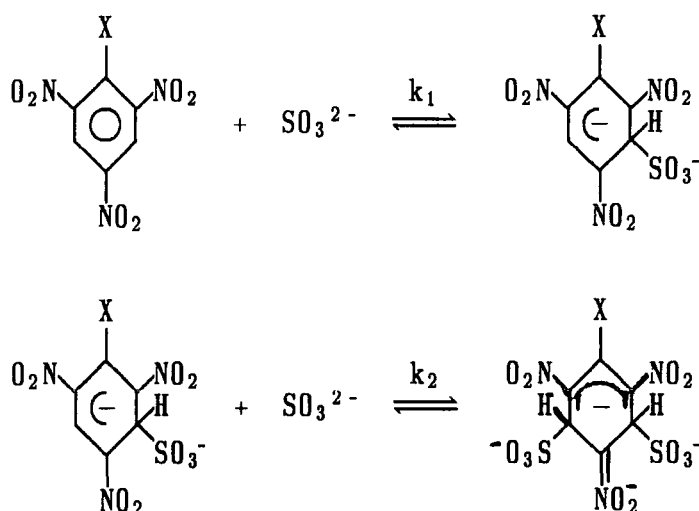


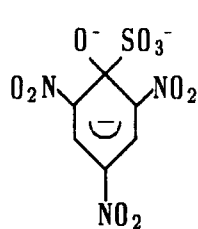
Table 1.14
Equilibrium constants for formation of adducts
with sodium sulphite in water

X	K ₁ /l mol ⁻¹	K ₂ /l mol ⁻¹	ref
H	286	9.3, 9.2	41
OMe	140	1400	46
Me	2.6	36	48
CH ₂ Cl	55	32	48
NH ₂	8.6x10 ³	20	46, 49
NHMe	6.8x10 ⁴	2 x 10 ³	46, 49
NMe ₂	3.0x10 ⁴	5.0x10 ⁴	46, 49

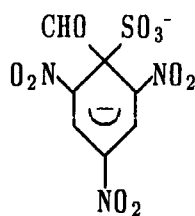
I=0.3M

The results show that there is some correlation of the values of K_2 with the size of the X-substituent. In the di-adducts the conjugation of the ring is broken so that the steric strain at C1 may be reduced relative to the parent molecules or 1:1 adducts. This steric relief would be expected to increase with the size of the X-substituent⁶⁴.

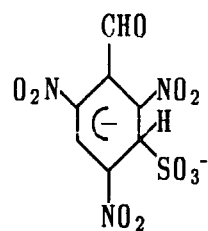
The failure to detect addition of sulphite to the 1-position has been ascribed largely to the steric strain effect associated with the addition of an extensively solvated sulphite ion to a carbon atom bearing a large X substituent. Two notable exceptions to this are the postulations of structures 1.15 and 1.16 for the adducts formed from picrate⁵¹ and 2,4,6-trinitrobenzaldehyde⁴⁷.



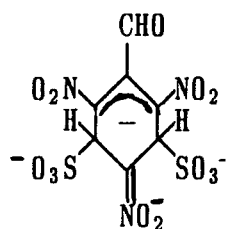
1.15



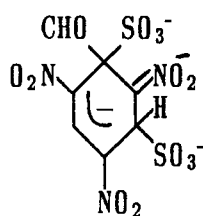
1.16



1.17



1.18

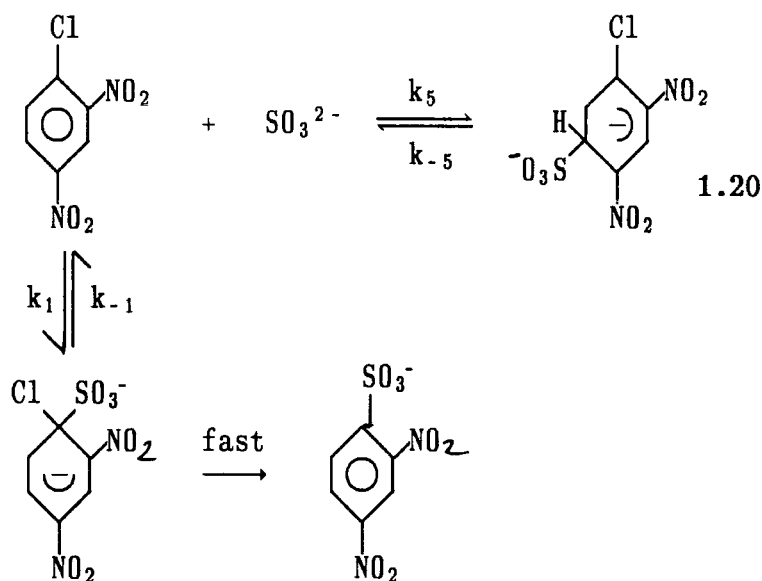


1.19

In the case of 2,4,6-trinitrobenzaldehyde, proton nmr studies showed that in aqueous solution the 1:2 adducts 1.18 and 1.19 were the only species present at equilibrium. However the isomeric 1:1 adducts could be observed by increasing the proportion of DMSO in the solvent⁴⁷.

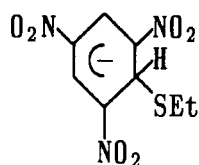
At low concentrations of sodium sulphite stopped flow spectrophotometry showed two reactions. The first was rapid and was attributed to sulphite addition to an unsubstituted ring position to form 1.17. The second reaction was slower and the observed rate constants were linearly dependent on sulphite at lower concentrations and independent of sulphite at higher concentrations. This kinetic dependence is consistent with isomerisation of the rapidly formed 1.17 to give 1.16.

The reaction of sulphite with 1-chloro-2,4-dinitrobenzene yields the σ -adduct 1.20 by attack at the unsubstituted 5-position. Attack at the 1-position, followed by rapid expulsion of chloride, is slower by a factor of $12^{5.3}$

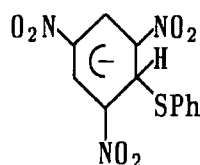


b) Thiolates

^1H nmr results for the interaction of TNB with thioethoxide and thiophenoxide ions show that the main interaction is to give an adduct by addition to a ring carbon carrying hydrogen⁵⁴. With thioethoxide ions in a solvent of 85/15 v/v DMSO/MeOH the spectrum contains resonances at δ 8.32 and 5.75 in the ratio 2:1 due to 1.21⁵⁴. The shift to high field of one of the protons reflects the change in hybridisation of one of the carbon atoms from sp^2 to sp^3 . With thiophenoxide a



1.21

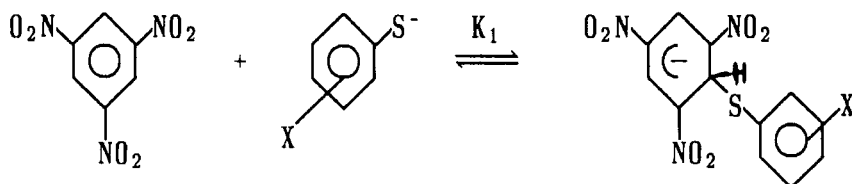


1.22

rapid exchange process gives a single combined resonance for the ring protons of 1.22 and TNB, the position of which depends on the concentration of thiophenoxide. When the concentration of thiophenoxide is increased so as to completely convert the TNB into the adduct 1.22, a limiting resonance of 7.45ppm is obtained which corresponds to the weighted average of the resonances observed in the thioethoxide adduct 1.21⁵⁴. Leshina *et al* have studied⁵⁷ the temperature dependence of the nmr spectra of the 1,3-adduct formed by addition of thiophenoxide to 2,4,6-trinitroanisole in a solvent of 25/75 DMSO/MeOH (v/v) to evaluate lifetimes, τ . At -40°C $\tau = 0.00118\text{s}$; at -35°C $\tau = 0.00059\text{s}$.

The UV/visible spectra of 1:1 adducts formed with thioethoxide and thiophenoxide ions in methanol have⁵⁴ absorption maxima at 460nm (sh 550nm) and 464nm (sh 560nm) respectively. Increasing the concentration of thioethoxide gives a different spectrum with a single absorption maximum at 510nm typical of 1:2 adducts. Values for the corresponding equilibrium constants, K_1 for the formation of the 1:1 adduct and K_2 for the formation of the 1:2 adduct, have been measured in methanol^{54,55}, ethanol, water and various mixtures⁵⁵. In the alcohols the major interaction of TNB with thioethoxide ions is to give a 1:1 adduct, K_2 being of the order of 10 l mol^{-1} in both solvents. In water, 1:2 adduct formation is the main interaction, reflecting the strong solvation of the multicharged species in the medium.

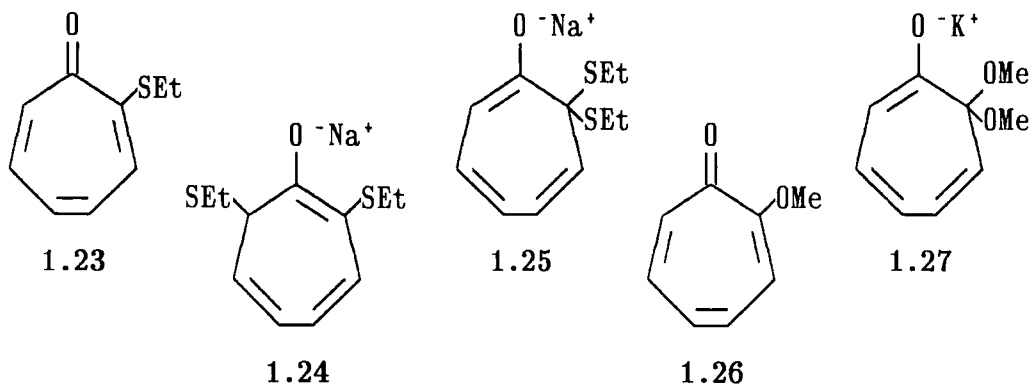
Equilibrium constants (K_1) have been obtained⁵⁶ for the 1:1 interaction of a series of substituted thiophenoxides with TNB in 95/5 EtOH/H₂O (v/v). A plot of $\log K_1$ vs. $\text{p}K_a$ for the thiophenoxides was linear with slope 1.24⁵⁶.



Carbon basicities (as measured by K_1 values) thus show a greater susceptibility to change in the X substituent than do proton basicities.

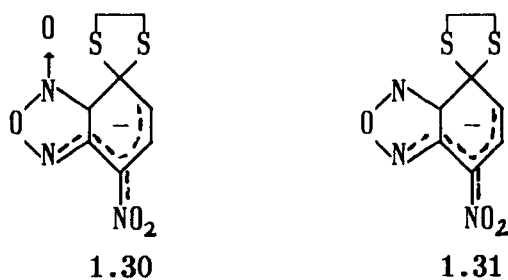
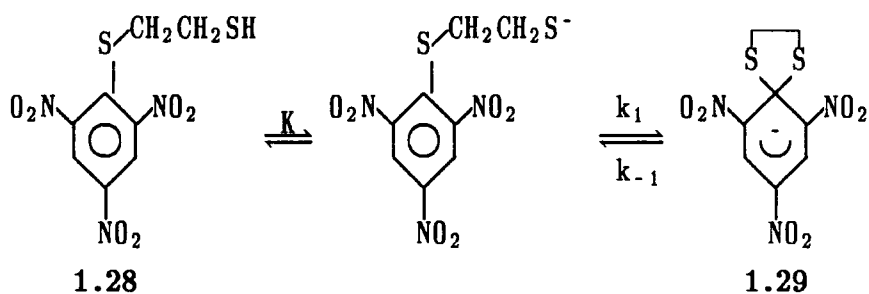
Crampton has measured the proton-nmr spectra of adducts formed with trinitroaniline and some sulphur bases; addition was found to occur at unsubstituted ring positions^{5,4} in contrast to oxygen bases where loss of an amino proton can occur. Thioethoxide anions have been shown to add to ethyl picrate^{5,8} and ethylthiopicate^{5,9,60} at both substituted and unsubstituted positions. When the substrate is ethyl picrate 1,1 and 1,3 complexes were reported in *ca* 1:1 ratios^{5,8}; when the substrate is ethylthiopicate the 1,3 complex predominates^{5,9,60}. The latter result is in direct contrast with its oxygen counterpart (and indeed alkoxide addition to alkyl 2,4,6-trinitrophenyl ethers generally) where the equilibrium constant for addition to a substituted position is larger by several orders of magnitude than the corresponding equilibrium constant for addition to unsubstituted positions.

The interaction of sodium thioethoxide and 2-ethylthiotropone 1.23 has been investigated by ¹H nmr⁶¹. The stable product on mixing the reagents in DMSO is 1.24 produced by base addition to the unsubstituted 7-position. Also seen in equilibrium with the latter are traces of the isomeric product 1.25⁶¹. By contrast the reaction of 2-methoxytropone 1.26 with potassium methoxide⁶² produces only the gem-type adduct 1.27 as a stable species⁶². Adducts produced by methoxide attack to the 7-position are short-lived.

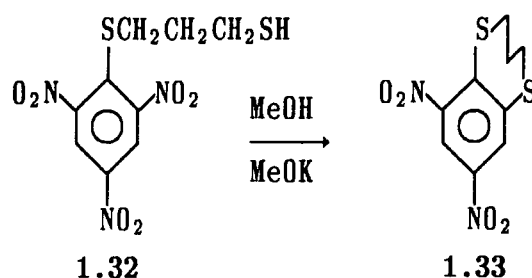


Spiro complexes

1-[(2-Mercaptoethyl)thio]-2,4,6-trinitrobenzene 1.28 cyclises in water⁶⁵ and methanol⁶⁷ to give the spirocomplex 1.29. It is half formed at pH5 in water⁶⁵. Similarly, 1.30 and 1.31 form from the parent nitrobenzofuroxan and benzofuroxan in water and methanol⁶⁶.



These adducts exhibit a remarkably high stability and their decomposition is not catalysed by H^+ . Their resistance to acids has been explained in terms of the low basicity of sulphur, a "soft" base relative to oxygen⁶⁵. Significantly a dramatic increase in the rate of decomposition of 1.29 occurs when Hg^{2+} , a soft acid, is added to the solution⁶⁵. Though the dithiolane adducts are apparently more stable than their oxygen counterparts, this stability is due to the greater acidities of thiols (reflected by higher K values) relative to alcohols rather than their K_1 values. Values of K_1 for internal cyclisation of dithiolane adducts are actually of the same order or lower than those for their oxygen analogues. This contrasts with the higher carbon basicities found for sulphite and thiolate ions relative to oxygen bases for reactions with TNB⁶⁵. Possible factors accounting for this behaviour are (i) differences in the stabilising effect of multiple alkoxy and thioalkoxy substitutions at sp^3 carbon atoms (as shown in the EtS^- /ethylthiopicrate system) and (ii) destabilisation of the sulphur complexes due to steric compression between the two sulphur atoms at C1 and between the dithiolane ring and *ortho* substituents⁶⁵. When 1.32 the propanedithiol analogue of 1.28 is treated with MeOK in methanol, 1H nmr and UV/visible spectroscopy indicate that σ -adducts are produced only as short-lived species, the final product isolated in low yield, being 1.33⁶⁷ and resulting from displacement of an *ortho*-nitro group.



Carbon bonded σ -adducts

(a) Cyanide adducts

Equilibrium and kinetic studies for the addition of cyanide to TNB to give 1.34 have mostly been carried out in alcohols. In lower alcohols the reaction is complicated by alcoholysis of the cyanide ion (eqn. 1.35) to yield the corresponding alkoxide ion. Formation of the 1:1 alkoxide-TNB adduct thus competes with the



formation of 1.34 in ethanol and propanol solvents. Changing the solvent from methanol to *t*-butanol greatly increases both k_1 and K_1 . The increase has now been explained in terms of increasing solvation of the cyanide ion on going from *t*-BuOH to EtOH or MeOH. Data for cyanide addition to the unsubstituted position of 1-X-2,4,6-trinitrobenzenes are shown in table 1.36. The reactions of cyanide with TNA and TNT yield exclusively the 1,3 adduct and surprisingly these were found to have stabilities comparable to that of 1.34.

Cyanide addition to 2,4,6-trinitroanisole in chloroform, however, forms both isomeric 1:1 adducts. At equilibrium the 1,3-adduct is favoured relative to the 1:1 adduct.⁷⁴

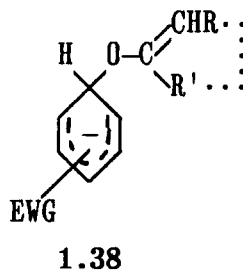
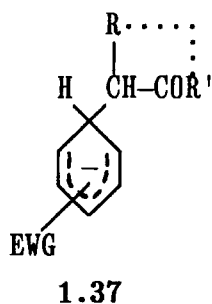
The cyanide adducts have much greater stabilities than expected on the basis of their hydrogen basicities. For example, the methoxide-TNB adduct and 1.34 have similar stabilities^{68,75} in methanol while the methoxide ion is some 3 orders of magnitude more basic than CN^- .^{72,73}

Table 1.36 Kinetic and Equilibrium data for cyanide addition to unsubstituted positions of 1-X-2,4,6-trinitrobenzenes.

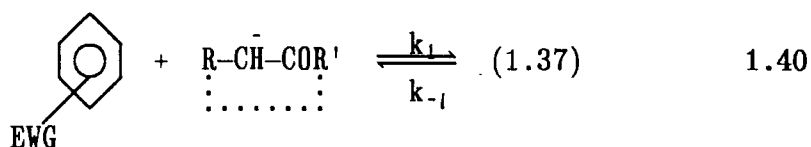
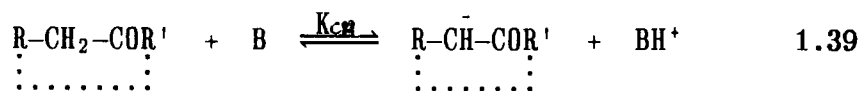
X	solvent	k_1/lmol^{-1}	k_{-1}/s^{-1}	K_1/lmol^{-1}	ref.
H	MeOH			39	68
H	EtOH			1265	68
H	EtOH			1.05×10^4	69
H	PrOH			1470	68
H	PrOH	932	<0.01	$>9 \times 10^4$	69
H	<i>i</i> -PrOH	2450	0.245	10^4	68,69
H	<i>i</i> -PrOH	2450	0.048	5.1×10^4	70
H	BuOH			2020	68
H	<i>t</i> -BuOH			5×10^5	68
H	<i>t</i> -BuOH	1.06×10^5	2.5	4.24×10^4	69
OMe	<i>i</i> -PrOH	344	0.031	1.12×10^4	70
Me	<i>i</i> -PrOH	32.6	0.002	2.01×10^4	70

Carbanions from Enolates

Enolate carbanions of ketones^{1-4,71,76-98}, aldehydes⁹⁹, esters^{80,87,100-104}, ketoesters^{77,80,87}, amides¹⁰⁵, and also compounds like creatinine¹⁰⁶⁻¹⁰⁹ add to activated aromatics to form carbon bonded adducts also known as Janovsky^{1,2} complexes. Enolate attack through oxygen to give 1.38 has never been observed in any of the studies.



The enolate adduct 1.37 usually forms in a two step process (equations 1.39, 1.40) in which the carbanion is generated in a rapid equilibrium process prior to the rate determining addition step. It has to be remembered that some carbanions



will be potentially ambidentate. The results in table 1.41 show that all the enolate anions have carbon basicities which are considerably greater than expected from their proton basicities⁸⁷.

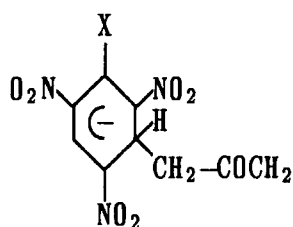
Table 4.41
Kinetic and Equilibrium data for the formation of enolate-TNB adducts
in methanol containing methoxide

parent carbonyl compound	K_{CH} lmol^{-1}	k_1 $\text{lmol}^{-1}\text{s}^{-1}$	k_{-1} s^{-1}	K_1 lmol^{-1}	ref
acetone	$ca10^{-6}$ *	2.5×10^6	4×10^{-4}	6.3×10^9	89
		3.3×10^6	8.2×10^{-6}	4×10^{11}	87
cyclohexanone	$ca10^{-4}$ *	1.5×10^5	6.88×10^{-4}	2.2×10^8	90
		1.6×10^5	1.76×10^{-4}	9.2×10^8	87
dimethylmalonate	0.5	2.5×10^5	20.5	1.2×10^4	87
methylcyanoacetate	54	1.3×10^5	62	1660	87
methylacetoacetate	418	5500	470	11.7	87

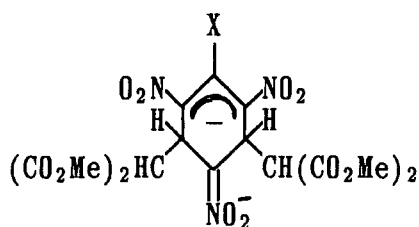
* apparent equilibria referring to a mixture of keto/enol forms of the parent molecules

Furthermore the acid catalysed decomposition of enolate-TNB adducts is very slow¹¹⁰ compared with that for alkoxy-TNB adducts. For example, in water values of k_{H^+} for the acid catalysed decomposition of the acetone and cyclohexanone-TNB adducts are $0.026 \text{ l mol}^{-1} \text{ s}^{-1}$ and $0.16 \text{ l mol}^{-1} \text{ s}^{-1}$ respectively¹¹⁰ while the value of k_{H^+} for the 1:1 hydroxide-TNB adduct is close to the diffusion controlled limit of $10^{10} \text{ l mol}^{-1} \text{ s}^{-1}$. Factors involved in reducing k_{H^+} for enolate adducts are thought to be¹¹⁰ protonation of an oxygen atom which is two atoms removed from the bond to be broken and a high degree of structural /electronic /solvational reorganisation accompanying the process.

Acetone reacts with substituted 1-X-2,4,6-trinitrobenzenes⁹¹⁻⁹⁴ ($X = \text{OEt}$, OPh , Cl , NMe_2 , Me , OMe , COOH , COOMe , SMe) to give exclusively the 1,3 adduct 1.42. The anion of dimethylmalonate reacts with 2,4,6-trinitroanisole^{100,102} to give



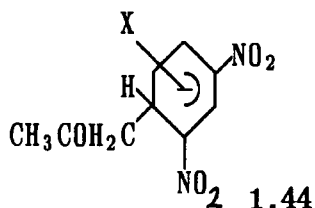
1.42



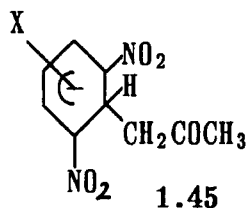
1.43

both 1,3 and 1,1 adducts while 1:2 adducts (1.43 $X = \text{H}$, Cl , OMe) have been obtained with dimethylmalonate and TNB⁸⁷, picryl chloride¹⁰³ and TNA¹⁰⁰

Acetone ions react with substituted 1-X-3,5-dinitrobenzenes and 1-X-2,4-dinitrobenzenes to form 1.44 and 1.45 in ratios depending on the nature of X.



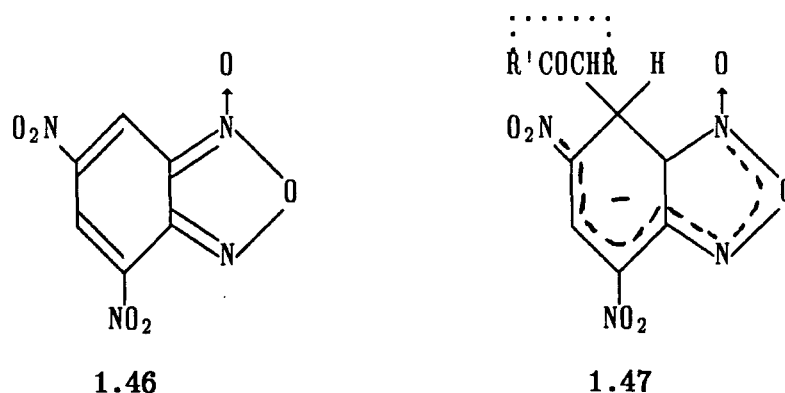
1.44



1.45

For instance 1-X-3,5-DNB (X = OMe, Me) yields only σ -adducts of the type 1.44⁹⁷ while in the case of X = CO₂Et^{95,97}, CF₃⁹⁵⁻⁹⁷, CO₂Me, COO⁻⁸³, CONH₂ and CON(Et)₂⁸⁶ mixtures of 1.44 and 1.45 are formed, 1.45 always being less stable and gradually isomerising to 1.44. Likewise, acetate ions react with 1-X-2,4-DNB to yield a mixture of the isomers in which 1.45 prevails for X = OMe, CO₂Me^{95,98}, F, Cl, Br, I¹¹¹, Me, Et, *i*-Pr, *t*-Bu⁹⁸ and 1.44 for X = SEt and SCN⁹⁵. The effect of the sulphur containing substituent has been attributed⁹⁵ to the high electron accepting capacity of the sulphur atom with its unoccupied 3d orbitals.

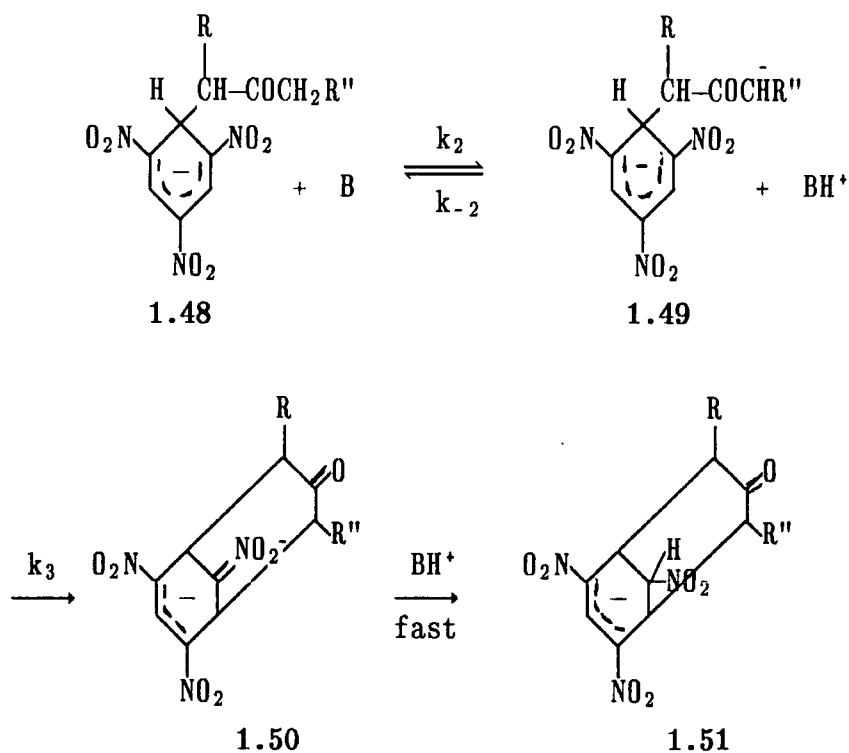
The super-electrophile 4,6-dinitrobenzofuroxan (1.46) has been shown to react with ketones of low acidity (such as acetone and cyclopentanone) in DMSO in the absence of added base to form adducts 1.47⁷⁷. These reactions are thought to result from attack of equilibrium concentrations of the weakly basic enol on DNBF⁷⁷.



Formation of bicyclic adducts

The adduct 1.37 is susceptible to cyclisation provided it possesses a potential nucleophilic site γ to the tetrahedral ring carbon (i.e. R' = CH₂R''). Thus various ketones and ketoesters (acetone, diethylketone, cyclohexanone, acetylacetone, dibenzylketone, methylacetoacetate etc.)^{80-82,112-116} readily form bicyclic adducts such as 1.51.

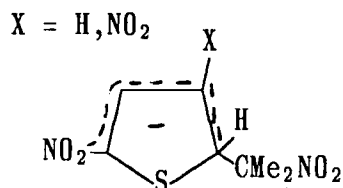
In most cases these reactions proceed as shown in the scheme. They involve deprotonation of the exocyclic carbonyl group followed by intramolecular nucleophilic attack of the resulting enolate side chain.



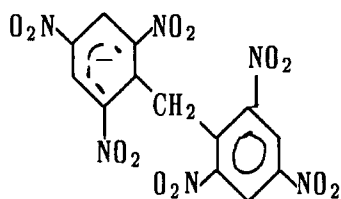
Other carbanions

Various other carbon acids add to activated aromatic compounds to form σ -adducts. These include nitroalkanes¹¹⁷⁻¹¹⁹, nitriles ($\text{CH}_2(\text{CN})_2$, $\text{CHEt}(\text{CN})_2$)¹²⁰ CH_3CN ¹²², PhCH_2CN ¹²¹) and haloforms (CHX_3 ; $\text{X} = \text{Cl, Br, I}$)¹²³⁻¹²⁵.

σ -Adducts have been observed from reaction of TNB with anions derived from nitromethane¹¹⁷, nitroethane and 2-nitropropane¹¹⁹. In the case of nitromethane and nitroethane addition to an unsubstituted ring position of 2,4,6-trinitrotoluene has also been observed¹¹⁹. The anion derived from 2-nitropropane adds in DMSO to 2-nitrothiophene and 2,4-dinitrothiophene to give 1.52 ($\text{X} = \text{H, NO}_2$).



1.52



1.53

Polynitroaromatics with ionisable side chains will also add to activated aromatic compounds. Thus the 2,4,6-trinitrobenzyl anion adds easily to TNB to give 1.53^{126,127}, while other adducts have been obtained with 2,4-dinitrotoluene¹²⁷, 4,6-dinitro-*m*-xylene¹²⁷ and 2,4,6-trinitro-*m*-xylene¹²⁶. In excessive base the latter substrate may lose protons from both methyl groups and thus form an adduct with two molecules of TNB¹²⁶.

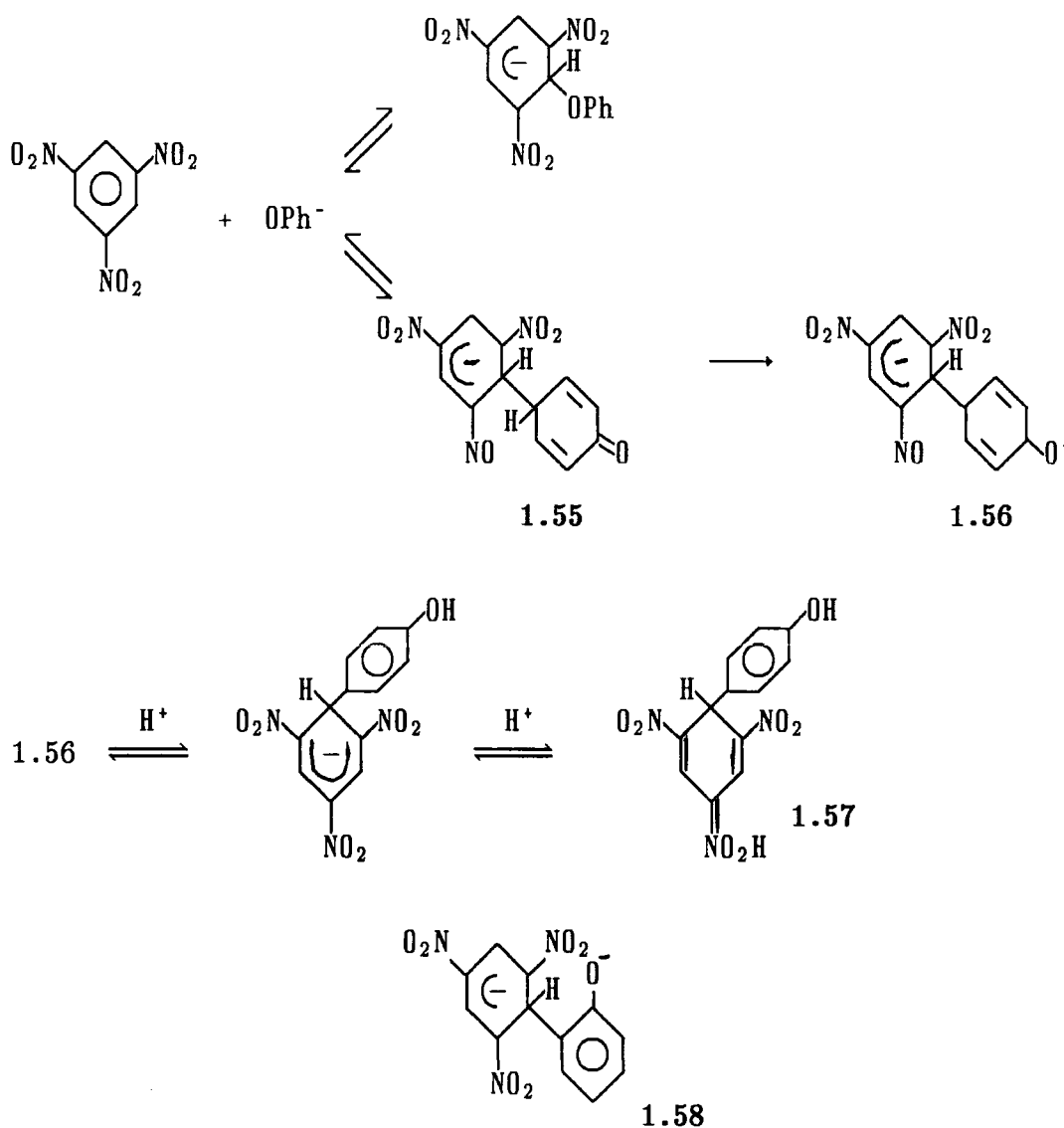
In a stopped-flow study of the interactions of 2,4,6-trinitrotoluene with sodium methoxide¹²⁸, Bernasconi observed three time processes. With [MeO⁻] >> [TNT], methoxide addition to an unsubstituted position of TNT (rapid) was observed along with ionisation of TNT. With [TNT] >> [MeO⁻], Janovsky addition of TNT⁻ to TNT was the predominant process¹²⁸.

σ -Adducts derived from species of very low acidity have also been the subject of a number of structural studies^{76,129}. In these cases the carbanions were often generated via organometallic species. Such adducts are often remarkably stable.

Ambident Nucleophiles

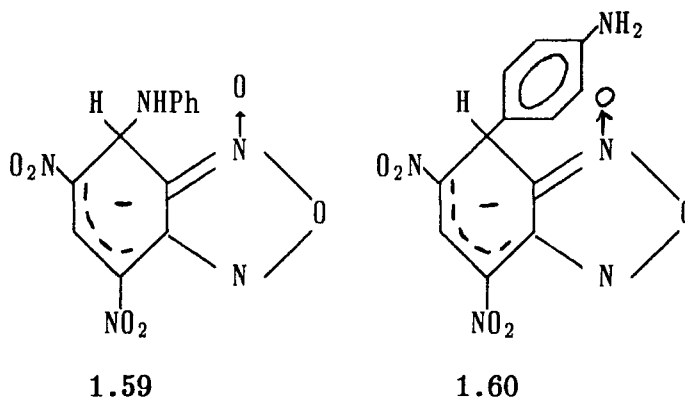
Phenoxide ions act as an ambident nucleophile forming both oxygen and carbon-bonded adducts with activated aromatics^{130,135}. While the oxygen bonded adducts are frequently detected as transient species resulting from a kinetically favoured addition, the formation of carbon-bonded adducts is essentially irreversible due to the rearomatization of intermediates of type 1.55.

The TNB adduct 1.56 does not decompose in acidic media and may be converted to 1.57, a nitronic acid, in a two-step protonation¹³².

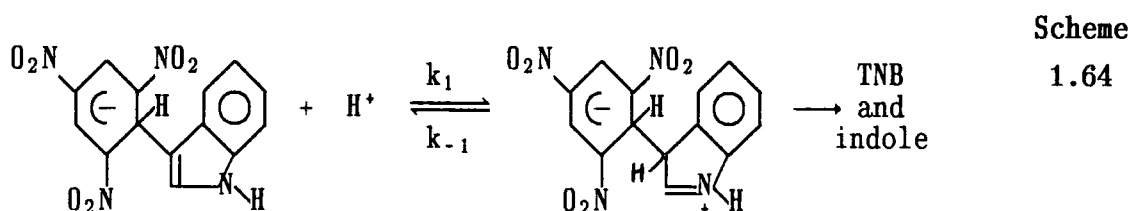
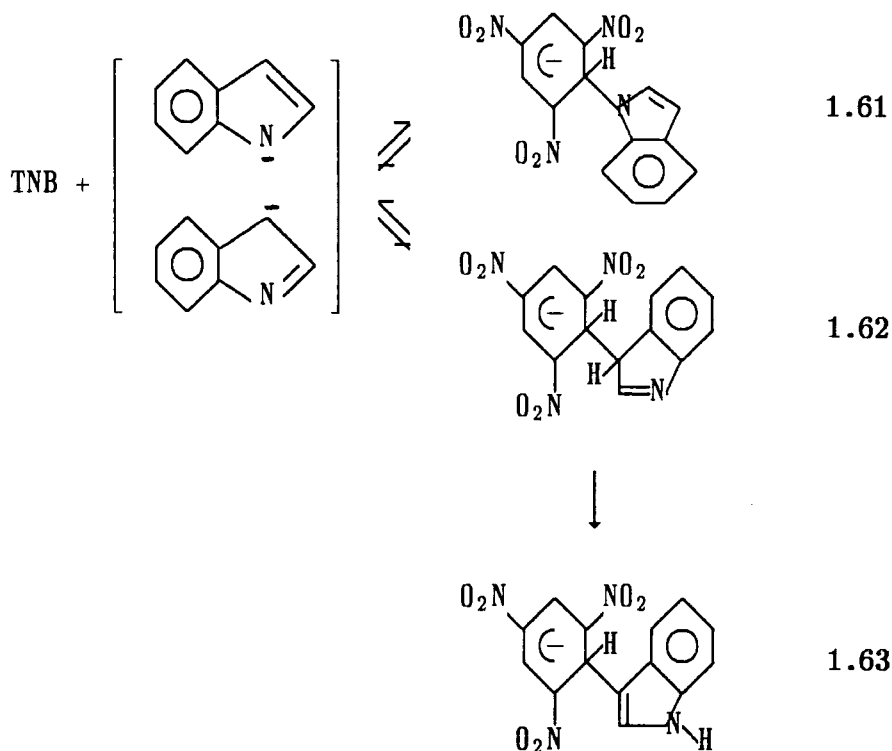


Also noted is the adduct 1.58 formed by bonding between an *ortho* carbon of phenoxide ion and an unsubstituted carbon of TNB¹³². *Ortho* addition also occurs with 4-substituted phenols¹³¹ and with the naphthoxide ion¹³⁶.

Aniline reacts with 4,6-dinitrobenzofuran to yield both N and C-bonded σ -adducts 1.59 and 1.60. The reaction of aniline with TNB is known¹³⁷ to give only an N-bonded adduct. Other ambident nucleophiles include pyrrolide, indolide



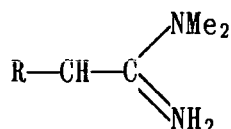
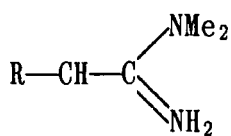
and imidazolide^{138,140} ions which react with TNB in DMSO to give initially N-bonded adducts which undergo subsequent conversion to C-bonded adducts. The reaction scheme for indolide is shown. The intermediate 1.62 is not observed suggesting that rearrangement to 1.63 is very rapid. The same is true for the pyrrolide and imidazolide analogues.



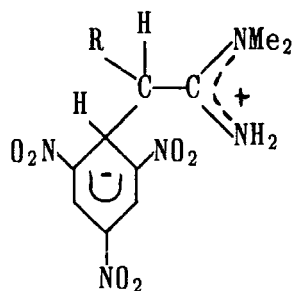
Although these σ -adducts are formed through pathways which are essentially irreversible, the adducts of pyrrole and indole derivatives decompose in aqueous acid solution to TNB and parent heterocycles¹⁴⁰. It has been suggested that the decomposition proceeds according to scheme 1.64 (shown for the indole adduct) with the proton transfer step being rate limiting^{141,142}

In contrast with its pyrrole and indole analogues, the carbon-bonded imidazole adduct does not decompose appreciably in aqueous acidic solution due to the protonation of the imidazole moiety¹⁴⁰.

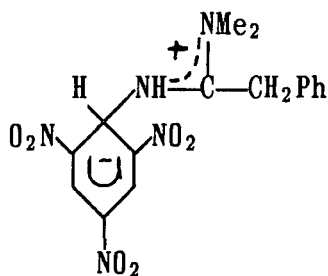
Amidines are another important class of ambident nucleophile. α -Substituted N,N-dimethylamidines **1.65** ($R = \text{CH}_3, \text{H}$) react with 1,3,5-trinitrobenzene in DMSO or ethanol to give solely the carbon-bonded zwitterionic adducts **1.66**¹⁴⁴. When $R = \text{Ph}$ only the bridged adduct **1.68** ($R = \text{Ph}$) can be isolated and this is believed to result from the cyclisation of the initially formed (though undetected) N-bonded adduct **1.67**^{143,144}. The carbon-bonded adducts **1.66** ($R = \text{CH}_3, \text{H}$) will cyclise in the presence of strong base to give **1.68** ($R = \text{CH}_3, \text{H}$)¹⁴⁵. These *meta*-bridging reactions lead to a useful synthesis of 6,7-benzomorphan¹⁴⁶.



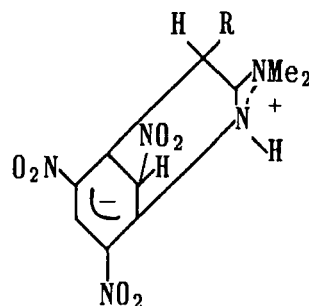
1.65



1.66



1.67



1.68

Quantitative Measurements of Nucleophilicity: Basicity, Nucleophilicity and Intrinsic barriers

Polar reagents fall into two categories: those which are "electrophilic", defined as electron seeking and those which are "nucleophilic", defined as nucleus seeking. Bunnett¹⁴⁸ has suggested that the term "nucleophile" be restricted to reagents that supply a pair of electrons to form a new bond with another atom. In its modern form, nucleophilicity is restricted to kinetic phenomena, describing the kinetic ability of a nucleophile in an addition or substitution process. Basicity on the other hand, is a thermodynamic term, describing the ability of an electron-rich species to displace an equilibrium. The term basicity, given alone, usually refers to hydrogen (Bronsted basicity) but may be usefully applied to other elements; thus carbon basicity¹⁴⁹ refers to the thermodynamic ability of a base to add to carbon. Bunnett¹⁴⁸ has listed several factors which contribute to overall nucleophile reactivity.

As the kinetic barrier to nucleophilic attack is affected by the thermodynamics of the reaction, kinetic data can only be meaningfully compared in systems which have the same equilibrium constant. By comparing systems for which the equilibrium constants are unity, the thermodynamic factor (ΔG^0) may be eliminated altogether leaving a purely kinetic factor known as the intrinsic barrier (ΔG_0^\ddagger) and the corresponding intrinsic rate constant k_0 . [For a reaction with forward and reverse rate constants k_1 and k_{-1} , k_0 is defined as $k_0 = k_1 = k_{-1}$ for $\Delta G^0 = 0$ ($K_1 = 1$)]. ΔG_0^\ddagger is related via transition state theory, to k_0 by expression 1.69

$$k_0 = \left[\frac{kT}{h} \right] K_0^\ddagger = \left[\frac{kT}{h} \right] e^{-\frac{\Delta G_0^\ddagger}{RT}} \quad 1.69$$

The theoretical and practical significance of intrinsic rate constants is that, at least in principle, they are representative of a whole reaction series and independent of the thermodynamics of a particular member within the series¹⁵¹. In practice, k_0 is obtained by extrapolation or interpolation of $\log k$ vs. $\log K$ plots. Reactions with high intrinsic barriers are associated with a large degree of electronic/structural and solvational reorganisation and a lack of synchronisation between concurrent reaction events such as bond formation / breakage, solvation / desolvation, development (loss) of resonance etc. Conversely, for reactions where the amount of electronic / structural and solvational reorganisation is minimal (and well synchronised) the intrinsic barrier is low^{150,151}.

Bernasconi has developed a rule known as the "principle of non-perfect synchronisation"¹⁵¹ which has been used to explain trends in intrinsic barrier resulting from substituent and solvent effects. According to this rule, product-stabilising factors that develop late along the reaction coordinate increase the barrier while reactant-stabilising factors that are lost late decrease the barrier; the converse is true for early development or early loss¹⁵¹. "Early" and "late" are defined in relation to the main process which may be bond formation/breakage or the transfer of charge from one reactant to another. For example, in the addition of thiolates to substituted α -nitrostilbenes¹⁵², there is evidence that the product stabilising factor (the formation of a soft-soft interaction) develops ahead of bond formation thereby decreasing the intrinsic barrier¹⁵². This contrasts with most other common product stabilising factors (for example resonance, solvation, intramolecular hydrogen bonding) whose development typically lags behind bond formation thereby increasing the intrinsic barrier¹⁵². The concept of intrinsic barrier was introduced by Marcus¹⁵³ in his theory of electron transfer reactions. One expression of Marcus theory, shown in 1.70 relates the reaction barrier (ΔG^\ddagger) to the intrinsic barrier (ΔG_0^\ddagger) and the free energy of the reaction¹⁴⁷.

$$\Delta G^\ddagger = \Delta G_0^\ddagger + \frac{1}{2}\Delta G^0 + \frac{\Delta G^0{}^2}{16\Delta G_0^\ddagger} \quad 1.70$$

The gradient $\frac{d \Delta G^\ddagger}{d \Delta G^0}$ (1.71) contains a term in ΔG^0 . A linear free energy relationship such as a Bronsted plot, will thus only be obtained strictly when $\Delta G^\ddagger \gg \Delta G^0$.

$$\frac{d \Delta G^\ddagger}{d \Delta G^0} = \frac{1}{2} \left[1 + \frac{\Delta G^0}{4\Delta G_0^\ddagger} \right] \quad 1.71$$

Quantitative studies of nucleophilicity can be said to have begun with the work of Bronsted and Pederson who noted a correlation of the rates (k_B) of nitramide decomposition with strength (pK_{HB}) of base (B^-).

$$\log k_{B^-} = \beta pK_{HB} + C \quad 1.72$$

The expression in 1.72 thus correlates hydrogen basicity with hydrogen nucleophilicity. The extended form of the Bronsted equation (with gradient $\beta_{nuc} = \frac{d \log k}{d pKa}$) allows for nucleophilic attack on various atomic centres and is much used.

A single-parameter linear free energy relationship for correlating nucleophilicity was presented by Swain and Scott (expression 1.73)

$$\log \left[\frac{k}{k_0} \right] = sn \quad 1.73$$

where the nucleophilicity constants n are defined by the reaction rate of methyl bromide ($s=1$) relative to that of water. This relationship implies that nucleophiles have the same relationship towards all reactive sites, but now ample

evidence exists that this is not the case. The Brønsted relationship exhibited a similar problem in that nucleophiles with different attacking atoms (e.g. oxygen, carbon, and nitrogen bases) gave separate correlations. Thus these one parameter expressions will not provide a correlation of all nucleophiles with all centres.

In 1954 Edwards¹⁵⁴ added polarisability (as measured by the oxidation potential of oxidative dimerisation of nucleophiles, E^0) as a second parameter to obtain the modified Brønsted equation 1.74 where k/k_0 is the rate constant for the

$$\log \left[\frac{k}{k_0} \right] = \alpha E_X + \beta H_X \quad 1.74$$

reaction of a substrate with a reagent X relative to that for reaction with water and

$$H_X = pK_{HX} + 1.74$$

$$E_X = E^0(X_2) + 2.60$$

Use of equation 1.74 allowed the correlation of a fair amount of data. However attempts to correlate data for methyl iodide and *trans*-Pt(py₂)Cl₂ reacting with a diverse set of nucleophiles failed. Other LFERs with three or more parameters have since been used with varying degrees of success.

The importance of polarisability in Edwards' expression led Pearson^{155,156} to formulate his principle of hard and soft acids and bases in which nucleophiles (bases) are classified as either polarisable (soft) or non-polarisable (hard). For soft nucleophiles α is large, for hard nucleophiles β is large. The principle states that hard acids (electrophiles) prefer to bind to hard bases, and soft acids prefer to bind to soft bases. For example the equilibrium constants⁵⁴ for the 1:1 interaction of 1,3,5-trinitrobenzene with thiophenoxide and phenoxide (reaction through oxygen) in methanol are 1.95 l mol⁻¹ and <2x10⁻³ l mol⁻¹ respectively. The pK_as of the compounds in methanol are reported as 10.9 (thiophenoxide)¹⁵⁸ and 14.1

(phenoxide)¹⁵⁷. Thus a comparison of carbon basicities shows a 10³-fold difference in favour of sulphur, a "soft" base, reacting with carbon, a "soft" acid, while a comparison of hydrogen basicities reveals again a 10³-fold difference in favour of the oxygen base (hard relative to sulphur) for reaction with protons, a hard acid.

In a conventional Brønsted plot, log k for the forward reaction is plotted against pK_a values for the nucleophiles. These latter form a "family" of structurally similar compounds, the basicities of which can be altered by remote substitutions. The gradient β_{nuc} describes the sensitivity of the reaction towards Brønsted basicity and may have implications in the structure of the transition state.

$$\log k = \beta_{\text{nuc}} \text{pK}_{\text{a}} + C \quad 1.75$$

In the reactions of α-nitrostilbenes with thiolate anions¹⁵² (equation 1.76)

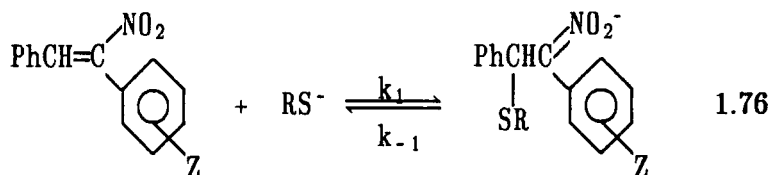
Bernasconi has determined β-values $\left[\beta_{\text{nuc}} = \frac{d \log k_1}{d \text{pK}_{\text{aRSH}}}, \beta_{1g} = \frac{d \log k_{-1}}{d \text{pK}_{\text{aRSH}}}, \beta_{\text{eq}} = \frac{d \log K_1}{d \text{pK}_{\text{aRSH}}} \right]$ by varying R in the nucleophile for reaction with α-

nitrostilbene, and Hammett ρ values (ρ(k₁), ρ(k₋₁), ρ(K₁)) by varying Z in the

electrophile for reaction with HOCH₂CH₂S⁻. Quantities β_{nuc}ⁿ $\left[= \frac{\beta_{\text{nuc}}}{\beta_{\text{eq}}} = \frac{d \log k_1}{d \log K_1} \right]$ by varying R

and α_{nuc}ⁿ $\left[= \frac{\rho(k_1)}{\rho(K_1)} = \frac{d \log k_1}{d \log K_1} \right]$ by varying Z

are used to determine I $\left[= \alpha_{\text{nuc}}^{\text{n}} - \beta_{\text{nuc}}^{\text{n}} \right]$, the degree of transition state imbalance.



The large value of I in this reaction (0.68) has been taken to indicate a strongly imbalanced transition state in which development of resonance and solvation at

from the thiophenoxide to the aromatic ring¹⁶¹. However the fact that rate constants k_1 are six orders of magnitude higher in the dinitro compound than in 1-chloro-4-nitrobenzene adds weight to the argument that such slopes do not give a good estimate of the degree of charge transfer in the transition state¹⁶¹.

Acidity functions in strongly basic solutions

Strongly basic solutions can be arbitrarily defined as those with an ionising power equal to or greater than 0.1M aqueous metal hydroxide solutions¹⁶³. Hammett first suggested a suitable acidity function to measure the relative ability of these solutions to ionise weak acids



and the acidity function can be defined as

$$H_- = \text{p}K_a + \log \left[\frac{[\text{A}^-]}{[\text{HA}]} \right] \quad 1.79$$

where $\frac{[\text{A}^-]}{[\text{HA}]}$ is the measured ionisation ratio of the indicator¹⁶³. The acidity function of the solution is equal to

$$H_- = \frac{-\log \gamma_A a_{\text{H}^+}}{\gamma_{\text{HA}}}$$

where γ denotes the activity coefficient of the indicator and a_{H^+} the hydrogen ion activity. The H_- function thus becomes identical with pH in dilute aqueous solution¹⁶³.

The H_- function has also been evaluated for various alcohol solutions of alkoxide. For dilute solutions (<0.1M base) there is a direct relationship between H_- and base concentration such that

$$H_- = C + \log[\text{OR}^-] \quad 1.80$$

where C is a constant dependent on the nature of the alcohol. Just as for aqueous

solutions, the increase in basicity soon becomes more rapid than suggested by expression 1.80. This can be attributed to the increasingly reduced solvation of the alkoxide ions with increasing concentration and their consequent rise in activity. The H_m acidity function¹⁶⁴ is defined by equation 1.81 and refers to methanol as the standard state

$$H_m = -\log \left[\frac{a_H + \gamma_{A^-}}{\gamma_{HA}} \right] = pK_{HA}^m + \log_{10} \frac{[A^-]}{[HA]} \quad 1.81$$

Other functions of this kind can be defined according to the charge type of the acid, i.e., the H_+ , H_0 , or H_2^- scales for the ionisation of double positively, positively or negatively charged acids.



In the case of base addition to the indicator (in water) the appropriate function is J_- which is defined in terms of the equilibrium



The acidity function is then

$$\begin{aligned} J_- &= \rho(KK_W) + \log \left[\frac{[BOH^-]}{[B]} \right] \quad 1.82 \\ &= -\log(a_{H^+} \gamma_{BOH^-} / a_{H_2O} \gamma_B) \end{aligned}$$

For alkoxide additions in alcohols the expression for J_- is analagous, K_W being replaced by the value for the autoprotolysis constant. In methanol the function is designated J_M ¹⁶⁴.

Acidity functions in mixed solvents

Mixed solvents such as H₂O/pyridine, H₂O/tetramethylsulphone, H₂O/DMSO¹⁶⁵, EtOH/DMSO¹⁶⁶ and MeOH/DMSO¹⁶⁷ containing constant concentrations of base have also been used to determine H₋ scales. A considerable increase in H₋ is observed in all cases as the proportion of the dipolar aprotic solvent is increased¹⁶³.

Use has been made¹⁶⁹ of Rochester's J_M function (equation 1.83) to determine equilibrium constants for the formation of methoxide adducts of low stability.

$$J_M = \rho(K_1 K_{MeOH}) + \log_{10} \frac{[\text{adduct}]}{[\text{parent}]} \quad 1.83$$

K_{MeOH} is the autoprotolysis constant of methanol and K₁ the equilibrium constant for the formation of the methoxide adduct in methanol.

A similar scale¹⁶⁸ describing the addition of methoxide to α -cyanostilbenes is described in chapter 5. A comparison of the J_M and H_M scales obtained in DMSO/MeOH solvent reveals rather similar behaviour. This probably arises from the fact that the major source of increase in basicity is due to desolvation of the methoxide ion will be independent of the indicator used¹⁶⁹.

References

- 1 JV Janovsky, L. Erb., *Ber.*, 1886,**19**,2155
- 2 JV Janovsky, *ibid.*, 1891,**24**,171
- 3 G Wilgerodt, *ibid.*, 1892,**25**,608
- 4 B von Bitto, *Liebigs Ann. Chem.*, 1892,**269**,377
- 5 MC Lobry de Brun, FH van Leent, *Rec. Trav. Chim.*, 1895,**14**,150
- 6 CL Jackson, WF Boos, *Amer. Chem. J.*, 1898,**20**,444
- 7 A Hantzsch, H Kissel, *Ber.*, 1899,**32**,3137
- 8 FH von Leent, *Rec. Trav. Chim.*, 1896,**15**,89
- 9 CL Jackson, FH Gazzolo, *J. Amer. Chem. Soc.*, 1900,**23**,376
- 10 J Meisenheimer, *Justus Liebigs Ann. Chem.*, 1902,**323**,205
- 11 R Destro, C Gramaccioli, M Simonetta, *Acta Crystallogr.*, 1968,**24**,1369
- 12 H Ueda, N Sakabe, J Tanaka, A Furusaki, *Bull. Chem. Soc. Jap.*, 1968,**41**,2866
- 13 MR Crampton, V Gold, *J. Chem. Soc.*, 1964, 4293
- 14 MJ Strauss, *Chem. Rev.*, 1970,**70**,667
- 15 E Buncel, AR Norris, KE Russell, *Quart. Rev. (London)*, 1968,**22**,123
- 16 J Hayami, S Otani, F Yamaguchi, Y Nishikawa, *Chem. Lett.*, 1987,739
RI Cattana, JO Singh, JD Anunziata, JJ Silber, *J. Chem. Soc. Perkin Trans. II*, 1987,79
- 17 R Bacaloglu, CA Bunton, G Cerichelli, *J. Am. Chem. Soc.*, 1987,**109**,621
- 18 GA Russell, EG Janzen, *J. Amer. Chem. Soc.*, 1967,**89**,300
- 19 GA Russell, EG Janzen, ET Strom, *ibid.*, 1964,**86**,1807
- 20 MR Crampton, V Gold, *J. Chem. Soc. (B)*, 1966,498
- 21 DN Brooke, MR Crampton, *J. Chem. Res.*, 1980 (S) 340; (M) 4401
- 22 EF Caldin, G Long, *Proc. R. Soc. London, Ser. A*, 1955,**228**,263
- 23 PCMF Castilho, MR Crampton, J Yarwood, *J. Chem. Res.*, 1989 (S) 370 ; (M) 2801
- 24 JF Bunnett, RE Zahler, *Chem. Rev.*, 1951,**49**,273
- 25 JF Bunnett, *Q. Rev. Chem. Soc.*, 1958,**12**,1

- 26 JF Bunnett, JJ Randall, *J. Am. Chem. Soc.*, 1958,**80**,6020
- 27 AJ Kirby, WP Jencks, *J. Am. Chem. Soc.*, 1965,**87**,3217
- 28 JF Bunnett, RH Garst, *ibid.*, 1965,**87**,3879
- 29 CF Bernasconi, MC Muller, P Schmid, *J. Org. Chem.*, 1979,**44**,3189
MR Crampton, B Gibson, *J. Chem. Soc., Perkin Trans.II*, 1981,533
MR Crampton, C Greenhalgh, *ibid.*, 1983,1175
MR Crampton, PJ Routledge, P Golding, *ibid.*, 1984,329
E Buncel, HW Leung, *J. Chem. Soc., Chem. Commun.*, 1975,19
E Buncel, W Eggiman, *J. Chem. Soc., Perkin Trans.II*, 1978,673
- 30 MR Crampton, PJ Routledge, *J. Chem. Soc. Perkin Trans.II*, 1984,573
- 31 NS Nudelman, PME Manicini, RD Martinez, LR Vottero, *J. Chem. Soc., Perkin Trans.II*, 1987,951
- 32 Y Hasegawa, *J. Chem. Soc. Perkin Trans. II*, 1985,87
- 33 CF Bernasconi, RH de Rossi, P Schmid, *J. Am. Chem. Soc.*, 1977,**99**,4090
- 34 CF Bernasconi, *Acc. Chem. Res.*, 1978,11,147
- 35 Y Hasegawa, *J. Org. Chem.*, 1985,**50**,649
- 36 E Buncel, MR Crampton, MJ Strauss, F Terrier, "*Electron Deficient aromatic and heteroaromatic base interactions*", Elsevier, Amsterdam 1984
- 37 Jon A Orvik, JF Bunnett, *J. Am. Chem. Soc.* 1970,**92**,2417
- 38 CA Fyfe, A Koll, SWH Damji, CO Malkiewich, PA Forte, *J. Chem. Soc., Chem. Commun.*, 1977,335
Can. J. Chem., 1977,**55**,1468
- 39 MR Crampton, *J. Chem. Soc. B.*, 1967,1341
- 40 RA Henry, *J. Org. Chem.*, 1962,**27**,2637
- 41 CF Bernasconi, RG Bergstrom, *J. Am. Chem. Soc.*, 1973,**95**,3603
- 42 MJ Strauss, SPB Taylor, *J. Am. Chem. Soc.*, 1973,**95**,3813
- 43 MR Crampton, MJ Willison, *J. Chem. Soc., Chem. Commun.*, 1973,215
- 44 MR Crampton, *J. Chem. Soc. Perkin Trans. II*, 1978,343
- 45 MR Crampton, MA El Ghariani, *J. Chem. Soc. B*, 1969,330
- 46 MR Crampton, MJ Willison, *J. Chem. Soc. Perkin Trans. II*, 1976,160
- 47 N Marendic, AR Norris, *Can. J. Chem.*, 1973,**51**,3927
- 48 DN Brooke, MR Crampton, *J. Chem. Soc. Perkin Trans. II*, 1980,1850
- 49 E Buncel, AR Norris, KE Russell, PJ Sheridan, *Can. J. Chem.*, 1974,**52**,25

- 50 MR Crampton, MA El Ghariani, *J. Chem. Soc. B*, 1970,391
- 51 EG Kaminskaya, SS Gitis, A Ya Kaminski, *J. Org. Chem. USSR*, 1979,15(4), 793
- 52 JF Bunnett, M Gisler, H Zollinger, *Helv. Chim. Acta.*, 1982,65,63
- 53 MR Crampton, C Greenhalgh, *J. Chem. Soc. Perkin Trans. II*, 1985,599
- 54 MR Crampton, *J. Chem. Soc.B*, 1968,1208
- 55 MR Crampton, MA El Ghariani, *ibid.*, 1971,1043
- 56 MR Crampton, *ibid.*,1971,2112
- 57 TV Leshina, KV Solova, SM Shein, *J. Org. Chem. USSR*, 1974,10,354
- 58 M Cavazza, G Morganti, A Guerriero, F Pietra, *Tetrahedron Lett.*, 1980, 3703
- 59 G Biggi, F Pietra, *J. Chem. Soc. Chem. Commun.*, 1973,229
- 60 G Biggi, F Pietra, *J. Chem. Soc. Perkin Trans. I*, 1973,1980
- 61 CA Veracini, F Pietra, *J. Chem. Soc. Chem. Commun.*,1974, 623
- 62 G Biggi, CA Veracini, F Pietra, *J. Chem. Soc. Chemm. Commun.*, 1973,523
- 63 F Terrier, *Chem. Rev.*, 1982,82(2),77
- 64 MR Crampton, *Adv. Phys. Org. Chem.*, 1969,7,211
- 65 MR Crampton, MJ Willison, *J. Chem. Soc. Perkin Trans. II*, 1976,901
- 66 G Ah-Kow, *Ph.D. Thesis, Paris*, 1979
- 67 G Biggi, F Pietra, *J. Chem. Soc. Chem. Commun.*, 1973,229
- 68 E Buncel, AR Norris, W Proudlock, KE Russell, *Can. J. Chem.*, 1969,47, 4129
- 69 LH Gan, AR Norris, *ibid.*,1974,52,1
- 70 LH Gan, AR Norris, *ibid.*, 1974,52,8
- 71 MJ Strauss, *Acc. Chem. Res.*, 1974,7,181
- 72 CH Rochester, B Rossall, *J. Chem. Soc. Perkin Trans. II*, 1967,743
- 73 CJM Stirling, *Acc. Chem. Res.*, 1979,12,198
CJM Stirling, M Varma, *J. Chem. Soc. Chem. Commun.*, 1981,553
- 74 AR Norris, *Can. J. Chem.*, 47,2895,1969
- 75 MR Crampton, HA Khan, *J. Chem. Soc. Perkin Trans. II*, 1973,710

- 76 GA Artamkina, MP Egorov, IP Beletskaya, *Chem. Rev.*, 1982,**82**,427
- 77 F Terrier, MP Simonnin, MJ Pouet, MJ Strauss, *J. Org. Chem.*, 1981,**46**, 3537
- 78 R Foster, CA Fyfe, *J. Chem. Soc. B*, 1966,53
- 79 CA Fyfe, *Tetrahedron Lett.*, 1968,659
- 80 MJ Strauss, TC Jensen, H Schran, K O'Connor, *J. Org. Chem.*, 1970,**35**,383
- 81 K Kohashi, Y Ohkura, T Momose, *Chem. Pharm. Bull.*, 1970,**18**,2151
- 82 MJ Strauss, SPB Taylor, *J. Org. Chem.*, 1973,**38**,856
- 83 MR Crampton, HA Khan, *J. Chem. Soc. Perkin Trans. II*, 1972 ,733
- 84 T Kabeya, K Kohashi, Y Ohkura, T Momose, *Chem. Pharm. Bull.*, 1973,**21**, 2168
- 85 V Kavalek, V Machacek, V Sterba, J. Subert, *Collect. Czect. Chem. Commun.*, 1974,**39**,2063
- 86 A Ashfaq, V Machacek, V Sterba, *ibid.*, 1975,**40**,1910
- 87 J Kolb, V Machacek, V Sterba, *ibid.*, 1976,**41**,1914
- 88 EG Kaminskaya, *Zh. Org. Khim*, 1978,**14**,2576
- 89 N Obi, M Kimura, *Chem. Pharm. Bull.*, 1972,**20**,2295
- 90 N Obi, H Kakizaki, M Kimura, *ibid.*, 1973,**21**,235
- 91 M Kimura, N Obi, M Kawazoe , *ibid.*, 1969,**17**,531
- 92 M Kimura, N Obi, M Kawazoe , *ibid.*, 1972,**20**,452
- 93 R Foster, CA Fyfe, PH Emslie, MJ Foreman, *Tetrahedron*, 1967,**23**,227
- 94 A Ya Kaminsky, SS Gitis, Yu D Grudtsyn, LI Khabarova, EG Kaminskaya, V Sh Golubchik, *Zh. Org. Khim.*, 1974,**10**,1205
- 95 SS Gitis, A Ya Kaminsky, EA Bronstein, EE Gol'teuzen, Yu D Grudtsyn, *Zh. Org. Khim.*, 1973,**9**,2091
- 96 MI Foreman, R Foster, *Can. J. Chem.*, 1969,**47**,729
- 97 SS Gitis, Yu P Grudtsyn, EA Bronshtein, EE Gol'teuzen, A Ya Kaminsky, *Dokl. Akad. Nauk. SSSR*, 1972,**203**,1063
- 98 SS Gitis *et al.*, *Teor. Exp. Khim.*, 1972,**8**,261
- 99 MJ Strauss, *Tetrahedron Lett.*, 1969,2021
- 100 J Kavalek, V Machacek, M Pastrnec, V Sterba, *Collect. Czech. Chem. Commun.*, 1977,**42**,2928

- 101 J Kavalek, A Ashfaq, V Sterba, *ibid.*, 1979,**44**,1453
- 102 V Machacek, V Sterba, A Lycka, *ibid.*, 1987,**52**,132
- 103 J Kavalek, M Pastrnek, V Sterba, *ibid.*, 1978,**43**,1401
- 104 NV Ignatev, VN Boiko, LM Yagupolskii, *Zh. Org. Chim.*, 1980,**16**,1501
- 105 SS Gitis, A Ya Kaminsky, EA Bronshtein, Yu D Grudtsyn, *Zh. Org. Khim.*, 1971,**7**,1830
- 106 K Kohashi, Y Tsuruta, Y Ohkura, *Chem. Pharm. Bull.*, 1978,**26**,2914
- 107 K Kohashi, Y Tsuruta, M Yamaguchi, Y Ohkura, *Chem. Pharm. Bull.*, 1979,**27**,2122
- 108 AR Butler, *Clin. Chim. Acta.*, 1975,**59**,227
- 109 AR Butler, *J. Chem. Soc. Perkin Trans. II*, 1975,853
- 110 RA Renfrow, MJ Strauss, F Terrier, *J. Org. Chem.*, 1980,**45**,471
- 111 SS Gitis *et al.*, *Zh. Org. Khim.*, 1975,**11**,2106
- 112 MJ Strauss, SPB Taylor, *J. Org. Chem.*, 1973,**38**,1330
- 113 MJ Strauss, SPB Taylor, H Shindo, *ibid.*, 1972,**37**, 3658
- 114 MJ Strauss, HF Schran, RR Bard, *ibid.*, 1973,**38**,3394
- 115 MJ Strauss, HF Schran, *Tetrahedron Lett.*, 1971,2349
- 116 K Kohashi, Y Ohkura, T Momose, *Chem. Pharm. Bull.*, 1971,**19**,645
- 117 CA Fyfe, *Can. J. Chem.*, 1968,**46**,3047
- 118 PJ Newcombe, RK Norris, *Aust. J. Chem.* 1978,**31**,2463
- 119 JPL Cox, MR Crampton, P Wight, *J. Chem. Soc. Perkin Trans. II*, 1988,25
- 120 MR Crampton, TP Kee, JR Wilcock, *Can. J. Chem.*, 1986,**64**,1714
- 121 A Hantzsch, N Picton, *Ber.*, 1909,**42**,2119
- 122 SS Gitis, IM Gershkovich, Yu D Grudtsyn, A Ya Kaminsky, *Zh. Org. Khim.*, 1975,**11**,1566
- 123 SM Shein, AD Kmelinskaya, VV Brovko, *J. Chem. Soc. Chem. Commun.*, 1969,1043
- 124 PJ Atkins, V Gold, *J. Chem. Soc. Chem. Commun.*, 1983,140
- 125 SM Sheinn, AD Khmelinskaya, *Zh. Org. Khim.*, 1972,**8**,1237
- 126 SS Gitis, A Ya Kaminsky, Yu D Grudtsyn, EE Gol'teuzen, *Dokl. Akad. Nauk., SSSR*, 1972,**206**,102

- 127 EE Gol'teuzen, Yu D Grudtsyn, SS Gitis, A Ya Kaminsky, *Zh. Org. Khim.*, 1972,8,16
- 128 CF Bernasconi, *J. Org. Chem.*, 1971,36,1671
- 129 SS Gitis, A Ya Kaminsky, *Usp. Khim.*, 1978,47,1970
- 130 SM Shein, OG Byval'kevich, *Zh. Org. Khim.*, 1972,8,328
- 131 SM Shein, OG Byval'kevich, *ibid.*, 1976,12,134
- 132 E Buncel, A Jonczyk, JGK Webb, *Can. J. Chem.*, 1975,53,3761
- 133 E Buncel, RA Renfrow, MJ Strauss, *J. Org. Chem.*, 1987,52,488
- 134 CF Bernasconi, MC Muller, *J. Am. Chem. Soc.*, 1978,55,530
- 135 E Buncel, W Eggiman, *Can. J. Chem.*, 1976,54,2436
- 136 V Machacek, V Sterba, A Sterbova, *Collect. Czech. Chem. Commun.*, 1976, 41,2556
- 137 E Buncel, W Eggiman, *J. Am. Chem. Soc.*, 1977,99,5958; *J. Chem. Soc. Perkin Trans. II*, 1978,673
- 138 JC Hallé, F Terrier, MJ Pouet, MP Simonnin, *J. Chem. Res.*, 1980,(S) 360
- 139 JC Hallé, MJ Pouet, MP Simonnin, F Debleds, F Terrier, *Can. J. Chem.*, 1982,60,1988
- 140 F Terrier, F Debleds, JF Verchère, Abstracts of the "Third International Conference on the Mechanisms of Reactions in Solution", Canterbury, England, July 1982.
- 141 AJ Kresge, Y Chiang, *J. Chem. Soc. B*, 1967,53
- 142 BC Challis, EM Millar, *J. Chem. Soc. Perkin Trans. II*, 1972,1116; *ibid.*, 1618
- 143 RR Bard, MJ Strauss, *J. Org. Chem.*, 1976,41,2421
- 144 RR Bard, MJ Strauss, *J. Am. Chem. Soc.*, 1975,97,3789
- 145 MJ Strauss, F Terrier, *Tetrahedron Lett.*, 1979,313
- 146 DC Palmer, MJ Strauss, *Chem. Rev.*, 1977,77,1
- 147 JM Harris, SP McManus ed., "Nucleophilicity", American Chemical Society, Washington, 1987
- 148 JF Bunnett, *Annu. Rev. Phys. Chem.*, 1963,14,271
- 149 J Hine, RD Weimar, *J. Am. Chem. Soc.*, 1965,87,3387
- 150 CF Bernasconi, *Pure and Appl. Chem.*, 1982,54,12,2335

- 151 CF Bernasconi, *Acc. Chem. Res.*, 1987,20,301
- 152 CF Bernasconi, RB Killion, *J. Am. Chem. Soc.*,1988,110,7506
- 153 RA Marcus, *Annu. Rev. Phys. Chem.*, 1964,15,155
- 154 JO Edwards, *J. Am. Chem. Soc.*,1954,76,1540; *ibid.*,1956,78,1819
- 155 RG Pearson, *Surv. Prog. Chem.*, 1969,5,1
- 156 RG Pearson, J Songstad, *J. Am. Chem. Soc.*,1967,89,1827
- 157 BD England, D House, *J. Chem. Soc.*,1962,4421
- 158 BW Clare, D Cook, ECF Ko, YC Mac, AJ Parker, *J. Am. Chem. Soc.*,1966,88,1911
- 159 A Pross, *J. Org. Chem.*, 1984,49,1811
- 160 FG Bordwell, DL Hughes, *J. Am. Chem. Soc.*, 1985,107,4737; 1986,108, 7300
- 161 MR Crampton, MJ Willison, *J. Chem. Soc. Perkin Trans.II*, 1974,238
- 162 G Bartoli, Li di Nunno, L Forlani, PE Todesco, *Internat. J. Sulfur Chem.*, C, 1971,77
- 163 K Bowden, *Chem. Rev.*, 1966,66,119
- 164 CH Rochester "*Acidity Functions*", Academic Press 1970
- 165 R Stewart, JP O'Donnell, *Can. J. Chem.*, 1964,42,1681,1694
- 166 K Bowden, R Stewart, *Tetrahedron*, 1965,21,261
- 167 R Stewart, JP O'Donnell, DJ Cram, B Rickborn, *Tetrahedron*, 1962,18,917
- 168 DJ Kroeger, R Stewart, *Can. J. Chem.*, 1967,45,2163
- 169 MR Crampton, MA El Ghariani, HA Khan, *J. Chem. Soc. Perkin Trans.II*, 1972,1178

Chapter 2

Experimental

Materials

a) Solvents

Water: Distilled water was boiled to expel dissolved carbon dioxide. A soda-lime guard tube was subsequently used for protection from the atmosphere.

Dimethyl sulphoxide: DMSO was refluxed with calcium hydride and fractionated under reduced pressure, the middle fraction being collected.

Dioxan: Analytical grade solvent was used as supplied.

Methanol: Analytical grade, used without further purification.

Deuterated solvents: D₂O and [²H₆]-DMSO were commercial samples of isotopic purity > 99% in glass phials containing 1 cm³ of solvent and were used as supplied.

b) Base solutions and nucleophiles

Sodium hydroxide: Sodium hydroxide solutions were prepared by dissolving analytical grade sodium hydroxide pellets in distilled water. Concentrations were determined by titration with standardised HCl solution using phenolphthalein as the indicator.

Tetramethylammonium hydroxide: Analytical grade material (*ca.* 2.7M in water) was used as supplied.

Sodium methoxide: Solutions of sodium methoxide were prepared by dissolving clean sodium metal in AnalaR methanol under nitrogen. Cloudiness in the more concentrated solutions was removed on standing. Concentrations were determined by titration with standardised HCl using phenolphthalein as the indicator.

Thiols: Ethanethiol, glutathione, ethyl-2-mercaptoacetate, thioglycolic acid and mercaptosuccinic acid were all commercial materials of the highest available purity and were used as supplied.

Substituted phenylacetonitriles: With the exception of the 3-nitro and 4-cyano substituted compounds, the preparations of which are described in chapter 5, all the phenylacetonitriles were commercial specimens of the highest available purity and were used as supplied.

Phenylnitromethane: Details of the preparation are given in chapter 5.

Ethylcyanoacetate and dimethylmalonate were both commercially available AnalaR grade reagents.

c) Added salts

Sodium chloride, used to maintain ionic strength, was a dried AnalaR reagent. Stock solutions in water were 1 – 4M and in methanol 0.1M

d) Aromatic compounds

1,3,5-trinitrobenzene (m.pt. 121°C lit¹ 122.5°C) and 2,4,6-trinitrotoluene were recrystallised commercial specimens.

Picryl chloride was a dried commercial sample of the highest available purity and was used without purification.

2,4,6-trinitroanisole (m.pt. 80°C lit² 78.5°C) was a prepared sample available from previous work³

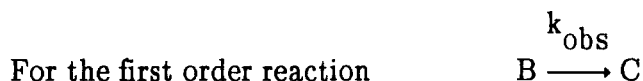
Ethylthiopicrate (m.pt. 45°C lit⁴ 45°C) was a prepared sample. Details of the preparation are given in chapter 4.

1-chloro-2,4-dinitrobenzene, 1-fluoro-2,4-dinitrobenzene and 2,4-dinitrophenol were the purest grade commercially available and were used as supplied.

Measurement techniques

a) UV/visible spectra

All UV/visible spectra were recorded using fresh solutions in 1 cm silica or quartz cells on either a Perkin Elmer Lambda 3 or a Philips PU8725 instrument at 25°C. The Perkin Elmer instrument was also used for the kinetic measurement of slow reactions ($t_{\frac{1}{2}} > ca. 1$ minute). All kinetic measurements were made under first order conditions and observed rate coefficients were determined by following the change in absorbance at an appropriate wavelength. Measured absorbance values were entered into a program running on an Apple][e microcomputer which calculated the observed rate constant based on the following derivation.



The rate of formation of C is given by
$$\frac{d[C]}{dt} = k_{obs}[B]$$

The reaction may be monitored by following an increase in absorbance (A) due to C. A_{∞} is the absorbance at the completion of the reaction and B, the concentration of which is proportional to $A_{\infty} - A$, is assumed not to absorb.

Thus,
$$\frac{dA}{dt} = k_{obs}(A_{\infty} - A)$$

$$\int_{A_0}^{A_t} \frac{dA}{A_{\infty} - A} = \int_0^t k_{obs} dt$$

$$\ln(A_{\infty} - A) \Big|_{A_0}^{A_t} = -k_{obs}t \Big|_0^t$$

$$\ln \left| \frac{A_{\infty} - A_t}{A_{\infty} - A_0} \right| = -k_{\text{obs}} t$$

Hence a plot of $\ln \left| A_{\infty} - A_t \right|$ vs t has gradient $-k_{\text{obs}}$. For very slow reactions or where A_{∞} was difficult to obtain accurately, the Guggenheim method was used. This involves plotting $\ln \left| A_{t+\tau} - A_t \right|$ against time where τ is some arbitrarily chosen constant time interval greater or equal to two half-lives. The gradient of the plot is equal to $-k_{\text{obs}}$.

b) Stopped flow spectrophotometry

This was the main technique employed for kinetic measurement in the present work. The instrument was a Hi-Tech SF-3L apparatus. Figure 2.1 shows a schematic representation of the apparatus. The two solutions A and B which undergo reaction are stored in glass reservoirs and from there they enter identical syringes. A single piston drives both syringes so that equal volumes of each solution are mixed at point M (halving the concentration of each solution) before passing into a thermostatted 2mm quartz cell at point O. Spent reactant solution is forced out into a stopping syringe, the plunger of which comes up abruptly against a block, thus stopping the flow. At the same time the oscilloscope time-base is triggered by a microswitch causing monitoring of the reaction at O to begin. This is done by passing a beam of monochromatic light of the appropriate wavelength through the cell. The reaction within the cell causes an increase or decrease in the transmitted light which is fed through a photomultiplier and displayed on an oscilloscope screen from where voltage changes can be read off. Changes in voltage are related to absorbance values via equation 2.2 where ΔV is the voltage change and V_0 is the applied voltage. For kinetic measurements,

$$A = \log_{10} \frac{I_0}{I} = \log_{10} \left| \frac{V_0}{V_0 - \Delta V} \right| \quad 2.2$$

scale readings were not converted into absorbance values but were used as a direct measure of concentration. This is valid for small ratios of $\Delta V/V_0$ where, to a good approximation, quadratic and higher terms may be neglected in the power series.

$$A = \log_{10} \left| \frac{V_0}{V_0 - \Delta V} \right| = \frac{1}{2.303} \left[\left[\frac{\Delta V}{V_0} \right] + \frac{1}{2} \left[\frac{\Delta V}{V_0} \right]^2 + \frac{1}{3} \left[\frac{\Delta V}{V_0} \right]^3 + \dots \right]$$

In practice V_0 was 6 – 8 volts, ΔV being kept smaller than 1 volt.

The stopped flow apparatus was connected for operation with an Apple IIe microcomputer which allowed for automatic data collection and Hi-Tech software were usually used for evaluation of rate coefficients.

The instrument was also used to determine absorbance values and spectral shapes of species present after short reaction times.

All stopped flow measurements were made at 25°C.

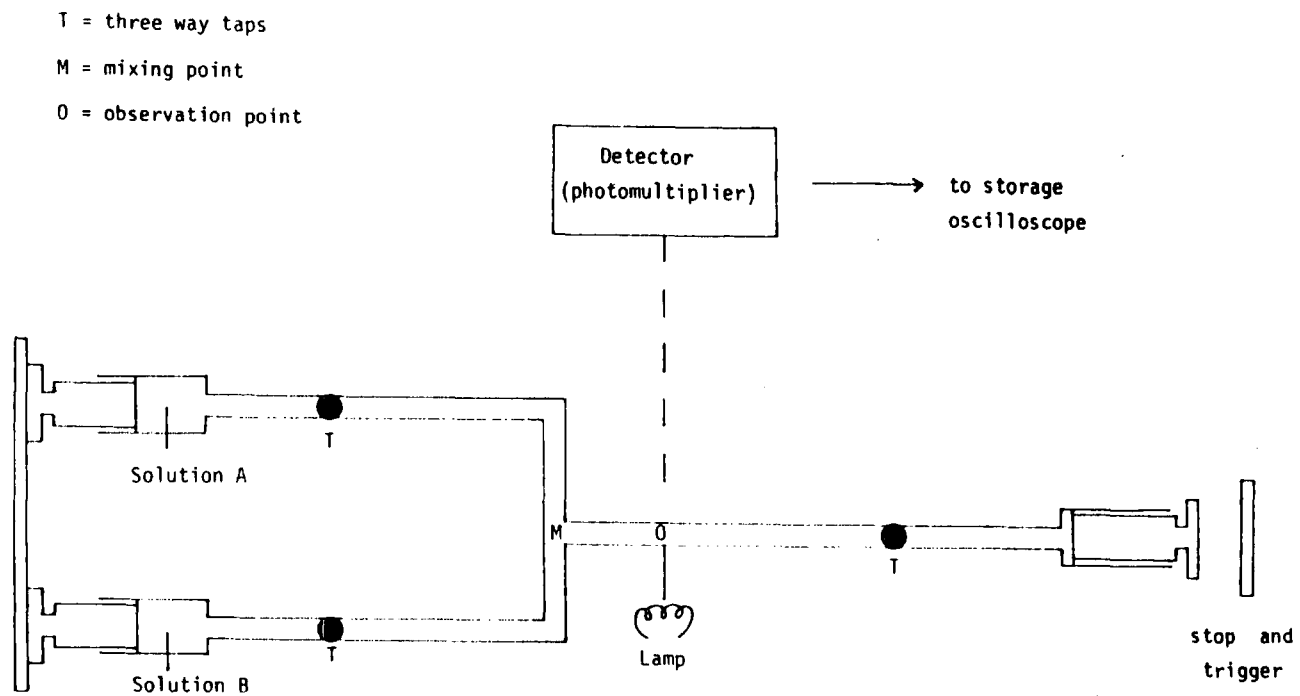
c) Stopped flow scanning spectrophotometry

Spectra of short-lived species were sometimes recorded by stopped flow scanning spectrophotometry. The instrument consisted of a Hi-Tech Spectrascan CU MG3000 unit mounted on a Hi-Tech SF-3L apparatus. Triggering of the microswitch caused a rapid scanning (up to 10 scans per second) from 200 – 600nm or from 350 – 850nm. Hi-Tech software were used for collection of data.

d) Temperature-jump spectrophotometry

Temperature-jump is one of the most important relaxation techniques for the measurement of rapid reactions. ($t_{\frac{1}{2}} < 10^{-2}$ s). A sudden change in temperature causes a change in the equilibrium position of the reaction mixture and the reaction is monitored as it relaxes into the new equilibrium position associated

Figure 2.1 Schematic representation of stopped-flow
UV/visible spectrophotometer



with the higher temperature. Most chemical equilibria are associated with a finite standard enthalpy of reaction (ΔH) and are thus temperature dependent according to the van't Hoff expression 2.3

$$\left[\frac{\partial \ln K}{\partial T} \right]_p = \frac{\Delta H}{RT^2} \quad 2.3$$

In this work temperature-jump measurements were made with an instrument supplied by Hartley measurements Ltd. consisting of a delay line energy storage system with a square heating pulse. A temperature-jump of 5°C was obtained by discharging 20kV from a capacitor of total discharge capacitance 0.05 μ F into the reaction cell (volume 0.5cm³) containing the conducting reaction mixture. NaCl was used as the electrolyte and the mixture was previously thermostatted to 20°C. Synchronous with the discharge, the oscilloscope was triggered for the observation of the relaxation effect. Monitoring was by spectrophotometric means, a monochromatic beam of light of suitable wavelength being passed through the reaction cell. Reported rate coefficients are the average of 5 to 10 determinations.

e) ¹H nmr spectroscopy

¹H nmr spectra were recorded on a Bruker AC 250 (250MHz) instrument though a Hitachi/Perkin Elmer R-24B (60MHz) instrument was sometimes used for initial investigations. All measurements are quoted as " δ " values relative to internal tetramethylsilane.

References

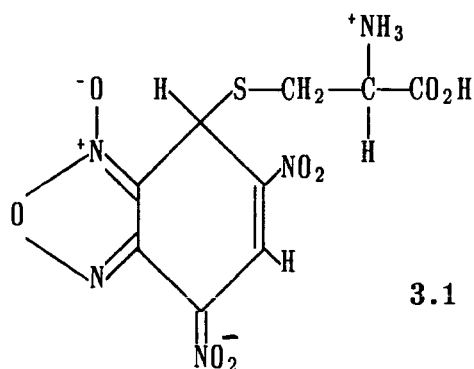
- 1 "*Dictionary of Organic Compounds*", Fourth edition, Eyre and Spottiswoode, 1964
- 2 A Hantzsch, H Gorke, *Ber.*, 1906,**39**,1097
- 3 MR Crampton, *J. Chem. Soc. Perkin Trans. II*, 1977,1442
- 4 CC Culvenor, W Davies, WE Savige, *J. Chem. Soc.*, 1952,4480
- 5 CF Bernasconi, "*Relaxation Kinetics*", Academic Press, New York, 1976

Chapter 3

Kinetic and Equilibrium Studies of the reactions of some thiolate ions with trinitro-aromatic compounds: Intrinsic reactivities

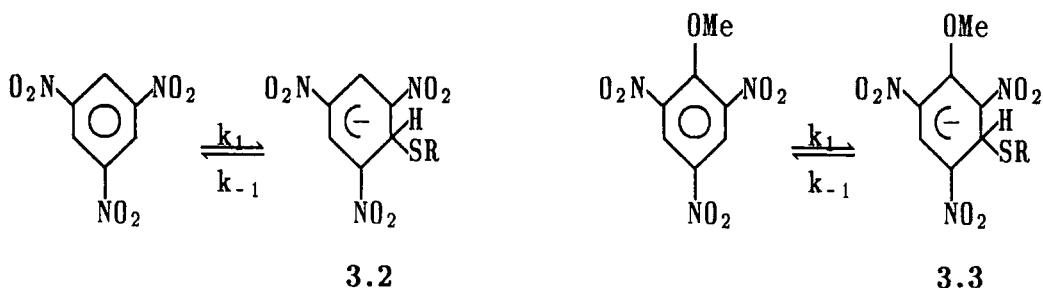
Introduction

Nitrobenzofuroxans have been observed as powerful inhibitors of nucleic acid biosynthesis with an especially toxic effect on leukocyte metabolism *in vitro*.^{1,2} This activity is thought to result from a primary interaction of such heterocycles with the intracellular thiol functionality producing, initially, the corresponding Meisenheimer adducts.^{1,2} In support of this proposal it has been noted that the cysteine complex of 4,6-dinitrobenzofuroxan 3.1 is completely formed in water at physiological pH.³ Similarly, 1,3,5-trinitrobenzene (TNB) has been shown to



inhibit the action of glutathione-S-transferase.⁴ The excretion of halogenated aromatic nitrocompounds is likely to involve reaction with glutathione in mammalian liver⁵ and the reactions of nitroaromatics with biologically active compounds are of interest as a means for the chemical modification of proteins.⁶ The initial step in these reactions is also thought to be σ -adduct formation by thiolate attack at an aromatic ring.^{7,8}

Values of equilibrium constants have been reported^{3,5,9-12} for the formation of σ -adducts by reaction of glutathione, ethanethiolate anions and substituted thiophenoxide ions at unsubstituted positions of 1,3,5-trinitrobenzene. However, kinetic data for such reactions are limited to one stopped-flow spectrophotometric study⁵ which will be discussed later, and an nmr study.⁹ The ¹H nmr spectra⁹ of sodium ethanethiolate with TNB in [²H₆]-DMSO/MeOH show line broadening in both the adduct 3.2 (RS = SEt) and TNB. This behaviour corresponds to a slow



(on an nmr time scale) interconversion of the adduct 3.2 (RS = SEt) and TNB⁹

Measurement of the line widths allowed the determination of the lifetimes τ and thus values of k_{-1} ($= \frac{1}{\tau}$). Values of k_{-1} , which were found to increase as the proportion of methanol in the solvent was increased, give a value (obtained by extrapolation of $\log k_1$ vs mol% DMSO) for $k_{-1} > 10^2 \text{ s}^{-1}$ in methanol. K_1 has the value⁹ of $3.5 \times 10^3 \text{ l mol}^{-1}$ in this medium. Similar behaviour was observed for thiophenoxide and TNB⁹. As the rate of interconversion was found to be much faster, spectra gave a combined resonance for the protons in TNB and in the adduct 3.2 (RS = C₆H₅S). In 85/15 [²H₆]-DMSO/MeOH (v/v) and at 31°C τ was found to be less than 10^{-3} s^{-1} giving $k_{-1} > 10^3 \text{ s}^{-1}$. The value of k_{-1} is expected to increase as the solvent becomes more methanol rich. Since the equilibrium constant K_1 for the formation of 3.2 (RS = C₆H₅S) has the value⁹ 1.95 l mol^{-1} , one may expect a relatively large intrinsic rate constant for the addition of thiophenoxide ions to trinitroactivated aromatics. A value of $k_{-1} = 1.7 \times 10^3 \text{ s}^{-1}$ has been determined¹³ for the formation of 3.3 (RS = C₆H₅S) by a similar method in a solvent of 25/75 [²H₆]-DMSO/MeOH (v/v) at -35°C.

This study reports kinetic and equilibrium data for the reactions of 1,3,5-trinitrobenzene and 2,4,6-trinitrotoluene with thiolate anions derived from thioglycolic acid (mercaptoacetic acid), thiomalic acid (mercaptosuccinic acid), glutathione and ethyl-2-mercaptoacetate. The results are used to determine intrinsic reactivities for the thiolate ions in adduct-forming reactions at the trinitro-activated aromatic ring.

Experimental

Kinetic measurements, made by both stopped flow and temperature jump spectrophotometry, were made under first order conditions with the concentration of the thiolate anion in large excess of the concentration of the nitrocompound.

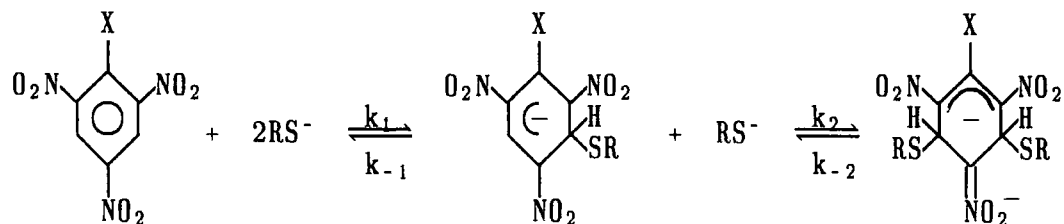
Thiolate anions were generated by ionisation of the parent thiol with sodium hydroxide, sufficient base being to ionise the carboxylic acid functions as well as the thiol group. Checks were occasionally made to determine whether complete ionisation of the thiol had taken place by varying the excess concentration of base. Typically, an excess concentration of $5 \times 10^{-3} \text{M}$ of hydroxide was used. For stopped-flow work one syringe contained a solution of the nitrocompound and the other contained a solution of the thiolate anion. However, for the reactions with glutathione one syringe contained the nitrocompound and glutathione and the other the sodium hydroxide solution. Solutions of thiolate ions are prone to oxidation and were used as quickly as possible. The stopped-flow spectrophotometer was also used to determine the spectral shapes of species after short reaction times. This involved measuring absorbances at individual wavelengths and building up spectra point by point. Reported rate constants are the average of at least five kinetic determinations. For temperature jump work, T-jumps of 5°C were obtained in a cell with a heated volume of 0.5 cm^3 . This was thermostatted to 20°C so that rate measurements refer to 25°C . Solutions of the aromatic nitrocompound and thiolate ion were used as rapidly as possible and were often freshly replaced. Again, reported rate constants are the average of at least five kinetic determinations.

Stock solutions of the nitrocompounds were prepared in dioxan. Measurements were made in a solvent consisting of 90/10 (v/v) water/dioxan or (in the case of glutathione) 99/1 (v/v) water/dioxan and the ionic strength was maintained to 0.25M with sodium chloride.

Results and Discussion

Kinetic and equilibrium measurements were made for the reactions of thiolate ions with TNB and with 2,4,6-trinitrotoluene (TNT). The thiolate anions were generated from the parent thiols by reaction with sodium hydroxide, sufficient base being added to ionise the carboxylic acid functions as well as the thiol group. A slight excess (usually $5 \times 10^{-3} \text{M}$) of base was used to ensure the complete ionisation of the thiols. These have pK_a s which vary from 7.9^{12} (ethyl-2-mercaptoacetate) to 11.1^{14} (thiomalate). The equilibrium constant for direct reaction of hydroxide ions with TNB has the value $1.6 \times 10^7 \text{ l mol}^{-1}$ so that negligible interference from this reaction was observed. Likewise in the reaction with TNT no evidence was found for the production of trinitrobenzyl anions ($\lambda_{\text{max}}^{18}$ in MeOH 370, 514, 620 nm) by abstraction of a side chain proton. The results indicate the formation of 1:1 and 1:2 adducts as shown in scheme 3.4 (next page). Slower irreversible reactions were also observed but not identified. All measurements were made with $[\text{RS}^-] \gg [\text{TNB}], [\text{TNT}]$ and it was found that formation of the 1:1 adducts was considerably faster than formation of the 1:2 adduct. The relevant rate expressions (derived in the appendix) for the fast and slow processes are 3.5 and 3.6

Scheme 3.4



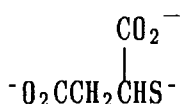
RS⁻

X = H, Me

thioglycolate



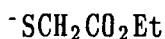
thiomalate



glutathione



ethyl 2-mercaptoacetate



$$k_{\text{fast}} = k_1 [\text{RS}^{-}] + k_{-1} \quad 3.5$$

$$k_{\text{slow}} = k_{-2} + \frac{k_2 K_1 [\text{RS}^{-}]^2}{1 + K_1 [\text{RS}^{-}]} \quad 3.6$$

Reactions with TNB

Visible spectra of TNB in the presence of low concentrations of thiolate ions show bands at 470 nm and 550 nm (shoulder). Previous measurements on related systems⁷⁻¹⁰ have shown these bands to be attributable to 1:1 adducts. With increasing concentration of thiolate a band at 500 nm, attributed to the formation of 1:2 adducts, grows at the expense of the bands. The 1:2 adducts have extinction

coefficients between $1.5 \times 10^4 \text{ l mol}^{-1} \text{ cm}^{-1}$ and $1.6 \times 10^4 \text{ l mol}^{-1} \text{ cm}^{-1}$ at λ_{max} . In the case of thioglycolate ions some decrease in the intensity of the spectrum due to the 1:2 adduct was observed at large concentrations ($[\text{SCH}_2\text{CO}_2^-] > 0.4\text{M}$) of nucleophile presumably owing to the formation of an adduct of 1:3 stoichiometry.

Formation of the 1:1 adducts was in all cases too fast for measurement by stopped-flow spectrophotometry, reaction being complete within the mixing time of the apparatus. However, temperature jump measurements could be used to monitor this process. In every case the oscilloscope traces showed that the temperature jump (a rise in temperature of 5°C) produced a decrease in absorbance implying that the formation of 1:1 adducts is an exothermic process. Similar decreases in absorbance were also noted in the temperature jump experiments with TNT.

a) Thioglycolate ions

Kinetic data for reaction with thioglycolate ions are in table 3.7. A linear plot of k_{fast} according to equation 3.5 gave values $k_1 = 1.4 \times 10^6 \text{ l mol}^{-1} \text{ s}^{-1}$ and $k_{-1} = 5500 \text{ s}^{-1}$ leading to a value of $K_1 (= k_1/k_{-1})$ of 250 l mol^{-1} . The best fit of the data for k_{slow} to expression 3.6 gave values $k_2 = 3300 \text{ l mol}^{-1} \text{ s}^{-1}$, $k_{-2} = 8 \text{ s}^{-1}$ and $K_1 = 220 \text{ l mol}^{-1}$. Values for K_1 and K_2 were independently determined by using absorbances measured by stopped-flow spectrophotometry at completion of the fast and slow reactions respectively. The data (table 3.8) lead to values $K_1 = 240 \text{ l mol}^{-1}$ and $K_2 = 500 \text{ l mol}^{-1}$ in reasonable agreement with those from obtained from kinetics. In order to calculate K_2 , use was made of the fact that the 1:2 adduct shows negligible absorbance at 600 nm.

b) Thiomalate ions

Kinetic data for reaction of TNB with thiomalate ions (table 3.9) lead to values $k_1 = 1.2 \times 10^6 \text{ l mol}^{-1} \text{ s}^{-1}$, $k_{-1} = 3 \times 10^4 \text{ s}^{-1}$, $k_2 = 250 \text{ l mol}^{-1} \text{ s}^{-1}$ and $k_{-2} = 33 \text{ s}^{-1}$.

Combination of rate coefficients yields values $K_1 = 40 \text{ l mol}^{-1}$ and $K_2 = 8 \text{ l mol}^{-1}$. The plot of data for k_{fast} is shown in figure 3.9. Absorbance values (table 3.10) lead to $K_1 = 33 \text{ l mol}^{-1}$ and $K_2 = 9 \text{ l mol}^{-1}$.

c) Glutathione ions

In the two previous studies of the reaction with TNB with glutathione in water it was assumed that only a 1:1 interaction was involved and equilibrium constants of 28 l mol^{-1} ⁵ and 42 l mol^{-1} ⁴ were reported. However visible spectra show that even at very low concentrations of glutathione both 1:1 and 1:2 adducts are present. Absorbance values (table 3.11) lead to values of $K_1 = 15 \pm 5 \text{ l mol}^{-1}$ and $K_2 = 300 \pm 100 \text{ l mol}^{-1}$. Data for the formation of the 1:2 adduct (table 3.12) are fit well by expression 3.6 with $k_2 = 17000 \text{ l mol}^{-1} \text{ s}^{-1}$, $k_{-2} = 53 \text{ s}^{-1}$ and $K_1 = 15 \text{ l mol}^{-1}$. Combination of rate coefficients gives $K_2 = 320 \text{ l mol}^{-1}$. These measurements refer to $I = 0.25\text{M}$. Gan⁵ has previously reported rate measurements in the range $100\text{-}130 \text{ s}^{-1}$ at lower (uncontrolled) ionic strength for the formation of what he believed to be a 1:1 adduct. Allowing for differences in ionic strength which will be important in the reactions of multicharged species (Gan noted that the addition of sodium chloride had great influence on the stability of the product) these rate constants are similar to those observed in this study for the formation of a 1:2 adduct.

Measurement of the rate of equilibration of the 1:1 adduct and TNB required T-jump spectrophotometry and values of k_{fast} at concentrations of glutathione anion of 0.010M ($(1.3 \pm 0.2) \times 10^5 \text{ s}^{-1}$) and 0.012M ($(1.5 \pm 0.2) \times 10^5 \text{ s}^{-1}$) were obtained. Using the known value of $K_1 = 15 \text{ l mol}^{-1}$ these rate constants lead to $k_1 = (1.8 \pm 0.6) \times 10^6 \text{ l mol}^{-1} \text{ s}^{-1}$ and $k_{-1} = (1.2 \pm 0.2) \times 10^5 \text{ s}^{-1}$. The precision is relatively low because of the small conversion of TNB to its adduct in these solutions.

d) ethyl-2-mercaptoacetate

The formation of both 1:1 and 1:2 adduct was too fast for measurement on a stopped-flow timescale. In 10/90 (v/v) dioxan/water and $I = 0.1M$, absorbance measurements (table 3.13) determined by conventional spectrophotometry allow the calculation of values of $K_1 = 17 \text{ l mol}^{-1}$ and $K_2 = 25 \text{ l mol}^{-1}$. In methanol the 1:1 adduct has a λ_{max} at 460 nm ($\epsilon = 2.2 \times 10^4 \text{ l mol cm}^{-1}$) and 540 nm (shoulder). At larger concentrations of thiolate a peak at 516 nm was attributed to the 1:2 adduct. Absorbance data (table 3.14) show that the main interaction is to give a 1:1 adduct, the ratio of $\text{Abs}(460\text{nm}) : \text{Abs}(500\text{nm})$ remaining constant up to $[\text{SCH}_2\text{CO}_2\text{Et}] = 0.01M$. Results are limited to a value $K_1 = 45 \pm 5 \text{ l mol}^{-1}$, K_2 being small.

The value of K_1 is larger in methanol than in water. Formation of a 1:1 adduct involves a dispersal of charge and is thus expected to be better solvated in methanol than in water!⁰ On the other hand, solvation of the 1:2 adduct, in which there is a localised negative charge on the nitrogroup, will be stronger in water!⁰ (a more polar solvent relative to methanol) leading to larger values of K_2 in this medium.

**Table 3.7 Kinetic data for the reaction of TNB with thioglycolate ions
in 90/10 water/dioxan**

10^3 [$\text{SCH}_2\text{CO}_2^-$] M	$10^{-3}k_{\text{fast}}$ s ⁻¹	k_{slow} s ⁻¹	k_{calc} s ⁻¹	
1.0	6.9	8	8	<p style="text-align: center;">$I = 0.25M$</p> <p>a measured by temperature jump spectrophotometry at 470 nm. b measured by stopped-flow spectrophotometry at 500nm as a colour-forming reaction c calculated from eqn.3.6 using $k_2=3300 \text{ l mol}^{-1}\text{s}^{-1}$, $k_{-2}=8 \text{ s}^{-1}$ and $K_1=220 \text{ l mol}^{-1}$</p>
2.0	8.1	110	10	
3.0	9.7	—		
4.0	11.0	16	14	
6.0		22	19	
8.0		26	25	
10.0		31	31	
12.0		37	36	

Table 3.8 Visible Absorbances and calculated equilibrium constants for the reaction of TNB with thioglycolate ions at 25°C with I = 0.25M

$10^3 [-SCH_2CO_2^-]$ M	a, b A_{450nm}^{init}	c K_1 $l\text{mol}^{-1}$	b A_{450nm}^{final}	b A_{600nm}^{final}	d $10^5 [1:1]$ M	e $10^5 [1:2]$ M	f $10^5 [TNB]$ M	K_1 $l\text{mol}^{-1}$	K_2 $l\text{mol}^{-1}$
0.5	0.19	250	0.19	0.062	1.13	0	8.87	250	
2.5	0.56	200	0.72	0.134	2.44	2.58	4.98	200	420
5.0	0.94	250	1.06	0.124	2.25	5.67	2.08	220	500
7.5	1.18	300	1.16	0.096	1.75	7.22	1.03	230	550
10.0	1.24	270	1.18	0.066	1.20	8.15	0.65	180	680
15.0	1.30	220	1.18	0.058	1.05	8.35	0.60		530
20.0	1.40	230	1.20	0.028	0.51	9.29	0.20		
40.0			1.17						

a measured by stopped-flow spectrophotometry at completion of the reaction forming the 1:1 adduct. b normalised to $1 \times 10^{-4} \text{M}$ TNB and a pathlength of 1cm. c A Benesi-Hildebrand plot of $A_{450nm}^{initial}$ gives a value for $\epsilon_{1:1}$ of $1.7 \times 10^4 \text{ l mol}^{-1} \text{ cm}^{-1}$. K_1 calculated as $A_{450nm}^{initial} / [1.7 - A_{450nm}^{initial}] [-SCH_2CO_2^-]$

d At $5 \times 10^{-4} \text{M} [-SCH_2CO_2^-]$ where there is no 1:2 adduct present the ratio of absorbances at 450nm and 600nm is 3.06. This leads to a value for $\epsilon_{1:1}$ of $5.5 \times 10^3 \text{ l mol}^{-1} \text{ cm}^{-1}$ at 600nm. Hence $[1:1] = A_{600nm}^{final} / 5.5 \times 10^3$

e From the most concentrated solutions $\epsilon_{1:2} = 1.2 \times 10^4 \text{ l mol}^{-1} \text{ cm}^{-1}$ at 450nm. $[1:2] = [A_{450nm}^{final} - 3.06 A_{600nm}^{final}] / 1.2 \times 10^4$

f $[TNB] = 1 \times 10^{-4} - [1:1] - [1:2]$

Table 3.9
Kinetic data for the reaction of TNB with thiomalate ions in
10/90 dioxan/H₂O (v/v) at 25^oC with I = 0.25M

10^3 [thio- malate] M	^a 10^{-4} k_{fast} s^{-1}	^b k_{slow} s^{-1}	^c k_{calc} s^{-1}
3.0	3.4		
8.0		34	33
9.0	4.1		
12		34	34
15	4.9		
20	5.2	35	35
30	6.7		
36	7.4		
40*		39	39
60*		43	43
80*		48	48

* I > 0.25M

- a measured by T-jump spectrophotometry at 470 nm
- b measured by stopped-flow spectrophotometry at 500 nm
- c calculated from expression 3.6 with $k_2 = 250 \text{ l mol}^{-1} \text{ s}^{-1}$, $k_{-2} = 33 \text{ s}^{-1}$ and $K_1 = 33 \text{ l mol}^{-1}$.

Fig 3.9

Reaction of thiomalate ions with TNB in 90/10 (v/v) dioxan/H₂O. Plot of kinetic data for 1:1 adduct formation.

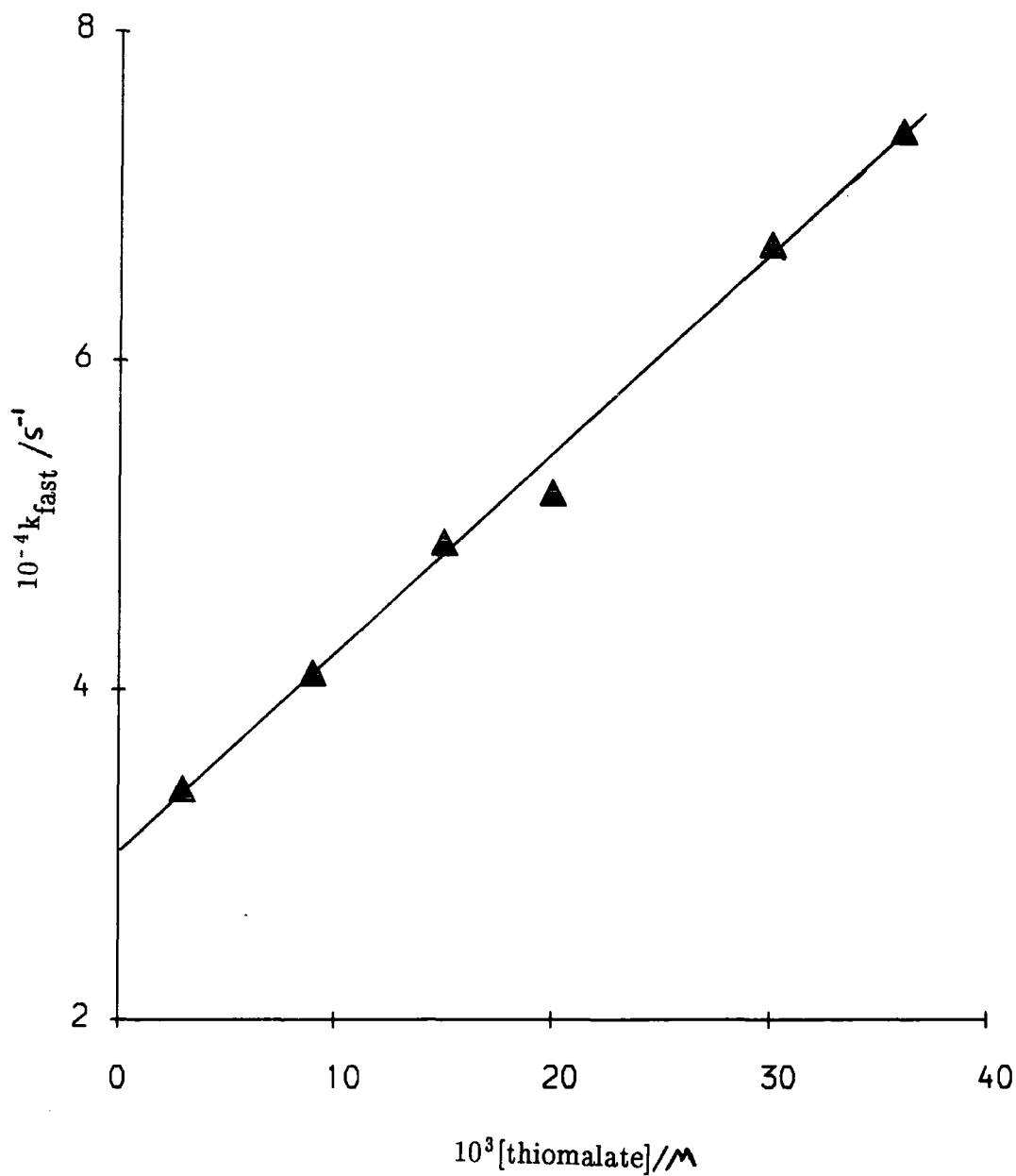


Table 3.10 Visible absorbances and calculated equilibrium constants for the reaction of TNB^a with thiomalate ions at 25°C

10 ² [thiomalate] M	A _{470nm} ^b init	K ₁ ^c l mol ⁻¹	A _{600nm} ^{b,d} init	A _{600nm} ^e final	A _{470nm} ^e final	equilibrium concentrations			K ₁ l mol ⁻¹	K ₂ l mol ⁻¹
						10 ⁵ [1:1] ^f M	10 ⁵ [1:2] ^f M	10 ⁵ [TNB] M		
1.2	0.50	30	0.14	0.14	0.52	2.64	0.14	7.22	30	—
1.6	0.70	36	0.20	0.18	0.72	3.40	0.57	6.03	35	10
4.0	1.12	36	0.30	0.24	1.14	4.53	2.15	3.32	34	12
6.0 [*]	1.26	33	0.36	0.26	1.26	4.91	2.52	2.57	32	9
8.0 [*]	1.40	35	0.40	0.28	1.40	5.28	3.02	1.67	39	7

* I > 0.25M

a Concentration is 1x10⁻⁴M

b Measured by stopped-flow spectrophotometry at completion of the reaction forming 1:1 adduct. Normalised to a pathlength of 1cm.

c Calculated as $A_{470nm}^{initial} / (1.9 - A_{470nm}^{initial})$ [thiomalate]

The extinction coefficient of 1.9x10⁴ l mol⁻¹cm⁻¹ for $\epsilon_{1:1}$ at 470nm was determined by a Benesi-Hildebrand plot.

d A Benesi-Hildebrand plot gave $\epsilon_{1:1} = 5.3 \times 10^3$ l mol⁻¹cm⁻¹ at 600nm.

e At completion of reactions forming 1:1 and 1:2 adducts normalised to a pathlength of 1cm.

f calculated as $A_{600nm}^{final} / 5.3 \times 10^3$

g calculated as $(A_{470nm}^{final} - 3.6 A_{600nm}^{final}) / 1.3 \times 10^4$

Visible spectra gave $\epsilon_{1:2} = 1.3 \times 10^4$ l mol⁻¹cm⁻¹ at 470nm.

h [TNB] = 1x10⁻⁴ - [1:1] - [1:2]

Table 3.11 Visible absorbances and calculated equilibrium constants for the reaction of TNB^a with glutathione anion in 99/1 (v/v) water/dioxan at 25°C with I = 0.25M

10 ³ [glutathione] M	b,c A _{500nm} ^{init}	d K ₁ l mol ⁻¹	b,e A _{500nm} ^{final}	b,e A _{600nm} ^{final}	equilibrium concentrations			K ₁ l mol ⁻¹	K ₂ l mol ⁻¹
					f 10 ⁵ [1:1] M	g 10 ⁵ [1:2] M	h 10 ⁵ [TNB] M		
2 [*]	—	—	†0.060	†0.014	0.28	0.12	9.60	15	
4	0.07	12	0.126	0.022	0.44	0.39	9.17	12	220
8	0.15	14	0.380	0.028	0.56	1.91	7.53	9	430
10	0.21	16	0.56	0.052	1.04	2.61	6.35	16	250
	0.21†								
12	0.25	17	0.64	0.044	0.88	3.28	5.84	13	310
15	0.32	15	0.78	0.050	1.00	4.06	4.94	13	270
20	—		1.08	0.040	0.80	6.19	3.01	13	390
50 [*]	—		1.54	0.027	0.54	9.41	0.05	—	350

* data at lower ionic strength

** I > 0.3M

† with [NaOH]_{excess} = 0.1M

a concentration is 1x10⁻⁴M. b normalised to a pathlength of 1cm. c measured at the completion of the rapid process forming 1:1 adduct

d calculated as $A_{500nm}^{initial} / [1.5 - A_{500nm}^{initial}]$ [glutathione] Assumes $\epsilon_{1:1} = 1.5 \times 10^4$ l mol⁻¹ cm⁻¹ at 500nm.

e absorbances measured at completion of both adduct forming processes.

f calculated as $A_{600nm}^{initial} / 5 \times 10^3$ Assumes $\epsilon_{1:1} = 5 \times 10^3$ l mol⁻¹ cm⁻¹ at 600nm similar to values of ϵ found for the TNB-thioglycolate and TNB-thiomalate adducts

g calculated as $[A_{500nm}^{final} - 3.0A_{600nm}^{final}] / 1.55 \times 10^4$ $\epsilon_{1:2}$ is likely to be ca 1.55x10⁴ l mol⁻¹ cm⁻¹ at 500nm

h [TNB] = 1x10⁻⁴ - [1:1] - [1:2]

Table 3.12 Kinetic data for the reaction of TNB with glutathione anion in 99/1 (v/v) water/dioxan at 25°C with I = 0.25M

10^3 [gluta- thione] M	10^{-5} k_{fast} s^{-1}	k_{slow} s^{-1}	k_{calc} s^{-1}
2		54	54
4		58	57
6		62	61
8		69	68
10	1.3± 2	74	75
12	1.5±0.2	83	84
14		93	94
16		106	106
20		134	132

- a measured by T-jump spectrophotometry at 470 nm
 b measured by stopped-flow spectrophotometry at 500 nm
 c calculated from expression 3.6 with $k_2 = 17000 \text{ l mol}^{-1} \text{ s}^{-1}$, $k_{-2} = 53 \text{ s}^{-1}$ and $K_1 = 15 \text{ l mol}^{-1}$.

Table 3.13 Equilibrium data for the reaction of ethyl-2-mercaptoacetate with TNB^a in methanol. Data at uncontrolled ionic strength

10^2 [-SCH ₂ CO ₂ Et] M	A_{460}	A_{516}	K_1 l mol^{-1}	$\frac{A_{460}}{A_{516}}$
0.1	.077	.037	36	2.1
0.2	0.16	0.07	39	2.3
0.4	0.34	0.14	46	2.4
0.6	0.48	0.20	47	2.4
1.0	0.73	0.32	50	2.3
2.0	1.07	0.55	47	1.9
3.0	1.28	0.73	46	1.8
4.0	1.42	0.86		1.6

a concentration is $1 \times 10^{-4} \text{ M}$

b normalised to a pathlength of 1 cm.

c calculated as

$$A_{460} / (2.2 - A_{460}) [-\text{SCH}_2\text{CO}_2\text{Et}]$$

The extinction coefficient

$$\text{of } \epsilon_{1:1} = 2.2 \times 10^4 \text{ l mol cm}^{-1}$$

was determined by a Benesi-Hildebrand plot.

Table 3.14
Equilibrium data for the reaction of ethyl 2-mercaptoacetate and TNB^a
in 10/90 dioxan/H₂O with I = 0.1M (NaCl)

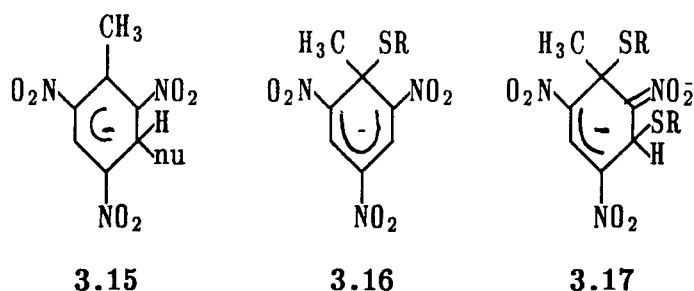
[⁻ SCH ₂ CO ₂ Et] M	b			c		d	
	A ₆₀₀	A ₅₀₀	A ₄₅₀	K ₁ l mol ⁻¹	K ₂ l mol ⁻¹	A ₅₀₀ ^{calc}	A ₄₅₀ ^{calc}
0.005	0.05	0.09	0.13	16	—	0.11	0.15
0.01	0.07	0.19	0.25	15	—	0.23	0.29
0.02	0.13	0.48	0.53	17	25	0.47	0.52
0.03	0.14	0.73	0.72	18	28	0.69	0.69
0.04	0.15	0.85	0.72	12	—	0.86	0.81
0.06	0.19	1.14	1.00	21	22	1.12	0.95
0.08	0.16	1.41	1.10		27		
0.10	0.18	1.49	1.16				
0.6	small	1.80	1.00				

- a** concentration is 1×10^{-4} M
- b** normalised to $l = 1$ cm. Absorbances determined by conventional spectrophotometry.
- c** calculated from the data at 450nm and 500nm using the extinction coefficients at 450nm $\epsilon_{1:1} = 1.8 \times 10^4$ l mol⁻¹ cm⁻¹ and $\epsilon_{1:2} = 1.0 \times 10^4$ l mol⁻¹ cm⁻¹ and at 500nm $\epsilon_{1:1} = 1.2 \times 10^4$ l mol⁻¹ cm⁻¹ and $\epsilon_{1:2} = 1.8 \times 10^4$ l mol⁻¹ cm⁻¹.
- d** calculated using the above extinction coefficients and $K_1 = 17$ l mol⁻¹, $K_2 = 25$ l mol⁻¹.

Reactions with TNT

The UV/visible spectra obtained with TNT and thiolate anions were qualitatively similar to those produced by corresponding reactions with TNB. At sufficiently low thiolate concentrations species with λ_{\max} 460nm and 550nm (shoulder), characteristic of 1:1 adducts were produced while at higher concentrations of thiolate ions 1:2 adducts with λ_{\max} 430nm ($\epsilon = 9 \times 10^3$ l mol cm⁻¹) were formed. Because of the low values of K_1 relative to K_2 spectra of the 1:1 adducts were conveniently determined by stopped-flow spectrophotometry by measuring absorbances at completion of the fast process at various wavelengths. Such a spectrum is shown in figure 3.18 for the reaction with thioglycolate. The initial spectrum (A) corresponds to the formation of a 1:1 adduct while the spectrum obtained at the completion of the slow reaction (B) corresponds to a mixture of 1:1 and 1:2 adducts.

In the case of TNT, addition of thiolate is possible at unsubstituted positions or at the -CH₃ substituted position of the aromatic ring. However, ¹H nmr has



been used to show that the addition of both cyanide²³ and sulphite¹⁹ to TNT occurs exclusively at an unsubstituted position to give adducts of structure 3.15. The 1:1 adducts formed by attack of hydride, acetate and dialkyl hydrogen phosphite ions also involve reaction at an unsubstituted position of TNT. Similarly the 1:2 adduct with sulphite¹⁹ has been shown (¹H nmr) to contain sulphite at two unsubstituted positions. Thus the adducts 3.16 and 3.17 may be discounted in favour of those shown in scheme 3.4 (X = CH₃).

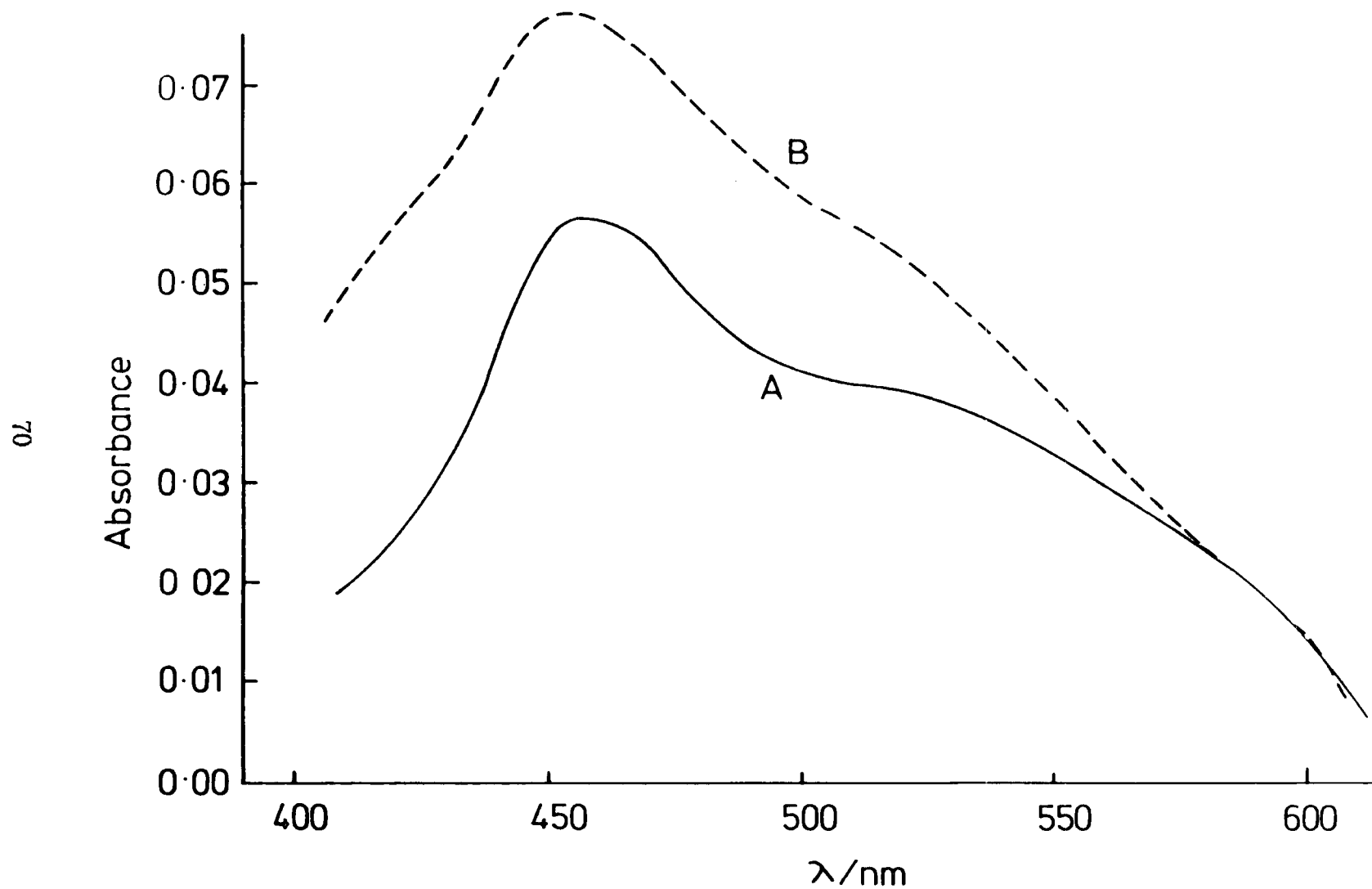


Figure 3.18 Visible spectra of TNT ($6 \times 10^{-4} \text{M}$) and mercaptoacetate ions ($5 \times 10^{-3} \text{M}$) measured by stopped-flow spectrophotometry, **A** at completion of rapid reaction (corresponds to 1:1 adduct) and **B** at completion of slow reaction (corresponds to a mixture of 1:1 and 1:2 adducts). Spectra have been normalised to 1cm pathlength

In the reaction of TNT with thiolate anions no evidence was found for the production of trinitrobenzyl anions. In contrast to what is observed in alcohols, Bernasconi²⁰ has shown that the trinitrobenzyl anion plays at most a very minor role in largely aqueous media. This was confirmed in the work of Bowden and Stewart²¹ who reported an insignificant amount of hydrogen exchange in TNT in experiments in an aqueous solvent containing 5-15 mol% of dimethyl sulphoxide.

Because of the low values of equilibrium constants for reaction with TNT, it was necessary to use relatively large concentrations of TNT (up to 6×10^{-4} M) and thiolate anions. Consequently it was not always possible to limit I to 0.25M.

a) Thioglycolate ions

Absorbances at completion of the fast process were measured at both 450nm and 600nm. In order to calculate values of K_1 the extinction coefficients 1.7×10^4 $\text{lmol}^{-1}\text{cm}^{-1}$ (450nm) and 5×10^3 $\text{lmol}^{-1}\text{cm}^{-1}$ (600nm) were assumed which are typical of 1:1 adducts. To obtain K_2 , the value of $\epsilon_{1:2} = 8 \times 10^3$ $\text{lmol}^{-1}\text{cm}^{-1}$ at 450nm was measured from visible spectra where complete conversion to the di-adduct had been achieved. Absorbance data (table 3.18) lead to values $K_1 = 1.1$ lmol^{-1} and $K_2 = 180 \pm 30$ lmol^{-1} . Values of k_{fast} obtained at 0.04M and 0.08M thioglycolate (both $(5 \pm 1) \times 10^4$ s^{-1}) approximate to k_{-1} giving a value for k_1 ($=K_1 \cdot k_{-1}$) of 5.5×10^4 $\text{lmol}^{-1}\text{s}^{-1}$. The values of k_{slow} are well fit with expression 3.6 and values of $k_2 = 5500$ $\text{lmol}^{-1}\text{s}^{-1}$, $k_{-2} = 28$ s^{-1} and $K_1 = 1.1$ lmol^{-1} . The value of K_2 thus obtained (200 lmol^{-1}) is in accord with the value obtained from absorbance data. The kinetic data are given in table 3.19.

b) Thiomalate ions

Equilibrium constants for reaction of TNT with thiomalate were low, necessitating the use of high concentrations of thiolate ions and it was therefore not possible to keep the ionic strength constant at 0.25M. As a consequence of the

triple negatively charged thiomalate anion this varies from $I = 0.25\text{M}$ to $> 3.0\text{M}$ for concentrations of thiomalate from 0.04M to 0.5M .

Absorbances (table 3.20) obtained at the completion of the fast 1:1 adduct forming process yield a value for $K_1 = 0.15 \text{ l mol}^{-1}$. Absorbances obtained at the completion of the slower process forming the 1:2 adduct allow the calculation of K_2 . The data in table 3.20 show that K_2 increases with ionic strength as expected for the reaction of multicharged species. However, the change in this value is not dramatic suggesting similar values in activity coefficient for the thiolate anion in the region of $I = 0.6$ to 3.0M . Rate data for the formation of the 1:2 adduct (table 3.21) again at uncontrolled ionic strength are reasonably well fit with values $k_2 = 3500 \text{ l mol}^{-1} \text{ s}^{-1}$ and $k_{-2} = 160 \text{ s}^{-1}$ (leading to $K_2 = 22 \text{ l mol}^{-1}$) although there is some deviation for the larger concentrations of thiomalate anion.

Temperature jump measurements at 470nm yield a value for k_{-1} of *ca.* $6 \times 10^4 \text{ s}^{-1}$. The value of $k_1 (=K_1 \cdot k_{-1})$ is thus $7.5 \times 10^3 \text{ l mol}^{-1} \text{ s}^{-1}$.

c) Glutathione ions

Measurements with glutathione were restricted to 1:1 adduct formation. Initial absorbances (table 3.22) gave a value for $K_1 = 0.12 \text{ l mol}^{-1}$. Measurements were made at both 470nm and 500nm and the extinction coefficients used to calculate K_1 ($\epsilon_{1:1} = 1.9 \times 10^4 \text{ l mol}^{-1} \text{ cm}^{-1}$ at 470nm and $\epsilon_{1:1} = 1.5 \times 10^4 \text{ l mol}^{-1} \text{ cm}^{-1}$ at 500nm) are typical of 1:1 adducts. Temperature-jump measurements gave $k_{-1} = 4 \times 10^4 \text{ s}^{-1}$ leading to $k_1 (=k_{-1} \cdot K_1) 5 \times 10^3 \text{ l mol}^{-1} \text{ s}^{-1}$.

Table 3.18 Visible absorbances and calculated equilibrium constants for the reaction of TNT^a with thioglycolate ions in 90/10 (v/v) dioxan/water at 25°C with I = 0.25M

[⁻ SCH ₂ CO ₂ ⁻] M	A _{450nm} ^{init} b,c	K ₁ d l mol ⁻¹	A _{450nm} ^{final} b	A _{600nm} ^{final} b	equilibrium concentrations			K ₁ l mol ⁻¹	K ₂ l mol ⁻¹
					10 ⁶ [1:1] e M	10 ⁶ [1:2] f M	10 ⁶ [TNB] g M		
0.005	0.0092	1.1	0.0133	0.0027	0.53	0.52	98.95	1.1	200
0.010	0.0175	1.0	0.0325	0.0052	1.04	1.85	97.11	1.1	180
0.020	0.0367	1.1	0.0833	0.0100	2.00	6.16	91.84	1.0	150

a Concentration is 1x10⁻⁴M. b Normalised to a pathlength of 1cm. c Initial absorbance due to formation of 1:1 adduct

d Calculated as $A_{450nm}^{initial} / [1.7 - A_{450nm}^{initial}] [^{-}SCH_2CO_2^{-}]$ Assumes $\epsilon_{1:1} = 1.7 \times 10^4 \text{ l mol}^{-1} \text{ cm}^{-1}$ at 450nm.

e Calculated as $A_{600nm}^{final} / 5 \times 10^3$ The ratio of $A_{450nm}^{initial} / A_{600nm}^{initial} = 3.4$

The value of $5 \times 10^3 \text{ l mol}^{-1} \text{ cm}^{-1}$ for the 1:1 adduct at 600nm is assumed similar to those obtained for adducts with TNB.

f Calculated as $[A_{450nm}^{final} - 3.4 A_{600nm}^{final}] / 8 \times 10^3$ The value of $\epsilon_{1:2} = 8 \times 10^3 \text{ l mol}^{-1} \text{ cm}^{-1}$ at 450nm was obtained from visible spectra at complete conversion of TNT to the 1:2 adduct.

$$g \quad [TNT] = 1 \times 10^{-4} - [1:1] - [1:2]$$

Table 3.19
Kinetic data for reaction of TNT with thioglycolate ions in 90/10 (v/v)
H₂O/dioxan at 25^oC with I = 0.25M

[thioglycolate] M	^a 10 ⁻⁴ k _{fast} s ⁻¹	^b k _{slow} s ⁻¹	^c k _{calc} s ⁻¹
0.01		28 ± 1	29
0.02		28	30
0.03		33	33
0.04	5 ± 1		
0.05		40	42
0.07		53	56
0.08	5 ± 1		
0.09 [*]		76	73
0.10 [*]		84	83

^{*}I > 0.25M

- a** measured by temperature jump spectrophotometry at 460 nm.
- b** measured by stopped-flow as a colour forming reaction at 430 nm.
- c** calculated from expression 3.6 with $k_2 = 5500 \text{ l mol}^{-1} \text{ s}^{-1}$, $k_{-2} = 28 \text{ s}^{-1}$ and $K_1 = 1.1 \text{ l mol}^{-1}$.

Table 3.20

Visible absorbances and calculated equilibrium constants for the reaction of TNT^a with thiomalate ions in 90/10 (v/v) dioxan/water at 25°C Data at variable ionic strength

[thiomalate] M	A _{470nm} ^{b,c} init	K ₁ ^d l mol ⁻¹	A _{470nm} ^b final	A _{600nm} ^{b,c} init	A _{600nm} ^b final	equilibrium concentrations			K ₁ l mol ⁻¹	K ₂ l mol ⁻¹
						10 ⁶ [1:1] ^e M	10 ⁶ [1:2] ^f M	10 ⁶ [TNB] ^g M		
0.04	0.0133	0.18	0.0133	0.0047	0.0047	0.67	0	99.33	0.17	
0.06	0.0160	0.14	0.0160	0.0063	0.0063	0.90	0	99.1	0.15	
0.08	0.0207	0.14								
0.10	0.0283	0.15	0.0283	0.0127	0.0080	1.14	0.88	97.98	0.12	8
0.20	0.0500	0.14	0.0633	0.0190	0.0120	1.71	4.43	93.86	0.09	13
0.30	—		0.160	0.0237	0.0157	2.24	17.32	80.44	0.09	26
0.40	—		0.313		0.0207	2.95	38.07	58.98	0.13	32
0.50	—		0.353		0.0230	3.29	43.07	53.64	0.12	26

a,b,c,d,e,f,g -see next page

footnotes to table 3.20

a concentration is $1 \times 10^{-4} \text{M}$

b normalised to a pathlength of 1cm.

c initial absorbances due to formation of 1:1 adduct

d calculated as $A_{470\text{nm}} / \left[1.9 - A_{470\text{nm}}^{\text{initial}} \right] [\text{thiomalate}]$

e calculated as $A_{600\text{nm}}^{\text{final}} / 7 \times 10^3$ Find $A_{470\text{nm}}^{\text{initial}} / A_{600\text{nm}}^{\text{initial}} = 2.8$ Thus $\epsilon_{1:1} = \frac{1.9 \times 10^4}{2.8} = 7 \times 10^3 \text{ l mol}^{-1} \text{ cm}^{-1}$ at 600nm.

f calculated as $\left[A_{470\text{nm}}^{\text{final}} - 2.8 A_{600\text{nm}}^{\text{final}} \right] / 6.7 \times 10^3$ Value of $\epsilon_{1:2} = 6.7 \times 10^3 \text{ l mol}^{-1} \text{ cm}^{-1}$ at 470nm determined from visible spectra at complete conversion of TNT to 1:2 adduct.

$$\mathbf{g} \text{ [TNT]} = 1 \times 10^{-4} - [1:1] - [1:2]$$

Table 3.21 Kinetic data for reaction of TNT with thiomalate ions in 90/10 (v/v) H₂O/dioxan at 25^oC

[thiomalate] M	^a 10 ⁻⁴ k _{fast} s ⁻¹	^b k _{slow} s ⁻¹	^c k _{calc} s ⁻¹
0.1		170 ± 20	170
0.2		180	180
0.3	5.4 ± 1	210	210
0.4		260	240
0.5	5.4 ± 1	330	280

- a** measured by temperature-jump spectrophotometry at 460nm.
b measured by stopped-flow as a colour forming process at 430nm or as a fading reaction at 600 nm.
c calculated from expression 3.6 with $k_2 = 3500 \text{ l mol}^{-1} \text{ s}^{-1}$, $k_{-2} = 160 \text{ s}^{-1}$ and $K_1 = 0.15 \text{ l mol}^{-1}$.

Table 3.22 Kinetic and equilibrium data for the reaction of TNT^a with glutathione ions in 99/1 H₂O/dioxan at 25^oC

[gluta-thione] M	^b initial A _{470nm}	^c K ₁ l mol ⁻¹	^b initial A _{500nm}	^d K ₁ l mol ⁻¹	^e 10 ⁻⁴ k _{fast} s ⁻¹
0.04	0.012	0.16	0.009	0.15	—
0.08	0.017	0.11	0.012	0.10	—
0.12	0.025	0.11	0.019	0.11	—
0.30	—	—	—	—	3.6 ± 1

- a** concentration is $1 \times 10^{-4} \text{ M}$
b absorbances determined at completion of the reaction forming 1:1 adduct.

c,d K_1 calculated as $A^{\text{initial}} / (A_{\infty} - A^{\text{initial}})[\text{glutathione}]$

with $A_{\infty} = 1.9$ at 470nm

$A_{\infty} = 1.5$ at 500nm

- e** determined by temperature jump spectrophotometry.

Comparisons and determination of intrinsic reactivities

Kinetic and equilibrium data for additions to TNB and TNT are summarised in table 3.23. Values of K_1 for 1:1 adduct formation are shown to decrease in the order thioglycolate > thiomalate > ethyl-2-mercaptoacetate > glutathione and show (in terms of $\log K_1$ values) a much smaller spread than the $\text{p}K_a$ values. The correlation between the two quantities is poor because of the importance of steric effects with the bulkier substituents. Thiomalate shows a lower affinity for TNB than expected from its $\text{p}K_a$ value and chain branching^{7,8} at the carbon atom α to the thiolate ion may be responsible. This will result in unfavourable steric interactions in the 1:1 adduct and it is likely that there will be a degree of electrostatic repulsion between the two negatively charged carboxylate groups and the negative charge delocalised in the nitro groups of the adduct. These factors will also contribute to the relatively low value of K_2 for the thiomalate anion. Although there is no chain branching at the α -carbon atom in glutathione, similar steric effects may contribute to the low value of K_1 obtained for TNB. Electrostatic effects, however, are likely to be less important in the 1:1 and 1:2 adducts formed from glutathione than in those formed from thiomalate. For the smaller thiolate ions (thioglycolate and ethyl-2-mercaptoacetate) where steric effects are relatively unimportant the larger value of K_1 for thioglycolate is reflected in its larger $\text{p}K_a$.

Values of K_1 for reaction with TNT are lower than those for reaction with TNB by factors 230 (thioglycolate), 220 (thiomalate) and 125 (glutathione). The inductive effect of the $-\text{CH}_3$ group will be an important factor in reducing adduct stability as will be the disruption of planarity of the *ortho* nitro groups with the ring^{18,19} thus reducing their electron withdrawing ability. A further factor thought to contribute to the low stability of the TNT adducts is the hydrophobic $-\text{CH}_3$ substituent which will hinder the solvation of the adducts.¹⁹ Values of K_2 for

reaction with TNT are not dissimilar to corresponding values obtained for TNB. The formation of 1:2 adducts relieves the steric strain between the $-\text{CH}_3$ substituent and the *ortho* nitro groups and is thus expected to be a relatively favoured process with respect to 1:1 adduct formation⁵. In the 1:2 adducts the rings are necessarily non-planar so that steric effects are also less important.

Bernasconi and Killion²⁴ have recently obtained a very low β_{nuc} value for thiolate addition to α -nitrostilbenes. In accord with their work, values of k_1 obtained for thiolate addition to TNB are very similar (in the range $1-2 \times 10^6 \text{ l mol}^{-1} \text{ s}^{-1}$) for thiols whose pK_a values vary from 8.7¹⁵ (glutathione) to 11.1¹⁴ (thiomalate). Comparison of the corresponding values for reaction with TNT, however, shows that they vary quite widely, with a tenfold difference in rate constant on going from thioglycolate ($k_1 = 5.5 \times 10^4 \text{ l mol}^{-1} \text{ s}^{-1}$) to glutathione ($k_1 = 5000 \text{ l mol}^{-1} \text{ s}^{-1}$). This is an unexpected result, as is the lower value of the reverse rate constant, k_{-1} , for glutathione attack to TNT than the corresponding value for attack to TNB.

Comparisons of nucleophilic reactivity may be usefully made²⁴⁻²⁶ in terms of intrinsic rate constants, k_0 , which can be obtained by interpolation or extrapolation of $\log k$ versus $\log K$ plots to $K = 1$ ($\Delta G^0 = 0$). Such plots, using the data for 1:1 adduct formation for each of the three thiolate ions are shown in figure 3.24 and gave the values of k_0 summarised in table 3.27. From literature values, intrinsic rate constants were also obtained for reactions of the sulphite ion^{19,22,28,29} and the hydroxide ion³¹ at unsubstituted ring positions of trinitro-activated aromatics. These plots are shown in figures 3.25 and 3.26.

The results show that the intrinsic reactivities of the three thiolate ions are closely similar and are considerably higher than that of the sulphite ion which in turn is higher than that of the hydroxide ion. The extent of electronic / structural and solvational reorganisation required during reaction is of major importance in determining intrinsic reactivities²⁶. In the three thiolate ions, all of which contain

Table 3.27 Intrinsic rate constants for reaction at an unsubstituted position of trinitro-activated aromatics

nucleophile	k_0	medium
glutathione	6×10^4	99/1 (v/v) water/dioxan
thioglycolate	5.6×10^4	90/10 (v/v) water/dioxan
thiomalate	5×10^4	90/10 (v/v) water/dioxan
sulphite	500 (360 [*])	water
hydroxide	10	water

* value determined using only data for TNB and TNT

carboxylic groups there is unlikely to be extensive delocalisation of the negative charge away from the sulphur atom so that electronic reorganisation will be minimal. There is also evidence³⁰ that thiolate ions are poorly solvated relative to alkoxide ions in hydrogen-bonding solvents and thus solvent reorganisation will also be kept to a minimum. In addition to these observations, it has also been suggested²⁴ that the enhanced intrinsic rate constants for thiolate ions derive from the development of a soft-soft interaction which has made more progress at the transition state than bond formation. This is an example of the operation of the principle of non-perfect synchronisation²⁷ where a product stabilising factor develops ahead of bond formation, thereby increasing k_0 .

In contrast to the thiolate ions, the negative charges in the sulphite ion will largely reside on oxygen atoms so that adduct formation, which involves reaction through the sulphur atom⁷⁻⁹ will require electronic/structural reorganisation with associated changes in solvation. Hence the lower value of k_0 .

The hydroxide ion will be very strongly solvated in water and the low intrinsic reactivity reflects the large amount of solvational reorganisation required during reaction. In addition, since oxygen is a "hard" base relative to sulphur, solvation of the adduct and delocalisation of charge into the ring will be the major product stabilising factors. These will lag behind bond formation and will, according to PNS²⁷, lower the intrinsic rate constant.

Table 3.23 Summary of Kinetic and Equilibrium data for addition of thiolate ions and other nucleophiles to unsubstituted positions of TNB and TNT at 25°C with I = 0.25M

nucleophile	sub- strate	K_1 l mol^{-1}	k_1 l $mol^{-1}s^{-1}$	k_{-1} s $^{-1}$	K_2 l mol^{-1}	k_2 l $mol^{-1}s^{-1}$	k_{-2} s $^{-1}$	pK _a	medium (v/v)
ethyl-2- mercapto- acetate ion	TNB	17	—	—	25	—	—	7.9 ^e	90/10 water/dioxan
thioglycolate ion	TNB	250	1.4x10 ⁶	5500	400	3300	8	10.7 ^f	90/10 water/dioxan
thiomalate ion	TNB	33	1.2x10 ⁶	3x10 ⁴	8	250	33	11.1 ^g	90/10 water/dioxan
glutathione ion	TNB	15	1.8x10 ⁶	1.2x10 ⁵	320	1.7x10 ⁴	53	8.7 ^h	99/1 water/dioxan
sulphite ^{*a}	TNB	27 } † 2 }	3.58x10 ⁴	130	9.2 } † 9.3 }	1.2 } † 195 }	0.13 } † 21 }	6.9	water
hydroxide ^b	TNB	3.73 (2.7) ^c	37.5	9.8	—	—	—	13.4 ^a	90/10 water/dioxan
thioglycolate ion	TNT	1.1	5.5x10 ⁴	5x10 ⁴	200	5500	28	10.7 ^f	90/10 water/dioxan
thiomalate ^{**} ion	TNT	0.15	7500	6x10 ⁴	22	3500	160	11.1 ^g	90/10 water/dioxan
glutathione ion	TNT	0.12	5000	4x10 ⁴	—	—	—	8.7 ^h	99/1 water dioxan
sulphite ^{*d}	TNT	2.6	800	800	36	42	1.16	6.9	water

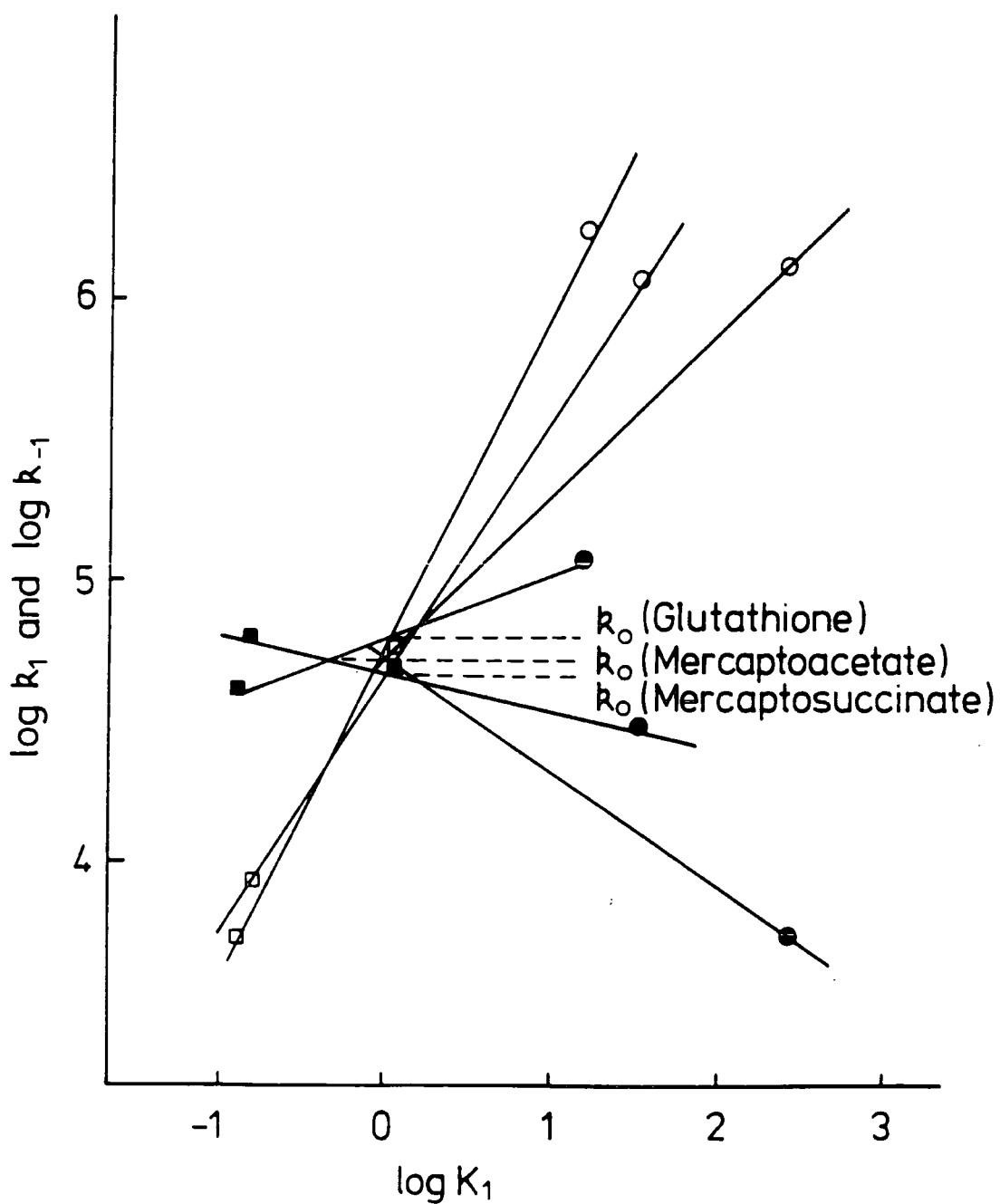


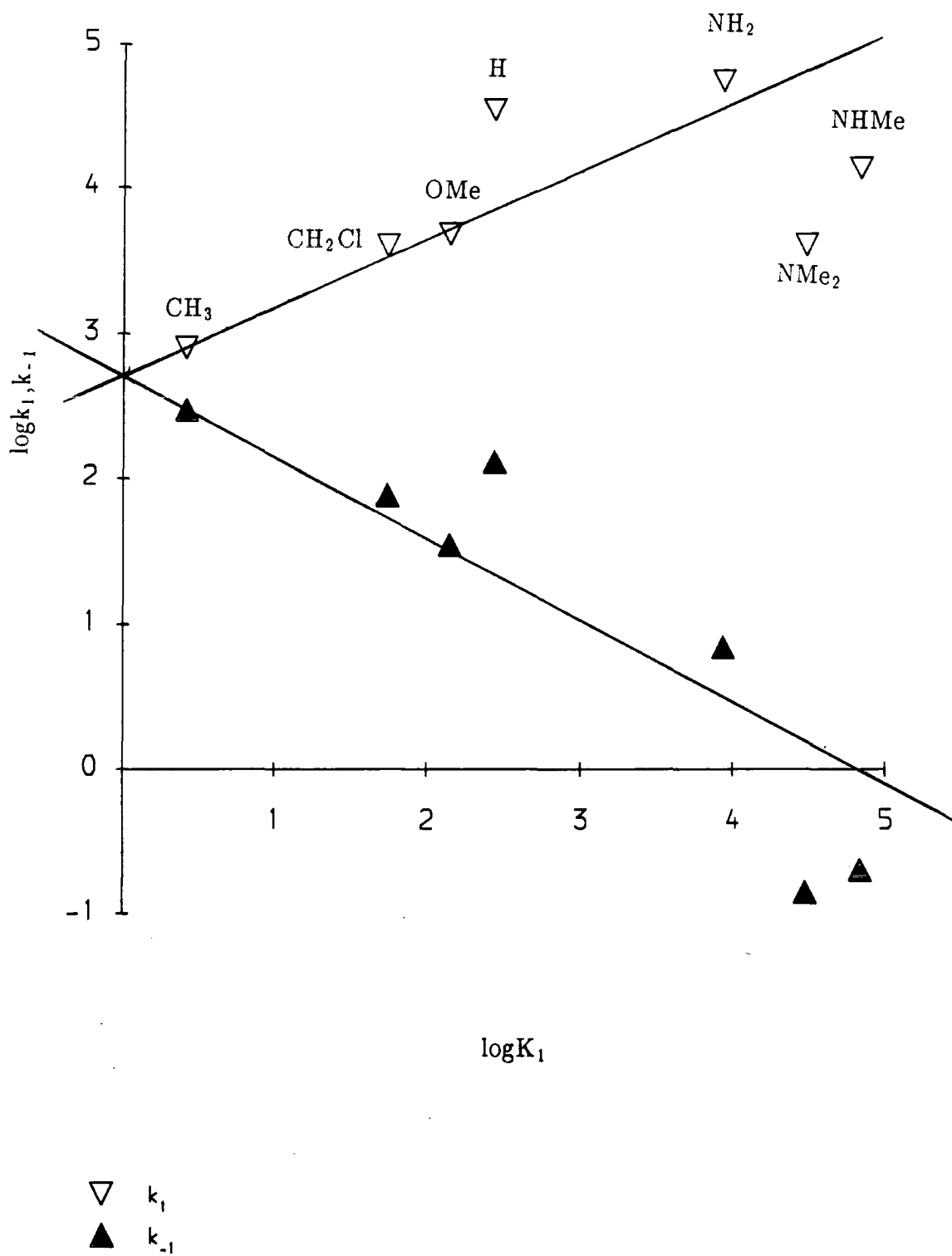
Figure 3.24

Determination of intrinsic reactivities

Reactions of thiolate ions at unsubstituted ring-positions of TNB (circles) and TNT (squares). Open symbols refer to k_1 and solid symbols to k_{-1}

Figure 3.25

Determination of intrinsic reactivities. Reactions of sulphite ions at unsubstituted positions of 1-X-2,4,6-trinitrobenzenes.



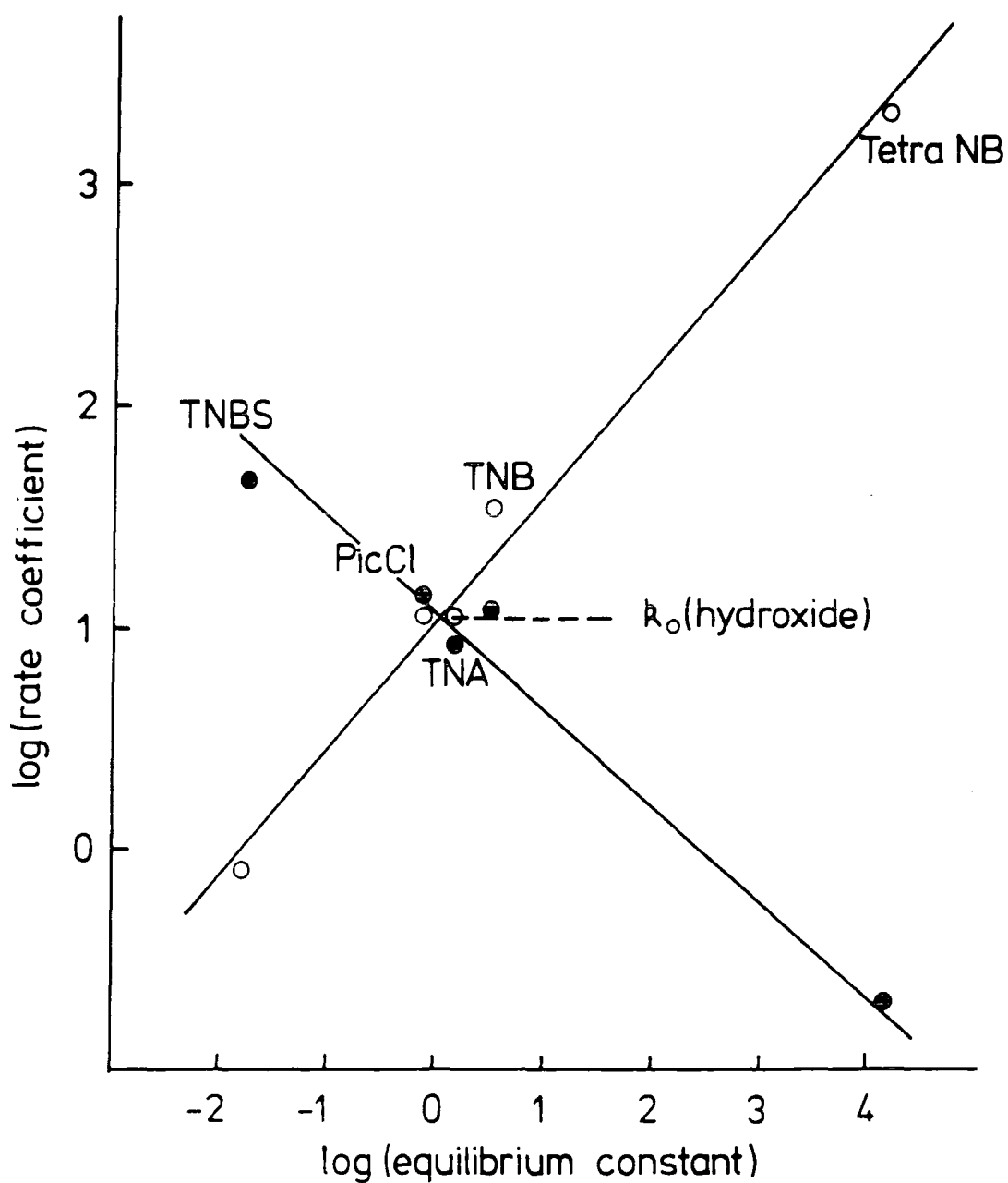


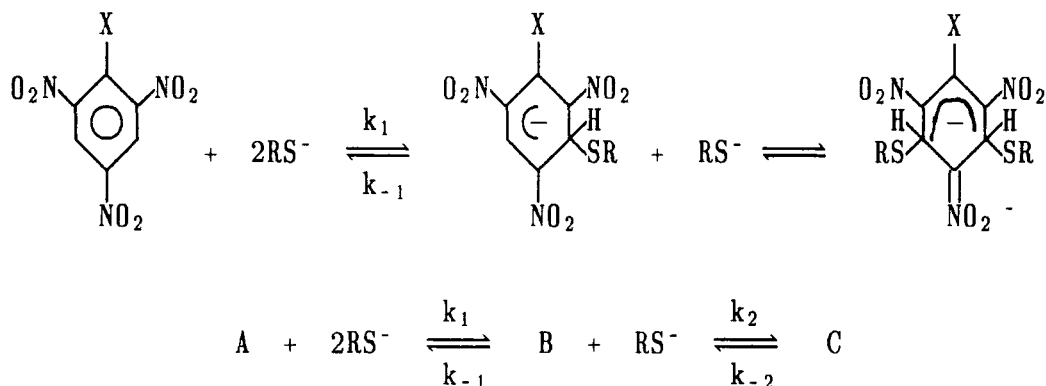
Figure 3.26

Determination of intrinsic reactivities

Reactions of hydroxide ions at unsubstituted ring-positions of nitro-aromatic compounds. Open symbols refer to k_1 and solid symbols refer to k_{-1} . Data from ref.31

Appendix

Derivation of rate expressions 3.5 and 3.6



Rapid process – formation of the 1:1 adduct.

The rate of loss of A is given by 3.28

$$\frac{-d[\text{A}]}{dt} = k_1 [\text{RS}^-] [\text{A}] - k_{-1} [\text{B}] \quad 3.28$$

The stoichiometric concentration of A, $[\text{A}]_0$ is $[\text{A}]_0 = [\text{A}] + [\text{B}]$

$$\text{Thus} \quad \frac{-d[\text{A}]}{dt} = k_1 [\text{RS}^-] [\text{A}] + k_{-1} ([\text{A}] - [\text{A}]_0) \quad 3.29$$

At equilibrium:

$$\frac{-d[\text{A}]}{dt}_{\text{eq}} = 0 = k_1 [\text{RS}^-] [\text{A}]_{\text{eq}} + k_{-1} ([\text{A}]_{\text{eq}} - [\text{A}]_0) \quad 3.30$$

Subtracting 3.30 from 3.29

$$\frac{-d[\text{A}]}{dt} = ([\text{A}] - [\text{A}]_{\text{eq}}) (k_1 [\text{RS}^-] + k_{-1})$$

$$\text{Thus} \quad \frac{-1}{[\text{A}] - [\text{A}]_{\text{eq}}} \frac{d[\text{A}]}{dt} = k_{\text{obs}} = k_1 [\text{RS}^-] + k_{-1} \quad [3.5]$$

Slow process – formation of the 1:2 adduct

The rate of formation of C is given by

$$\frac{d[C]}{dt} = k_2 [B] [RS^-] - k_{-2} [C] \quad 3.31$$

Use $K_1 = \frac{[B]}{[A][RS^-]}$ together with $[A]_0 = [A] + [B] + [C]$ to obtain [B]
in terms of [C]

$$[B] = \frac{([A]_0 - [C])K_1 [RS^-]}{1 + K_1 [RS^-]} \quad 3.32$$

Substitute for [B] in 3.31 to obtain

$$\frac{d[C]}{dt} = \frac{K_1 k_2 ([A]_0 - [C]) [RS^-]^2}{1 + K_1 [RS^-]} - k_{-2} [C] \quad 3.33$$

At equilibrium

$$\frac{d[C]}{dt}_{eq} = 0 = \frac{K_1 k_2 ([A]_0 - [C]_{eq}) [RS^-]^2}{1 + K_1 [RS^-]} - k_{-2} [C]_{eq} \quad 3.34$$

Subtracting 3.34 from 3.33

$$\frac{d[C]}{dt} = ([C]_{eq} - [C]) \left[\frac{K_1 k_2 [RS^-]^2}{1 + K_1 [RS^-]} + k_{-2} \right] \quad 3.35$$

Thus
$$\frac{1}{[C]_{eq} - [C]} \frac{d[C]}{dt} = k_{obs} = k_{-2} + \frac{K_1 k_2 [RS^-]^2}{1 + K_1 [RS^-]} \quad [3.6]$$

References

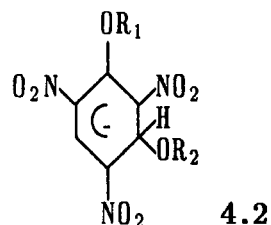
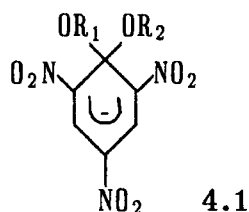
- 1 PB Ghosh, MW Whitehouse, *J. Med. Chem.*, 1968,**11**,305
MW Whitehouse, PB Gosh, *Biochem. Pharmacol.*, 1968,**17**,158
- 2 PB Ghosh, B Ternai, MW Whitehouse, *J. Med. Chem.*, 1972,**15**,255
- 3 MJ Strauss, A De Fusco, F Terrier, *Tetrahedron Lett.*, 1981,**22**,1945
- 4 AG Clark, M Sinclair, *Biochem. Pharmacol.*, 1988,**37**,259
- 5 L-H Gan, *Aust. J. Chem.*, 1977,**30**,1475
- 6 RB Freedman, GK Raddon, *Biochem. J.*, 1968,**108**,383
A Kotaki, M Harada, K Yagi, *J. Biochem.*,1964,**55**,553
- 7 E Buncel, MR Crampton, MJ Strauss, F Terrier, "*Electron Deficient aromatic- and heteroaromatic- base interactions*", Elsevier, Amsterdam 1984
- 8 F Terrier, *Chem. Rev.*,1982,**82**,77
- 9 MR Crampton, *J. Chem. Soc. (B)*, 1968,1208
- 10 MR Crampton, MA El-Ghariani, *J. Chem. Soc. (B)*, 1971,1043
- 11 MR Crampton, *J. Chem. Soc. (B)*, 1971,2112
- 12 MM Kreevoy, ET Harper, RE Duvall, AS Wilgus, LT Ditsch, *J. Am. Chem. Soc.*, 1960,**82**,4899
- 13 RJ Irving, L Nelander, I Wadso, *Acta. Chem. Scand.*, 1964,**18**,769
- 14 O Makitie, A Ilvonen, *Acta. Chem. Scand.*, 1972,**26**,847
- 15 FA Isherwood, *Symp. Biochem. Soc.*, 1957,**17**,3
- 16 T Abe, *Bull. Chem. Soc. Jap.*, 1960,**33**,41
V Gold, CH Rochester, *J. Chem. Soc.*, 1964,1710
- 17 CF Bernasconi, *J. Am. Chem. Soc.*, 1970,**92**,4682
- 18 DN Brooke, MR Crampton, *J. Chem. Res.*, 1980(S) 340, (M)4401
- 19 DN Brooke, MR Crampton, *J. Chem. Soc. Perkin Trans. II*, 1980,1850
- 20 CF Bernasconi, *J. Org. Chem.*, 1971,**36**,1671
- 21 K Bowden, R Stewart, *Tetrahedron*, 1965,**21**,261
- 22 CF Bernasconi, RG Bergstrom, *J. Am. Chem. Soc.*, 1973,**95**,3603
- 23 E Buncel, AR Norris, W Proudlock, *Can. J. Chem.*, 1968,**46**,2759

- 24 CF Bernasconi, RB Killion, *J. Am. Chem. Soc.*, 1988,110,7506
- 25 JPL Cox, MR Crampton, P Wight, *J. Chem. Soc. Perkin Trans. II*, 1988,25
- 26 CF Bernasconi, *Pure Appl. Chem.*, 1982,54,2335
- 27 CF Bernasconi, *Acc. Chem. Res.*, 1987,20,301
- 28 MR Crampton, MJ Willison, *J. Chem. Soc. Perkin Trans. II*, 1976,160
- 29 E Buncel, AR Norris, KE Russell, PJ Sheridan, *Can. J. Chem.*, 1974,52,25
- 30 MR Crampton, "*Chemistry of the thiol group*", ed. S Patai, Wiley, 1974, 3779
- 31 B Gibson, MR Crampton, *J. Chem. Soc. Perkin Trans. II*, 1979, 648

Chapter 4
**Kinetic and Thermodynamic preferences in the reactions of
thiolate ions with 1-substituted-2,4,6-trinitrobenzenes**

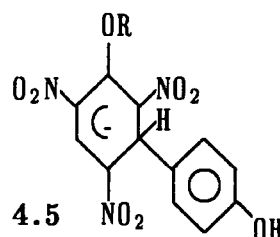
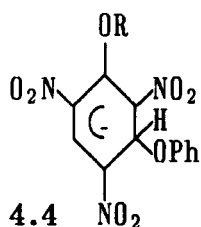
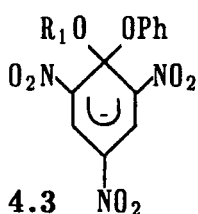
Introduction

Much evidence has been obtained from nmr and kinetic studies^{1,2} to show that alkoxide ion attack at unsubstituted ring positions of 2,4,6-trinitrophenyl ethers is a faster process than isomeric attack at the substituted 1-position but leads to thermodynamically less stable products. The greater stability of 1,1-adducts 4.1,



relative to 1,3-adducts 4.2, has been attributed³ to the release, in going to 4.1, of steric compression between the alkoxy substituent and the *ortho*-nitrogroup in the starting aromatic compound and to the particular stability of a saturated carbon atom substituted with two electronegative groups.

Similarly it has been shown^{4,5} that hydroxide ion attack at unsubstituted positions of 1-substituted-2,4,6-trinitrobenzenes is at least an order of magnitude slower than attack at the 1-position. However, on changing the nucleophile to phenoxide ion the behaviour is exactly reversed⁶. Thus the reaction of phenoxide

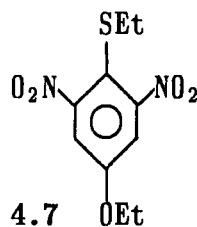
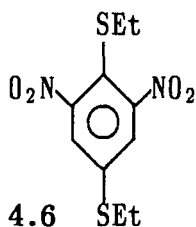


ions with 2,4,6-trinitroanisole and 2,4,6-trinitrophenyl phenyl ether results in the respective kinetically favoured 1,1 oxygen bonded adducts 4.3 (R = Ph, Me) and the thermodynamically preferred 1,3-adducts 4.4 (R = Ph, Me)⁶. In both cases the final stable product, according to ¹H nmr spectroscopy, is not the 1,3 O-bonded

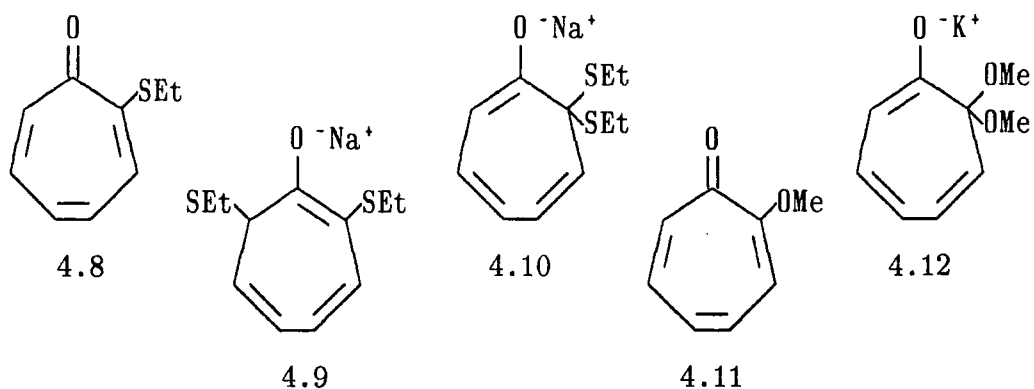
adduct 4.4 but 4.5 (R = Ph, Me) which results from *para*-carbon attack of phenoxide as an ambident nucleophile at unsubstituted positions of the substrate⁶. In a stopped-flow kinetic study of the interaction of phenoxide with 2,4,6-trinitroanisole in DMSO/H₂O solvent, Bernasconi and Muller⁷ were able to observe only the O-bonded 1,1 adduct 4.3 (R = Me) but not 4.4 or 4.5. Instead the reaction proceeded to give the 1,3 hydroxide adduct and finally picrate (via the 1,1 hydroxide adduct).

Pietra and co-workers have reported nmr measurements¹¹⁻¹³ in dimethyl sulphoxide showing that the reaction of ethanethiolate anions with ethylpicrate (2,4,6-trinitroanisole) and ethylthiopicate yield mixtures of 1,1- and 1,3-adducts in comparable concentrations thus indicating similar thermodynamic stabilities for these adducts. Interestingly, the reaction of ethoxide with ethylthiopicate in DMSO yields exclusively the 1,3-adduct!³ Also of interest in these reactions is the known ability^{16,17} of thioalkyl or thiophenyl functions to activate the substitution, by nucleophiles, of *ortho* and *para* nitrogroups. Thus among the final products in the reactions of ethylthiopicate with ethanethiolate ions and ethoxide ions were 4.6 and 4.7!^{1,13} In the reaction of *p*-tolylthiopicate with sodium toluene-*p*-thiolate, the rapid decay of the initially formed σ -adducts was too fast for ¹H nmr. However, products due to the substitution of both *ortho* and *para*-nitrogroups were observed!²

The reaction of sodium ethanethiolate with 2-ethylthiotropone (4.8) produces 4.9 which originates from base addition to the unsubstituted 7-position. Also seen in equilibrium with the latter were traces of the isomeric product 4.10!⁴



By contrast the reaction of 2-methoxytropone (4.11) with KOMe¹⁵ yielded only the *gem*-type adduct 4.12 as a stable species. Adducts produced by methoxide attack to the 7-position were observed only as transient species.



In contrast to the wealth of information available for the σ -adduct forming reactions of oxygen nucleophiles there have been few studies of the biologically important σ -adduct forming reactions of thiolate anions⁸⁻¹⁰

This study reports kinetic, equilibrium and ¹H nmr data for the reactions of some thiolate anions with 1-substituted 2,4,6-trinitrobenzenes. For comparison some data for hydroxide ion attack are also included.

Experimental

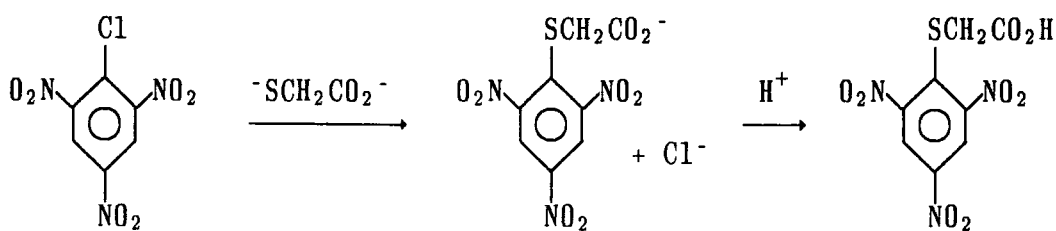
Preparation of trinitrophenylthioglycolic acid^{1 8}

To picryl chloride (10g) was added with stirring a solution in ethanol/H₂O containing 1.1 mol equivalents of thioglycolic acid and two equivalents of base (sodium bicarbonate or sodium acetate). The mixture was maintained at 40^oC for 1½ hours after which most of the ethanol was removed (rotary evaporator) and the resulting mixture acidified to pH 1 or 2 with dilute aqueous hydrochloric acid to obtain an oil. ¹H nmr of the dried material in [²H₆]-DMSO showed resonances (δ_{ring} 9.11(s), δ_{CH_2} 3.83(s), δ_{COOH} 11.3(s) (sometimes broadened)) due to the product as well as those due to 2,4,6-trinitrophenetole (δ_{ring} 9.2(s), δ_{CH_2} 4.5(q), δ_{CH_3} 1.4(t)) and picric acid (δ_{ring} 8.62(s)). At this stage the crude material contained about 90% of the required product.

The reaction was also repeated using the solvent hexamethylphosphoramide instead of ethanol but a similar oily and impure product was obtained.

Some effort was made to separate the components on a silica gel (particle size 0.040-0.063mm) column. 4g of the crude material was dissolved in ethylacetate which was also used as the eluting solvent. Several fractions were collected and these can be divided into three main groups. The first contained excess 2,4,6-trinitrophenetole and picric acid as expected from preliminary TLC studies. The middle fractions contained trinitrophenylthioglycolic acid and ¹H nmr showed them to be mostly free from impurities. The amount of product collected, however, was very small due to the formation of large quantities of a decomposition product: the final fractions washed off the column with methanol contained a black material. ¹H nmr of the dried material in [²H₆]-DMSO showed four bands of equal intensity δ 9.0 – 9.2

A few crystals of the required product were obtained from the middle fraction. These decomposed on heating. A solution made up in water (1 x 10⁻⁴M) gave a UV/visible spectrum with λ_{max} 360nm. A solution made up in 0.1M sodium

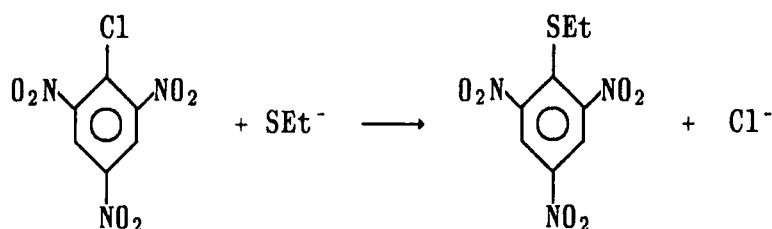


hydroxide did not show complete conversion to picrate after considerable periods of time.

Because of the doubtful purity of the final product, the trinitrophenylthioglycolic acid was not used in kinetic studies.

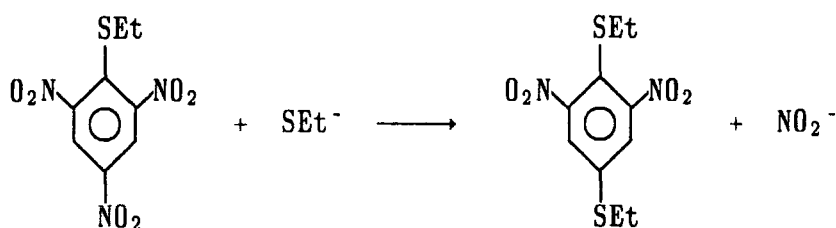
Preparation of ethylthiopicrate

A mixture of sodium acetate (2.8g) was gradually added, with stirring, to a warmed mixture of picryl chloride (10g) and ethanethiol (*ca.* 2.8g) in ethanol. After 15 minutes the reaction mixture was allowed to cool, water was added and a fine yellow precipitate was observed. The solid was extracted several times into ether which was washed with water and dried with anhydrous sodium sulphate. The ether was then evaporated leaving a solid product which was twice recrystallised from methanol giving yellow needles m.pt. 44–45⁰C (lit. 45⁰C). The ¹H nmr spectrum, shown in table 4.13, indicated the product to be free from impurities. Elemental analysis (% by mass) gave C 37.0, N 16.1, H 2.6 (calc for C₈H₇N₃O₆S : C 35.2, N 15.4, H 2.6)



Preparation of 1,4-bisethylthio-2,6-dinitrobenzene

To a solution of ethylthiopicrate (*ca.* 5g) in DMSO at room temperature was added with stirring an excess (1.2 mol equivalents) of ethanethiol and 1 mol equivalent of sodium methoxide (*ca.* 4M in methanol). The solution immediately became dark red. After one hour sufficient water was added to give a precipitate of 1,4-bisethylthio-2,6-dinitrobenzene. Recrystallisation from petroleum ether (b.p. 40°C) gave pale yellow needles m.pt. 88°C, lit.^{1,2} 90°C. Elemental analysis (% by mass) gave: C 41.0, N 9.5, H 4.0 (calc for C₁₀H₁₂N₂O₄S₂ : C 41.7, N 9.7, H 4.2). The ¹H nmr spectrum is shown in table 4.18



¹H nmr spectra

¹H nmr spectra were recorded in a solvent of [²H₆]-DMSO or [²H₆]-DMSO/D₂O containing up to 15% D₂O by volume. Substrate concentrations were 0.1 – 0.3M with nucleophile, substrate mole ratios varying from 0 to 4. Thiolate ions were generated *in situ* by reaction of the parent thiol in [²H₆]-DMSO with deuterioxide ions in D₂O. As the thioglycolic acid was a solution (80% by mass) in H₂O, the compound was reacted with one equivalent of sodium hydroxide, dried, and the resulting sodium salt made up in D₂O. The thiolate anion was generated by further reaction with OD⁻.

All measurements refer to internal tetramethylsilane.

Kinetic measurements

Kinetic measurements, obtained using conventional or stopped-flow spectrophotometry, were made under first order conditions with the concentration of the nucleophile usually in large excess of that of the nitrocompound. Reported rate coefficients are the mean of at least five separate determinations.

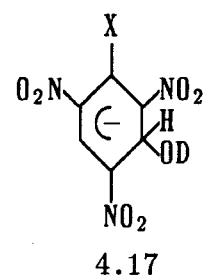
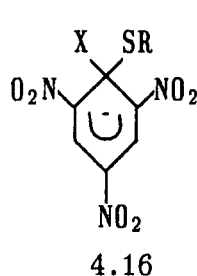
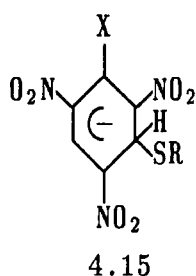
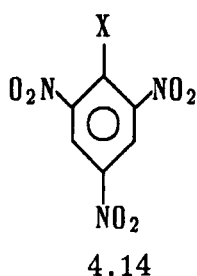
Solutions of thiolate ions were, because of their instability, generated immediately before use from the parent thiol and sodium hydroxide solution, enough hydroxide being added to ionise both carboxyl and thiol groups. A slight excess, usually $5 \times 10^{-3} \text{ M}$, of sodium hydroxide was used to ensure complete ionisation; checks were made to confirm that the excess hydroxide did not affect the observed kinetics. Measurements were made in water containing 1% or 2% dioxan which was used to prepare stock solutions of the nitrocompounds. Unless otherwise stated the ionic strength was maintained at 0.25M with sodium chloride.

The stopped-flow apparatus was also used to determine spectral shapes of species present after short reaction times. This involved measuring absorbances at individual wavelengths and building up spectra point by point.

Results and discussion

^1H nmr measurements

^1H nmr measurements shown in table 4.13 relate to the following structures:



In adducts of type 4.15 where addition of thiolate is at an unsubstituted position, the spectra showed two characteristic bands of equal intensity at *ca.* δ 8.3 and 5.9

due to ring hydrogens. Adducts of type 4.16 gave a single band due to ring hydrogens at *ca.* δ 8.4. Small bands slightly to high field of adducts 4.15 were sometimes observed and were attributed to the competitive addition of OD^- to unsubstituted ring position to yield adducts of structure 4.17. These resonances were also determined in separate experiments by addition of OD^- to the substrate in the absence of thiol.

Nmr spectra obtained within two minutes after mixing the reagents, before appreciable decomposition has occurred, allowed the relative proportion of the 1,1-adduct and 1,3-adducts to be determined. When ethylthiopicrate (4.14, $\text{X} = \text{SEt}$) was the substrate, ethanethiolate attack favoured the formation of the 1,3-adduct 4.15 ($\text{X} = \text{RS} = \text{SEt}$) over the 1,1-adduct 4.16 ($\text{X} = \text{RS} = \text{SEt}$) in a ratio of 3:1; with thioglycolate as the nucleophile only bands due to the 1,3-adduct 4.15 ($\text{X} = \text{SEt}$, $\text{RS} = \text{SCH}_2\text{CO}_2^-$) were observed. A band at δ 8.09 also present in the initial spectrum may be attributed to either 4.19 ($\text{RS}_1 = \text{SEt}$, $\text{RS}_2 = \text{SCH}_2\text{CO}_2^-$) or 4.19 ($\text{RS}_1 = \text{RS}_2 = \text{SCH}_2\text{CO}_2^-$). Formation of the latter product would involve substitution of thioethoxide by thioglycolate followed by displacement of the *para*-nitrogroup.

In contrast, spectra obtained for ethyl picrate (4.14 $\text{X} = \text{OEt}$) with both ethanethiolate and thioglycolate ions show that the 1,1-adducts 4.16 ($\text{X} = \text{OEt}$, $\text{RS} = \text{SEt}$, $\text{SCH}_2\text{CO}_2^-$) are favoured relative to the corresponding 1,3-adducts 4.15 ($\text{X} = \text{OEt}$, $\text{RS} = \text{SEt}$, $\text{SCH}_2\text{CO}_2^-$) in the ratio of 1.2:1. These results are in general agreement with Pietra's findings^{1,13} that the 1,1- and 1,3-adducts have rather similar stabilities in these systems.

In all cases the concentrations of the adducts gradually diminished with time. In the reaction of ethylthiopicrate with ethanethiolate anions, the bands due to the adducts were replaced with those due to 4.19 ($\text{RS}_1 = \text{RS}_2 = \text{SEt}$) and small amounts of 4.20 ($\text{RS}_1 = \text{RS}_2 = \text{SEt}$) as well as those due to the formation of picrate. The formation of 4.19 was found to be fairly rapid and was sometimes

observed in the initial spectra. When a large excess of ethanethiolate was used bands in the region $\delta 7.2 - 8.1$ were also observed, presumably indicating further substitution of nitrogroups.

The reaction of ethylpicrate with ethanethiolate also yielded 4.19 ($RS_1 = RS_2 = SEt$) and 4.20 ($RS_1 = RS_2 = SEt$); the reaction here involves substitution of ethoxide by ethanethiolate followed by displacement of nitrogroups. 4.19 ($RS_1 = RS_2 = SEt$) was also isolated as a crystalline solid by reaction of ethanethiolate with ethylpicrate.

The reaction of ethylpicrate with excess $^-SCH_2CO_2^-$ in dimethylsulphoxide yielded a mixture of products which were identified by 1H nmr. Data are summarised in table 4.18.

It is well known that DMSO stabilises 1:1 adducts relative to those of 1:2 stoichiometry! Attempts to obtain spectra of 1:2 adducts by increasing the proportion of D_2O in the solvent were unsuccessful due to problems of solubility.

The interaction of thioglycolate ions with picryl chloride was also studied by 1H nmr. Spectra taken within two minutes of mixing the reagents do not, however, show the formation of 1,3-adducts, presumably due to their rapid decay. When 1 equivalent of thioglycolate was used the products were solely picrate (δ_{ring} 8.63) and 4.14 ($X = ^-SCH_2CO_2^-$) (δ_{ring} 9.06, δ_{CH_2} 3.83). When 2 equivalents of $^-SCH_2CO_2^-$ were used the initial spectrum contained an extra band (δ 8.24) which may possibly be attributed to 4.19 ($RS_1 = RS_2 = ^-SCH_2CO_2^-$). After 24 hours the appearance of further bands (δ 8.01, 8.16, 8.42) was noted.

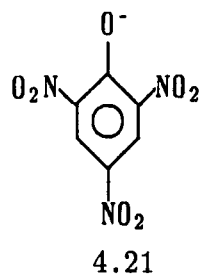
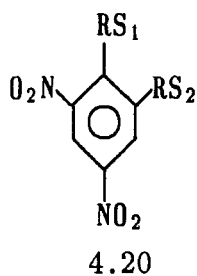
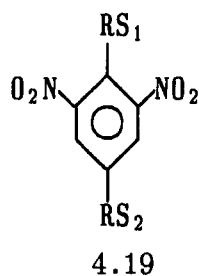


Table 4.13

 ^1H nmr Chemical shifts for parent structures and adducts

structure	ring	methylene ^c	methyl ^c	other
4.14 ^a X = OCH ₂ CH ₃	9.08(s)	4.26(q)	1.34(t)	
4.14 ^a X = SCH ₂ CH ₃	9.11(s)	2.95(q)	1.15(t)	
4.14 ^a X = SCH ₂ CO ₂ H	9.08(s)	3.83(s)		11.3(COOH)
4.15 { b { X = SCH ₂ CH ₃ SR = SCH ₂ CH ₃	5.97, 8.32	2.9(q) 2.5(q)	NM ^d	
4.15 { b { X = SCH ₂ CH ₃ SR = SCH ₂ CO ₂ ⁻	5.96, 8.30	NM	NM	
4.15 { b { X = OCH ₂ CH ₃ SR = SCH ₂ CH ₃	5.85, 8.33	4.0(q) 2.5(q)	NM	
4.15 { b { X = OCH ₂ CH ₃ SR = SCH ₂ CO ₂ ⁻	5.75, 8.33	4.1(q) 3.1(s)	1.3(t)	
4.16 { b { X = SCH ₂ CH ₃ SR = SCH ₂ CH ₃	8.36(s)	2.5 (q)	NM	
4.16 { b { X = OCH ₂ CH ₃ SR = SCH ₂ CH ₃	8.47(s)	3.26(q) 2.37(q)	1.08(t)	
4.16 { b { X = OCH ₂ CH ₃ SR = SCH ₂ CH ₃	8.46(s)	3.27(q) 2.9 (s)	1.08(t)	
4.17 ^b X = SCH ₂ CH ₃	8.34, 6.22	2.55(q)	1.1 (t)	
4.17 ^b X = OCH ₂ CH ₃	8.38, 6.14	4.03(q)	1.28(t)	

a solvent is [²H₆]-DMSO.

b solvent is [²H₆]-DMSO / D₂O containing at most 15% D₂O by volume.

c coupling J = 7Hz is observed between methylene and protons.

d not measured.

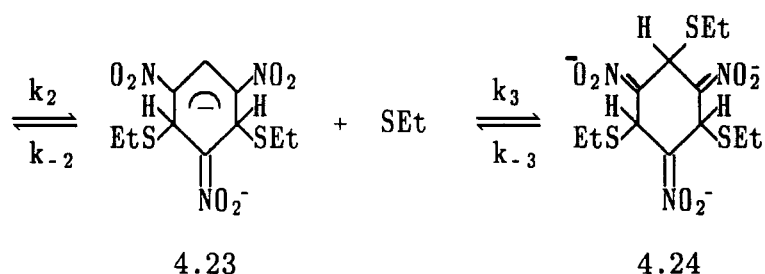
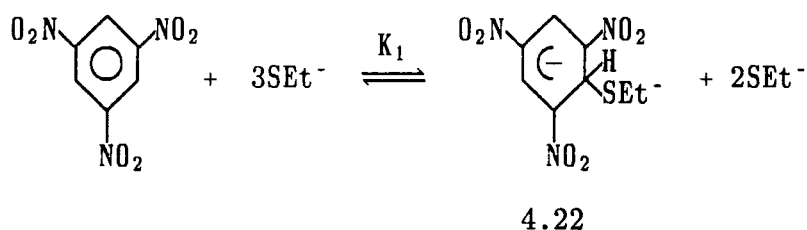
Table 4.18
 ^1H nmr data for substituted products in $[\text{}^2\text{H}_6]\text{-DMSO}$

structure	ring	methylene	methyl
4.19 $\begin{cases} \text{RS}_1 = \text{SCH}_2\text{CH}_3 \\ \text{RS}_2 = \text{SCH}_2\text{CH}_3 \end{cases}$	8.10 2H(s)	3.18 2H(q) 2.86 2H(q)	1.27 3H(t) 1.11 3H(t)
4.20 $\begin{cases} \text{RS}_1 = \text{SCH}_2\text{CH}_3 \\ \text{RS}_2 = \text{SCH}_2\text{CH}_3 \end{cases}$	8.51 1H(d), 8.22 1H(d) $J \approx 2$ Hz	NM NM	NM NM
4.20 $\begin{cases} \text{RS}_1 = \text{SCH}_2\text{CH}_3 \\ \text{RS}_2 = \text{SCH}_2\text{CO}_2^- \end{cases}$	8.50 1H(d), 8.28 1H(d) $J \approx 2$ Hz	3.17 2H(q) NM	1.30 3H(t) NM
4.19 $\begin{cases} \text{RS}_1 = \text{SCH}_2\text{CH}_3 \\ \text{RS}_2 = \text{SCH}_3\text{CO}_2^- \end{cases}$	8.17 2H	2.85 2H(q) 4.02 2H(s)	1.11 3H(t)
4.19 $\begin{cases} \text{RS}_1 = \text{SCH}_3\text{CO}_2^- \\ \text{RS}_2 = \text{SCH}_3\text{CO}_2^- \end{cases}$	8.10	NM	
4.21 (picrate)	8.62		

Kinetics and Equilibria

1,3,5-Trinitrobenzene and ethanethiolate anions

The UV/visible spectra of 1,3,5-TNB with ethanethiolate anions in water show that the major interaction is to give the di-adduct 4.23 with a λ_{\max} of 500nm. The spectrum of the 1:1 adduct, not directly obtainable in water, could be obtained in 60/40 DMSO/H₂O (v/v) and had a λ_{\max} of 470nm in this solvent. In water the 1:1 adduct 4.22 is known⁸ to have a λ_{\max} of 460nm ($\epsilon = 2.5 \times 10^4 \text{ l mol}^{-1} \text{ cm}^{-1}$). With $[\text{SEt}^-] > 0.01\text{M}$ in water, noticeable decreases in the intensity of the absorbance due to the 1:2 adduct were observed. The decrease was attributed to the formation of an adduct of 1:3 stoichiometry, 4.24, which is not



expected to absorb in the visible region²¹. Kinetic and equilibrium data, obtained by stopped-flow spectrophotometry are shown in table 4.25. Absorbance values, measured at completion of the most rapid colour-forming reaction at 460nm gave a value of $K_1 = 200 \text{ l mol}^{-1}$ for formation of 4.22. However the rate of this reaction was too rapid for measurement by the stopped-flow method. Unfortunately, temperature-jump measurements were not possible because the high equilibrium conversion to the adduct 4.23, even at low nucleophile concentrations, resulted in



very low equilibrium concentrations of the 1:1 adduct. The rate expression for the equilibration of adducts 4.22 and 4.23 is given in 4.26 and values, k_{calc} , calculated with $k_2 = 3 \times 10^4 \text{ l mol}^{-1} \text{ s}^{-1}$, $k_{-2} = 3 \text{ s}^{-1}$, and $K_1 = 180 \text{ l mol}^{-1}$ give a good fit with experimental values, $k_{\text{obs},2}$. The value thus obtained for $K_2 (= k_2/k_{-2})$ of $1 \times 10^4 \text{ l mol}^{-1}$ agrees well with the literature value^{8,20} of $1.2 \times 10^4 \text{ l mol}^{-1}$ determined from absorbance values. The high value of K_2 relative to K_1 is attributed²⁰ to the strong solvation by water of the negative charges localised on nitrogroups in the di-adduct.

$$k_{\text{obs},2} = k_{-2} + \frac{k_2 K_1 [\text{RS}^-]^2}{1 + K_1 [\text{RS}^-]} \quad 4.26$$

$$k_{\text{obs},3} = k_{-3} + \frac{k_3 K_1 K_2 [\text{RS}^-]^3}{1 + K_1 [\text{RS}^-] + K_1 K_2 [\text{RS}^-]^2} \quad 4.27$$

$$k_{\text{obs},3} = k_{-3} + k_3 [\text{RS}^-] \quad 4.28$$

The rates of the fading process for the conversion of the 1:2 adduct to the 1:3 adduct were measured at 460nm. The rate expression for the reaction, 4.27, simplifies to 4.28 since here $K_2 K_1 [\text{RS}^-] \gg 1 + K_1 [\text{RS}^-]$. A linear plot of the data in table 4.25 gave values of $k_3 = 900 \text{ l mol}^{-1} \text{ s}^{-1}$ and $k_{-3} 10 \text{ s}^{-1}$. Because of this fading process it was not possible to obtain directly a value for the extinction coefficient of the 1:2 adduct at λ_{max} . However, the values of $K_3 = 90 \text{ l mol}^{-1}$ and $K_2 = 1 \times 10^4 \text{ l mol}^{-1}$ obtained from kinetics are in accord with an extinction coefficient of $1.6 \times 10^4 \text{ l mol}^{-1} \text{ cm}^{-1}$ for the 1:2 adduct at 500nm: calculated equilibrium absorbances, A_{calc} , shown in table 4.25 and obtained with $\epsilon_{1:2} = 1.6 \times 10^4 \text{ l mol}^{-1} \text{ cm}^{-1}$, $\epsilon_{1:1} = 1.8 \times 10^4 \text{ l mol}^{-1} \text{ cm}^{-1}$, $K_1 = 200 \text{ l mol}^{-1}$, $K_2 = 1 \times 10^4 \text{ l mol}^{-1}$ and $K_3 = 90 \text{ l mol}^{-1}$, are in excellent agreement with the

experimentally determined values, A_{500}^{final} . This value of the extinction coefficient for the 1:2 adduct at λ_{max} is similar to those previously obtained for TNB and thiolate anions derived from thioglycolic acid, mercaptosuccinic acid and glutathione.

In the reaction of 1,3,5-trinitrobenzene with sodium sulphite in water, three rate processes were observed due to the formation of a 1:1 adduct and two *cis*- and *trans*- isomeric 1:2 adducts^{2,2}. The possibility that the third rate process in the reaction of ethanethiolate ions with TNB may represent formation of an isomeric 1:2 adduct is, however, not compatible with the visible spectra. In this case the 1:2 adduct is likely to exist predominantly in the *trans*- form^{2,3}

Equilibrium data for the reaction of ethanethiolate anions with TNB were also obtained in 60/40 (v/v) DMSO/H₂O. The λ_{max} of the 1:2 adduct is shifted to 522nm in this solvent. Because of the large equilibrium conversion of TNB to both 1:1 and 1:2 adducts even at low concentrations of ethanethiolate anion, the data do not permit calculation of K_1 . The value of K_2 calculated from absorbances is *ca.* 1000 l mol⁻¹ while K_1 is estimated at >10⁴ l mol⁻¹. These values illustrate the ability of DMSO to stabilise 1:1 adducts at the expense of 1:2 adducts.

Table 4.29
Equilibrium data for TNB and ethanethiolate ions in 60/40 DMSO/H₂O
I = 0.25M (NaCl)

$10^3 [\text{SEt}^-]$ M	a A_{600}	a A_{522}	b $10^4 [1:1]$ M	c $10^4 [1:2]$ M	d $10^4 [\text{TNB}]$ M	e $10^{-2} K_2$ l mol^{-1}
0.25	0.86	1.51	0.86	—	0.13	—
0.5	0.75	1.81	0.75	0.17	0.08	—
1.0	0.53	2.57	0.53	0.47	nil	9
1.5	0.32	2.40	0.32	0.52	0.16	11
2.0	0.34	2.55	0.34	0.56	0.10	8
3.0	0.26	2.98	0.26	0.74	nil	10
4.0	0.22	3.54	—	0.89	—	—
8.0	0.10	3.36	0.10	0.89	0.01	11
12.0	0.12	3.56				

- a** normalised to $1 \times 10^4 \text{M}$ TNB and a pathlength of 1cm.
- b** calculated as $A_{600}/1 \times 10^4$. It is assumed that the 1:2 adduct does not absorb at this wavelength.
- c** calculated as $(A_{522} - 1.7A_{600})/3.55 \times 10^4$.
 For $[\text{SEt}^-] = 2.5 \times 10^{-4} \text{M}$ the spectrum is essentially that of the 1:1 adduct with $A_{522}/A_{600} \approx 1.7$
- d** calculated as $1 \times 10^{-4} \text{M} - [1:1] - [1:2]$
- e** calculated as $[1:2] / [1:1][\text{SEt}^-]$

Table 4.25 Kinetic and equilibrium data for the reaction of trinitrobenzene^a with SET⁻ in water at 25°C with I = 0.25M

$10^3 [\text{SEt}^-]$ M	^b $A_{460\text{nm}}^{\text{init}}$	^c $A_{460\text{nm}}^{\text{final}}$	^d K_1 l mol ⁻¹	^b $A_{500\text{nm}}^{\text{init}}$	^c $A_{500\text{nm}}^{\text{final}}$	^e $A_{500\text{nm}}^{\text{calc}}$	$k_{\text{obs},2}$ s ⁻¹	^f k_{calc} s ⁻¹	^g K_3 l mol ⁻¹	^h $k_{\text{obs},3}$ s ⁻¹	ⁱ k_{calc} s ⁻¹
0.25					—	—	3.4	3.3			
0.50	0.19	0.55	165	0.15	0.61	0.60	4.6	4.2			
1.0	0.41	1.00	196	0.28	1.11	1.05	7.0	7.6			
1.5	0.61	1.18	215	0.40	1.18	1.21	11.5	12.5			
2.0	0.67	1.07	183	0.49	1.29	1.25	19	18.9			
4.0	1.10	1.01	196	1.00	1.08	1.16				13.2	13.6
6.0					—	—			—	15.4	15.4
8.0					0.97*	0.93			81	17.3	17.2
10.0					—	—			—	18.8	19.0
12.0					0.75*	0.77			94	20.7	20.8
15.0										22.6	23.5
18.0										24.9	26.2
20.0					0.57*	0.57			90		
40.0					0.34*	0.35			92		
60.0					0.21*	0.25			110		

1048

* obtained by conventional spectrophotometry

a Absorbances normalised to $1 \times 10^{-4} \text{M}$ TNB and a pathlength of $l=1 \text{cm}$.

b At completion of fast reaction forming a 1:1 adduct.

c At completion of all adduct forming reactions.

d Calculated as
$$A_{460}^{\text{initial}} / \left[2.5 - A_{460}^{\text{initial}} \right] [\text{SEt}^-]$$

Assuming an extinction coefficient of $2.5 \times 10^4 \text{ l mol}^{-1} \text{ cm}^{-1}$ for the 1:1 adduct

e Final equilibrium absorbance

f calculated with $k_2 = 3 \times 10^4 \text{ l mol}^{-1} \text{ s}^{-1}$, $k_{-2} = 3 \text{ s}^{-1}$ and $K_1 = 180 \text{ l mol}^{-1}$ according to expression 4.26

g calculated as
$$\left[1.6 - A_{500}^{\text{final}} \right] / A_{500}^{\text{final}} [\text{SEt}^-] \quad \text{Assumes } \epsilon_{1:2} = 1.6 \times 10^4$$

$\text{l mol}^{-1} \text{ cm}^{-1}$ at 500nm.

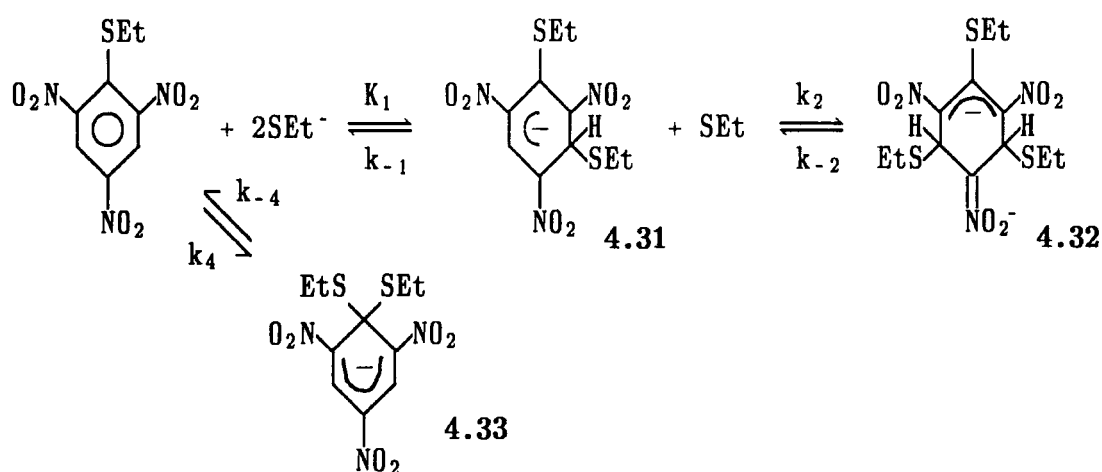
h Fading at 460nm.

i Calculated with $k_3 = 900 \text{ l mol}^{-1} \text{ s}^{-1}$ and $k_{-1} = 10 \text{ s}^{-1}$ according to expression 4.28.

Ethylthiopicrate and ethanethiolate ions

Visible spectra in water indicate that even at low concentrations of ethanethiolate anion, the substrate is largely converted to a 1:2 adduct (λ_{\max} 435, $\epsilon \approx 1 \times 10^4 \text{ l mol}^{-1} \text{ cm}^{-1}$). The λ_{\max} for this adduct shifts progressively to longer wavelengths in solvents containing increasing proportions of DMSO reaching 490nm in 60/40 (v/v) DMSO/H₂O. In the latter medium the spectra of the 1:1 adduct(s) show maxima at 470nm and 540nm (shoulder) while in 80/20 (v/v) DMSO/H₂O the adduct has a λ_{\max} 465nm.

Stopped-flow measurements in water provided evidence for three reversible processes. The most rapid reaction, attributed to attack at an unsubstituted position to give 4.31 was too fast for kinetic measurements but absorbance values taken at the completion of the reaction (table 4.30) at 440nm and 500nm lead to a value of K_1 of 85 l mol^{-1} . The spectrum of the adduct 4.31, obtained by measuring such absorbances at various wavelengths, has a λ_{\max} of *ca.* 440nm where the absorbance of ethylthiopicrate (λ_{\max} 355nm, $\epsilon \approx 5500 \text{ l mol}^{-1} \text{ cm}^{-1}$) was found to be negligible. At low nucleophile concentrations, $[\text{EtS}^-] \leq 10^{-3} \text{ M}$, a second process attributable to 1:1 adduct formation was observed. This process had a very low amplitude and the value of the rate constant, $30 \pm 10 \text{ s}^{-1}$, was independent of the nucleophile concentration. The large uncertainty in this value arises from the use



of a double exponential curve fitting procedure. This process is thought to represent equilibration with the adduct 4.33.

The assignment of the faster more intense process to the formation of 4.31 is based on the nmr results given previously which show that at equilibrium 4.31 is quite strongly favoured relative to 4.33, and also by analogy with the results for attack of ethanethiolate ions on TNB where reaction at an unsubstituted position

Table 4.30

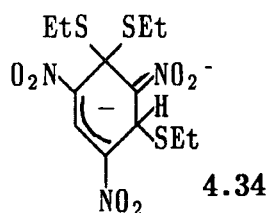
Kinetic and equilibrium data for the reaction of ethylthiopicrate in water at 25°C

$10^3 [\text{SEt}^-]$ M	^a A_{440}^{init}	^b K_1 l mol^{-1}	^a A_{500}^{init}	^c K_1 l mol^{-1}	^d A_{500}^{final}	$k_{\text{obs},2}$ s^{-1}	^e k_{calc}	^d A_{440}^{final}	^f A_{calc}
0.20			0.019	88					
0.25	0.056	115				1.4	2	0.488	0.484
0.50	0.107	113				4.0	5	0.734	0.742
0.75	0.123	87				—			
1.00	0.150	81	0.083	82	0.315	14	16	0.862	0.857
1.50	0.223	84	0.125	85	0.344	38	33	0.946	0.871
2.00	0.296	87	0.162	86	0.340	65	56	0.866	0.891
2.00						85	84		
3.00						126	117		
4.00						191	194		

- a** Absorbances at the completion of the fast 1:1 adduct forming reaction, normalised to a pathlength of 1 cm.
- b** Calc. as $A_{440}/(2.0-A_{440})[\text{SEt}^-]$. Assumes $\epsilon_{1:1} = 2.0 \times 10^4 \text{ l mol}^{-1} \text{ cm}^{-1}$ at 440nm.
- c** Calc. as $A_{500}/(1.1-A_{500})[\text{SEt}^-]$. Assumes $\epsilon_{1:1} = 1.1 \times 10^4 \text{ l mol}^{-1} \text{ cm}^{-1}$ at 500nm.
- d** Final equilibrium absorbances at completion of all adduct forming reactions
- e** Calc. from eqn 4.26 with $k_2 = 1.9 \times 10^5 \text{ l mol}^{-1} \text{ s}^{-1}$, $k_{-2} = 1 \text{ s}^{-1}$, and $K_1 = 85 \text{ l mol}^{-1}$
- f** Calc. with $K_1 = 85 \text{ l mol}^{-1}$, $K_4 = 28 \text{ l mol}^{-1}$, $K_2 = 2 \times 10^5 \text{ l mol}^{-1}$, $\epsilon_{1:1} = 2.0 \times 10^4 \text{ l mol}^{-1} \text{ cm}^{-1}$ and using a measured value of $9 \times 10^3 \text{ l mol}^{-1} \text{ cm}^{-1}$ for $\epsilon_{1:2}$

was found to be extremely rapid. On this basis a value for K_4 of *ca.* 28 l mol^{-1} (one third of the value for K_1) may be obtained. The measured value of 30 s^{-1} thus represents k_{-4} and leads to a value for $k_4 (= K_4 \cdot k_{-4})$ of $840 \pm 300 \text{ l mol}^{-1} \text{ s}^{-1}$.

The major measurable rate process in water involved formation of the 1:2 adduct and with $[\text{SEt}^-] > 10^{-3} \text{ M}$ this process became faster than the equilibration with 4.33 which was no longer observable. Values of $k_{\text{obs},2}$ in table 4.30 give a good fit with equation 4.26 with $k_2 = 1.9 \times 10^5 \text{ l mol}^{-1} \text{ s}^{-1}$, $k_{-2} = 1 \pm 1 \text{ s}^{-1}$ and $K_1 = 85 \text{ l mol}^{-1}$. The high uncertainty in the value of k_{-2} makes it unprofitable to obtain a value for K_2 by combination of rate coefficients. However the equilibrium absorbances at completion of these reactions are in accord with a value of $K_2 = 2 \times 10^5 \text{ l mol}^{-1}$ implying $k_{-2} \text{ ca. } 1 \text{ s}^{-1}$. The very high value of k_2 for the formation of the 1:2 adduct is in accord with nucleophilic attack at an unsubstituted ring position and is more compatible with structure 4.32 rather than 4.34 for the 1:2 adduct. The formation of 4.34 (which would thus involve nucleophilic attack on equilibrium concentrations of 4.33) cannot be a significant process since $k_{\text{obs},2}$ exceeds the rate of formation of 4.33.



All the adduct forming reactions were followed by slower irreversible processes. Because of the low solubility of the parent aromatic compound in aqueous solutions no attempt was made to identify the final products.

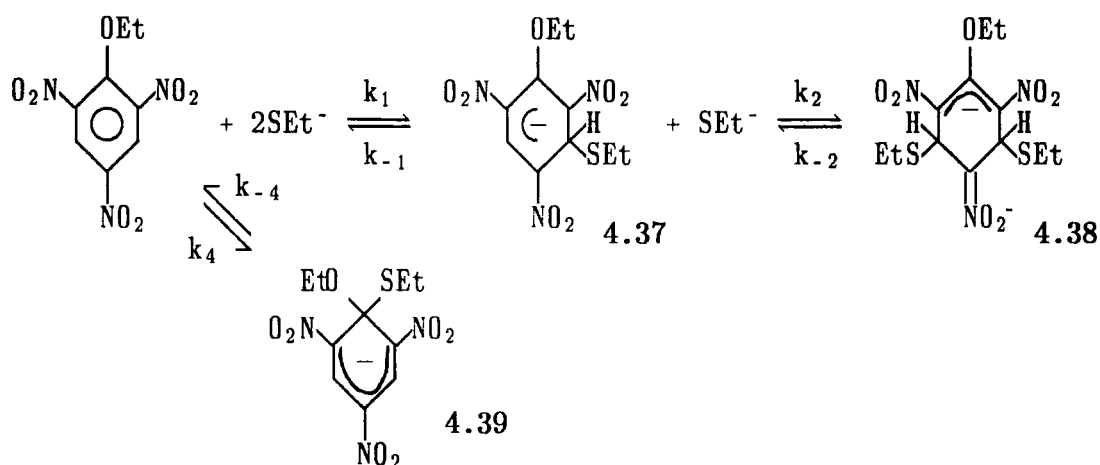
Ethylpicrate and ethanethiolate anions

The behaviour in water was qualitatively similar to that observed with ethylthiopicate in that there was evidence for the formation of two isomeric 1:1

adducts, while formation of a 1:2 adduct was dominant. The UV/visible spectrum of the 1:1 adducts, not directly obtainable in H₂O, was found to have a λ_{max} of 445nm in 50/50 (v/v) DMSO/H₂O. With the nucleophile in excess of the nitro-compound, three reversible processes were observable by stopped-flow spectrophotometry. The most rapid process, attributed to the formation of the 1,3-adduct was too fast for kinetic measurements but absorbances gave a value for K_1 of 90 lmol^{-1} , assuming an extinction coefficient of $2.0 \times 10^4 \text{lmol}^{-1} \text{cm}^{-1}$ at λ_{max} .

At low concentrations of ethanethiolate ($< 2 \times 10^{-3} \text{M}$) two further processes were observed, both colour forming at 430nm and 445nm. The first which is attributed to equilibration with 4.39, was not the dominant process, in terms of amplitude, even at the lowest concentration ($2.5 \times 10^{-4} \text{M}$) of ethanethiolate. Rate measurements, $k_{\text{obs},4}$, obtained by a double exponential curve fitting procedure gave a value of *ca.* 14s^{-1} which approximates to k_{-4} . The second process, attributed to the formation of the di-adduct 4.38, very rapidly increased in rate and amplitude with increasing $[\text{SEt}^-]$ and, with $[\text{SEt}^-] \geq 2 \times 10^{-3} \text{M}$, "overtook" the formation of 4.39 which could no longer be observed. In table 4.35, values of $k_{\text{obs},2}$ are compared with values k_{calc} obtained from equation 4.26 and values $k_2 = 1 \times 10^5 \text{dm}^3 \text{mol}^{-1} \text{s}^{-1}$, $k_{-2} = 2 \text{s}^{-1}$, $K_1 = 90 \text{lmol}^{-1}$. Absorbances, however, give a value for K_2 of *ca.* $2.5 \times 10^4 \text{lmol}^{-1}$. The poor agreement between $k_{\text{obs},2}$ and k_{calc} is likely to be the result of interference between the two processes forming adducts 4.39 and 4.38.

In order to limit formation of the 1:2 adduct and thus obtain more information about formation of 4.39, measurements (shown in table 4.36) were also made with $[\text{ethylpicrate}] > [\text{ethanethiolate}]$. Values of A_{initial} , measured at 500nm, increase with excess $[\text{hydroxide}]$ due to the increased ionisation of the thiol. Thus solutions of $2 \times 10^{-4} \text{M}$ of the thiol containing 1 equivalent of hydroxide are less than half ionised. Complete ionisation, shown by effectively constant values of A_{initial} , was achieved at $1 \times 10^{-3} \text{M}$ or $2 \times 10^{-3} \text{M}$ excess hydroxide. Values of A_{final} however,



increase with excess hydroxide even when A_{initial} is constant. This increase is attributed to the formation of a 1,3-hydroxide adduct. Hence K_4 was calculated when the concentration of excess hydroxide was small. In order to do so, values of A_{initial} are taken to be directly proportional to the degree of ionisation of the thiol. Values of $K_1 = 95 \text{ l mol}^{-1}$ and $K_4 = 110 \text{ l mol}^{-1}$ were obtained for these two processes indicating a slightly greater thermodynamic stability for the adduct by attack at the 1-position. This is in agreement with the nmr data in DMSO/water.

Formation of 4.39 was observed with a rate constant ($=k_{-4}$) of 13 s^{-1} . Thus $k_4 (=k_{-4} \cdot K_4) = 1400 \text{ l mol}^{-1} \text{ s}^{-1}$.

Table 4.36 Kinetic and equilibrium data for the 1:1 adduct forming reactions of ethanethiolate ions with ethylpicrate in 10/90 dioxan/H₂O (v/v)

I = 0.25M (NaCl) Data at 500nm

10 ⁴ [Ethyl picrate] M	10 ⁴ [EtSH] M	10 ³ [OH] excess M	a A ₅₀₀ ^{init}	b A ₅₀₀ ^{final}	c K ₁ l mol ⁻¹	d K ₄ l mol ⁻¹	k _{obs} s ⁻¹
5	2	nil	0.035	0.058	95	90	13
		ca 0.25	0.067	0.067			
		0.5	0.094	0.219			
		1.0	0.105	0.235			
		2.0	0.108	0.242			
5	4	0.5	0.148	0.292	97	107	13
		1.0	0.189	0.403			
		2.0	0.215	0.469			
		3.0	0.215	0.488			13
5	1	1	0.063	0.108	140	115	
		2	0.075	0.168			
		3	0.078	0.190			
3	2	nil	0.025	0.041	97	116	13
		0.5	0.054	0.102			
		1	0.063	0.131			
		2	0.067	0.137			
		4	0.067	0.150			

a absorbance at completion of the very rapid reaction forming the 1,3 adduct, normalised to a pathlength of 1 cm.

b absorbance at completion of the 1,1 and 1,3 adduct forming reactions.

c calculated with $\epsilon_{1:1} = 1.2 \times 10^4 \text{ l mol}^{-1} \text{ cm}^{-1}$. Account is taken of the depletion of S⁻Et and ethylpicrate.

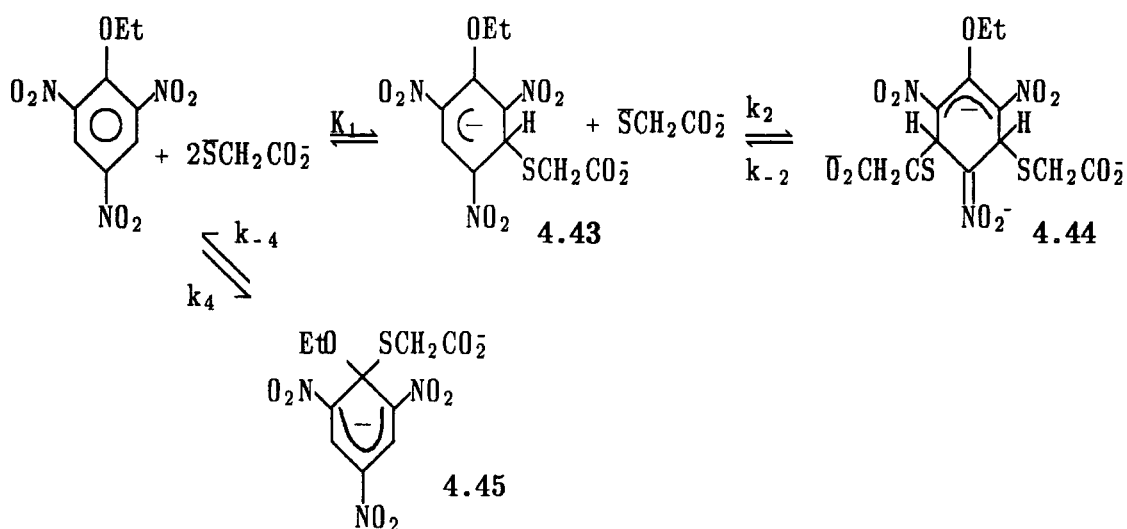
d calculated with $\epsilon_{1:1} = 1.2 \times 10^4 \text{ l mol}^{-1} \text{ cm}^{-1}$ using $[\text{SEt}^-] = \frac{A_{\text{initial}} [\text{EtSH}]_0}{A_{\infty}}$

where A_{∞} is the initial absorbance corresponding to complete ionisation of the thiol.

Ethylpicrate and thioglycolate anions

There was evidence for the formation of 1:1 adducts (λ_{\max} 440nm) and a 1:2 adduct (λ_{\max} 426nm, $\epsilon = 9.5 \times 10^3 \text{ l mol}^{-1} \text{ cm}^{-1}$). Spectra are shown in figures 4.40 and 4.41.

Stopped-flow measurements in water showed three reversible processes as before. Nucleophile attack at an unsubstituted position to form 4.43 was too fast for kinetic measurement. Values of the equilibrium constant were best calculated with an extinction coefficient of $1.9 \times 10^4 \text{ l mol}^{-1} \text{ cm}^{-1}$ at 440nm to give $K_1 = 45 \text{ l mol}^{-1}$. Data are shown in table 4.40. Unfortunately there was strong interference between the rate processes forming 4.44 and 4.45 and it was only possible to determine a value of k_{-4} of 25 s^{-1} . In 75/25 water/DMSO where the processes were



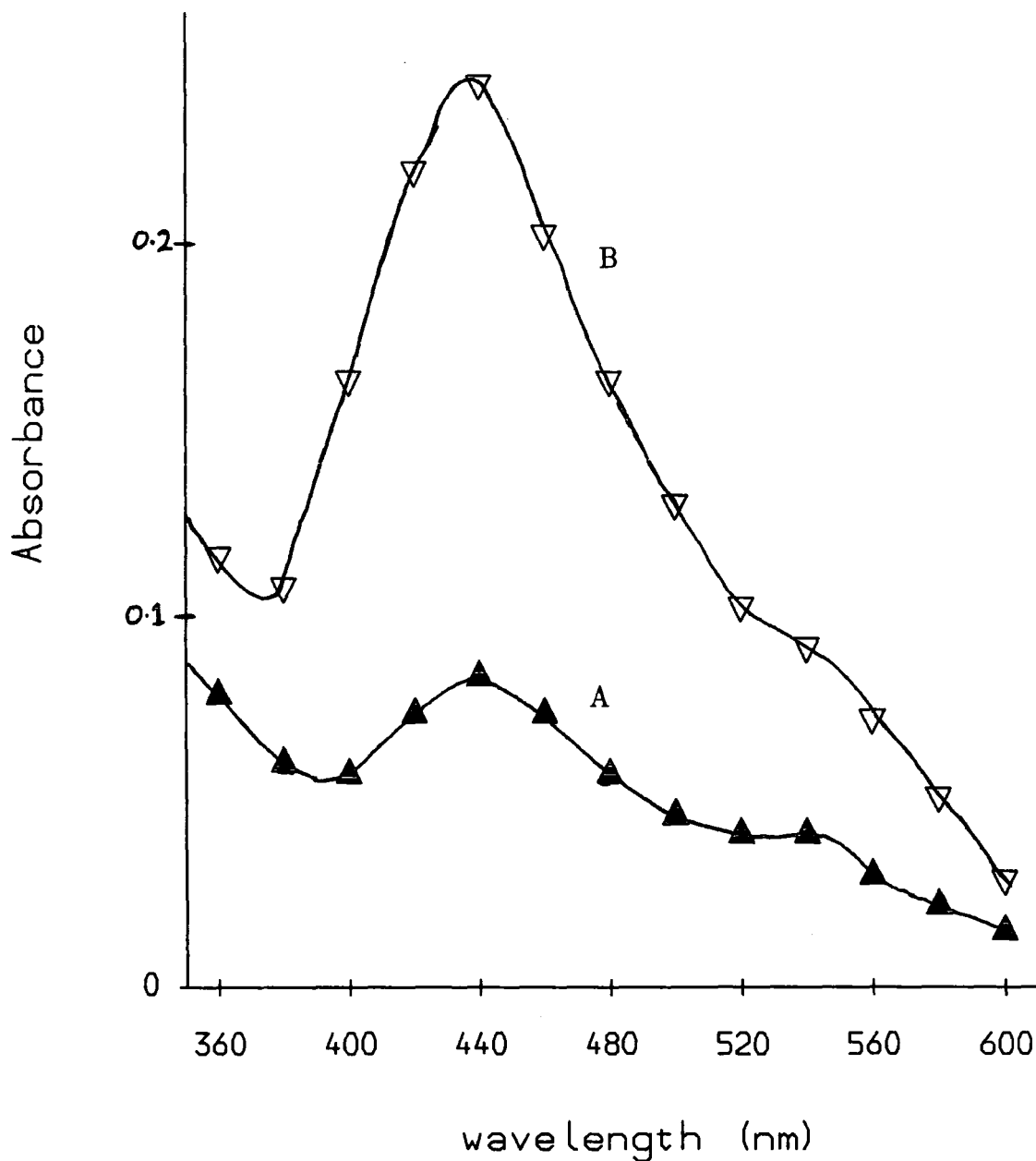
better separated values $k_2 = 1.9 \times 10^4 \text{ l mol}^{-1} \text{ s}^{-1}$ and $k_{-2} = 10 \text{ s}^{-1}$ were obtained leading to a value of $K_2 = 1.9 \times 10^3 \text{ l mol}^{-1}$. In this solvent (table 4.42) the value of the equilibrium constant K_1 was increased to 190 l mol^{-1} . The value of K_4 was not measured but the accompanying increase in this equilibrium constant is expected² to involve an increase in the rate coefficient k_4 and a decrease in k_{-4} (not measured). Thus values of $k_{\text{obs},2}$, which were independent of wavelength,

were found to be greater than values $k_{\text{obs},4}$.

In water the absorbances are in accord with a value of *ca.* $2.5 \times 10^3 \text{ l mol}^{-1}$ for K_2 . Absorbance values, calculated with this equilibrium constant and known values of extinction coefficient are compared (table 4.40) with experimentally obtained absorbance measurements.

Using $[\text{ethylpicrate}] > [\text{S-CH}_2\text{CO}_2^-]$ where 1:2 adduct formation was relatively disfavoured (table 4.41) it was possible to obtain values of equilibrium constants ($K_1 = 50 \text{ l mol}^{-1}$, $K_4 = 50 \text{ l mol}^{-1}$) for the two isomeric adducts in reasonable agreement with nmr data. The slightly larger value of K_1 is probably a solvent effect on going from water to 10/90 dioxan/ H_2O (v/v). The rate of equilibration with 4.45 was also determined yielding a value of $k_{-1} = 25 \text{ s}^{-1}$ as before.

Figure 4.40



Visible spectra of ethylpicrate ($1 \times 10^{-4} \text{M}$) and $\text{SCH}_2\text{CO}_2^-$ ($1 \times 10^{-3} \text{M}$) in water
Measured by stopped-flow spectrophotometry and normalised to a pathlength of 1cm. Spectrum A was measured at the completion of the rapid reaction and corresponds to that of the 1,3-adduct 4.43. Spectrum B was measured at the completion of all adduct-forming reactions and corresponds to a mixture of the isomeric 1:1 adducts 4.43, 4.45 and the 1:2 adduct 4.44.

BISA

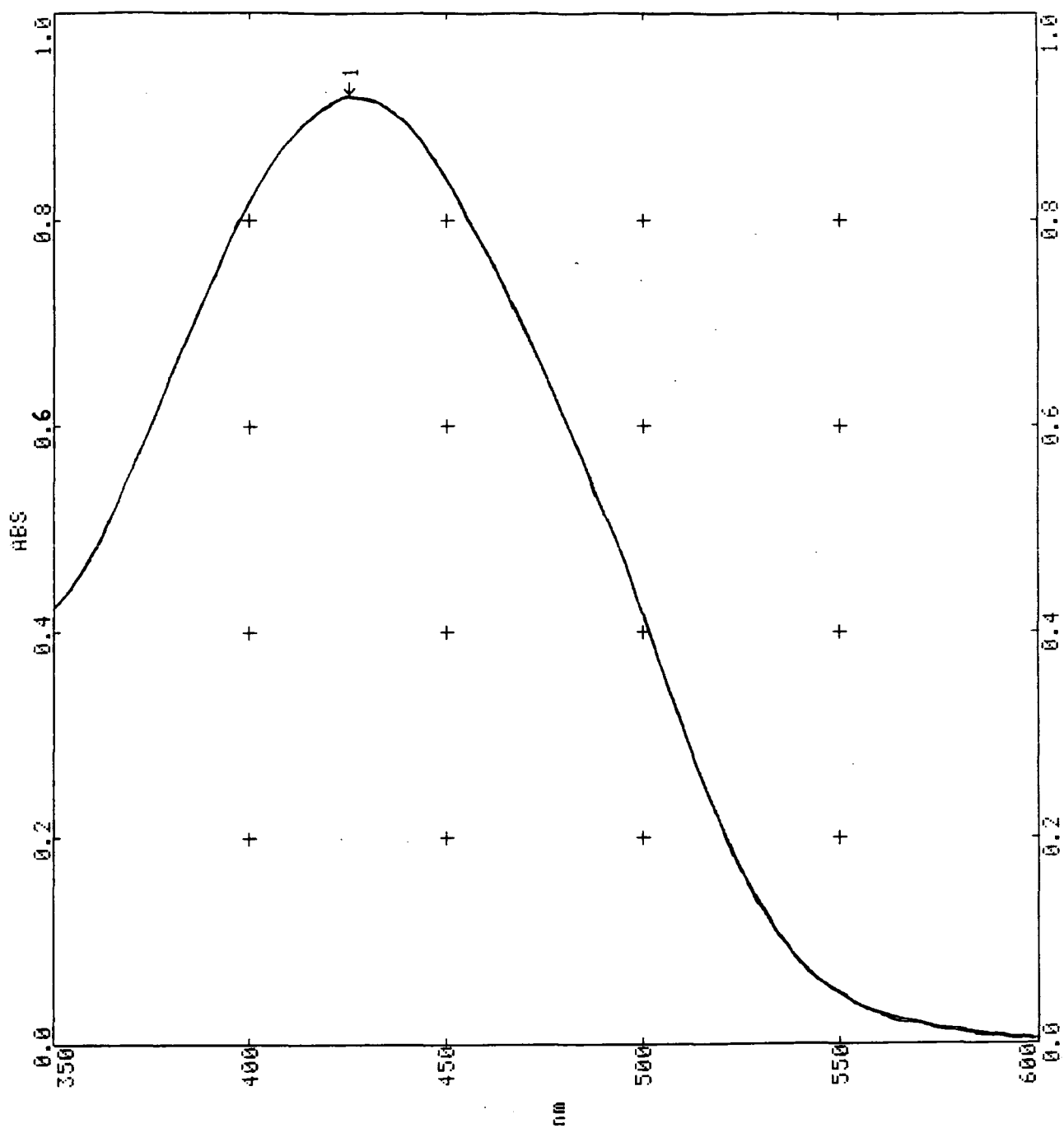


Figure 4.41

Visible spectrum of the 1:2 adduct formed from ethylpicrate ($1 \times 10^{-4} \text{M}$) and $-\text{SCH}_2\text{CO}_2^-$ (0.05M). Spectrum normalised to a pathlength of 1cm.

Table 4.40
Kinetic and Equilibrium data for the reaction of ethylpicrate
with thioglycolate ions in water at 25°C I = 0.25M

$10^3 [-SCH_2CO_2^-]$ M	a	c	b	d	$k_{obs,4}$ s ⁻¹	a	b	e
	A_{440}^{init}	K_1 l mol ⁻¹	A_{440}^{final}	A_{440}^{calc}		A_{500}^{init}	A_{500}^{final}	A_{500}^{calc}
0.5					25			
1	0.084	46	0.240	0.23	26	0.050	0.122	0.12
2	0.163	47	0.460	0.46	26	0.097	0.221	0.23
2	0.161	46	0.441	0.46				
3	0.252	51	0.642	0.53		0.145	0.272	0.31
4	0.290	45	0.733	0.73		0.193	0.288	0.35
4	0.324	51	0.727	0.73				
5	0.360	47	0.792	0.79				
6	0.416	47	0.855	0.81				
7	0.465	46	0.868	0.86				
8	0.524	48	0.830	0.88				
10	0.568	43	0.900	0.90				

- a at completion of the most rapid reaction forming a 1,3 adduct. } normalised to 1×10^{-4} M ethylpicrate and a pathlength of 1 cm.
- b at completion of all adduct forming reactions }

c calculated as

$$\frac{A_{440}^{initial}}{(1.9 - A_{440}^{initial}) [-SCH_2CO_2^-]}$$

- d Absorbances calculated with $K_1=45$ l mol⁻¹, $K_4=45$ l mol⁻¹, $K_2=2.5 \times 10^3$ l mol⁻¹, $\epsilon_{1:1}^{440} = 1.9 \times 10^4$ l mol⁻¹ cm⁻¹ and the measured value of $\epsilon_{1:2}^{440} = 9 \times 10^3$ l mol⁻¹ cm⁻¹
- e Absorbances calculated with the above equilibrium constants, $\epsilon_{1:1}^{500} = 1.1 \times 10^4$ l mol⁻¹ cm⁻¹ and the measured value of $\epsilon_{1:2}^{500} = 4 \times 10^3$ l mol⁻¹ cm⁻¹

Table 4.41 Kinetic and equilibrium data for the reaction of $^-SCH_2CO_2^-$ ions with ethylpicrate in 10/90 dioxan/ H_2O at $25^\circ C$ with $I = 0.25M$

10^4 [Ethyl- picrate] M	10^4 [thiol] M	10^3 [OH $^-$] excess M	a A_{500}^{init}	b A_{500}^{final}	c K_1 $l\text{mol}^{-1}$	c K_4 $l\text{mol}^{-1}$	$k_{obs,4}$ s^{-1}
5	2	nil	0.017	0.030		40	26
		0.5	0.034	0.067		50	26
		1.0	0.056	0.113	48	52	25
		3.0	0.054	—	47		
5	4	0.5	0.099	0.177		35	25
		1.0	0.099	0.183	43	40	
3	2	0.5	0.035	0.062		50	24
		1.0	0.038	0.071	54	50	
		ca 3	0.030	0.071	43	61	

10^3 [$^-SCH_2CO_2^-$] M	a,e $A_{440}^{initial}$	d K_1 $l\text{mol}^{-1}$	b,e A_{440}^{final}
2.0	0.21	52	
4.0	0.37	50	0.73
6.0	0.56	57	0.93
10.0	0.75	52	0.99

- a at completion of the most rapid reaction forming a 1,3 adduct.
- b at completion of all adduct forming reactions
- c calculated with $\epsilon_{1:2}^{500} = 1.2 \times 10^4 \text{ lmol}^{-1} \text{ cm}^{-1}$
- d calculated as $A_{440}^{initial} / [2.2 - A_{440}^{initial}] [^-SCH_2CO_2^-]$
- e normalised to $1 \times 10^{-4} M$ ethylpicrate

Table 4.42
Kinetic and equilibrium data for the reaction of ethylpicrate
with $^-SCH_2CO_2^-$ in 27/75 DMSO/H₂O (v/v) with I = 0.25M

a	b	c
$10^3 [^-SCH_2CO_2^-]$ M	A_{440}^{init} K_1 l mol ⁻¹	$k_{obs,2}$ k_{calc} s ⁻¹
0.5	0.19 210	10 11
1	0.33 200	14 13
2	0.48 160	22 21
3	0.58	31 31
4	0.94 220	44 43
5		53 56
6	1.00 170	71 71
7		87 86
8	1.15 170	106 102
9		125 118

a absorbance due to formation of 1,1-adduct

b calculated as

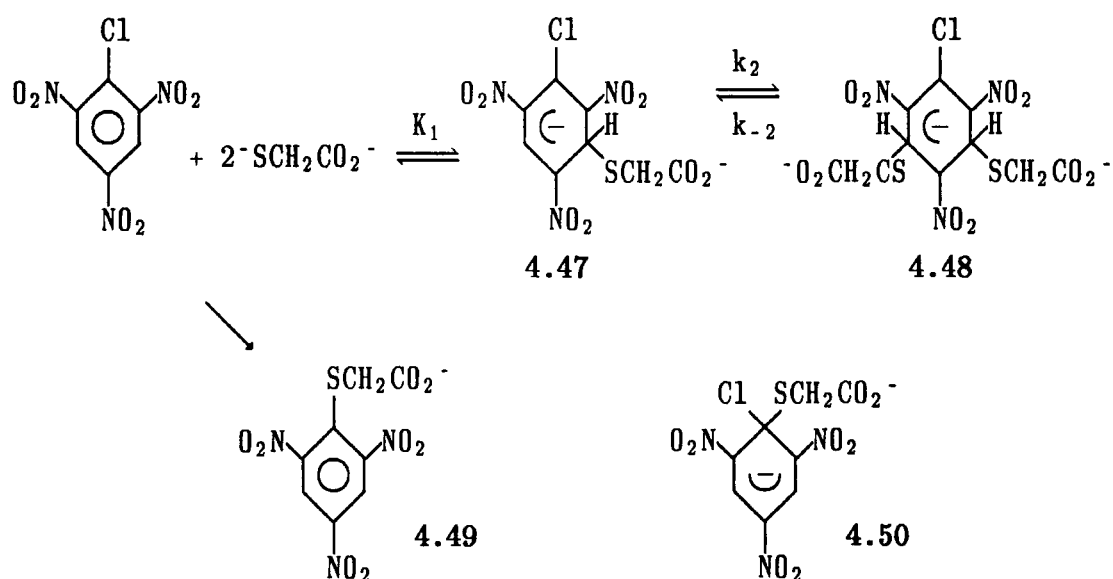
$$\frac{A_{440}^{initial}}{(2.0 - A_{440}^{initial}) [^-SCH_2CO_2^-]}$$

c calculated with $k_2 = 1.9 \times 10^4$ l mol⁻¹ s⁻¹, $k_{-2} = 10$ s⁻¹ and
 $K_1 = 190$ l mol⁻¹ according to expression 4.26

Picryl chloride and thioglycolate ions

When aqueous solutions of picryl chloride and thioglycolate ions ($<2 \times 10^{-3} \text{ M}$) were mixed, UV/visible spectra, taken as soon as possible after mixing the reagents, showed the production of a species with λ_{max} 360nm (quite distinct from the UV/visible spectrum of picrate in water with λ_{max} 356nm) which was taken to be the substituted product 4.49. At higher concentrations of thioglycolate the spectrum of a 1:2 adduct (λ_{max} 428nm $\epsilon \approx 1 \times 10^4 \text{ l mol}^{-1} \text{ cm}^{-1}$) was observed.

Stopped-flow measurements in water with the nucleophile in excess of the substrate concentration indicated three processes all colour forming at 445nm and 500nm. Absorbance measurements at the completion of the initial rapid process gave a value of $K_1 = 18 \text{ l mol}^{-1}$ for the formation of 4.47. The other two processes were attributed to the formation of 4.49, resulting from nucleophilic attack at the 1-position of picryl chloride and to the formation of 4.48. These two processes were slightly interfering but since equilibration of 4.47 and 4.48 was always a faster process than formation of 4.49, it was possible to obtain individual rate constants. Measurements of $k_{\text{obs},2}$ at both wavelengths were in good agreement and were usually obtained by an extrapolation of the linear portion of the absorbance vs. time plot to obtain an infinity value or sometimes by a double exponential curve



fitting procedure. It was sometimes possible to obtain absorbance values at the reactions forming 4.47 and 4.48. These are consistent with a value for K_2 of 1000 l mol^{-1} . Values of A_{calc} , shown in the table, were calculated by using measurements of $\epsilon_{1:2}$ obtained from spectra ($[\text{S}^-] > 0.1\text{M}$) where conversion to the di-adduct was complete. Rate data lead to values $k_2 = 2.6 \times 10^4 \text{ l mol}^{-1} \text{ s}^{-1}$ and $k_{-2} = 25 \text{ s}^{-1}$.

Rates of the slow process, $k_{\text{obs},4}$, are unlikely to be of high accuracy. Production of 4.49 involves formation of the intermediate 4.50 from which expulsion of chloride is expected to be rapid. Nucleophilic attack on picryl chloride is thus rate determining and expression 4.51, derived in the appendix, thus applies. A value for k_4 of *ca.* $1000 \text{ l mol}^{-1} \text{ s}^{-1}$ is in reasonable agreement with observed values for $[\text{S}^-] < 6 \times 10^{-3} \text{M}$. 4.49 is also expected to react with excess thioglycolate ions to give σ -adducts. Such reactions will become more important as $[\text{S}^-]$ is increased and may be one cause of the deviation shown between the observed and calculated values for larger $[\text{S}^-]$.

$$k_{\text{obs},4} = \frac{k_4 [\text{S}^-]}{1 + K_1 [\text{S}^-] + K_1 K_2 [\text{S}^-]^2} \quad 4.51$$

Ethylpicrate and thiomalate ($[\text{S}^-(\text{CO}_2^-)\text{CH}_2\text{CO}_2^-]$) ions

Visible spectra indicate that with $[\text{RS}^-] < 0.03\text{M}$ the parent is in equilibrium with 1:1 adducts, (see figure 4.52) λ_{max} 440nm and 530nm (shoulder). At higher concentrations there is progressive conversion to a 1:2 adduct (λ_{max} 430nm $\epsilon = 9 \times 10^3 \text{ l mol}^{-1} \text{ cm}^{-1}$). Stopped-flow measurements indicate the formation of two 1:1 adducts. Absorbances obtained at the completion of the rapid process forming a 1,3-adduct lead to a value of $K_1 = 8 \text{ l mol}^{-1}$. The measurable rate process associated with the formation of the 1,1-adduct gives a value of k_{-4} of 33 s^{-1} while absorbances lead to a value of $K_4 = 10 \text{ l mol}^{-1}$. Data are shown in table 4.52.

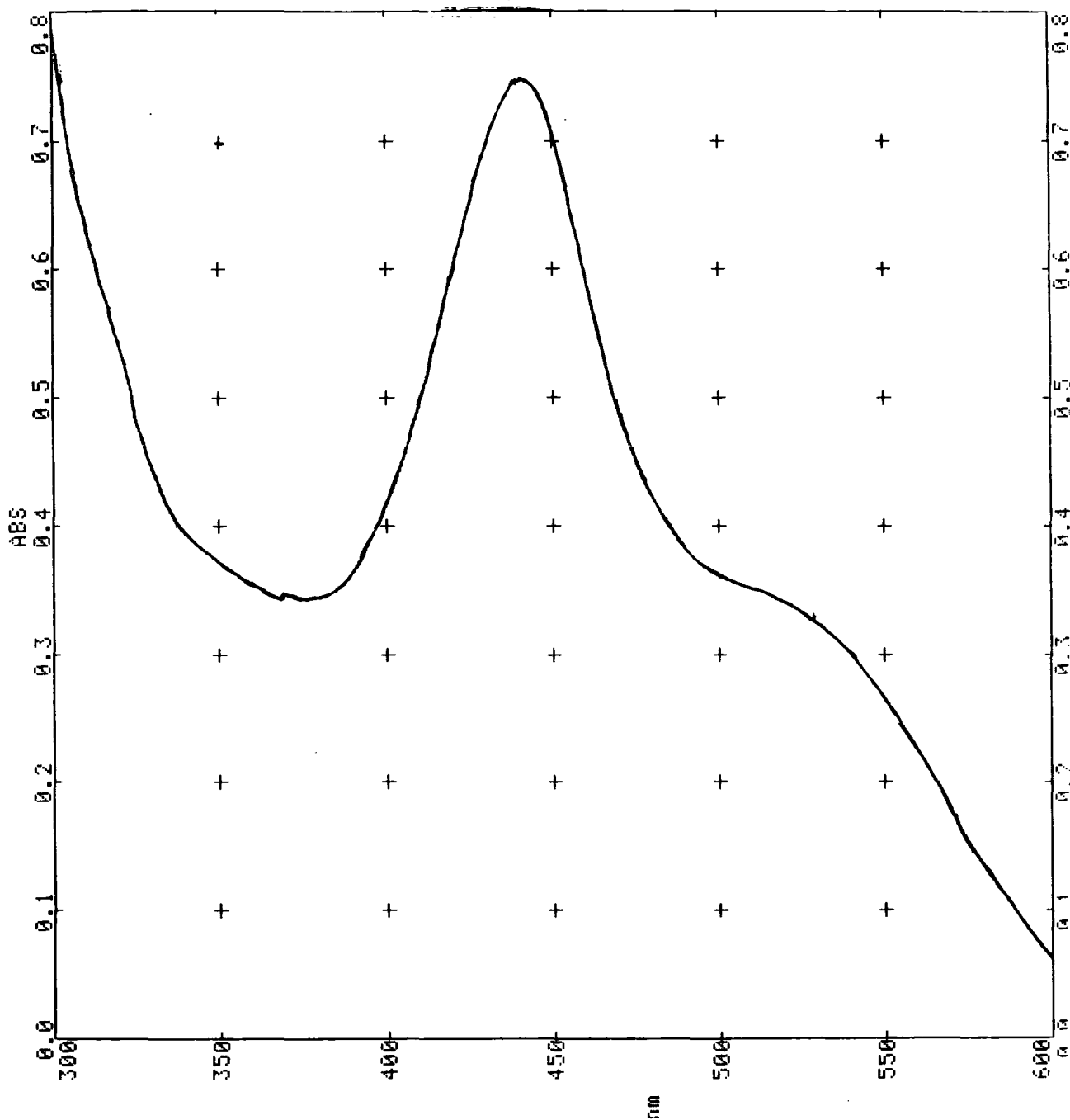


Figure 4.52

Visible spectra of the 1:1 adducts formed from ethylpicrate ($2 \times 10^{-4} \text{M}$) and $^-\text{SCH}(\text{CO}_2^-)\text{CH}_2\text{CO}_2^-$ (0.02M). Spectra normalised to a pathlength of 1cm.

Table 4.46

Kinetic and equilibrium data for the reaction of picryl chloride with thioglycolate ions in water at 25°C with I=0.25M

$10^3 [-SCH_2CO_2^-]$ M	^a A_{445nm}^{init}	^c K_1 l mol ⁻¹	^a A_{500nm}^{init}	^d K_1 l mol ⁻¹	^e $k_{obs,2}$ k_{calc} s ⁻¹ s ⁻¹		^b A_{445}	^f A_{calc}	^b A_{500}	^g A_{calc}	^{k_{obs,4}} k_{calc} s ⁻¹ s ⁻¹	^h k_{calc} s ⁻¹	ⁱ A_{445nm}^{final}
1.0	0.030	15	—	—	26	25	not measurable		—	—	0.8	1.0	0.175
2.0	0.074	19	0.041	18	27	27			0.053	0.062	1.4	1.8	0.408
4.0	0.144	19	0.086	19	29	32			0.141	0.138	3.4	3.0	0.731
6.0	0.173	16	0.102	15	35	40			0.195	0.203	4.0	3.4	0.779
8.0	0.246	17	0.147	17	44	51			0.253	0.251	(7.9)	3.5	0.796
10.0	0.318	19			65	65	0.675	0.665					0.850
12.0					79	80	0.682	0.726			(7.5)	3.2	0.820
16.0					130	117	0.730	0.801			(4.5)	2.7	0.868

a at completion of formation of 1,3-adduct } normalised to a pathlength of 1cm

b at completion of all adduct forming reactions } and 1×10^{-4} M picryl chloride.

c calculated as $A_{445nm}^{initial} / \left[2.0 - A_{445nm}^{initial} \right] [-SCH_2CO_2^-]$ Assuming a value of $\epsilon_{1:1}(445nm) = 2.0 \times 10^4$ l mol⁻¹ cm⁻¹

d calculated as $A_{500nm}^{initial} / \left[1.2 - A_{500nm}^{initial} \right] [-SCH_2CO_2^-]$ Assuming a value of $\epsilon_{1:1}(500nm) = 1.2 \times 10^4$ l mol⁻¹ cm⁻¹

e calculated with $k_2 = 2.6 \times 10^4$ l mol⁻¹ s⁻¹, $k_{-2} = 25$ s⁻¹ and $K_1 = 18$ l mol⁻¹ from equation 4.26

- f calculated with $K_2 = 1000 \text{ l mol}^{-1}$, $K_1 = 18 \text{ l mol}^{-1}$, $\epsilon_{1:1} = 2 \times 10^4 \text{ l mol}^{-1} \text{ cm}^{-1}$ and $\epsilon_{1:2} = 9 \times 10^3 \text{ l mol}^{-1} \text{ cm}^{-1}$
- g calculated with $K_2 = 1000 \text{ l mol}^{-1}$, $K_1 = 18 \text{ l mol}^{-1}$, $\epsilon_{1:1} = 1.2 \times 10^4 \text{ l mol}^{-1} \text{ cm}^{-1}$ and $\epsilon_{1:2} = 3.5 \times 10^3 \text{ l mol}^{-1} \text{ cm}^{-1}$
- h calculated with $K_2 = 1000 \text{ l mol}^{-1}$, $K_1 = 18 \text{ l mol}^{-1}$ and $k_4 = 1000 \text{ l mol}^{-1} \text{ s}^{-1}$ from equation 4.51
- i final absorbance at completion of all reactions.

12/19

Table 4.52 Kinetic and equilibrium data for the reactions of ethylpicrate with thiomalate ions in water at 25°C with I=0.25M

$10^2 [MS^-]$ M	A_{440nm}^{init} ^a	K_1 ^b l mol ⁻¹	A_{440nm}^{final} ^c	$K_{1,4}$ ^{b,e} l mol ⁻¹	A_{500nm}^{init} ^a	K_1 ^d l mol ⁻¹	A_{500nm}^{final} ^c	$K_{1,4}$ ^{d,e} l mol ⁻¹	k_{obs}^{440} s ⁻¹	k_{obs}^{500} s ⁻¹
0.1 [*]	0.020	10	0.050	26	0.010	8	0.025	21	—	—
0.2 [*]	0.031	8	0.076	20	0.018	8	0.041	18	32	32
0.3 [*]	0.039	7	0.085	15	0.022	6	0.049	14		34
0.4 [*]	0.051	7	0.111	15	0.030	6	0.061	13		
0.4 [*]	(0.055)	7	(0.121)	16						
0.5	0.088	9	0.210	23	0.041	7		—		34
0.8	0.103	7	0.289	21	0.079	9	0.173	21		
0.8	(0.108)	7	(0.312)	23	(0.074)	8	(0.174)	21		
1.0	0.13	7	0.32	19	0.08	7	0.16	15		—
1.2	0.15	7	0.38	20	0.12	9	0.23	20	33	35
1.4	0.19	8	0.47	22	—	—	—	—		
2.0	0.24	7	0.57	20	0.13	6	0.28	15		
3.0	0.29	6	0.60	16	0.21	7	0.35	14		
4.0	0.46	8	0.90	20	0.29	8	0.46	16		
5.0	0.56	8	—	—	0.31	7	—	—		

122

Footnotes to table 4.52

* solvent is 10/90 (v/v) dioxan/water.

a absorbance at completion of formation of the 1,3-adduct normalised to $1 \times 10^{-4} \text{M}$ ethylpicrate and a pathlength of 1cm.

b calculated as $A_{440} / (2.0 - A_{440}) [\text{MS}^-]$ Assuming $\epsilon_{1:1} = 2.0 \times 10^4 \text{ l mol}^{-1} \text{ cm}^{-1}$ at 440nm.

c absorbance at completion of formation of both 1:1 adducts

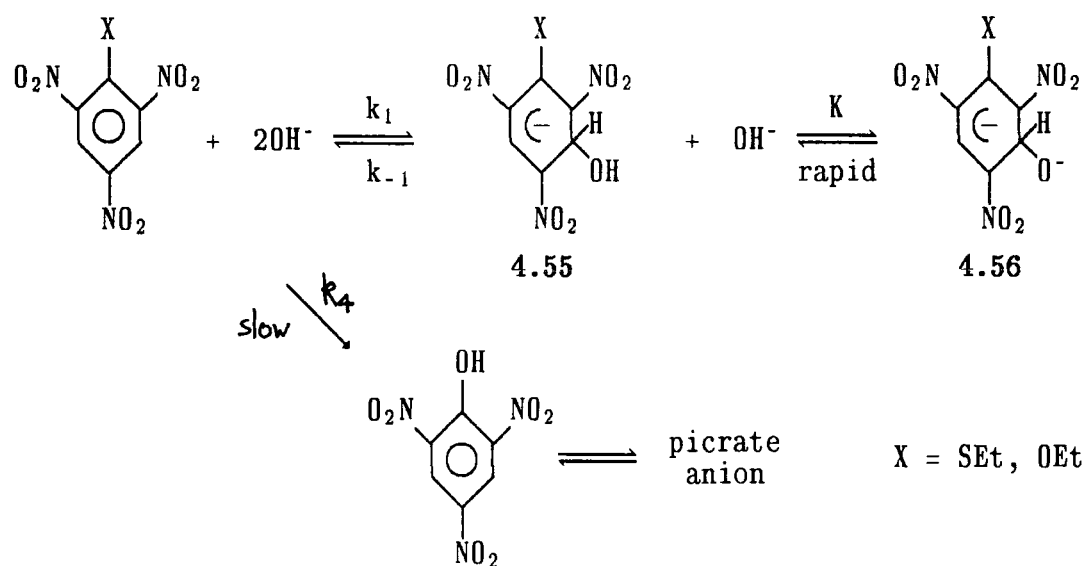
d calculated as $A_{500} / (1.2 - A_{500}) [\text{MS}^-]$ Assuming $\epsilon_{1:1} = 1.2 \times 10^4 \text{ l mol}^{-1} \text{ cm}^{-1}$ at 500nm.

e $K_{1,4} = K_1 + K_4$

(Bracketed values are those obtained with 0.01M excess hydroxide instead of the usual $5 \times 10^{-3} \text{M}$ excess.)

Reactions of ethylthiopicate and ethylpicrate with hydroxide ions.

On mixing solutions of the nitrocompounds with sodium hydroxide the red colour due to the formation of adducts gradually faded to give picrate with its distinctive visible spectrum (λ_{\max} 356nm). Data are interpreted according to the scheme below which allows for the rapid ionisation of adducts 4.55 to give the di-anions 4.56. Expression 4.57 (derived in the appendix) is the relevant expression for the more rapid process; the apparent equilibrium constant K_c is related to K_1 in expression 4.58.



$$k_{\text{fast}} = k_1 [\text{OH}^-] + \frac{k_{-1}}{1 + K[\text{OH}^-]} \quad \text{4.57}$$

$$K_c = K_1 (1 + K[\text{OH}^-]) \quad \text{4.58}$$

$$k_{\text{slow}} = k_4 [\text{OH}^-] \quad \text{4.59}$$

In both reactions, the ionic strength was maintained to $I = 1.0\text{M}$ with NaCl. In order to minimise turbulence, for $[\text{OH}^-] \leq 0.5\text{M}$, solutions of identical ionic strength were mixed in the stopped-flow apparatus.

With ethylthiopicrate values of k_{calc} calculated with $k_1 = 4.8 \text{ l mol}^{-1} \text{ s}^{-1}$, $k_{-1} = 8.3 \text{ s}^{-1}$ and $K = 8 \text{ l mol}^{-1}$ give excellent agreement with observed rate constants. Absorbance values used to obtain values of K_c are in best agreement with calculated values (using K_1 and K determined from kinetics with an extinction coefficient of $1.2 \times 10^4 \text{ l mol}^{-1} \text{ cm}^{-1}$ for 4.55 and 4.56. With ethylpicrate values of $k_1 8.1 \text{ l mol}^{-1} \text{ s}^{-1}$, $k_{-1} = 8.6 \text{ s}^{-1}$ and $K = 2.2 \text{ l mol}^{-1}$ are obtained. Values of K_c (calculated with $\epsilon = 1.2 \times 10^4 \text{ l mol}^{-1} \text{ cm}^{-1}$ for 4.55 and 4.56) are in complete accord with the kinetically determined measurements. Interestingly the value of K (for ionisation of 4.55) for ethylthiopicrate (8 l mol^{-1}) is larger than the corresponding values for ethylpicrate (2.2 l mol^{-1}) and TNA⁴ (2 l mol^{-1} ; $I = 1\text{M}$). These results are in accord with the larger values of σ for sulphur containing substituents at *meta*-positions of the ring than the corresponding values for oxygen containing substituents:^{3,7} For example, for $X = \text{SMe}$, $\sigma_{\text{meta}}^- = 0.167$ while for $X = \text{OMe}$, $\sigma_{\text{meta}}^- = 0.100$ ^{3,7}

In both reactions there was some evidence for the formation of 1:2 adducts at large concentrations of hydroxide but no rate measurements were made for this process.

Rate constants, k_{slow} , were obtained by measuring the rate of picrate formation in dilute solutions of sodium hydroxide where there was little conversion of parent to the adducts 4.55 or 4.56. Equation 4.59 thus applies and values of k_4 obtained were $0.1 \text{ l mol}^{-1} \text{ s}^{-1}$ (ethylthiopicrate) and $0.8 \text{ l mol}^{-1} \text{ s}^{-1}$ (ethylpicrate).

The data are given in tables 4.53 and 4.54.

Table 4.53
Reaction of ethylpicrate^a with hydroxide ions in water at 25°C
with I = 1.0M (NaCl)

[OH ⁻] M	b,e A _{500nm}	c K _c l mol ⁻¹	d K _c ^{calc} l mol ⁻¹	e k _{fast} s ⁻¹	f k _{calc} s ⁻¹	e,g k _{slow} s ⁻¹
0.02	—	—	—	—	—	0.016*
0.04	0.045	0.97	1.02	8.3	8.2	0.033
0.06	0.069	1.02	1.07	8.2	8.1	—
0.08	—	—	—	—	—	0.071
0.10	0.121	1.12	1.15	8.0	7.9	0.085
0.15	—	—	—	7.8	7.7	0.122
0.20	0.250	1.32	1.36	7.7	7.6	0.154
0.30	0.388	1.59	1.56	7.6	7.6	
0.40	0.491	1.73	1.77	7.9	7.8	
0.50	0.610	2.07	1.97	8.2	8.1	
0.60	0.746	2.74	2.19	8.4	8.6	
0.70	0.774	2.59	2.39	8.9	9.0	
0.80	0.821	2.71	2.60	9.6	9.6	
1.00	—	—	—	11.2	10.8	

- a** concentration is 1×10^4 M
- b** absorbance at completion of adduct forming reactions normalised to a pathlength of 1 cm.
- c** calculated as $A_{500} / (1.2 - A_{500})[\text{OH}^-]$ assuming an extinction coefficient of $1.2 \times 10^4 \text{ l mol}^{-1} \text{ cm}^{-1}$ for the hydroxy-adduct and di-anion.
- d** calculated with $K = 2.2 \text{ l mol}^{-1}$ and $K_1 = 0.94 \text{ l mol}^{-1}$ obtained from kinetics.
- e** obtained by stopped-flow spectrophotometry except * obtained by conventional spectrophotometry.
- f** calculated with $K = 2.2 \text{ l mol}^{-1}$, $k_1 = 8.1 \text{ l mol}^{-1} \text{ s}^{-1}$ and $k_{-1} = 8.6 \text{ s}^{-1}$ using expression 4.57
- g** colour-forming at 360nm.

Table 4.54
 Reaction of ethylthiopicrate^a with hydroxide ions in water at 25°C
 with I = 1.0M (NaCl)

[OH ⁻] M	b, e A _{500nm}	c K _c l mol ⁻¹	d K _c ^{calc} l mol ⁻¹	e k _{fast} s ⁻¹	f k _{calc} s ⁻¹	g k _{slow} s ⁻¹
0.02						1.9x10 ⁻³
0.03				6.7	6.8	
0.05				6.2	6.2	4.8x10 ⁻³
0.10	0.095	0.86	1.04	5.1	5.1	8.6x10 ⁻³
0.15	—			4.5	4.5	
0.20	0.213	1.08	1.50	4.2	4.2	
0.30	0.403	1.69	1.97	3.9	3.9	
0.40	0.580	2.33	2.43	3.9	3.9	
0.50	0.721	3.01	2.89	4.1	4.1	
0.60	0.809	3.44	3.35	4.3	4.3	
0.80				5.0	5.0	
1.00				6.2	5.7	

- a concentration is 1×10^4 M
 b absorbance at completion of adduct forming reactions normalised to a pathlength of 1 cm.
 c calculated as $A_{500} / (1.2 - A_{500})[\text{OH}^-]$ assuming an extinction coefficient of $1.2 \times 10^4 \text{ l mol}^{-1} \text{ cm}^{-1}$ for the hydroxy-adduct and di-anion.
 d calculated with $K = 8 \text{ l mol}^{-1}$ and $K_1 = 0.58 \text{ l mol}^{-1}$ obtained from kinetics using expression 4.58
 e obtained by stopped-flow spectrophotometry.
 f calculated with $K = 8 \text{ l mol}^{-1}$, $k_1 = 4.8 \text{ l mol}^{-1} \text{ s}^{-1}$ and $k_{-1} = 8.3 \text{ s}^{-1}$ using expression 4.57
 g obtained by conventional spectrophotometry at 360nm.

Conclusions and Comparisons

Data, summarised in table 4.60, show that values of the equilibrium constant K_1 for attack at unsubstituted ring positions are reduced by the presence of substituents at the 1-position of the substrate. For example with SEt^- as the nucleophile K_1 is reduced from 200 l mol^{-1} for TNB to 95 l mol^{-1} and 85 l mol^{-1} for ethylpicrate and ethylthiopicate respectively. These reductions in equilibrium constant can be attributed to the steric effect of the 1-substituent which results in distortion from the ring plane of the adjacent nitro-groups thus reducing their electron withdrawing ability. This steric effect is more important in picryl chloride than the electron withdrawing nature of the chlorine substituent; the value of K_1 for $^- \text{SCH}_2\text{CO}_2^-$ is reduced by a factor of 14 on going from TNB to picryl chloride. Other factors such as solvation differences will also play a part in determining relative stabilities of the adducts.

For a given nucleophile, values of K_2 are seen to increase with increasing size of the 1-substituent ($\text{SEt} > \text{OEt} > \text{H}$ and $\text{OEt} > \text{Cl} > \text{H}$). Similar trends have been observed previously in the reactions of sodium sulphite with 1-substituted-2,4,6-trinitrobenzenes.^{2,6,1} The increase has been attributed to the release of steric strain at Cl in the 1:2 adducts relative to 1:1 adducts or parent molecules. The degree of steric relief on forming 1:2 adducts would be expected to increase with increasing size of the 1-substituent.

The values of K_2 for thioglycolate (and thiomalate) ions are much reduced relative to corresponding values for ethanethiolate ions partly owing to electrostatic repulsion between the negatively charged carboxyl groups and the negative charge in the initially formed 1:1 adduct.

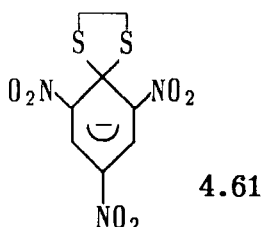
Measurement of rate coefficients k_1 and k_{-1} for thiolate addition was not possible by a stopped-flow method. However values of k_1 for the reaction of TNB with anions derived from glutathione, thioglycolic and thiomalic acids are in the

range $1 - 2 \times 10^6 \text{ l mol}^{-1} \text{ s}^{-1}$ with values of K_1 ranging from 15 (glutathione) to 250 l mol^{-1} (thioglycolate). Related to this, Bernasconi and Killion³¹ have recently found a very low β_{nuc} value for thiolate addition to α -nitrostilbenes indicating a small dependence of the forward rate constant on thiolate basicity. Values of k_1 for thiolate addition to ethylthiopicate, ethylpicrate and picryl chloride are thus expected to have values of *ca.* $10^6 \text{ l mol}^{-1} \text{ s}^{-1}$. Since values of K_1 are *ca.* 10^2 l mol^{-1} the values of k_{-1} (k_1/K_1) will be *ca.* 10^4 s^{-1} . The measured values of k_4 for thiolate attack to the 1-substituted position are all *ca.* $10^3 \text{ l mol}^{-1} \text{ s}^{-1}$. Hence the thiolate anions, like alkoxide but unlike phenoxide, show strong kinetic preference for attack at unsubstituted positions of the aromatic ring. A similar kinetic preference has been demonstrated in the reactions of 1-substituted-2,4,6-trinitrobenzenes with carbanions^{2,8} Interestingly the values of k_4 given in the table show little dependence on the nature of the 1-substituent ($-\text{OEt}$, $-\text{SEt}$ or $-\text{Cl}$).

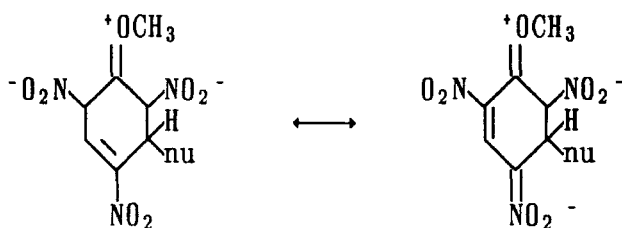
In a given system values obtained for K_1 and K_4 in aqueous are broadly similar indicating that the adducts formed from thiolate attack at unsubstituted positions and at $-\text{SEt}$ (or $-\text{OEt}$) substituted positions have similar thermodynamic stabilities. This is also shown in the nmr data in $[\text{}^2\text{H}_6]\text{-DMSO}/\text{H}_2\text{O}$.

By contrast, alkoxide addition to 2,4,6-trinitrophenyl ethers produces 1,1-adducts (by addition at a substituted ring position) which have considerably greater stabilities than their isomeric 1,3-adducts.¹ The larger stability of the 1,1 adducts is probably primarily related to the special stabilising effect of two electronegative substituents attached to an sp^3 hybridised carbon atom^{2,3,27} This stabilisation is expected to be much less important with two sulphur atoms at C1 or with a combination of oxygen and sulphur, sulphur being less electronegative than oxygen^{1,2} Both these latter types of adducts will also be destabilised by increasing steric interactions as alkoxy groups are changed to the more bulky thioalkoxy groups. Such steric factors are thought to contribute to the low stability of

dithiolane adducts such as 4.61 relative to their oxygen analogues³³ The slightly greater stability of the 1,3-adducts formed from ethylthiopicrate and SEt^- over the 1,1 isomeric adduct has been attributed¹¹ to the tendency of bivalent sulphur to accept electrons by d-orbital participation. Clearly this cannot operate in the 1,1 adduct.

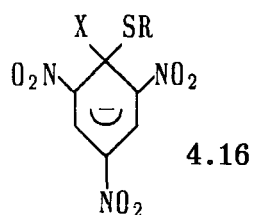


Similarly, the reaction of TNA with cyanide in chloroform²⁹ and of TNA with dimethylmalonate ions in DMSO³⁰ both yield mixtures of the isomeric 1:1 adducts, the 1,3-adducts being slightly favoured at equilibrium relative to the 1,1-adducts. The fact that the 1,3-adducts can benefit from resonance stabilisation involving both methoxy and nitro-groups²³ may be significant here.



Comparisons of equilibrium values (table 4.60) for hydroxide attack with those for corresponding attack of thiolate ions reveals the much lower thermodynamic affinity of the oxygen base ("hard" relative to sulphur) with aromatic carbon (a "soft" acid). Values of rate coefficients for hydroxide attack are also much lower, as expected.

Previous work has shown that the intrinsic barrier (for reaction at a trinitro-activated ring) for thiolate ions is much lower than that for hydroxide ions. These differences can be explained by the poorer solvation in water of thiolate ions relative to hydroxide ions^{3,2} and, in the case of thiolate addition, by the development of a "soft - soft" interaction ahead of bond formation.^{3,1} A consequence of the lower energy barrier to reaction with thiolate ions than with oxygen bases is that during the nucleophilic substitution of ethylpicrate with thiolate ions intermediates of structure 4.16 (X = OEt) are observable. Thus 4.16 (X = OEt) will release thiolate ions in preference to ethoxide. In contrast the



intermediate 4.16 (X=OH,R=Et) formed by hydroxide attack on ethylthiopicate is not observed since it is unstable with respect to loss of thioethoxide. These observations confirm the theoretical predictions of Miller^{3,4}.

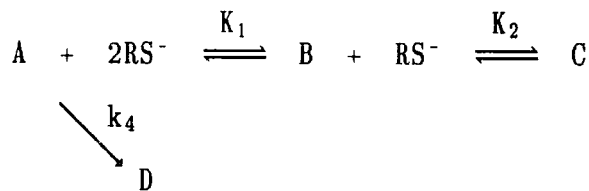
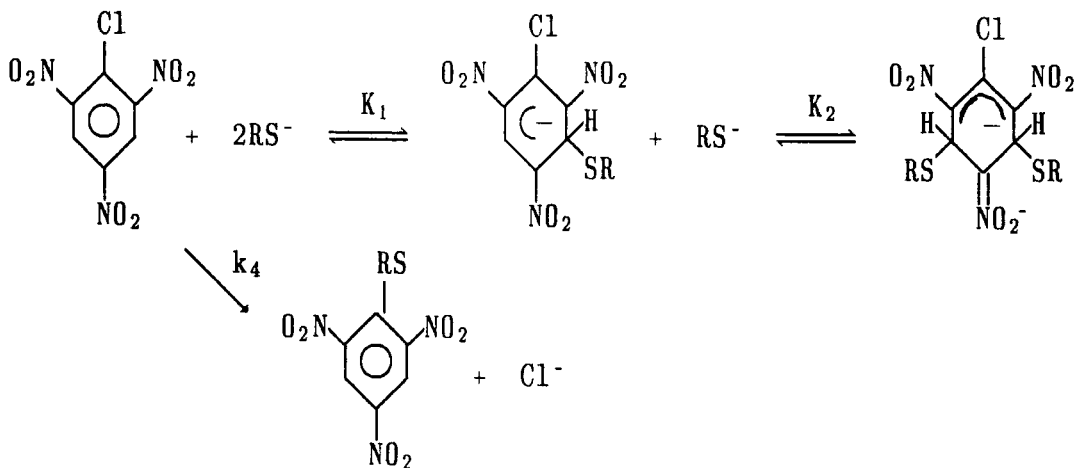
Table 4.60 Summary of kinetic and equilibrium data for adduct formation in water with $I = 0.25M$

parent	nucleophile	k_1 $l\text{mol}^{-1}\text{s}^{-1}$	k_{-1} s^{-1}	K_1 $l\text{mol}^{-1}$	k_4 $l\text{mol}^{-1}\text{s}^{-1}$	k_{-4} s^{-1}	K_4 $l\text{mol}^{-1}$	k_2 $l\text{mol}^{-1}\text{s}^{-1}$	k_{-2} s^{-1}	K_2 $l\text{mol}^{-1}$	pK_a
TNB ^a ethylthiopicrate	SEt^-	—	—	200	—	—	—	3×10^4	3	1×10^4	10.6^j
	SEt^-	—	—	85	840	30	28	1.9×10^5	1	2×10^5	10.6^j
ethylpicrate TNB ^b	SEt^-	—	—	95	1430	13	110	—	—	2.5×10^4	10.6^j
	$^-\text{SCH}_2\text{CO}_2^-$	1.4×10^6	5500	250	—	—	—	3.3×10^3	8	400	10.7^j
ethylpicrate picryl chloride	$^-\text{SCH}_2\text{CO}_2^-$	—	—	45	1125	25	45	1.9×10^4 ⁱ	10^i	900^i	10.7^j
	$^-\text{SCH}_2\text{CO}_2^-$	—	—	18	1000	—	—	2.6×10^4	25	1000	10.7^j
ethylpicrate TNB ^b	$^-\text{SCH}(\text{CO}_2^-)\text{CH}_2\text{CO}_2^-$	—	—	8	330	33	10	—	—	—	11.1^k
	$^-\text{SCH}(\text{CO}_2^-)\text{CH}_2\text{CO}_2^-$	1.2×10^6	3×10^4	33	—	—	—	250	33	8	11.1^k
TNB ^c	OH^-	37.5	9.8	3.73 $(2.7)^{d,e}$	—	—	—	—	—	—	13.4^l
TNA ^f	OH^-	12	8.3	1.4	1.4^*	—	—	—	—	—	13.4^l
picryl chloride ^g ethylpicrate ^h ethylthiopicrate ^h	OH^-	12	1.4	0.4	0.4	—	—	—	—	—	13.4^l
	OH^-	8.1	8.6	0.8	0.8	—	—	—	—	—	13.4^l
	OH^-	4.8	8.3	0.1	0.1	—	—	—	—	—	13.4^l

a values also obtained for $k_3=900 \text{ l mol}^{-1}\text{s}^{-1}$ and $k_{-3}=10 \text{ s}^{-1}$ b data in 10/90 (v/v) dioxan/ H_2O c ref. 23, data in 10/90 (v/v) dioxan/ H_2O $I=0.5M$ d ref. 24 e ref. 25 f ref. 4 $I=1M$ (NaCl) except * $I=2M$ (NaCl) g ref. 4 $I=2M$ (NaCl) $I=1M$ (NaCl) i data refer to 25/75 (v/v) DMSO/ H_2O j ref. 35. Value in water. k ref. 36. Value in water. l ref. 23. Value in 10/90 (v/v) dioxan/ H_2O

Appendix

Derivation of rate expression 4.51



$$\frac{d[D]}{dt} = k_4 [A] [RS^-]$$

The stoichiometric concentration of A is given by

$$[A]_0 = [A] + [B] + [C] + [D]$$

The equilibrium constants K_1 and K_2 are defined by:

$$K_1 = \frac{[B]}{[RS^-][A]} \quad K_2 = \frac{[C]}{[B][RS^-]}$$

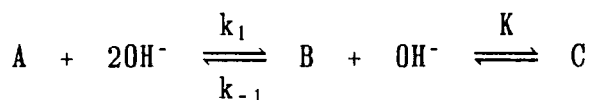
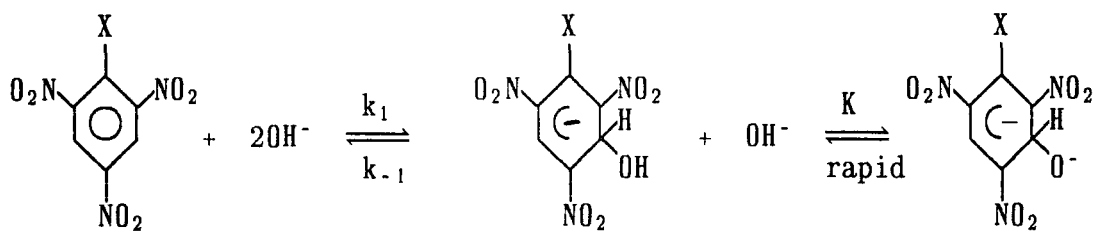
The above three equations are used to obtain $[A]$ in terms of $[D]$:

$$[A] = \frac{[A]_0 - [D]}{1 + K_1 [RS^-] + K_1 K_2 [RS^-]^2}$$

Hence
$$\frac{d[D]}{dt} = \frac{k_4 ([A]_0 - [D]) [RS^-]}{1 + K_1 [RS^-] + K_1 K_2 [RS^-]^2}$$

And
$$k_{\text{obs}} = \frac{1}{([A]_0 - [D])} \frac{d[D]}{dt} = \frac{k_4 [RS^-]}{1 + K_1 [RS^-] + K_1 K_2 [RS^-]^2} \quad 4.51$$

Derivation of rate expression 4.57



The rate of loss of A is given by
$$-\frac{d[A]}{dt} = k_1 [A] [OH^-] - k_{-1} [B]$$

The stoichiometric concentration of A is
$$[A]_0 = [A] + [B] + [C]$$

K is defined as
$$K = \frac{[C]}{[B] [OH^-]}$$

Thus
$$[B] = \frac{[A]_0 - [A]}{1 + K [OH^-]}$$

Hence
$$-\frac{d[A]}{dt} = k_1 [A] [OH^-] + \frac{k_{-1} ([A] - [A]_0)}{1 + K [OH^-]}$$

At equilibrium

$$-\frac{d[A]}{dt} = 0 = k_1 [A]_{\text{eq}} [\text{OH}^-] + \frac{k_{-1} ([A]_{\text{eq}} - [A]_0)}{1 + K[\text{OH}^-]}$$

Subtracting

$$-\frac{d[A]}{dt} = ([A] - [A]_{\text{eq}}) \left[k_1 [\text{OH}^-] + \frac{k_{-1}}{1 + K[\text{OH}^-]} \right]$$

$$\frac{-1}{([A] - [A]_{\text{eq}})} \frac{d[A]}{dt} = k_{\text{obs}} = k_1 [\text{OH}^-] + \frac{k_{-1}}{1 + K[\text{OH}^-]} \quad \mathbf{4.57}$$

References

- 1 F Terrier, *Chem. Rev.*, 1982,82,77
- 2 E Buncl, MR Crampton, MJ Strauss, F Terrier, "*Electron Deficient Aromatic- and Heteroaromatic-Base Interactions*", Elsevier, Amsterdam, 1984
- 3 MJ Strauss, *Chem. Rev.*, 1970,70,667
- 4 B Gibson, MR Crampton, *J. Chem. Soc. Perkin Trans. II*, 1979,648
- 5 MR Crampton, C Greenhalgh, *ibid.*, 1986,187
- 6 E Buncl, JM Dust, A Jonczyk, I Onyido. Personal Communication
- 7 CF Bernasconi, MC Muller, *J. Am. Chem. Soc.*,1978,100,5530
- 8 MR Crampton, *J. Chem. Soc. (B)*, 1968,1208
- 9 TV Leshina, KV Solodova, SM Shein, *J. Org. Chem., USSR*, 1974,10,354
- 10 L-H Gan, *Aust. J. Chem.*, 1977,30,1475
- 11 G Biggi, F Pietra, *J. Chem. Soc., Chem. Commun.*, 1973,229
- 12 G Biggi, F Pietra, *J. Chem. Soc. Perkin Trans. I*, 1973,1980
- 13 M Cavazza, G Morganti, A Guerriero, F Pietra, *Tetrahedron Lett.*, 1980,21,3703
- 14 CA Veracini, F Pietra, *J. Chem. Soc., Chem. Commun.*, 1974,623
- 15 G Biggi, CA Veracini, F Pietra, *ibid.*, 1974, 523
- 16 P Cogolli, L Testaferri, M Tingoli, M Tiecco, *J. Org. Chem.*, 1979,44,2636
- 17 JR Beck, JA Yahner, *ibid.*, 1978,43,2048
- 18 A Kotaki, M Harada, K Yagi, *J. Biochem.*, 1964,55,553
- 19 CC Culvenor, W Davies, WE Savige, *J. Chem. Soc.*, 1952,4480
- 20 MR Crampton, MA El Ghariani, *J. Chem. Soc (B)*, 1971,1043
- 21 T Abe, *Bull. Chem. Soc.*, Japan, 1966,627
CH Rochester, *J. Chem. Soc.*, 1965,2404
- 22 CF Bernasconi, RG Bergstrom, *J. Am. Chem. Soc.*, 1973,95,3603
- 23 CF Bernasconi, *J. Am. Chem. Soc.*, 1970,92,4682
- 24 T Abe, *Bull. Chem. Soc.*, Japan, 1960,33,41
- 25 V Gold, CH Rochester, *J. Chem. Soc.*, 1964,1710

- 26 MR Crampton, *J. Chem. Soc. (B)*, 1967,1341
E Buncl, AR Norris, KE Russel, PJ Sheridan, *Can. J. Chem.*, 1974,52,25
MR Crampton, MJ Willison, *J. Chem. Soc. Perkin Trans. II*, 1976,16
- 27 J Hine, *J. Am. Chem. Soc.*, 1963,85,3239
CL Liotta *ibid.*, 1967,89,5911
- 28 J Kavalek, V Machacek, M Pastrnek, V Sterba, *Collect. Czech. Chem. Commun.*, 1977,42,2928
J Kavalek, M Pastrnek, V Sterba, *ibid.*,1978,43,1401
- 29 AR Norris, *Can. J. Chem.*, 1969,47,2895
- 30 V Machacek, V Sterba, A Lycka, *Collect. Czech. Chem. Commun.*, 1987,52,132
- 31 CF Bernasconi, RB Killion, *J. Am. Chem. Soc.*, 1988,110,7506
- 32 MR Crampton, "*Chemistry of the Thiol Group*", Ed. S. Patai, Wiley, 1974, 379
- 33 MR Crampton, MJ Willison, *J. Chem. Soc. Perkin Trans. II*, 1976,901
- 34 J Miller, "*Aromatic Nucleophilic Substitution*", Elsevier, Amsterdam, 1968
- 35 RJ Irving, L Nelander, I Wadso, *Acta. Chem. Scand.*, 1964,18,769
- 36 O Makitie, A Ilvonen, *ibid.*, 1972,26,847
- 37 Tseng Kuang-Chih, *Acta Chim. Sinica*, 1966,32,107

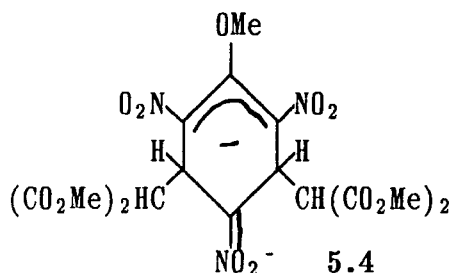
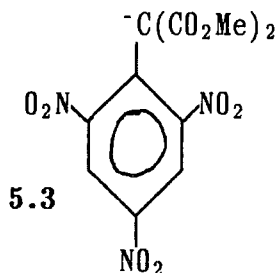
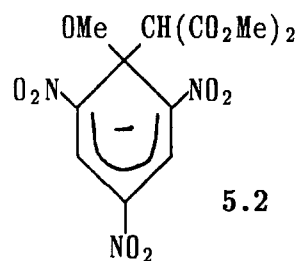
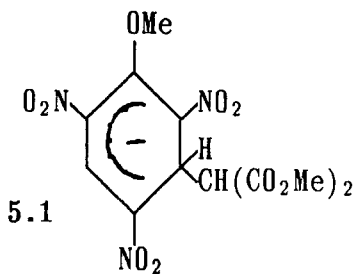
Chapter 5
**Kinetic and Equilibrium Studies of the reactions of some
carbanions with trinitroaromatic compounds.**

There have been several kinetic and structural investigations of the σ -adducts obtained from tri-nitroactivated aromatics and carbanions. Such studies have involved reactions with anions derived from nitroalkanes^{1,2} esters³⁻⁹ and nitriles¹⁰. However, the amount of data available is small compared to that for addition of oxygen bases.

Carbanion addition to 1-X-2,4,6-trinitrobenzenes gives carbon-bonded 1:1 (and in some cases 1:2) σ -adducts by addition to unsubstituted ring positions. If X is a poor leaving group then stable σ -adducts may also be produced by carbanion attack at the 1-position⁵.

Thus when 2,4,6-trinitroanisole and the sodium salt of dimethylmalonate were mixed in [²H₆]-DMSO, ¹H nmr showed signals⁵ entirely due to 5.1 (H₃ = 5.55 (dd), H₅ = 8.34 (d), J₃ = 5.4 Hz, J₄ = 1.5 Hz) and 5.2 (H₃ = H₅ = 8.61 (s)). The intensity of the signals for 5.2 increased at the expense of those for 5.1. After about an hour the ratio [5.1] / [5.2] remained practically unchanged at a value of 1.3 ± 0.1 indicating the 1,3-adduct to have a slightly greater thermodynamic stability than the 1,1-adduct. Very gradually, small amounts of the anion of the substitution product 5.3 appeared⁵. A stopped-flow spectrophotometric study⁷ in methanol showed that addition of the dimethylmalonate anion to the 3-position of trinitroanisole was very much more rapid than addition to the 1-position. A process faster than the latter was the formation of diadduct 5.4 for which there was kinetic and spectroscopic evidence⁷. On changing the solvent from methanol to 80/20 (v/v) MeOH/ DMSO the equilibrium constant for the formation of diadduct 5.4 from 5.1 decreased while the equilibrium constant for formation of 5.1 from 2,4,6-trinitroanisole increased⁷.

Leffek^{8,9} observed transient species in the substitution reactions of diethylmalonate anions with picryl chloride and picryl bromide in benzene/DMSO mixtures which he assumed to be 1,1-adducts, with the rate limiting step being expulsion of the halide. In fact the rate limiting step is expected^{10,11} to be



formation of the 1,1-adduct. Recent ^1H nmr studies⁵ on picryl chloride with dimethylmalonate anions in DMSO confirm Leffek's "intermediates" as 1,3-adducts; at no stage in the substitution reaction was a 1,1-adduct observed.

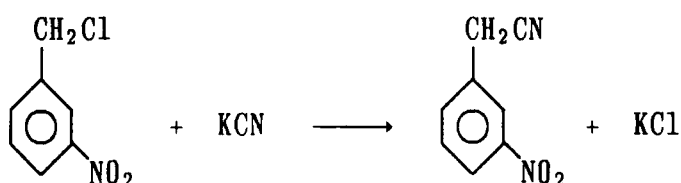
In the present work kinetic and equilibrium data are obtained for the reactions of 1-X-2,4,6-trinitrobenzenes ($X = \text{H}, \text{Cl}, \text{Me}$) with anions derived from dimethylmalonate, ethylcyanoacetate and various substituted phenylacetonitriles. The data are used to calculate values of intrinsic rate constants (k_0) for reaction at an unsubstituted ring position.

Also investigated is the interaction of 1,3,5-trinitrobenzene with the phenyl-nitromethane anion.

Experimental

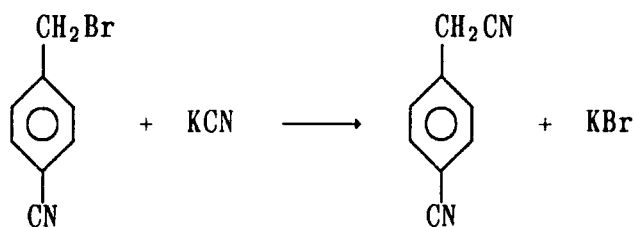
a) Preparation of 3-nitrophenylacetonitrile^{1,2}

10g of 3-nitrobenzyl chloride and 4.2g (1.1 equivalents) of potassium cyanide were dissolved in a mixture of ethanol and water (<100ml) at a temperature between 50 to 60°C (water bath). The reaction was allowed to continue at this temperature with constant stirring for 2 hours. The reaction mixture was then allowed to cool, iced water was added and the product extracted into diethyl ether. This layer was washed with water and then dried with anhydrous sodium sulphate. The ether was evaporated leaving a solid product which was recrystallised from ethanol. Elemental analysis and ¹H nmr showed that this product consisted entirely of 3-nitrophenylacetonitrile (40%) and starting material. Because of difficulties in separation, the reaction was repeated using 3 equivalents of potassium cyanide and a longer reaction time (≈15 hours). The product was extracted into ether as before; the reaction had produced a dark coloured by-product which mostly remained in the aqueous layer. The product, obtained in poor yield was recrystallised several times from ethanol to give pale crystals of m.pt. 60-61°C (lit.^{1,2} 61-62°C). ¹H nmr in [²H₆]-DMSO gave the expected spectrum (see table 5.10) and indicated the product to be free from impurities. Elemental analysis (% by mass) gave C 59.1, H 3.7, N 17.0 (calc. for C₈H₆N₂O₂ : C 59.2, H 3.7, N 17.3)



b) Preparation of 4-cyanophenylacetonitrile¹³

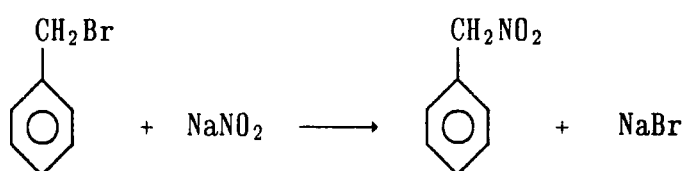
4-cyanophenylacetonitrile was prepared using 4-cyanobenzyl bromide and 1.1 equivalents of KCN in the same way as the 3-nitro derivative. Pouring the reaction mixture into ice water yielded solid material which was filtered off. Here the reaction time was found to be much shorter (<2 hours) and the product was obtained in good yield. Recrystallization from methanol gave pale yellow needles m.pt. 100°C (lit!³ 100°C). Elemental analysis (% by mass) gave: C 76.5, H 4.3, N 19.0 (calc. for C₉H₆N₂ : C 76.1, H 4.2, N 19.7)



c) Preparation of phenylnitromethane¹⁴

Benzyl bromide (51g, 0.30 mol) was poured into a stirred mixture of 600 ml of dimethylformamide, 36g of sodium nitrite (0.52 mol) and 40g of urea maintained at -20°C to -15°C. After 5 hours the reaction mixture was poured into 1.5l of ice water. The product was then extracted from the aqueous phase using several portions of diethyl ether. The combined extracts were washed, dried with anhydrous sodium sulphate and the ether was removed leaving a liquid. This was distilled at reduced pressure using a Fischer distillation apparatus. During distillation three main fractions were noted: 40°C /4mm due to benzyl nitrite, 79°C /4mm and 92°C /4mm due to phenylnitromethane (lit!⁴ 76°C /2mm). During the collection of the phenylnitromethane fraction some decomposition of the liquid was found to occur, with the pale product becoming gradually discoloured. This decomposition was probably a consequence of the higher than recommended¹⁴ temperatures used. It was not possible to obtain a smaller

working pressure then 4mm/Hg. The fractions containing phenylnitromethane were analysed by mass spectroscopy. The major impurities were found to be benzylalcohol, isocyanobenzene and starting material. There were also small amounts of benzaldehyde and benzylnitrile. The reaction was repeated with increased amounts of sodium nitrite and urea in order to convert more of the starting material. Again distilled, the purest sample obtained was about 90% in phenylnitromethane with impurities solely of benzaldehyde and isocyanobenzene (HPLC). Again the samples were discoloured, and they became darker on standing. The distilled product was used promptly.



^1H nmr in $[\text{}^2\text{H}_6]$ -DMSO : ring protons 7.4 – 7.5 ppm (multiplet), 5H
 methylene protons 5.75 ppm (singlet) , 2H

d) ^1H nmr spectra

Spectra of substituted phenylacetonitriles were recorded in $[\text{}^2\text{H}_6]$ -DMSO or $[\text{}^2\text{H}_6]$ -DMSO/MeOH. In order to generate the anions, sodium methoxide in methanol was added to the parent compound in $[\text{}^2\text{H}_6]$ -DMSO. Spectra were taken as soon as possible after mixing the reagents. All measurements refer to internal tetramethylsilane.

e) Stopped flow scanning spectrophotometry

This was the technique used to obtain the UV/visible spectra of anions of several substituted phenylacetonitriles. One syringe of the stopped flow apparatus contained a solution of the carbon acid in methanol/DMSO solvent, the other a solution of sodium methoxide in methanol/DMSO.

f) Kinetic measurements

Kinetic measurements, by both conventional and stopped flow spectrophotometry, were made under first order conditions with the concentration of both the carbon acid and sodium methoxide in large excess of the concentration of the nitro compound.

In the stopped flow experiments one syringe contained a mixture of the carbon compound and the aromatic nitro-compound while the other contained sodium methoxide in methanol. Reported rate constants are the average of at least five kinetic determinations.

For kinetic measurements made by conventional spectrophotometry small volumes of the reagents were added to solutions of sodium methoxide in methanol, the latter thermostatted at 25°C. The kinetic runs were started as soon as possible after mixing the reagents. Infinity measurements were taken after 10 half-lives. For very slow reactions the Guggenheim method was used to calculate rate constants. In these cases the reaction was continued for at least 3 half-lives. Reported rate constants are the average of at least two kinetic runs.

Values of A_{∞} were occasionally determined by using a very large excess of carbon compound and sodium methoxide over the substrate concentration.

Stock solutions of carbon acids (between 0.2M - 1.0M) were either in methanol or dioxan. Stock solutions of the aromatic nitrocompounds (usually 0.01M - 0.02M) were in dioxan.

All kinetic measurements were made at constant ionic strength (0.01M). Adjustments were made by addition of a solution of sodium chloride (0.1M) in methanol.

g) Determination of Equilibrium acidities

Carbanions were generated in methanol or DMSO/methanol by reaction with methoxide. Equilibrium acidities (with the exception of dimethylmalonate where conventional spectrophotometry was used) were determined by stopped flow

spectrophotometry as the decomposition of the carbanions was found to be fairly rapid. One syringe contained a solution of the carbon acid, the other a solution of sodium methoxide. Absorbance data were obtained at or near the λ_{max} of the carbanions.

DMSO/MeOH solutions were made up by volume and knowledge of the densities of the components allowed the calculation of the mol % DMSO.

Results and Discussion

i) Acidities of dimethylmalonate and ethylcyanoacetate

Carbanions were generated in methanol by reaction with methoxide



$$K_{CH} = \frac{K_a}{K_m} \quad 5.6$$

$R_1 = R_2 = CO_2Me$ (DMM); $R_1 = CN, R_2 = CO_2Et$ (ECA)

In the case of ethylcyanoacetate, forming or fading reactions were observed following on from the rapid ionisation. Slow fading reactions were also observed with dimethylmalonate at high concentrations of methoxide; here absorbance values were extrapolated to zero time. Results are reported in tables 5.7 and 5.8

carbon acid	$K_{CH} / \text{lmol}^{-1}$	ref
malononitrile $CH_2(CN)_2$	600	10
methyl cyanoacetate $CH_2CNC O_2Me$	54	3
DMM	0.5	3
DMM	0.45	†
ECA	24	†
nitromethane	22	2
nitroethane	500	2
nitropropane	$>10^3$	2

Table 5.9

Equilibrium acidities
of carbon acids in
methanol

† this work

K_{CH} values for these and other carbanions are shown in table 5.9. The smaller value of K_{CH} for ethylcyanoacetate relative to methylcyanoacetate may be

attributed to the greater electron releasing effect of the ethyl group (relative to the methyl group) and perhaps a larger degree of steric inhibition of solvation in the ethylcyanoacetate anion!⁵ The series of carbon acids dimethylmalonate, methylcyanoacetate and malononitrile illustrates the large acidifying effect of the cyano substituent. The increasing acidity shown in the series nitromethane, nitroethane and 2-nitropropane has been attributed to the stabilising influence of methyl substituents attached to an sp^2 hybridised carbon!⁶

K_{CH} is related by equation 5.6 to K_a , the acid dissociation constant, and to K_m , the autoprotolysis constant of methanol. The value for pK_m is given!⁵ as 16.92.

[NaOMe] lmol ⁻¹	Absorbance ^b (at 258 nm)	K _{CH} ^c lmol ⁻¹
0.004	0.007	0.70
0.008	0.010	0.50
0.012	0.013	0.44
0.020	0.020	0.40
0.030	0.030	0.40
0.050	0.055	0.45
0.080	0.10	0.52
0.100	0.11	0.46
0.150	0.18	0.52
0.20	0.37	
0.40	1.09	
0.6	1.51	
0.8	2.03	
1.0	2.32	
1.4	2.48	
1.8	2.50	
2.0	2.50	

Table 5.7

Equilibrium data for reaction
of dimethylmalonate^a with
sodium methoxide in methanol
at 25^o C

- a Concentration is $1 \times 10^{-4} \text{M}$
- b Values determined by conventional spectrophotometry. Absorbtion is due to the carbanion. The absorbtion due to the parent at 258 nm is negligibly small. Values correspond to a cell of 1 cm pathlength.
- c Calculated as $\frac{A}{(2.5 - A) [\text{NaOMe}]}$ where A represents absorbance.

[NaOMe] l mol ⁻¹	Absorbance ^b (at 245 nm)	K _{CH} ^c l mol ⁻¹
0.002	0.076	24
0.004	0.137	23
0.006	0.218	26
0.008	0.273	25
0.010	0.330	25
0.012	0.365	24
0.014	0.405	24
0.018	0.480	23
0.022	0.583	25
0.026	0.629	24
0.030	0.694	25
0.036	0.724	22
0.042	0.824	24
0.050	0.915	26
0.10	1.148	24
0.20	1.387	
0.30	1.559	
0.40	1.677	
0.50	1.633	
0.70	1.633	

Table 5.8

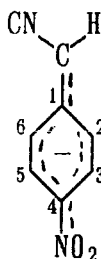
Equilibrium data for reaction
of ethylmalonate^a with
sodium methoxide in methanol
at 25^o C

- a Concentration is 1×10^{-4} M
- b Values determined by stopped flow spectrophotometry. Absorbtion is due to the carbanion. The absorbtion due to the parent at 245 nm is negligibly small. Values correspond to a cell of 1 cm pathlength.
- c Calculated as $\frac{A}{(1.63 - A) [\text{NaOMe}]}$ where A represents absorbance.

ii) Acidities of substituted phenylacetonitriles

a) ^1H nmr spectra

The ionisation of 4-nitrophenylacetonitrile has been previously studied¹⁷ by ^1H nmr. The results indicate that ionisation occurs by loss of a methylene proton. The spectrum of the anion in DMSO/MeOH solvent shows two resonances at *ca.* 6.35 ppm and 7.45 ppm due to the ring protons and a resonance at 4.05 ppm (in 70 mol% DMSO) due to methylene protons!⁷ This latter has an intensity representing a single hydrogen. In the anion the bond from the side chain carbon to the ring will have partial double bond character. Thus rotation about this bond



will be hindered. As a result, spectra of the anion are complicated by the non-equivalence of protons at C-2 and C-6 (and those at C-3 and C-5).

Spectra measured with a deficiency of base (sodium methoxide) show that there is a rapid interconversion between neutral molecule and anion!⁷ Increasing the proportion of DMSO in the solvent was found to decrease the rate of this process. Thus in a solvent of 50 mol% DMSO broad bands are observed for the ring protons in positions intermediate to those of the anion and parent compound while in 80 mol% DMSO separate bands are observed for the ring protons of each!⁷ ^1H nmr data for some phenylacetonitriles are shown in table 5.10. Spectra, taken as soon as possible after addition of methoxide to the parent in DMSO-d_6 , show the production of anions. These are unstable and gradually decompose. In the anion, ring proton resonances are shifted to high field in keeping with the

increased electron density in the ring. Because of the use of deuterated solvent it was not possible to determine methylene proton resonances in the anion.

The rate of interconversion between anion and neutral molecule is relatively slow for these phenylacetonitriles; separate resonances due to each were observed throughout and in the case of the ortho-cyano derivative in a solvent containing 40% methanol by volume. It was only possible to completely ionise the phenylacetonitriles in solvents containing large proportions of DMSO. This indicates the much smaller acidity of these compounds relative to the 4-nitro derivative. The positions of the ring proton resonances in the anion are strongly dependent on solvent composition. Increasing the proportion of methanol in the solvent shifts these resonances to lower field. This may be attributed, perhaps, to a greater amount of negative charge delocalised onto the cyano group in more methanolic solvent.

The ^1H nmr spectra of phenylacetonitrile show small bands due to the decomposition product (7.9 (multiplet), 7.27 (multiplet) in 86 vol% DMSO; 7.9 (multiplet), 7.28 (multiplet) in 98 vol% DMSO). Possibilities for the decomposition product include carbanion attack at the cyano-group of a second molecule of phenylacetonitrile or the base catalysed reaction of phenylacetonitrile with alcohols to form imidates^{3 8} ($\text{Ph}-\text{CH}_2-\text{C}(\text{NH})-\text{OMe}$).

b) UV/visible spectra

UV/visible spectra of the phenylacetonitriles in methanol are typical^{1 8} of those for substituted benzenes showing one fundamental band and much less intense features at higher wavelength.

4-Nitrophenylacetonitrile can be completely converted to its anion in methanol. The spectrum of the anion is similar to those obtained in several alcoholic media^{1 9} but quite different to that in water. In solvents containing water there is evidence^{2 0, 2 1} that the anion exists in two forms, one unspecifically solvated and

the other in which a molecule of water is hydrogen bonded to the nitro- group. Both forms have characteristic visible spectra.²⁰ In water, the hydrogen bonded form predominates.

Table 5.10

¹H nmr data for phenylacetonitriles and their anions

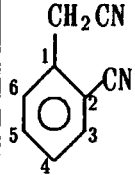
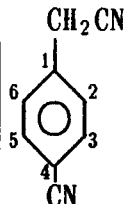
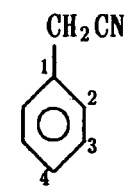
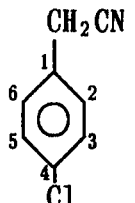
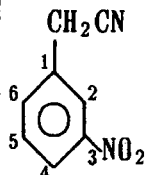
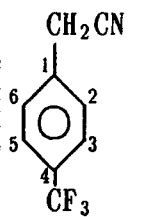
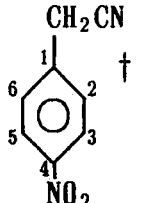
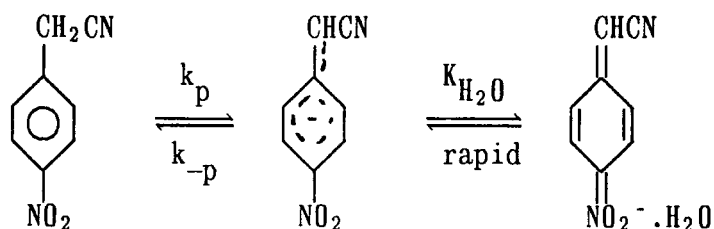
carbon acid	solvent	[NaOMe] /M stoic.	[carbon acid] /M stoic.	[anion] [parent]	CHEMICAL SHIFTS ppm		
					NEUTRAL MOLECULE*		ANION*
					ring protons	methylene protons	ring protons
	DMSO	—	0.30	—	7.4–8.0 (multiplet)	4.30	
	89/11 DMSO/MeOH (v/v)	0.5	0.3	6.5	7.3–7.8 (multiplet)	—	H ₃ =6.83(d) H ₄ =5.83(t) H ₅ =6.77(t) H ₆ =6.57(d)
	60/40 DMSO/MeOH (v/v)	0.3	0.19	3.5	7.3–7.8 (multiplet)	—	H ₃ =7.18(d) H ₄ =6.4(t) H ₅ =7.4(t) H ₆ =6.95(d)
	DMSO	—	0.3	—	H ₂ =H ₆ =7.58(d) H ₃ =H ₅ =7.89(d)	4.20	
	90/10 DMSO/MeOH (v/v)	0.45	0.5	>8	H ₂ =H ₆ =7.50(d) H ₃ =H ₅ =7.76(d)		H ₂ =H ₆ =6.33(d) H ₃ =H ₅ =6.87(d)
	DMSO	—	0.3		7.40 (multiplet)	4.04	—
	98/2 DMSO/MeOH (v/v)	0.1	0.1	—	none observed	—	H ₂ =H ₆ =6.55(d) H ₄ =6.38(t) H ₃ =H ₅ =6.88(t)
	92/8 DMSO/MeOH (v/v)	0.4	0.1	2.5	7.33 (multiplet)	—	H ₂ =H ₆ =6.8(d) H ₄ =6.58(t) H ₃ =H ₅ =7.0(t)
	86/14 DMSO/MeOH (v/v)	0.8	0.1	2.3	7.34 (multiplet)		H ₂ =H ₆ =6.9(d) H ₄ =6.7(t) H ₃ =H ₅ =7.05(t)
	DMSO	—	0.3		H ₂ =H ₆ =7.38(d) H ₃ =H ₅ =7.48(d)	4.06	
	90/10 DMSO/MeOH (v/v)	0.6	0.3	3	H ₂ =H ₆ =7.33(d) H ₃ =H ₅ =7.93(d)	—	H ₂ =H ₆ =6.60(d) H ₃ =H ₅ =6.91(d)

Table 5.10 continued

					CHEMICAL SHIFTS ppm		
carbon acid	solvent	[NaOMe] /M stoic.	[carbon acid] /M stoic.	[anion] [parent]	NEUTRAL MOLECULE*		ANION*
					ring protons	methylene protons	ring protons
	DMSO	—	0.3	—	H ₂ =8.26(s) H ₄ =8.22(d) H ₅ =7.72(t) H ₆ =7.85(d)	4.26	
	DMSO	—	0.3	—	H ₂ =H ₆ =7.61(d) H ₃ =H ₅ =7.79(d)	4.21	
	DMSO	—	0.5	—	H ₂ =H ₆ =7.65(d) H ₃ =H ₅ =8.28	4.28	
	64/36 DMSO/MeOH (v/v)	ca.0.5	ca.0.5				H ₂ =H ₆ =6.35 H ₃ =H ₅ =7.46

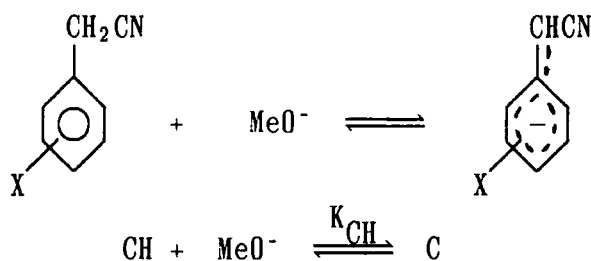
† data from
ref. 17* J_{ortho} only measured. All ca. 8Hz§ Measured from
relative intensities



In methanol the pink solution due to the anion (with a λ_{max} of 520 nm) gradually turns blue due to the formation of a decomposition product (λ_{max} 580 nm).

Formation of anions from other phenylacetonitriles could only be observed in DMSO/MeOH solvent. Decomposition of the anions was found to be fairly rapid, with the exception of the anion formed from the 2-cyano derivative which was stable for a much longer period. Spectra obtained by stopped flow scanning spectrophotometry are shown in Figure 5.11A. The anions absorb strongly in the visible region and (with the exceptions of the 3-NO₂ and 2-CN derivatives) have extinction coefficients of around $3 \times 10^4 \text{ l mol}^{-1} \text{ cm}^{-1}$. Data are summarised in table 5.11B

c) Determination of Equilibrium acidities



The value of K_{CH} for 4-nitrophenylacetonitrile was determined in methanol by using stopped flow spectrophotometry. Absorbance data shown in table 5.16 lead to a value $1.17 \pm 0.05 \text{ l mol}^{-1}$ in good agreement with a previously obtained value¹⁹ of $\text{p}K_{\text{B}} = 0.03$. ($K_{\text{CH}} = 1.1 \text{ l mol}^{-1}$)

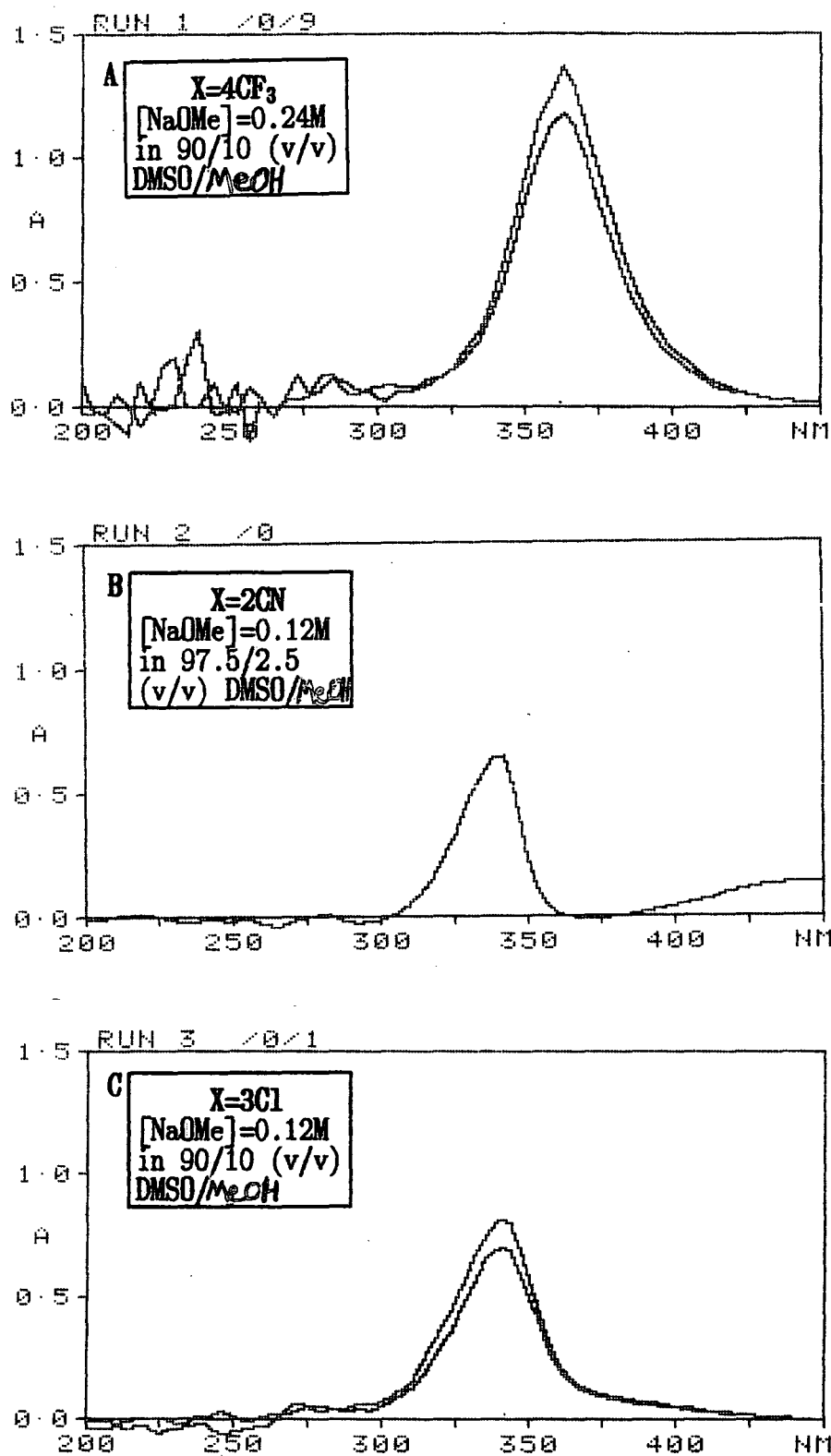


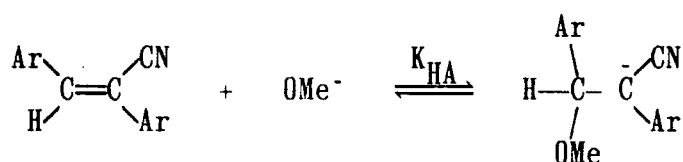
Figure 5.11A Visible spectra of the anions of some X-substituted phenylacetonitriles in DMSO/MeOH obtained by stopped-flow scanning spectrophotometry

Spectra are normalised to 0.2cm cells and 2×10^{-4} M of the carbon compound. The initial spectrum was obtained within ca. 30ms after mixing the reagents. Repeat scans obtained after intervals of 0.9s (A) and 0.1s (C) from the initial scans are of lower intensities than the initial scans.

Initial spectra of A and B correspond to complete conversion of carbon compound to anion.

In order to determine values of K_{CH} in methanol for the other phenylacetonitriles, use was made of the greatly enhanced basicity of methoxide ions in dimethylsulphoxide.^{2,3} Ratios $[\text{C}^-] / [\text{CH}]$ were obtained spectrophotometrically for several phenylacetonitriles for known sodium methoxide concentrations in varying DMSO/MeOH compositions. The rates of ionisation of these compounds were found always to be extremely rapid and were too fast to measure on a stopped flow timescale. Since it was not possible to construct an acidity scale using the conventional technique^{2,2} of overlapping indicators due to the sparsity of data, it was necessary to resort to using a published acidity scale^{2,3}.

Several acidity scales using DMSO as a cosolvent have been established.^{2,3-26} The most suitable^{2,3} is based on methoxide addition to α -cyanostilbenes. Because the methoxide ion acts as a nucleophile (or Lewis base) rather than a Brønsted-Lowry base, the scale is designated J_m .



Both the addition product AOMe^- and the phenylacetonitrile anion contain a negative charge delocalised onto a system containing an aromatic ring with a cyano-group attached to side-chain carbon atom. Hence the acidity function dependence of these two types of compound is likely to be closely similar.

The addition reaction shown in equation 5.12 can be expressed in terms of the equilibrium :



The equilibrium constant K_{HA} is therefore

$$K_{HA} = \frac{a_{AOMe^-} a_{H^+}}{a_A a_{MeOH}} = \frac{[AOMe^-]}{[A]} \times \frac{a_{H^+} \gamma_{AOMe^-}}{a_{MeOH} \gamma_A}$$

$$= \frac{[AOMe^-]}{[A]} \times j_m \quad \text{with} \quad j_m = \frac{a_{H^+} \gamma_{AOMe^-}}{a_{MeOH} \gamma_A}$$

Taking negative logarithm gives

$$J_m = -\log j_m = pK_{HA} + \log \frac{[AOMe^-]}{[A]} \quad 5.14$$

This differs from the H_m scale which is defined²⁴ as

$$H_m = -\log h_m = pK_{HA} + \log \frac{[A]}{[HA]} \quad \text{with} \quad h_m = \frac{a_{H^+} \gamma_{A^-}}{\gamma_{HA}}$$

If the activity coefficient ratios $\frac{\gamma_{A^-}}{\gamma_{HA}}$ and $\frac{\gamma_{AOMe^-}}{\gamma_A}$ are identical and if the activity of the alcohol is unity then j_m and h_m become identical. J_m and H_m values should be very close in dilute basic solutions²³

If it is assumed that the J_m scale describes well the ionisation behaviour of phenylacetonitriles in DMSO/MeOH mixtures, then in order to calculate values of $\log \frac{[C^-]}{[CH]}$ in methanol, a further assumption is made that values of ΔJ_m [$\Delta J_m = J_m$ (for a given DMSO/MeOH composition) - J_m (methanol)] are constant for various concentrations of sodium methoxide. The published scale uses a (constant) sodium methoxide concentration of 0.01M; sodium methoxide concentrations of up to 0.10M were used to determine values of $\log \frac{[C^-]}{[CH]}$ for the

phenylacetonitriles.

Values of K_{CH} are calculated using the expression

$$\log K_{\text{CH}} = \log \frac{[\text{C}^-]}{[\text{CH}]} - \Delta J_{\text{m}} - \log [\text{NaOMe}] \quad 5.15$$

Data for 9 substituted phenylacetonitriles and diphenylacetonitrile are shown in tables 5.16 to 5.26. In order to obtain the values of ΔJ_{m} shown in the tables, some interpolation of J_{m} values to the required mol% DMSO was necessary. These values are shown in table 5.11C. Values of $\log \frac{[\text{C}^-]}{[\text{CH}]}$ plotted versus mol% DMSO match closely the form of the J_{m} vs. mol% DMSO plot, the latter (for mol% DMSO >50) being a gentle curve of increasing gradient.

For each phenylacetonitrile, calculated values of K_{CH} (in MeOH) are generally fairly constant for the range of DMSO/MeOH compositions studied. There is however a small decrease in K_{CH} as the solvent becomes more methanol rich. This may be (partly) due to the decrease, in more methanolic solvent, in the values of extinction coefficient (for which assumed values of A_{m} were taken) and accompanying shifts in λ_{max} . Data are summarised in table 5.27.

Values of K_{CH} encompass 9 orders of magnitude from the 4-nitro derivative ($K_{\text{CH}} = 1.17 \text{ l mol}^{-1}$) to the 3-methoxy derivative ($K_{\text{CH}} = 6 \times 10^9 \text{ l mol}^{-1}$). It was not possible to ionise phenylacetonitrile (benzyl cyanide) completely even in the most DMSO rich solvent. In Figure 5.27 values of $\log K_{\text{CH}}$ are correlated with substituent constants σ^- in a Hammett relationship. σ^- Values are suitable when there is through resonance between a reaction site that becomes electron rich and a *para*-substituent?⁷ The value for the 4-nitro substituent is not included in the correlation. The plot gives a reasonable straight line with a ρ value of 4.99. The value of K_{CH} for 4-nitrophenylacetonitrile is thus some two orders of magnitude higher than would be predicted from this plot. The anomalous equilibrium acidity of this compound has been previously noted?⁰ It may perhaps be attributed to

some specific hydrogen bonding interaction involving the para-nitro group as was shown to be the case in aqueous solvents?^{20,21} However this argument seems unlikely given that the same deviation from the Hammett plot occurs with 4-nitrophenylacetonitrile in DMSO which cannot³⁵ act as an H-bond donor. The ρ value for 8 substituted phenylacetonitriles in DMSO has been reported³² as 5.9; the pK_a values of phenylacetonitrile³² ($\sigma^- = 0$) and 4-nitrophenylacetonitrile²⁰ ($\sigma^- = 1.297^{28}$) are 21.9 and 12.3 respectively. Thus the 4-nitro compound is likely to be about two orders of magnitude more acidic in this medium than the ρ value would have predicted.

Values of K_{CH} in MeOH for the 2-CN and 4-CN derivatives are closely similar. In both of these compounds the negative charge can be delocalised directly onto the nitrogen atom. Steric effects in proton transfer reactions in protic solvents are expected³² to be unimportant.

The pK_a values of the phenylacetonitriles are larger by about 4 units in methanol compared with the corresponding values in DMSO; the results reflect the good ability of DMSO to solvate species containing delocalised negative charges.

C-H acid	pK_a (MeOH)	pK_a (DMSO)
phenylacetonitrile	25.4 [*]	21.9 ^a
diphenylacetonitrile	21.7	17.5 ^b
4-nitrophenylacetonitrile	16.9	12.3 ^c

* estimated from Hammett plot
a=ref 32, b=ref 33, c=ref 20

As anions in which the negative charge resides largely in the aromatic ring, stabilisation by hydrogen bonding in methanol will be relatively unimportant.³⁵ The stronger solvation in DMSO can be attributed to the larger dipole and polarisability properties of the solvent.³⁵ The converse situation in which pK_a

increases on going from protic solvent (H_2O) to DMSO is exemplified by nitroalkanes. In these anions the negative charge is largely situated on the oxygen atoms. Hydrogen bonding in H_2O therefore becomes very important and so the acidity is reduced on going to DMSO.^{3,5}

The Hammett plot has been used to estimate the acidities in methanol for phenylacetonitriles with substituents H, 3-Me, and 4-Me. These values of K_{CH} are also shown in table 5.27

Phenylnitromethane

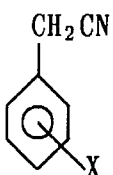
The sample used to obtain spectra was about 80% in phenylnitromethane with impurities solely of benzaldehyde and isocyanobenzene.

Complete conversion to the anion could be achieved using (for a solution containing a concentration of *ca.* $1 \times 10^{-4} \text{M}$ phenylnitromethane) very low concentrations ($2 \times 10^{-3} \text{M}$) of sodium hydroxide in water or sodium methoxide in methanol, consistent with a $\text{p}K_{\text{a}}$ of 10.3 in water.^{3,4} The anions appeared to be very stable in both media.

The λ_{max} of the anions formed in water and methanol were 294 nm and 302 nm respectively. The value of the extinction coefficient in water was estimated at $2.8 \times 10^4 \text{ l mol}^{-1} \text{ cm}^{-1}$. This value is rather higher than that in the literature^{3,4} ($\lambda_{\text{max}}^{289} \epsilon = 2.14 \times 10^4 \text{ l mol}^{-1} \text{ cm}^{-1}$). The value of the extinction coefficient, also estimated at $2.8 \times 10^4 \text{ l mol}^{-1} \text{ cm}^{-1}$ in methanol is very similar to the values observed for the phenylacetonitriles. In both cases the neutral molecule only showed a small absorbance at the λ_{max} of the carbanion.

Malonic acid $\text{HO}_2\text{CCH}_2\text{CO}_2\text{H}$

For this material there were problems of solubility in methanol and no kinetic or equilibrium measurements were made. On addition of sodium methoxide to a dilute solution of $\text{HO}_2\text{CCH}_2\text{CO}_2\text{H}$ in methanol, a white precipitate of the disodium salt is observed. Further ionisation of malonic acid to produce the carbanion is expected to be relatively unfavoured.

Table 5.11 B
 UV / visible spectra of 

X	parent: in MeOH		anion: in DMSO/ † MeOH mixtures	
	λ_{\max} nm	$10^{-4}\epsilon$ $\text{l mol}^{-1}\text{cm}^{-1}$	λ_{\max} nm	$10^{-4}\epsilon$ $\text{l mol}^{-1}\text{cm}^{-1}$
4-NO ₂	262	1.06	520	3.0
4-CN	229	1.35	390	3.6
3NO ₂	207	1.13	330	2.3
4-CF ₃	209	0.78	360	3.4
3CF ₃	207	0.83	330	3.1
3Cl	213	0.88	340	3.2
4-Cl	219	1.12	345	3.0
3-OMe	224	0.58	330	2.6
H	207	0.83		
3-Me	214	0.61		
4Me	213	0.65		
2-CN	227	1.16	340	1.8
3,5- <i>bis</i> CF ₃	209	0.68	355	2.7

* in MeOH

† approximate values: ϵ and λ_{\max} have a slight dependence on solvent composition

Table 5.11 C

J_m Values for DMSO/methanol containing 0.01M sodium methoxide

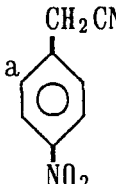
mol% DMSO in DMSO/MeOH	J_m^a	J_m^b	ΔJ_m^c	mol% DMSO in DMSO/MeOH	J_m^a	J_m^b	ΔJ_m^c
0.00	11.73			54.79	16.82		
0.68	11.83			57.1		17.03	5.30
2.32	12.03			59.61	17.25		
5.39	12.37			60.1		17.29	5.56
8.75	12.72			63.1		17.53	5.80
15.30	13.38			64.32	17.63		
20.60	13.87			69.5		18.13	6.40
25.54	14.29			69.63	18.4		
30.47	14.72			74.26	18.59		
35.14	15.12			76.4		18.82	7.09
36.3		15.22	3.49	78.52	19.05		
39.88	15.53			83.52	19.61		
41.1		15.64	3.91	83.7		19.65	7.90
44.05	15.89			87.5		20.08	8.35
46.1		16.07	4.34	88.24	20.17		
48.7		16.29	4.56	91.6		20.74	9.01
49.95	16.40			93.98	21.14		
51.4		46.53	4.80	97.61	21.65		
54.2		16.77	5.04				

a. literature values from reference 23

b. interpolated value

c. $\Delta J_m = J_m - J_m(\text{mol\% DMSO} = 0)$

Table 5.16

Equilibrium data for reaction of  with sodium methoxide at 25⁰ C

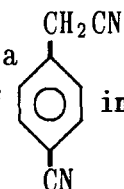
[NaOMe] /MeOH	b A _{520nm}	b A _{528nm}	c K _{CH} /l mol ⁻¹
0	negligible absorbance		
0.004	0.015		1.25
0.008	0.027		1.13
0.012	0.038		1.07
0.016	0.055		1.16
0.020	0.066		1.12
0.025	0.086		1.18
0.030	0.100		1.15
0.040	0.137		1.19
0.050	0.169		1.19
0.060	0.205		1.21
0.080	0.296		
0.10	0.365		
0.12	0.440		
0.14	0.500		
0.20	0.706		
0.40	1.322		
0.60	1.998	1.871	
0.80	2.310	2.218	
1.40	3.010	2.798	
1.80	3.010	2.897	
2.10	3.010	2.782	

a concentration is $1 \times 10^4 \text{M}$

b normalised to $l = 1 \text{ cm}$. Absorbances obtained by stopped flow spectrophotometry.

c calculated as
$$K_{\text{CH}} = \frac{A_{520}}{(3.01 - A_{520}) [\text{NaOMe}]}$$

Table 5.17

Equilibrium data for ionisation of  in DMSO/MeOH mixtures at 25^o C

vol% DMSO	mol% DMSO	^b A _{388nm}	[NaOMe] /M	^c log $\frac{[\text{carbanion}]}{[\text{parent}]}$	ΔJ_m	^e 10 ⁴ K _{CH} /l mol ⁻¹
75		3.48	0.05			
		3.61	0.10			
		3.64	0.20			
70	57.1	2.67	0.05	0.45	5.30	2.8
		3.16	0.10	0.84		3.5
		3.54	0.3			
		3.62	0.4			
		3.62	0.5			
65	51.4	1.59	0.05	-0.10 ^d	4.80	2.5
		2.18	0.10	0.19		2.4
60	46.1	0.70	0.05	-0.62 ^d	4.34	2.2
		1.25	0.10	-0.27		2.5
55	41.1	0.26	0.05	-1.11 ^d	3.91	1.9
		0.53	0.10	-0.76		2.1

a concentration is 1 x 10⁴M

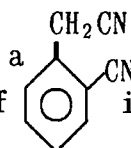
b normalised to a pathlength of 1cm

$$c \quad \frac{[\text{carbanion}]}{[\text{parent}]} = \frac{A_{340}}{A_{\infty} - A_{340}}$$

d calculated with a value of A_∞ = 3.6

e calculated according to expression 5.15

Table 5.18

Equilibrium data for ionisation of  in DMSO/MeOH mixtures at 25^o C

vol% DMSO	mol% DMSO	^b A _{340nm}	[NaOMe] /M	^c log $\frac{[\text{carbanion}]}{[\text{parent}]}$	ΔJ_m	$10^4 K_{CH}^e$ /l mol ⁻¹
80	69.5	1.74	0.05			
		1.74	0.10			
		1.69	0.40			
70	57.1	1.41	0.05	0.54	5.30	3.5
		1.60	0.10	0.88		
		1.81	0.20			
		1.81	0.4			
		0.04	nil			
65	51.4	0.88	0.05	-0.06	4.80	3.6
		1.29	0.10	0.34		
		1.82	0.20			
		1.87	0.4			
60	46.1	0.40	0.05	-0.58 ^d	4.34	3.5
		0.74	0.10	-0.17		
		1.79	0.4			
		0.04	nil			
55	41.1	0.20	0.05	-1.41 ^d	3.91	2.5
		0.36	0.10	-1.05		
		0.04	nil			
50	36.5	0.104	0.05	-1.41 ^d	3.49	2.5
		0.180	0.10	-1.05		
		0.04	nil			
45	31.8	0.057	0.05			
		0.080	0.10			
		0.031	nil			

a concentration is $1 \times 10^4 M$

b normalised to pathlength of 1cm

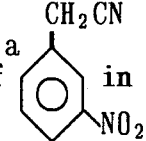
$$c \quad \frac{[\text{carbanion}]}{[\text{parent}]} = \frac{A_{340} - A'}{A_w - A_{340}}$$

d calculated with $A_w = 1.8$

where A' is eq^m absorbance due to the parent molecule

e calculated according to expression 5.15

Table 5.19

Equilibrium data for ionisation of  in DMSO/MeOH mixtures at 25^o C

vol% DMSO	mol% DMSO	b A _{328nm}	[NaOMe] /M	c log $\frac{[\text{carbanion}]}{[\text{parent}]}$	ΔJ_m	e 10 ⁶ K _{CH} /l mol ⁻¹
90	83.7	2.27	0.05			
		2.27	0.10			
		2.27	0.24			
85	76.4	1.75	0.05	0.52	7.09	5.4
		2.04	0.10	0.95		7.2
80	69.5	0.88	0.05	-0.21	6.40	4.9
		1.25	0.10	0.09		4.8
		2.26	0.47			
75	63.1	0.23	0.05	-0.05 ^d	5.80	2.8
		0.48	0.10	-0.60		4.0
70	57.1	0.11	0.05	-1.55 ^d	5.30	2.8
		0.17	0.10	-1.24		2.9
65	51.4	0.054	nil			
		0.063	0.05			
		0.078	0.10			

a concentration is 1 x 10⁴M

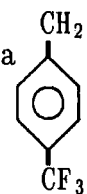
b normalised to a pathlength of 1cm

c $\frac{[\text{carbanion}]}{[\text{parent}]} = \frac{A_{328} - A'}{A_{\infty} - A_{328}}$ where A' is the equilibrium due to the parent molecule

d calculated with a value of A_∞ = 2.25

e calculated according to expression 5.15

Table 5.20

Equilibrium data for ionisation of  in DMSO/MeOH mixtures at 25 °C

vol% DMSO	mol% DMSO	λ /nm	Abs ^b	[NaOMe] /M	$\log \frac{[\text{carbanion}]}{[\text{parent}]}$ ^c	ΔJ_m	$10^6 K_{CH}$ /l mol ⁻¹ ^d
90	83.7	363	3.21	0.05	1.09		3.1
			3.47	0.10			
			3.47	0.24			
85	76.4	363	2.58	0.05	0.50	7.09	5.1
			3.03	0.10	0.91		6.7
			3.40	0.24			
			3.40	0.36			
80	69.5	363	1.53	0.05	-0.07	6.40	6.7
			1.94	0.10	0.14		5.5
			3.30	0.36			
			3.34	0.48			
75	63.1	360	0.33	0.05	-0.95	5.80	3.6
			0.80	0.10	-0.49		5.1
			3.03	0.48			
			3.27	0.60			
70	57.1	360	0.12	0.05	-1.42	5.30	3.8
			0.23	0.10	-1.12		3.8
65	51.4		0.03	0.05		4.80	
			0.06	0.10			

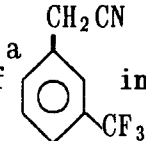
a concentration is $1 \times 10^{-4} M$

b normalised to a pathlength of 1cm

$$c \quad \frac{[\text{carbanion}]}{[\text{parent}]} = \frac{\text{Abs}}{A_m - \text{Abs}}$$

d calculated according to expression 5.15

Table 5.21

Equilibrium data for ionisation of  in DMSO/MeOH mixtures at 25^o C

vol% DMSO	mol% DMSO	b A _{330nm}	[NaOMe] /M	^c log $\frac{[\text{carbanion}]}{[\text{parent}]}$	ΔJ_m	^d 10 ⁷ K _{CH} /l mol ⁻¹
95	91.6	3.08	0.05			
		3.08	0.10			
		3.08	0.24			
90	83.7	2.40	0.05	0.50	7.90	8.0
		2.73	0.10	0.80		7.9
		3.16	0.48			
85	76.4	0.66	0.05	-0.55	7.09	4.6
		1.30	0.10	-0.12		6.2
		3.01	0.36			
80	69.5	0.14	0.05	-1.31	6.40	3.9
		0.31	0.10	-0.94		4.6
		3.01	0.72			
75	63.1	0.043	0.05	-1.84	5.80	4.6
		0.080	0.10	-1.56		4.4
70	57.1	0.010	0.05	-2.47	5.30	3.3
		0.021	0.10	-2.15		3.5

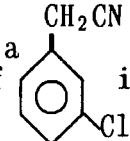
a concentration is 1 x 10⁴M

b normalised to a pathlength of 1cm

$$c \quad \frac{[\text{carbanion}]}{[\text{parent}]} = \frac{A_{330}}{A_{\infty} - A_{330}}$$

d calculated according to expression 5.15

Table 5.22

Equilibrium data for ionisation of  in DMSO/MeOH mixtures at 25°C

vol% DMSO	mol% DMSO	λ/nm	Abs ^b	[NaOMe] /M	$\log \frac{[\text{carbanion}]^c}{[\text{parent}]}$	ΔJ_m	$10^7 K_{\text{CH}}^d$ /l mol ⁻¹
95	91.6	342	2.80	0.05	0.94	9.01	1.7
			3.01	0.10	—		
			3.12	0.24	—		
90	83.7	342	1.29	0.05	-0.15	7.90	1.8
			2.11	0.10	0.32		
			3.12	0.24	—		
85	76.4	342	0.29	0.05	-0.99	7.09	1.7
			0.59	0.10	-0.063		
80	69.5	340	0.062	0.05	-1.71	6.40	1.6
			0.111	0.10	-1.45		
			3.25	0.72			
			3.24	0.96			
75	63.1	340	0.013	0.05	-2.39	5.80	1.3
			0.020	0.10	-2.20		
70	57.1	340	0.0027	0.05			
			0.0057	0.10			

a concentration is $1 \times 10^4 \text{M}$

b normalised to a pathlength of 1cm

$$c \quad \frac{[\text{carbanion}]}{[\text{parent}]} = \frac{\text{Abs}}{A_{\infty} - \text{Abs}}$$

d calculated according to expression 5.15

Table 5.23

Equilibrium data for ionisation of  in DMSO/MeOH mixtures at 25^o C

vol% DMSO	mol% DMSO	^b A _{345nm}	[NaOMe] /M	^c log $\frac{[\text{carbanion}]}{[\text{parent}]}$	ΔJ_m	^d 10 ⁸ K _{CH} /l mol ⁻¹
95	91.6	2.95	0.17		9.01	
		2.86	0.20			
		3.00	0.24			
		2.42	0.05			
		2.83	0.10			
90	83.7	0.36	0.05	-0.87	7.90	3.4
		0.76	0.10	-0.47		4.3
		3.00	0.48			
85	76.4	0.061	0.05	-1.68	7.09	3.4
		0.122	0.10	-1.37		3.5
80	69.5	0.0122	0.05	-2.39	6.40	3.2
		0.0252	0.10	-2.07		3.4
75	63.1	0.0024	0.05	-3.10	5.80	2.5
		0.0049	0.10	-2.79		2.6

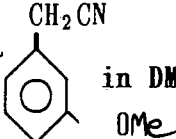
a concentration is 1 x 10⁴M

b normalised to a pathlength of 1cm

$$c \quad \frac{[\text{carbanion}]}{[\text{parent}]} = \frac{A_{345}}{A_w - A_{335}}$$

d calculated according to expression 5.15

Table 5.24

Equilibrium data for ionisation of ^a  in DMSO/MeOH mixtures at 25^o C

vol% DMSO	mol% DMSO	^b A _{330nm}	[NaOMe] /M	^c log $\frac{[\text{carbanion}]}{[\text{parent}]}$	ΔJ_m	^d 10 ⁸ K _{CH} /lmol ⁻¹
98.75	97.8	2.58	0.113			
97.5	95.7	2.56	0.057			
95	91.6	1.66	0.113	0.27	9.01	-
		0.40	0.031	-0.73		5.9
92.5	87.5	0.09	0.031	-1.44	8.35	5.4
		0.21	0.062	-1.05		6.4
90	83.7	0.021	0.031	-1.91	7.90	3.5
		0.044	0.062	-1.75		3.6

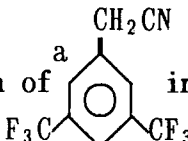
a concentration is 1 x 10⁴M

b normalised to a pathlength of 1cm

$$c \quad \frac{[\text{carbanion}]}{[\text{parent}]} = \frac{A}{A_{\infty} - A} \quad A_{\infty} = 2.56$$

d calculated according to expression 5.15

Table 5.25

Equilibrium data for ionisation of  in DMSO/MeOH mixtures at 25^o C

vol% DMSO	mol% DMSO	^b A _{355nm}	[NaOMe] /M	^c log $\frac{[\text{carbanion}]}{[\text{parent}]}$	ΔJ_m	^d 10 ⁴ K _{CH} /l mol ⁻¹
80	69.5	2.74	0.05			
		2.72	0.10			
75	63.1	2.24	0.05	0.67	5.80	1.5
		2.45	0.10	0.96		1.4
		2.72	0.3			
		2.72	0.6			
70	57.1	1.51	0.05	0.09	5.30	1.2
		1.94	0.10	0.38		1.2
		2.74	0.70			
67.5	54.2	1.04	0.05	-0.21	5.04	1.1
		1.56	0.10	0.13		1.2
65	51.4	0.64	0.05	-0.51	4.80	1.0
		1.09	0.10	-0.18		1.1
62.5	48.7	0.39	0.05	-0.78	4.56	0.9
		0.69	0.10	-0.47		0.9
60	46.1	0.21	0.05	-1.08	4.34	0.8
		0.44	0.10	-0.71		0.9

a concentration is 1 x 10⁴M

b normalised to a pathlength of 1cm

$$c \quad \frac{[\text{carbanion}]}{[\text{parent}]} = \frac{A_{355}}{A_{\infty} - A_{355}}$$

d calculated according to expression 5.15

Table 5.26

Equilibrium data for ionisation of diphenylacetonitrile^a
in DMSO/MeOH mixtures at 25^o C

vol% DMSO	mol% DMSO	b $A_{395\text{nm}}$	[NaOMe] /M	log ^c $\frac{[\text{carbanion}]}{[\text{parent}]}$	ΔH_R	e $10^5 K_{CH}$ /l mol ⁻¹
90	83.7	2.21	0.34			
85	76.4	2.26	0.2		7.09	1.6
		2.15	0.10	1.29		
		2.04	0.05	1.01		
80	69.5	2.29	0.45		6.40	1.7
		2.08	0.23			
		1.85	0.10	0.62		
		1.50	0.05	0.28		
75	63.1	1.00	0.10 ^d	-0.10	5.80	1.3
		0.65	0.05	-0.39		
72.5	60.1	0.71	0.10 ^d	-0.34	5.56	1.3
		0.39	0.05	-0.68		
70	57.1	0.41	0.10 ^d	-0.65	5.30	1.1
		0.22	0.05	-0.97		
65	51.4	0.15	0.1 ^d			
		0.07	0.05			

a concentration is $1 \times 10^4 \text{M}$

b normalised to a pathlength of 1cm

$$c \quad \frac{[\text{carbanion}]}{[\text{parent}]} = \frac{A_{395}}{A_{\infty} - A_{395}}$$

d calculated with $A_{\infty} = 2.26$

e calculated according to expression 5.15

Figure 5.27

Correlation of $\log K_{\text{CH}}$ with σ^- for substituted phenylacetonitriles.

* σ^- from ref. 29 except for 4-chlorophenylacetonitrile (ref.28)

slope = $\rho = 4.99$

intercept ($\sigma^- = 0$) = -8.56

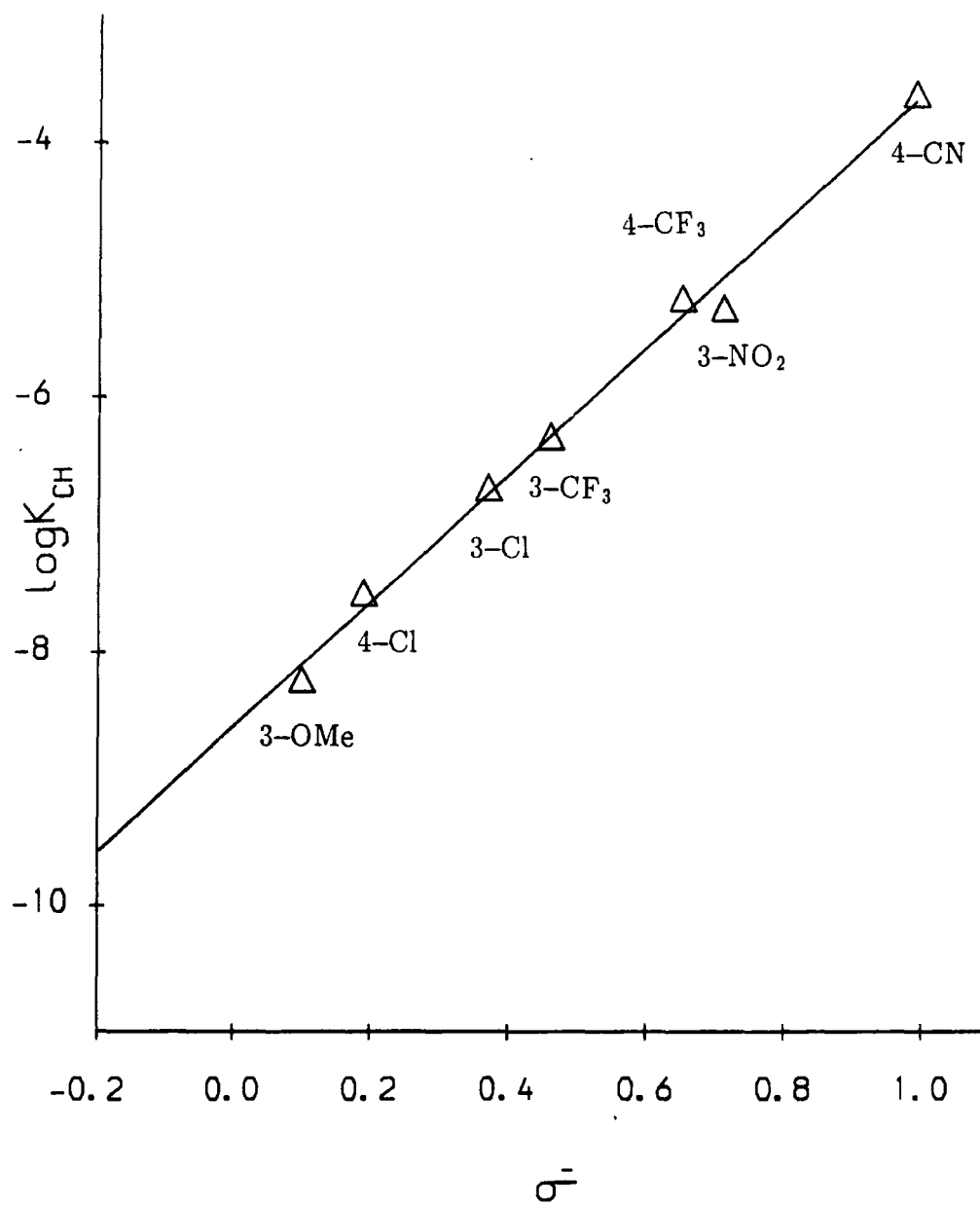


Table 5.27

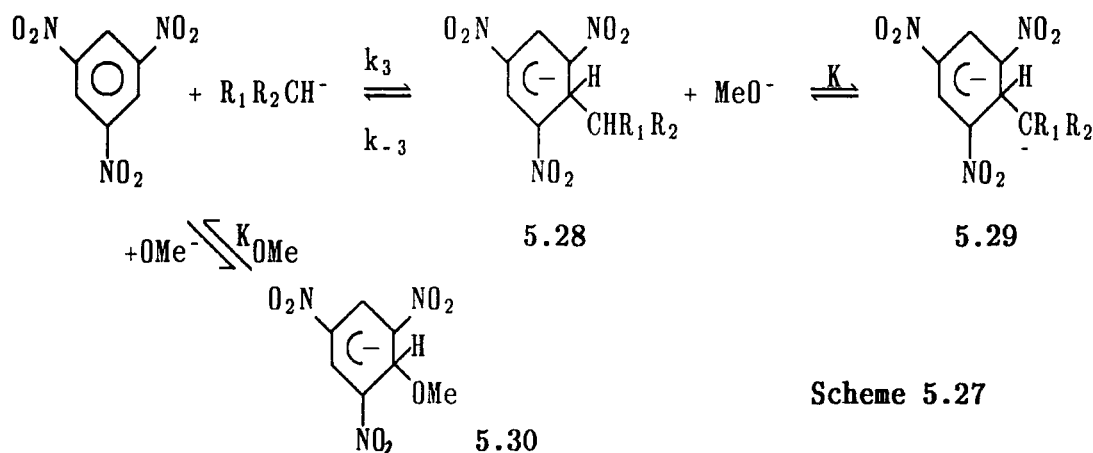
Estimated equilibrium acidities of X-substituted phenylacetonitriles in methanol

X	K_{CH} l mol^{-1}	σ^- ^a	σ^- ^b	K_{CH} l mol^{-1}	$\text{p}K_{\text{a}}$
4-NO ₂	1.17	1.297	1.23		16.85
4-CN	2.5×10^{-4}	1.019	0.99		20.5
2-CN	3.5×10^{-4}	—	—		20.4
3NO ₂	5×10^{-6}	0.756	0.71		22.2
4-CF ₃	6×10^{-6}	0.648	0.65		22.1
3-CF ₃	5×10^{-7}	0.430	0.46		23.2
3-Cl	2×10^{-7}	0.363	0.37		23.6
4-Cl	3×10^{-8}	0.192			24.4
3-OMe	6×10^{-9}	0.100	0.10		25.1
H		0		3×10^{-9} ^c	25.4
			0	3×10^{-9} ^d	25.6
3-Me		-0.086		1×10^{-9} ^c	25.9
				1×10^{-9} ^d	25.9
4-Me		-0.215		3×10^{-10} ^c	26.4
			-0.14	6×10^{-10} ^d	26.3
3,5-bis-CF ₃	1.2×10^{-4}	—	—		20.8
diphenyl- acetonitrile	1.5×10^{-5}	—	—		21.7

a data from ref. 28**b** data from ref. 29**c** calculated from $\log K_{\text{CH}} = 4.74\sigma^- - 8.50$ **d** calculated from $\log K_{\text{CH}} = 4.99\sigma^- - 8.56$

iii) Reactions with 1,3,5-trinitrobenzene (TNB)

Kinetic and absorbance data are interpreted according to scheme 5.27 which allows for the rapid reaction³⁶ of methoxide ion with TNB to give the adduct 5.30. This reaction, which has³⁷ an equilibrium constant K_{OMe} of 17 l mol^{-1} was minimised by working with $[\text{NaOMe}] \leq 0.01\text{M}$.



The scheme allows for the subsequent ionisation of the adduct 5.28. It is expected that 5.28 should be a stronger acid than $\text{R}_1\text{R}_2\text{CH}_2$ since the $\text{C}_6\text{H}_2(\text{NO}_2)_3^-$ group is electron withdrawing relative to hydrogen.^{39,40} The proton transfer involving the formation of 5.29 is likely to be rapid. Assuming the rapid formation of carbanion, the relevant rate expression (derived in the appendix) is 5.31 where K is the equilibrium constant for ionisation of 5.28 by methoxide. K is expected to be sensitive to ionic strength; this was maintained at 0.01M with sodium chloride.

$$k_{\text{obs}} = \frac{k_3 [\text{R}_1\text{R}_2\text{CH}^-]}{1 + K_{\text{OMe}} [\text{MeO}^-]} + \frac{k_{-3}}{1 + K [\text{MeO}^-]} \quad 5.31$$

$$K_{\text{obs}} = \frac{A}{(A_{\infty} - A) [\text{R}_1\text{R}_2\text{CH}^-]} \quad 5.32$$

$$K_{\text{obs}} = K_3 (1 + K [\text{MeO}^-]) \quad 5.33$$

The observed equilibrium constant, K_{obs} , is defined in expression 5.32 where A is the measured absorbance and A_{∞} is the absorbance value at complete conversion of TNB to adduct(s). It is assumed that adducts 5.28 and 5.29 have identical extinction coefficients at a given wavelength. Expression 5.33 relates K_{obs} to K_3 ($= k_3/k_{-3}$).

a) Reaction with dimethylmalonate and ethylcyanoacetate anions.

The visible spectra of 1:1 adducts formed with dimethylmalonate and ethylcyanoacetate anions had λ_{max} at 460nm ($\epsilon \approx 2.1 \times 10^4 \text{ l mol}^{-1} \text{ cm}^{-1}$) and 450nm ($\epsilon \approx 2.2 \times 10^4 \text{ l mol}^{-1} \text{ cm}^{-1}$) respectively, both with broad shoulders at 520nm, typical of carbon-bonded σ -adducts^{2,10}

Rate and absorbance data, obtained by stopped flow spectrophotometry, are shown in tables 5.34 and 5.35. Values of A_{∞} were obtained by using very large concentrations of carbanion and sodium methoxide. Data were obtained at λ_{max} (and also at 550nm for dimethylmalonate).

In the case of dimethylmalonate because of its very low value of K_{CH} the stoichiometric concentration of methoxide is depleted by at most 5%. Thus plots of k_{obs} vs $[\text{DMM}^-] / 1 + K[\text{MeO}^-]$ for each of the three methoxide concentrations are found to be linear with slopes of $2.3 \times 10^5 \text{ l mol}^{-1} \text{ s}^{-1}$ ($[\text{NaOMe}] = 2.5 \times 10^{-3} \text{ M}$), $2.5 \times 10^5 \text{ l mol}^{-1} \text{ s}^{-1}$ ($[\text{NaOMe}] = 5 \times 10^{-3} \text{ M}$) and $2.4 \times 10^5 \text{ l mol}^{-1} \text{ s}^{-1}$ ($[\text{NaOMe}] = 0.01 \text{ M}$). The value of the three intercepts (all at 24 s^{-1}) were found to be identical within experimental error, thus indicating a value for $K < 10 \text{ l mol}^{-1}$. This is borne out by the low dependence of K_{obs} on $[\text{NaOMe}]$; values at $5 \times 10^{-1} \text{ M}$ and 0.01 M sodium methoxide concentrations obtained from equilibrium absorbances are both *ca* $10,000 \text{ l mol}^{-1}$. This value is in good agreement with that obtained from combination of k_3 and k_{-3} values.

No evidence was obtained for the formation of a diadduct, though slower irreversible reactions leading to a fading of the 1:1 adduct (no change in spectral

shape) were noted. A 1:2 adduct has previously been obtained³ with dimethylmalonate and TNB in methanol. The reported equilibrium constant³ has the value 275 l mol^{-1} . Given the very low concentrations of dimethylmalonate anion generated in solution ($<3 \times 10^{-4} \text{ M}$) in this study, the 1:2 adduct would not have been in detectable concentration at equilibrium.

The results for ethylcyanoacetate are given in table 5.35 and indicate substantial ionisation of the adduct 5.28 ($R_1 = \text{CN}$, $R_2 = \text{CO}_2\text{Et}$) in line with the larger value of K_{CH} for the carbon acid. A plot of K_{obs} values derived from absorbance data vs $[\text{NaOMe}]_{\text{eq}}$ is poor with a high degree of scatter. A best fit according to expression 5.33 yields values of $K_3 = 2700 \text{ l mol}^{-1}$ and $KK_3 = 5 \times 10^5 \text{ l}^2 \text{ mol}^{-2}$. Rate constants, k_{calc} , calculated from expression 5.31 with $k_3 = 9.3 \times 10^4 \text{ l mol}^{-1} \text{ s}^{-1}$, $k_{-3} = 40 \text{ s}^{-1}$ and $K = 230 \text{ l mol}^{-1}$ agree well, throughout the entire range of carbanion and residual methoxide concentrations, with those obtained experimentally. Combination of rate coefficients gives a value of $K_3 = 2330 \text{ l mol}^{-1}$. Data are summarised in table 5.69.

b) Reactions with phenylacetonitriles

The UV/visible spectra of the 1:1 adducts formed from TNB and X-substituted phenylacetonitriles had λ_{max} centred on 450nm ($X = 4\text{-NO}_2, 4\text{-CN}, 2\text{-CN}, 4\text{-CF}_3, 3\text{-CF}_3, 3\text{-Cl}, 4\text{-Cl}$) or 455 nm ($X = 3\text{-MeO}, \text{H}, 3\text{-Me}, 4\text{-Me}$) and shoulders at 520-540nm. The di-substituted *bis* 3,5- CF_3 derivative also gave a 1:1 adduct with $\lambda_{\text{max}} = 450\text{nm}$.

4-Nitrophenylacetonitrile (PNPA)

At 450 nm the carbanion itself absorbs strongly, having an extinction coefficient of $2.0 \times 10^4 \text{ l mol}^{-1} \text{ cm}^{-1}$ at this wavelength. In order to determine values of K_{obs} , it was necessary to subtract from total absorbances the absorbance due to the carbanion. The error associated with these values is therefore large. At

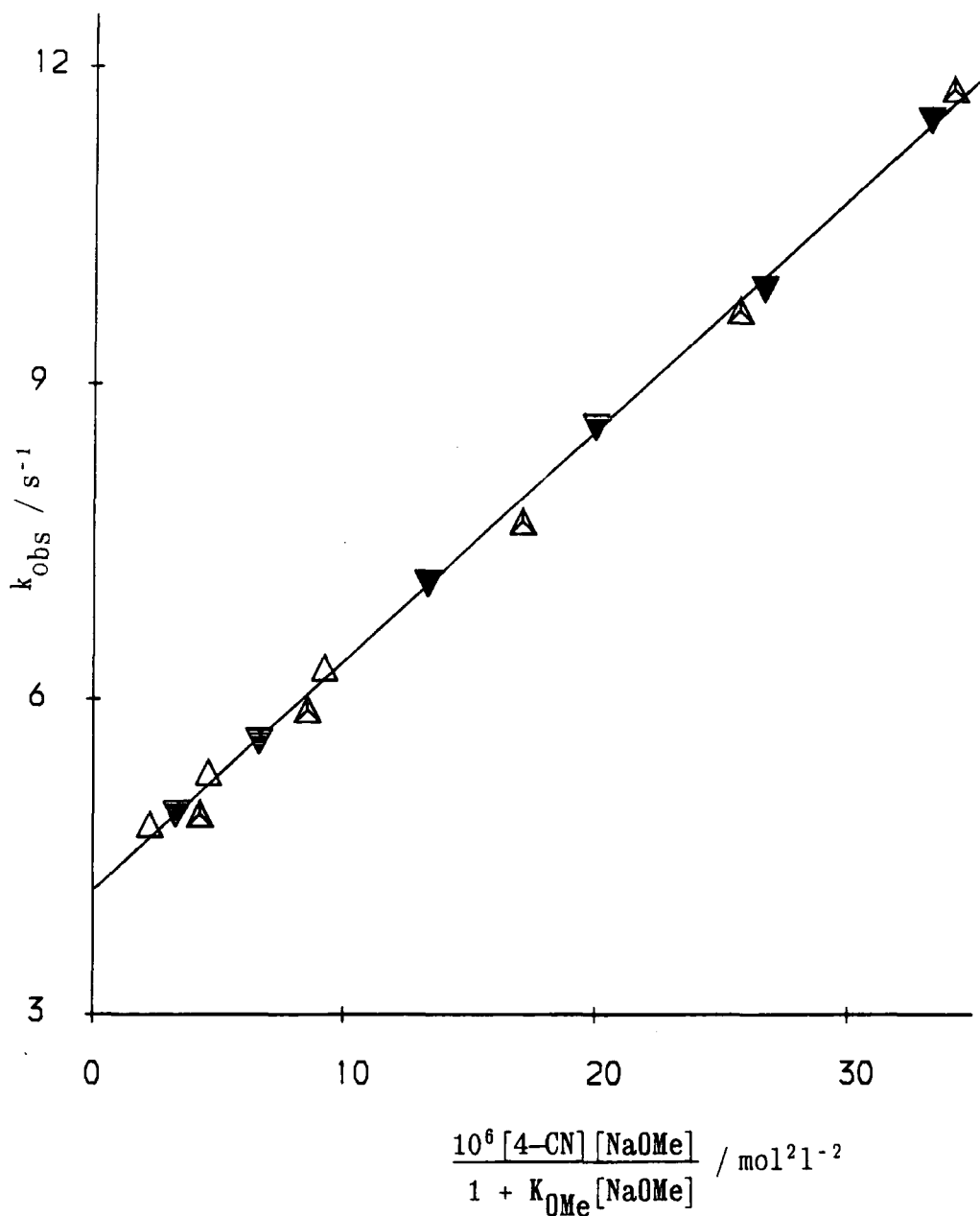
a given methoxide concentration plots according to equation 5.31 of $[\text{PNPA}^-] / 1 + K_{\text{OMe}}[\text{NaOMe}]$ are linear with an average gradient of $9.6 \times 10^5 \text{ l mol}^{-1} \text{ s}^{-1}$. The intercepts vary for each sodium methoxide concentration thus indicating ionisation of the adduct 5.28. Values of $k_3 = 9.6 \times 10^5 \text{ l mol}^{-1} \text{ s}^{-1}$, $k_{-3} = 18 \text{ s}^{-1}$ and $K = 40 \text{ l mol}^{-1}$ are consistent with the rate data and the values of K_{obs} derived from absorbances. Kinetic and equilibrium data are given in table 5.36.

For the remaining 11 phenylacetone nitriles the values of K_{CH} in methanol are small ($< 10^{-3} \text{ l mol}^{-1}$) and the concentration of the carbanion thus approximates to $K_{\text{CH}}[\text{NaOMe}][\text{R}_1\text{R}_2\text{CH}_2]$. It was therefore convenient to calculate products $k_3 K_{\text{CH}}$ from kinetic data and $K_{\text{obs}} K_{\text{CH}}$ from absorbance data. There was no evidence for ionisation of the adduct 5.28 in any of these phenylacetone nitriles; for a given compound, plots of $[\text{R}_1\text{R}_2\text{CH}_2][\text{NaOMe}] / (1 + K_{\text{OMe}}[\text{NaOMe}])$ were linear for each methoxide concentration studied with identical slopes and intercepts. Three such plots for the 4-cyano (fig. 5.37), 4-trifluoromethyl (fig. 5.39) and 3-methyl (fig. 5.46) derivatives are shown.

Values of $K_{\text{obs}} K_{\text{CH}}$ ($\equiv K_3 K_{\text{CH}}$) showed no dependence on methoxide concentration within experimental error. Values of $K_3 K_{\text{CH}}$ calculated from absorbances and kinetics agree well. This is the most direct evidence that formation of the carbanion does not represent the rate limiting step in these reactions.

Figure 5.37

Reaction of 4-cyanophenylacetonitrile ions with TNB in MeOH. Plot of kinetic data for 1:1 adduct formation.



- ▲ 0.01M [NaOMe]
- ▼ 7.5×10^{-3} M [NaOMe]
- △ 5×10^{-3} M [NaOMe]

Figure 5.39

Reaction of 4-trifluoromethylphenylacetonitrile ions with TNB in MeOH. Plot of kinetic data for 1:1 adduct formation.

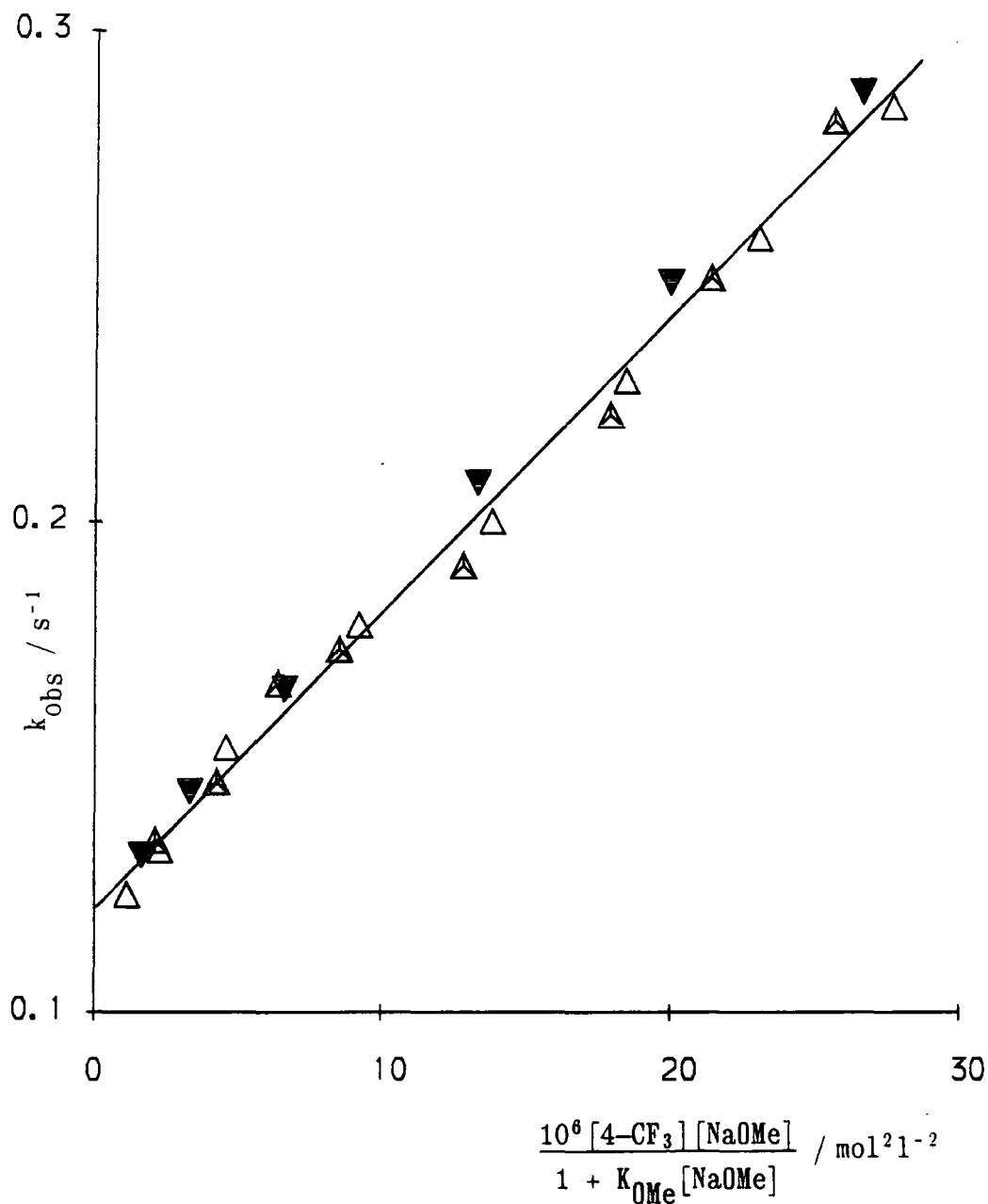
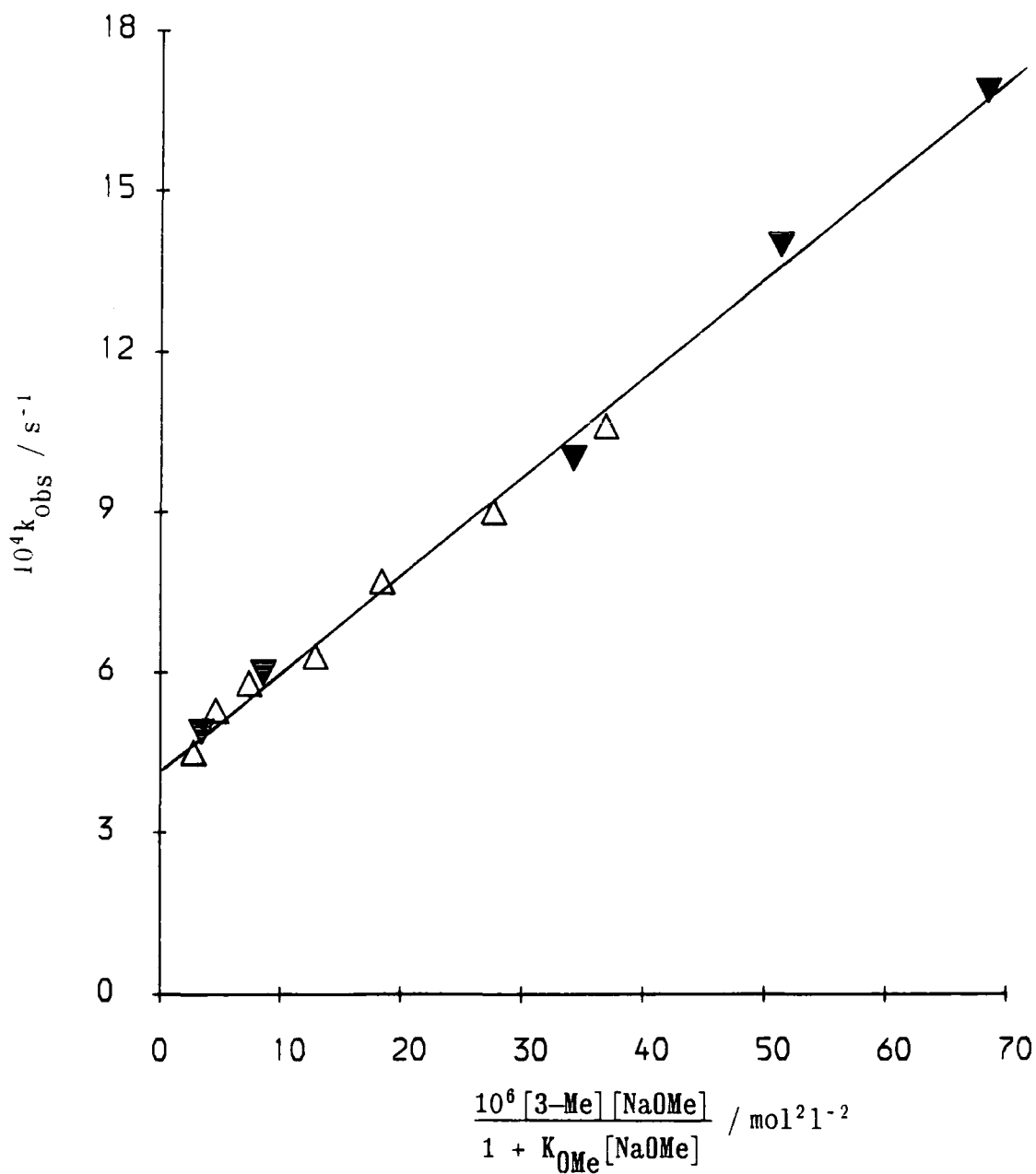


Figure 5.46

Reaction of 3-methylphenylacetonitrile ions with TNB in MeOH. Plot of kinetic data for 1:1 adduct formation.



- ▼ 0.01M [NaOMe]
- △ $5 \times 10^{-3} \text{M}$ [NaOMe]

The adducts formed were stable for several minutes before fading. The fading process only interfered noticeably with the kinetics of the reaction of 4-methylphenylacetonitrile with TNB ($t_{\frac{1}{2}} \approx 50$ minutes). The value of K_3K_{CH} calculated from absorbances is much smaller than the kinetically obtained value.

Data are summarised in table 5.49. Diphenylacetonitrile was found to be unreactive with TNB. This is likely to be due to the crowding effect of the two bulky phenyl groups and the cyano group attached to the carbon atom through which reaction occurs.

With the exception of the 2-cyano compound values of K_3 are all *ca.* $5 \times 10^4 \text{ l}^2\text{mol}^{-2}$. The independence of these values on the nature of the substituent shows that the electronic effects of the substituents in the ionisation reaction and in addition to the aromatic ring compensate each other almost exactly. The ρ value for ionisation has been shown to be *ca.* 5; it follows that the $\rho(K_3)$ value for reaction of the phenylacetonitrile anions with TNB will be close to -5 . There is similar compensation in the reaction of thiophenolate anions with TNB;^{3,9} where the ρ value for ionisation of the thiophenol (3.03) and for attack at the aromatic ring (-3.33) are nearly equal and of opposite sign. The lower value of K_3K_{CH} for the 2-cyano derivative ($1.8 \times 10^4 \text{ l}^2\text{mol}^{-2}$) can be attributed to a steric effect caused by the proximity of the *ortho*-cyano substituent to the adjacent nitro group in the adduct.^{3,4}

For the series of compounds from the 4-chloro to the 4-methyl substituents values of k_3 are all *ca.* $10^{10} \text{ l mol}^{-1}\text{s}^{-1}$ which is of the order of the diffusion controlled rate for common solvents.^{2,7}

The method of calculating values of K_{CH} in methanol, using an acidity function approach, may lead to substantial errors. Hence values of K_{CH} and thus values of k_3 may be in error by a factor of 10 or possibly more.

c) Phenylnitromethane

No reaction was observed with TNB and phenylnitromethane anions in methanol. Since the adduct produced would exist almost entirely in the ionised form, K_3 must be very small indeed. However, it was possible to generate a 1:1 adduct in solutions of DMSO/MeOH. To minimise production of the methoxide-TNB adduct a slight deficiency of sodium methoxide was used to ionise the phenylnitromethane. By increasing the amount of DMSO in the solvent there is a danger that the impurities in the sample of phenylnitromethane may become reactive. HPLC only detected two impurities (benzaldehyde and isocyanobenzene) which are unlikely to be reactive. However there is the possibility of further trace impurities in the sample.

The adduct produced (in DMSO > 80% by volume) was a deep red colour with a λ_{\max} of *ca.* 455 nm. This contrasts with the amber colour of the TNB-methoxide adduct λ_{\max} 427 nm (MeOH), 434 nm (99/1 (v/v) DMSO/MeOH). No equilibrium or kinetic measurements were made.

Table 5.34 Kinetic and Absorbance data for the reaction of 1,3,5-TNB with dimethylmalonate anion in MeOH at 25°C
Ionic strength maintained at 0.01M with NaCl

[DMM] M	10 ³ [NaOMe] M	10 ⁵ [DMM] M ^a	460nm k _{obs} s ⁻¹	550nm k _{obs} s ⁻¹	b,c A ₄₆₀	b,d A _{0Me}	10 ⁻² k _{obs} l mol ⁻¹ ^e	b,c A ₅₅₀	b,d A _{0Me}	10 ⁻² K _{obs} l mol ⁻¹ ^e
0.01	2.5	1.12	27	26	0.21	0.06	73	0.11	0.02	74
0.02	2.5	2.23	29	28	0.32	0.06	67	0.17	0.02	66
0.04	2.5	4.32	34	34	0.51	0.05	69	0.30	0.02	73
0.06	2.5	6.57	38	38	0.71	0.05	75	0.43	0.01	84
0.08	2.5	8.68	43	42	0.91	0.04	88	0.51	0.01	85
0.10	2.5	10.75	49	49	1.10	0.03	105	0.58	0.01	87
.0015	5.0	0.34		24	-	-	-	-	-	-
.0025	5.0	0.56		25	0.23	0.12	108	0.10	0.04	98
0.005	5.0	1.12		27	0.34	0.11	120	0.16	0.04	104
0.01	5.0	2.23		30	0.46	0.10	102	0.23	0.03	93
0.02	5.0	4.45		35	0.73	0.08	111	0.40	0.03	105
0.03	5.0	6.65		39	0.95	0.07	120	0.56	0.02	129
0.04	5.0	8.82		45	1.06	0.06	115	0.62	0.02	119
0.05	5.0	10.98		50	1.10	0.06	100	0.64	0.02	103
0.06	5.0	13.12		54	1.21	0.05	105	-	-	-
.0025	10.0	1.12	26	-	0.39	0.20	102	-	-	-
0.005	10.0	2.23	29	29	0.55	0.18	111	0.25	0.06	91
0.010	10.0	4.46	34	34	0.77	0.15	109	0.40	0.05	99
0.015	10.0	6.64	37	38	0.98	0.13	120	0.49	0.04	97
0.02	10.0	8.88	40	41	1.03	0.12	100	0.57	0.04	96
0.03	10.0	13.26	49	50	1.19	0.10	96	0.67	0.03	93
0.04	10.0	17.61	60	60	1.34	0.09	100	0.80	0.02	114
0.05	10.0	21.91	-	69	1.56	0.06	140	0.93	-	-
0.06	10.0	26.18	-	79	1.62	0.05	139	0.95	-	-
0.30	10.0				2.06			1.19		
0.40	10.0				2.04			1.19		

Legend for Table 5.34

- a** concentration of dimethylmalonate anion calculated with $K_{CH} = 0.45 \text{ l mol}^{-1}$
- b** absorbances correspond to a pathlength of 1cm and a TNB concentration of $1 \times 10^{-4} \text{ M}$
- c** equilibrium absorbances due to both methoxide and dimethylmalonate adducts
- d** absorbance due to methoxide adduct at equilibrium. Calculated as

$$A_{\text{OMe}^-} = A_{\text{OMe}}' \cdot \left(1 - \frac{A}{A_{\infty}}\right)$$

where A_{OMe}' is the absorbance due to the methoxide adduct in the absence of dimethylmalonate. The calculation uses extinction coefficients for the methoxide adduct of $1.7 \times 10^4 \text{ l mol}^{-1} \text{ cm}^{-1}$ and $0.5 \times 10^4 \text{ l mol}^{-1} \text{ cm}^{-1}$ at 460nm and 550nm respectively.

- e** Calculated as

$$\frac{A - A_{\text{OMe}}}{(A_{\infty} - A) [\text{DMM}^-]} \quad \text{using} \quad \begin{aligned} A_{\infty}^{460} &= 2.05 \\ A_{\infty}^{550} &= 1.19 \end{aligned}$$

Table 5.35

Kinetic and Absorbance data for the reaction of
 1,3,5-TNB with ethylcyanoacetate anion in MeOH at 25°C
 Ionic strength maintained at 0.01M with NaCl

10^1 [ECA] M	10^3 [NaOMe] M	10^4 [DMM] M	10^3 [OMe ⁻] M _{eq}	A_{450} b,c	A_{OMe} b,d	10^{-2} k_{obs} l mol ⁻¹	k_{obs}^{450} s ⁻¹	k_{calc} s ⁻¹
0.5	2.5	0.28	2.47	0.32	0.06	49	29.3	28.0
1.0	2.5	0.55	2.44	—	—	—	31.5	30.5
2.0	2.5	1.09	2.39	0.67	0.05	37	38.4	35.6
0.2	5.0	0.21	4.98	0.25	0.12	32	20.4	20.4
0.5	5.0	0.53	4.95	0.62	0.10	63	23.7	23.0
1.0	5.0	1.05	4.89	0.74	0.09	42	27.7	27.8
1.5	5.0	1.56	4.84	1.02	0.07	50	32.1	32.6
2.0	5.0	2.06	4.79	1.01	0.07	38	36.0	36.7
3.0	5.0	3.04	4.70	1.03	0.07	27	43.3	45.4
4.0	5.0	3.98	4.60	1.41	0.05	42	52.7	53.8
8.0	5.0	7.42	4.53	1.64	0.03	38	83.1	83.7
0.5	7.5	0.76	7.42	0.90	0.11	79	21.2	21.1
2.0	7.5	2.95	7.21	1.55	0.06	76	39.8	39.5
5.0	7.5	7.01	6.80	1.86	0.03	72	75.9	74.0
0.2	10.0	0.39	9.96	0.59	0.18	64	15.7	15.3
0.5	10.0	0.96	9.90	1.02	0.13	76	20.2	19.8
0.5	10.0	0.96	9.90	0.92	0.14	63	19.8	19.8
0.75	10.0	1.43	9.86	1.17	0.12	70	23.8	23.6
1.0	10.0	1.91	9.81	1.25	0.11	62	28.5	27.5
2.0	10.0	3.75	9.62	1.53	0.07	57	42.5	42.4
6.0	10.0	10.60	8.94	1.95	0.03	68	98.5	98.7
10.0	10.0	16.67	8.33	—	—	—	141	149
10.0	40.0			2.22				
20.0	40.0			2.22				

Legend for Table 5.35

- a** concentration of ethylcyanoacetate anion calculated with $K_{CH} = 24 \text{ l mol}^{-1}$
- b** absorbances correspond to a pathlength of 1cm and a TNB concentration of $1 \times 10^{-4} \text{ M}$
- c** equilibrium absorbances due to both methoxide and dimethylmalonate adducts
- d** absorbance due to methoxide adduct at equilibrium. Calculated as

$$A_{\text{OMe}^-} = A'_{\text{OMe}^-} \cdot \left(1 - \frac{A}{A_{\infty}}\right)$$

where A'_{OMe^-} is the absorbance due to the methoxide adduct in the absence of ethylcyanoacetate. The calculation uses an extinction coefficient for the methoxide adduct of $1.7 \times 10^4 \text{ l mol}^{-1} \text{ cm}^{-1}$ at 450nm.

- e** Calculated as

$$\frac{A_{450} - A_{\text{OMe}^-}}{(2.22 - A_{450}) [\text{ECA}^-]}$$

- f** calculated using expression 5.31 with $K_{\text{OMe}^-} = 17 \text{ l mol}^{-1}$, $k_3 = 9.3 \times 10^4 \text{ l mol}^{-1} \text{ s}^{-1}$, $k_{-3} = 40 \text{ s}^{-1}$ and $K = 230 \text{ l mol}^{-1}$

Table 5.36

Kinetic and equilibrium data for the reaction of 4-nitrophenylacetonitrile ions
with TNB in methanol at 25°C I = 0.01M (NaCl)

10^3 [NaOMe] M	10^4 [PNPA] M	10^5 [TNB] M	10^6 [PNPA ⁻] M	^a A_{450} ^b	^{b,c} A_{PNPA^-}	k_{obs} s ⁻¹	k_{calc} s ⁻¹	^d A_{450} ^{b,e}	A_{OMe^-} ^{b,f}	$10^{-4}K_{\text{obs}}$ ^g l mol ⁻¹	$10^4 \frac{A_{\text{PNPA}^-}}{[\text{PNPA}]}$ calc
1.5	8	10	1.40	0.247	0.026	18.8	18.3	0.221	0.038	6.6	1.86
1.5	16	6	2.80	0.296	0.050	20.3	19.6	0.410	0.034	7.5	1.79
2.5	4	10	1.17	0.243	0.020	17.5	17.4	0.223	0.062	7.0	2.08
2.5	10	6	2.91	0.313	0.052	19.1	19.0	0.435	0.056	7.4	2.02
2.5	24	5	6.98	0.534	0.141	23.5	22.8	0.786	0.045	7.5	2.02
2.5	38	3	11.03	0.541	—	28.4	26.5	1.105	0.034	8.9	—
5.0	4	10	2.33	0.410	0.040	17.6	17.1	0.370	0.111	6.1	1.72
5.0	6	8	3.49	0.426	0.063	18.6	18.1	0.454	0.106	5.7	1.81
5.0	10	5	5.81	0.451	0.108	20.1	20.1	0.686	0.092	6.8	1.86
5.0	24	3	13.92	0.580	0.262	27.5	27.3	1.060	0.069	6.2	1.88
5.0	36	3	20.85	0.714	0.387	32.4	33.4	1.090	0.067	4.4	1.86
5.0	48	3	27.76	0.931	0.548	39.1	39.6	1.277	0.056	4.8	1.97

table 5.36 continued

10^3 [NaOMe] M	10^4 [PNPA] M	10^5 [TNB] M	10^6 [PNPA ⁻] M	A_{450} ^a	A_{PNPA^-} ^b	k_{obs} ^c s ⁻¹	k_{calc} ^d s ⁻¹	A_{450} ^{b,e}	A_{OMe^-} ^{b,f}	$10^{-4}K_{\text{obs}}$ ^g lmol ⁻¹	$10^4 \frac{A_{\text{PNPA}^-}}{[\text{PNPA}^-]}_{\text{calc}}$
7.5	2	10	1.74	0.454	0.041	15.6	15.3	0.413	0.156	8.3	2.36
7.5	6	5	5.22	0.436	0.106	17.9	18.3	0.660	0.135	6.5	2.03
7.5	12	4	10.42	0.647	0.193	22.0	22.7	1.135	0.093	9.4	1.85
7.5	20	3	17.36	0.737	0.347	27.4	28.6	1.300	0.079	7.8	2.00
7.5	28	3	24.28	0.921	0.485	33.2	34.5	1.453	0.065	7.7	2.00
7.5	36	3	31.18	1.087	0.625	41.0	40.4	1.540	0.058	7.2	2.00
10.0	2	8	2.31	0.502	0.051	14.8	14.8	0.564	0.184	—	2.17
10.0	4	5	4.62	0.444	0.091	16.1	16.6	0.708	0.168	7.8	1.95
10.0	8	5	9.24	0.625	0.180	18.7	20.4	0.890	0.147	6.1	1.95
10.0	16	3	18.47	0.771	0.393	24.6	28.0	1.260	0.106	6.6	2.13
10.0	20	3	23.08	0.915	0.472	29.9	31.8	1.477	0.081	8.4	2.05
10.0	24	3	27.68	0.999	—	31.6	35.6	1.485	0.080	7.1	—
10.0	30	3	34.58	1.202	—	39.6	41.2	1.710	0.056	9.4	—

a calculated with $K_{\text{CH}} = 1.17 \text{ lmol}^{-1}$ **b** normalised to a pathlength of 1cm **c** experimentally measured absorbances due to PNPA⁻ anion
d calculated with $k_3 = 9.6 \times 10^5 \text{ lmol}^{-1}\text{s}^{-1}$, $k_{-3} = 18 \text{ s}^{-1}$ and $K = 40 \text{ lmol}^{-1}$ according to expression 5.31
e absorbance minus absorbance of PNPA⁻ and normalised to $1 \times 10^{-4} \text{ M TNB}$ **f** equilibrium absorbance due to methoxide adduct, calculated
 $\epsilon_{\text{OMe}} = 1.7 \times 10^4 \text{ lmol}^{-1}\text{cm}^{-1}$ and $K_{\text{OMe}} = 17 \text{ lmol}^{-1}$ **g** calculated as
$$\frac{A_{450} - A_{\text{OMe}}}{(2.2 - A_{450}) [\text{PNPA}^-]}$$

Table 5.37

Kinetic and absorbance data obtained by
stopped flow spectrophotometry for the reaction of
4-cyanophenylacetonitrile with TNB in methanol at 25⁰ C

I = 0.01M (NaCl)

10^3 [NaOMe] M	10^3 [4-CN] M	10^5 [TNB] M	a A_{450}	k_{450}^{obs} s^{-1}	a, b A_{450}	a, c A_{OMe^-}	10^{-4} $K_3 K_{CH}$ $l^2 mol^{-2}$
10	0.5	10	0.49	4.9	0.49	0.19	3.5
10	1.0	6	0.50	5.9	0.83	0.15	5.0
10	2.0	4	0.44	7.7	1.08	0.13	4.2
10	3.0	3	0.41	9.7	1.32	0.09	4.7
10	4.0	2	0.32	11.8	1.51	0.08	5.2
7.5	0.5	8	0.36	4.9	0.45	0.15	4.6
7.5	0.5	16	—	4.9	—	—	—
7.5	1.0	6	0.44	5.6	0.73	0.13	5.4
7.5	2.0	4	0.43	7.1	1.05	0.10	5.5
7.5	3.0	3	0.42	8.6	1.36	0.07	6.8
7.5	4.0	2	0.35	9.9	1.66	0.05	9.9
7.5	5.0	2	0.36	11.5	1.69	0.04	8.6
7.5	nil	8	.156		.195	—	
5.0	0.5	10	—	4.8	—		
5.0	1.0	6	—	5.3	—		
5.0	2.0	4	0.34	6.3	0.83	0.08	5.7

a Absorbances normalised to a pathlength of 1cm.

b absorbance normalised to 1×10^{-4} M TNB. The absorbance due to 4-cyanophenylacetonitrile ($\epsilon = 4 \text{ l mol}^{-1} \text{ cm}^{-1}$ at 450 nm) has been subtracted.

c equilibrium absorbance due to the methoxide adduct

d calculated as

$$\frac{A_{450} - A_{OMe}}{(2.2 - A_{450}) [4-CN] [NaOMe]}$$

Table 5.38

Kinetic and Equilibrium data for the reaction of TNB with
2-cyanophenylacetonitrile in MeOH at 25°C I=0.01M (NaCl)

$10^3 [\text{NaOMe}]$ /M	$10^3 [2\text{-CN}]$ /M	$10^5 [\text{TNB}]$ /M	A_{450}^a	A_{OCN}^b	k_{obs}^c /s ⁻¹	A_{450}^d	A_{OMe}^e	$10^{-4} k_3 K_{\text{CH}}$ l ² mol ⁻²
10.0	nil	10	0.26	—	—	0.26		
10.0	1.0	8	0.43	—	18.0	0.48	0.20	1.6
10.0	2.0	5	0.41	.085	19.7	0.65	0.18	1.5
10.0	4.0	3	0.46	.190	24.0	0.90	0.15	1.4
10.0	6.0	3	0.57	0.28	27.5	0.97	0.15	1.1
10.0	8.0	3	0.75	0.37	33.5	1.27	0.11	1.6
10.0	10.0	2	0.75	0.46	37.8	1.45	0.09	1.8
10.0	12.0	2	0.90	—	42.7	1.65		
7.5	nil	10	0.20	—	—			
7.5	1.0	10	0.45	—	17.0	0.40	0.16	1.8
7.5	2.0	6	0.42	.085	19.0	0.55	0.15	1.6
7.5	3.0	4	0.41	—	20.0	0.67	0.14	1.5
7.5	5.0	3	0.50	0.24	23.8	0.87	0.12	1.5
7.5	8.0	3	0.75	0.41	30.2	1.13	0.10	1.6
7.5	11.0	2	0.78	0.55	34.1	1.15	0.10	1.2
7.5	14.0	3	—	—	40.7			

a measured absorbance due to TNB methoxy and carbanion adducts and to 2-cyanophenylacetonitrile (the neutral molecule) normalised to a pathlength of 1 cm..

b measured absorbance due to phenylacetonitrile normalised to a pathlength of 1 cm.

c obtained by stopped flow spectrophotometry at 450 nm.

d absorbance due to TNB-methoxy and carbanion adducts normalised to a pathlength of 1 cm and 1×10^{-4} M TNB.

e equilibrium absorbance due to TNB-methoxy adduct calculated as:

$$\left(1 - \frac{A_{450}}{2.2}\right) \times A'_{\text{OMe}} \quad \text{Where } A'_{\text{OMe}} = \text{absorbance due to the methoxy adduct in the absence of competition.}$$

f calculated as
$$\frac{A_{450} - A_{\text{OMe}}}{(2.2 - A_{450}) [\text{NaOMe}] [2\text{-CN}]}$$

Table 5.39

Rate and Equilibrium data for the reaction of TNB^a with
4-trifluoromethylphenylacetonitrile in MeOH at 25°C

$10^3 [\text{NaOMe}]$ /M	$10^3 [4\text{-CF}_3]$ /M	^b A_{450}	^c A_{OMe}	^d $10^{-4} K_3 K_{\text{CH}}$ $\text{l}^2 \text{mol}^{-2}$	^e k_{obs} /s ⁻¹
5.0	0.25	0.22	0.12	3.9	0.124
5.0	0.50	0.31	0.11	4.1	0.133
5.0	1.00	0.45	0.11	3.8	0.154
5.0	2.00	0.70	0.09	3.9	0.179
5.0	3.00	0.82	0.08	3.4	0.200
5.0	4.00	0.96	0.08	3.4	0.229
5.0	5.00	1.10	0.07	3.6	0.258
5.0	6.00	1.16	0.06	3.4	0.285
7.5	0.25	0.38	0.16	6.3	0.132
7.5	0.50	0.50	0.15	5.3	0.145
7.5	1.00	0.72	0.13	5.1	0.166
7.5	2.00	1.10	0.10	5.8	0.208
7.5	3.00	1.37	0.08	6.5	0.249
7.5	4.00	1.62	0.05	—	0.288
10.0	0.25	0.42	0.20	4.8	0.135
10.0	0.25	0.46	0.20	5.8	0.135
10.0	0.50	0.60	0.18	5.1	0.147
10.0	0.75	0.74	0.17	5.0	0.164
10.0	1.00	0.88	0.15	5.3	0.175
10.0	1.00	0.84	0.15	4.9	0.173
10.0	1.50	1.00	0.13	4.6	0.191
10.0	2.00	1.18	0.12	5.0	0.222
10.0	2.50	1.22	0.11	4.3	0.250
10.0	3.00	1.39	0.09	5.0	0.282

a concentration is 10^{-4} M.

c equilibrium absorbance due to
TNB methoxide adduct.

d calculated as $\frac{A_{450} - A_{\text{OMe}}}{(2.25 - A_{450}) [4\text{-CF}_3] [\text{NaOMe}]}$

b absorbance due to adducts formed
from methoxide and carbanion.

Normalised to a pathlength of 1cm.

e obtained by stopped flow spectro-
photometry

Table 5.40

Kinetic and Equilibrium data for the reaction of TNB^a with
3-trifluoromethylphenylacetonitrile in MeOH at 25^oC

$10^3 [\text{NaOMe}]$ /M	$10^3 [3\text{-CF}_3]$ /M	b, c A_{450}	b, d A_{OMe}	e $10^{-4} K_3 K_{\text{CH}}$ $\text{l}^2 \text{mol}^{-2}$	f $10^2 k_{\text{obs}}$ /s ⁻¹
5.0	0.5	0.32	0.12	4.2	2.55
5.0	1.0	0.49	0.11	4.4	2.66
5.0	2.0	0.68	0.10	3.7	3.04
5.0	4.0	0.99	0.08	3.7	3.78
5.0	6.0	1.37	0.05	5.1	4.61
5.0	8.0	—	—	—	5.57
10.0	0.25	0.43	0.21	4.9	2.39
10.0	0.50	0.59	0.19	4.9	2.64
10.0	0.75	0.63	0.19	3.7	2.77
10.0	1.00	0.76	0.17	4.0	3.07
10.0	1.25	0.89	0.16	4.4	3.14
10.0	1.75	1.09	0.13	4.8	3.52
10.0	2.00	1.14	0.13	4.6	3.78
10.0	2.50	1.32	0.11	5.3	4.20
10.0	3.00	1.31	0.11	4.3	4.53
10.0	3.50	1.14	0.10	4.6	4.96
10.0	4.00	1.48	0.09	4.6	5.57
20.0	30.0	2.23			
20.0	40.0	2.23			

a concentration is $1 \times 10^{-4} \text{M}$

b normalised to pathlength of 1 cm.

c absorbance due to carbanion
and methoxy adducts.

d absorbance due to methoxy
adduct at equilibrium

f calculated as
$$\frac{A_{450} - A_{\text{OMe}}}{(2.23 - A_{450}) [\text{NaOMe}] [3\text{-CF}_3]}$$

f obtained by stopped flow spectrophotometry at 450 nm.

Table 5.41

Kinetic and Equilibrium data for the reaction of TNB^a with
3-chlorophenylacetonitrile in MeOH at 25°C I = 0.01M (NaCl)

$10^3 [\text{NaOMe}]$ /M	$10^3 [3\text{-Cl}]$ /M	k_{obs}^{450} /s ⁻¹	A_{450}^b	A_{OMe}^c	$10^{-4} K_3 K_{\text{CH}}^d$ l ² mol ⁻²
2.5	1.0	0.015	0.34	0.06	5.2
2.5	2.0	0.018	0.50	0.06	4.4
5.0	1	0.017	0.62	0.20	4.5
5.0	2	0.020	0.91	0.17	4.7
5.0	3	0.023	1.18	0.14	5.3
5.0	4	0.027	1.27	0.13	4.6
5.0	5	0.029	1.37	0.12	4.4
5.0	6	0.032	1.45	0.11	4.3
10.0	1	0.017	1.05	0.15	6.2
10.0	1	0.018	1.02	0.15	5.9
10.0	1.5	0.021	1.25	0.13	6.0
10.0	2.0	0.024	1.34	0.12	5.3
10.0	2.5	0.028	1.50	0.10	5.6
10.0	3.0	0.029	1.58	0.10	5.4
10.0	3.5	0.034	1.59	0.09	4.7
10.0	4.0	0.036	1.69	0.08	
10.0	20.0	—	2.48		
10.0	30.0	—	2.50		
10.0	nil	—	0.14		
5.0	nil	—	0.26		

a concentration is 1×10^{-4} M

b absorbance due to carbanion and methoxy adducts normalised to a pathlength of 1 cm.

c equilibrium absorbance due to methoxide adduct.

d calculated as
$$\frac{A_{450} - A_{\text{OMe}}}{(2.5 - A_{450}) [\text{NaOMe}] [3\text{-Cl}]}$$

Table 5.42

Kinetic and Equilibrium data for the reaction of TNB^a with
4-chlorophenylacetonitrile in MeOH at 25^oC I = 0.01M (NaCl)

$10^3 [\text{NaOMe}]$ /M	$10^3 [4\text{-Cl}]$ /M	^b A_{450}	^c A_{OMe}	^d $10^{-4} K_3 K_{\text{CH}}$ $\text{l}^2 \text{mol}^{-2}$	^e $10^3 k_{\text{obs}}$ /s ⁻¹
5.0	1.0	0.61	0.09	6.3	3.6
5.0	2.0	0.88	0.07	5.8	4.4
5.0	3.0	1.05	0.06	5.4	5.3
5.0	4.0	1.26	0.05	6.0	6.0
5.0	nil	0.24	—	—	
10.0	0.5	0.59	0.18	4.9	
10.0	1.0	0.95	0.14	6.1	4.3
10.0	1.5	1.15	0.19	6.1	5.0
10.0	2.0	1.32	0.12	5.2	5.8
10.0	2.5	1.45	0.10	6.6	6.6
10.0	3.0	1.56	0.09	7.0	7.1
10.0	3.5	1.58	0.07	6.3	8.2
10.0	4.0	1.59	0.07	5.6	9.0
10.0	4.5	1.60	0.07	5.1	9.8
10.0	5.0	1.83	0.07		9.8
10.0	nil	0.24			
10.0	20	2.27			
10.0	25	2.26			

a concentration is $1 \times 10^{-4} \text{M}$

c equilibrium absorbance due to
the methoxy adduct, calculated

as

$$\frac{A_{450} - A_{\text{OMe}}}{(2.27 - A_{450}) [4\text{-Cl}] [\text{NaOMe}]}$$

b absorbance due to adducts

corresponds to pathlength of 1cm.

d calculated as

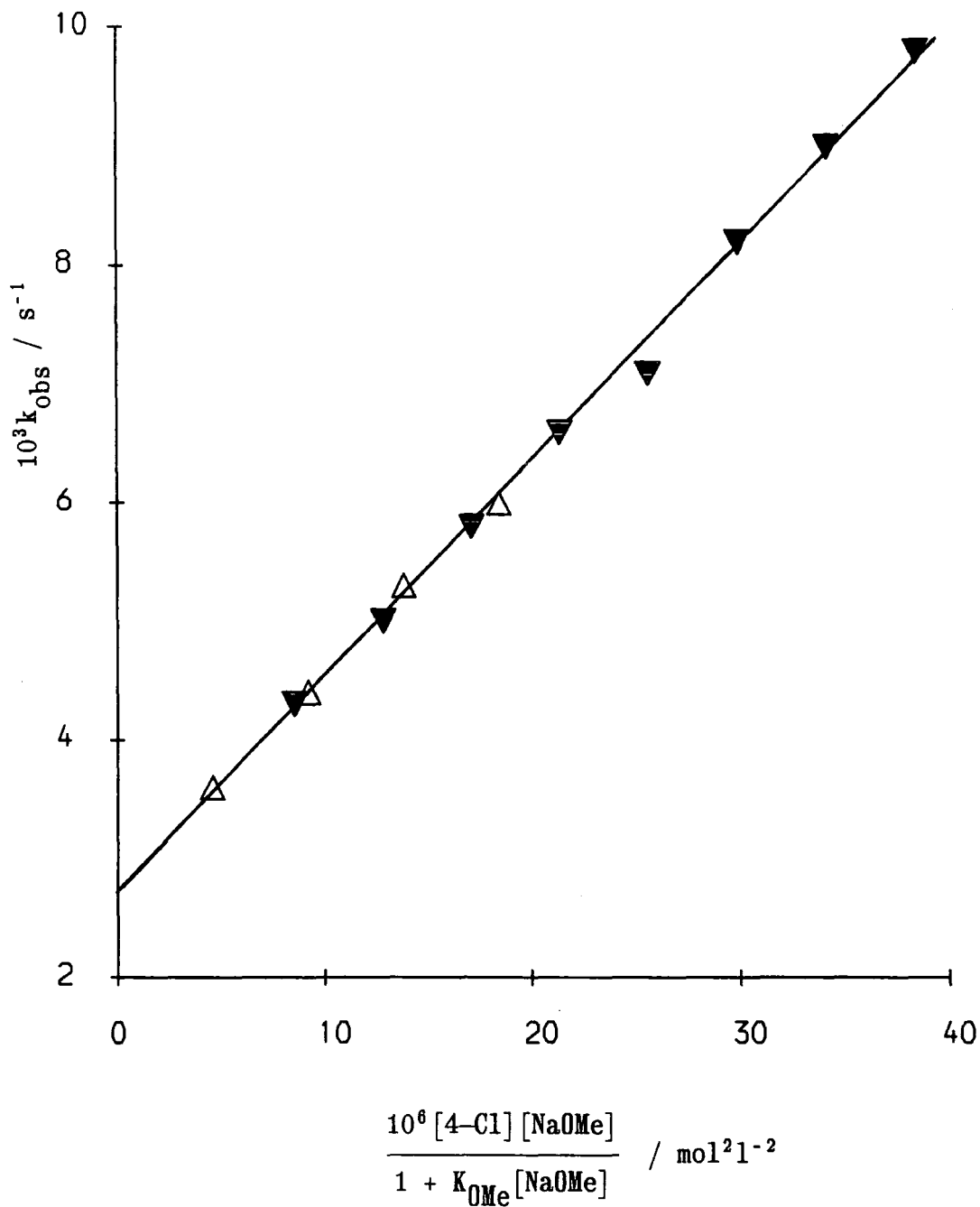
$$A_{\text{OMe}} = A_{\text{OMe}}' \left[1 - \frac{A_{450}}{2.27} \right]$$

where A_{OMe}' is the absorbance
due to the methoxy adduct in
the absence of competition.

e determined by conventional spectrophotometry at 450 nm.

Figure 5.42

Reaction of 4-chlorophenylacetonitrile ions with TNB in MeOH. Plot of kinetic data for 1:1 adduct formation.



- ▼ = 0.01M NaOMe
△ = $5 \times 10^{-3} \text{M}$ NaOMe

Table 5.43

Kinetic and Equilibrium data for the reaction of TNB^a with
3-methoxyphenylacetonitrile in MeOH at 25°C

$10^3 [\text{NaOMe}]$ /M	$10^3 [3\text{-MeO}]$ /M	$10^3 k_{\text{obs}}$ /s ⁻¹	A_{455}	$A_{0\text{Me}}$	$10^{-4} K_3 K_{\text{CH}}$ l ² mol ⁻²
5.0	1.0	1.17	0.57	0.10	5.8
5.0	2.0	1.62	0.90	0.08	6.3
5.0	3.0	1.90	1.12	0.07	6.5
5.0	4.0	2.11	1.24	0.06	6.1
5.0	6.0	2.81	1.47	0.04	6.5
5.0	8.0	3.45	—		
5.0	10.0	4.00	1.71		
10.0	1.0	1.76	0.85	0.15	5.2
10.0	1.5	2.35	—		
10.0	2.0	2.43	1.20	0.11	5.5
10.0	3.0	3.10	1.43	0.09	5.8
10.0	4.0	3.74	1.63	0.06	6.9
10.0	5.0	4.32	1.67	0.06	6.1

a concentration is 1×10^{-4} M

b measured by conventional spectrophotometry at 455 nm.

c absorbance due to adducts normalised to a pathlength of 1 cm.

d equilibrium absorbance due to TNB methoxy adduct.

e calculated as
$$\frac{A_{455} - A_{0\text{Me}}}{(2.2 - A_{455}) [3\text{-MeO}] [\text{NaOMe}]}$$

Table 5.45
Kinetic and Equilibrium data for the reaction of TNB^a with
phenylacetonitrile in MeOH at 25^o C

$10^3 [\text{NaOMe}]$ /M	10^3 [PhCH ₂ CN] /M	10^3 b k_{obs} /s ⁻¹	A_{455} c	A_{OMe} d	$10^{-4} K_3 K_{\text{CH}}$ e l ² mol ⁻²
10.0	100.0	23.2	2.15		
10.0	80.0	18.8	2.15		
10.0	60.0	14.3			
10.0	40.0	9.6			
10.0	20.0	5.2			
10.0	10.0	3.3			
10.0	20.0	5.0			
10.0	2.0	1.10			
10.0	1.0	0.83	1.06	0.13	8.5
5.0	40.0	5.10			
5.0	20.0	2.90			
5.0	18.0	2.45			
5.0	14.0	1.92	1.68	0.03	5.0
5.0	10.0	1.66	1.54	0.04	4.9
5.0	8.0	1.43	1.48	0.04	5.4
5.0	6.0	1.17	1.28	0.05	4.7
5.0	4.0	0.93	1.02	0.07	4.2
5.0	3.0	0.88	0.91	0.08	4.5
5.0	2.0	0.79			
5.0	1.0	0.70	0.48	0.10	4.6

a concentration is 1×10^{-4} M

b determined by stopped flow and conventional spectrophotometry

c absorbance due to adducts corresponds to a pathlength of 1 cm.

d equilibrium absorbance due to methoxy adduct.

e calculated as

$$\frac{A_{455}}{(2.15 - A_{455}) [\text{NaOMe}] [\text{PhCH}_2\text{CN}]}$$

Table 5.46

Kinetic and Equilibrium data for the reaction of TNB^a with
3-methylphenylacetonitrile in MeOH at 25^oC I = 0.01M (NaCl)

$10^3 [\text{NaOMe}]$ /M	$10^3 [3\text{-Me}]$ /M	$10^4 k_{\text{obs}}$ /s ⁻¹	A_{455} ^c	$A_{0\text{Me}}$ ^d	$10^{-4} K_3 K_{\text{CH}}$ ^e l ² mol ⁻²
5.0	0.6	4.5	0.42	0.11	5.8
5.0	1.0	5.3	0.56	0.10	5.6
5.0	1.6	5.8	0.66	0.09	4.6
5.0	2.8	6.3	1.00	0.07	5.5
5.0	4.0	7.6	1.22	0.07	5.9
5.0	6.0	9.0	1.33	0.05	4.9
5.0	8.0	10.6	1.41	0.05	4.3
10.0	0.4	4.9	0.48	0.19	4.2
10.0	1.0	6.0	—		
10.0	4.0	10.0	1.32	0.10	3.5
10.0	6.0	14.0	1.46	0.08	3.1
10.0	8.0	16.9	1.71	0.06	4.2

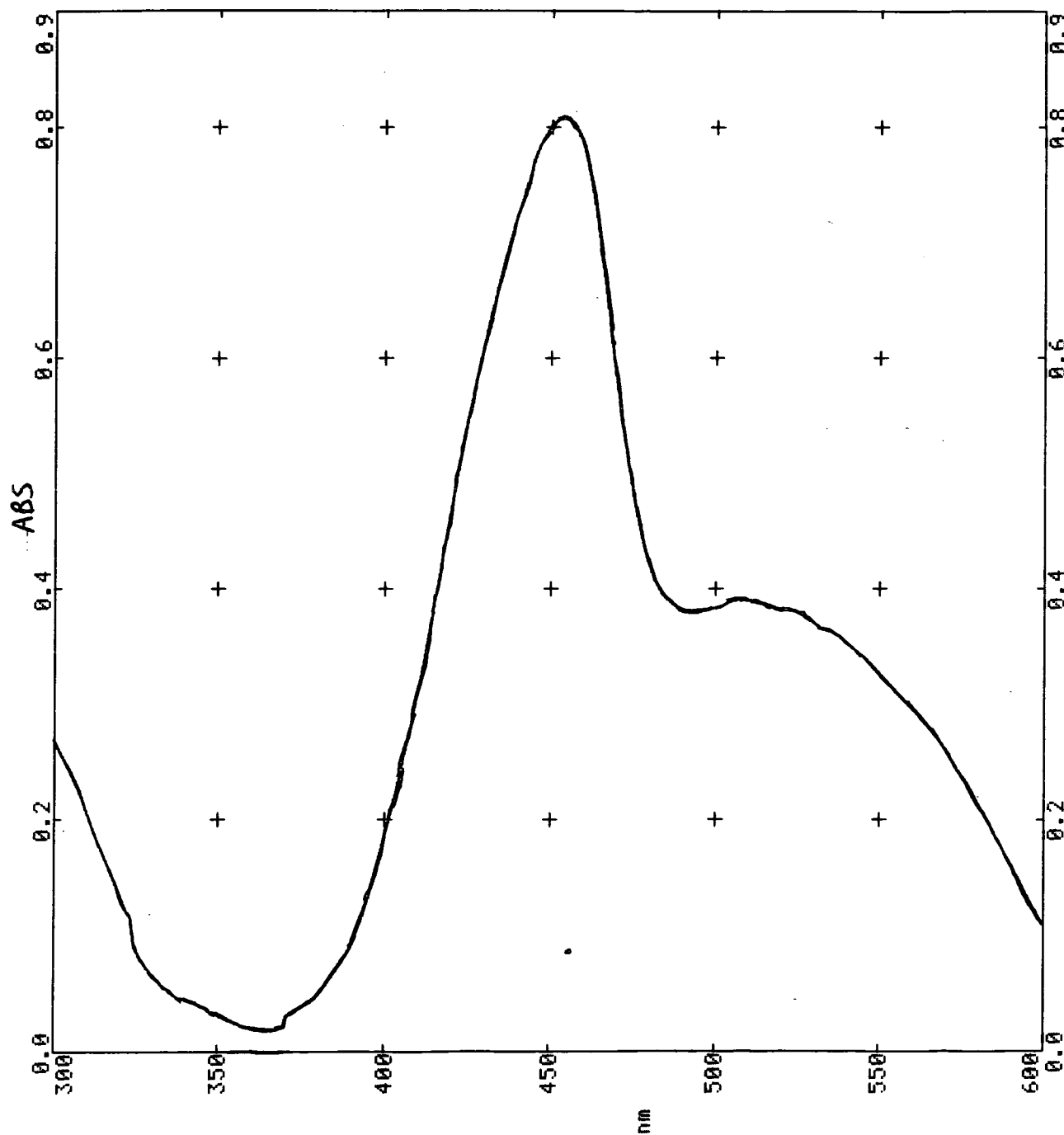
a concentration is 1×10^{-4} M

b determined by conventional spectrophotometry at 455 nm.

c absorbance due to adducts formed from TNB with 3-methylphenylacetonitrile and methoxide normalised to a pathlength of 1 cm.

d equilibrium absorbance due to methoxide-TNB adduct.

e calculated as
$$\frac{A_{455} - A_{0\text{Me}}}{(2.2 - A_{455}) [3\text{-Me}] [\text{NaOMe}]}$$



Visible spectrum of the 1:1 adduct formed from TNB ($1.5 \times 10^{-4} \text{ M}$) and 3-methylphenylacetonitrile ions ($[3\text{-Me}] = 1 \times 10^{-3} \text{ M}$, $[\text{NaOMe}] = 5 \times 10^{-3} \text{ M}$) at completion of the reaction. Normalised to a 1cm pathlength.

Table 5.47
Kinetic and Equilibrium data for the reaction of TNB^a with
4-methylphenylacetonitrile in MeOH at 25^oC

$10^3 [\text{NaOMe}]$ /M	$10^3 [4\text{-Me}]$ /M	10^4 b k_{obs} /s ⁻¹	A_{455} c	A_{OMe} d	$10^{-4} K_3 K_{\text{CH}}$ e l ² mol ⁻²
5.0	1	2.29	0.57	0.10	5.8
5.0	2	3.10	0.70	0.09	4.1
5.0	4	5.67			
5.0	6	6.70			
5.0	6	4.65			
10.0	0.5	2.32	0.49	0.19	3.5
10.0	1.0	3.22	—		
10.0	1.5	3.59	0.87	0.15	3.6
10.0	2.0	4.29	0.99	0.14	3.5
10.0	2.5	5.16			

- a concentration is $1 \times 10^{-4} \text{M}$
- b determined by conventional spectrophotometry at 455 nm. This reaction was accompanied by a slower colour fading process.
- c absorbance due to adducts formed from TNB with 4-methylphenylacetonitrile and methoxide normalised to a pathlength of 1 cm.
- d equilibrium absorbance due to methoxide-TNB adduct.
- e calculated as

$$\frac{A_{455} - A_{\text{OMe}}}{(2.2 - A_{455}) [4\text{-Me}] [\text{NaOMe}]}$$

Table 5.48
 Kinetic data for the reaction of
 3,5-*bis*-trifluoromethylphenylacetonitrile
 with TNB in MeOH at 25^oC I = 0.01M (NaCl)

$10^3 [\text{NaOMe}]$ /M	$10^3 [\text{bisCF}_3]$ /M	$k_{\text{obs}}^{\text{a}}$ s ⁻¹
10.0	0.6	3.5
10.0	1	3.9
10.0	2	4.9
10.0	4	7.4
10.0	6	9.6
10.0	8	11.6
7.5	1	3.4
7.5	2	4.4
7.5	4	6.4
7.5	6	8.3
7.5	8	10.0
7.5	10	11.6
5.0	2	4.0
5.0	4	5.3
5.0	6	6.5
5.0	10	8.9

a determined by stopped flow spectrophotometry at 450 nm.

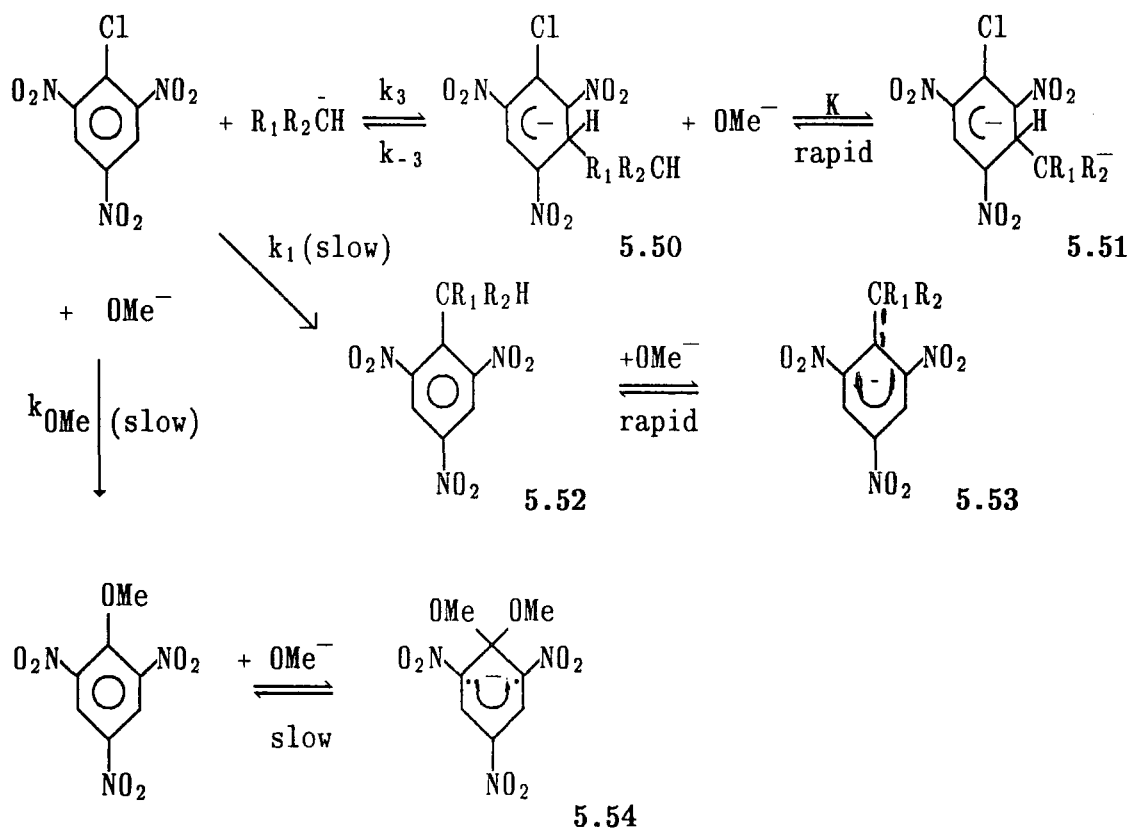
Table 5.49
Kinetic and equilibrium data for the reaction of substituted phenylacetonitriles with
1,3,5-trinitrobenzene in methanol

substituent	σ^-	K_{CH} l mol ⁻¹	pK _a	$k_3 K_{CH}$ l ² mol ⁻²	k_{-3} s ⁻¹	$10^{-4} K_3 K_{CH}$ l mol ⁻¹	log ₁₀ k ₃	log ₁₀ K ₃
4-NO ₂	1.297	1.17	16.85	1.1 x 10 ⁶	18	6.2	6.0	4.7
4-CN	1.019	2.5 x 10 ⁻⁴	20.5	2.2 x 10 ⁵	4.1	5.4	8.9	8.3
4-CF ₃	0.648	6 x 10 ⁻⁶	22.1	6070	0.122	5.0	9.0	9.9
3-CF ₃	0.430	5 x 10 ⁻⁷	23.2	900	0.022	4.0	9.3	10.9
3-Cl	0.363	2 x 10 ⁻⁷	23.6	680	0.013	5.2	9.5	11.4
4-Cl	0.192	3 x 10 ⁻⁸	24.4	180	2.8x10 ⁻³	6.4	9.8	12.3
3-MeO	0.100	6 x 10 ⁻⁹	25.1	70	1.1x10 ⁻³	6.4	10.1	13.0
H	0	3 x 10 ⁻⁹	25.4	25	6.0x10 ⁻⁴	4.2	9.9	13.1
3-Me	-0.086	1 x 10 ⁻⁹	25.9	19	4.2x10 ⁻⁴	4.5	10.3	13.7
4-Me	-0.215	6 x 10 ⁻¹⁰	26.1	<10 [*]	<1.7x10 ⁻⁴		<10.2	
3,5 bis CF ₃	—	1.2 x 10 ⁻⁴	20.8	1.35x10 ⁵	2.8	4.8		8.6
2-CN	—	3.5 x 10 ⁻⁴	20.4	2.7x10 ⁵	15	1.8		7.7

* assuming a value of $K_3 K_{CH} < 6 \times 10^4$ l² mol⁻²

iv) Reactions with picryl chloride

There is considerable evidence^{10,11,41-43} that nucleophilic attack at unsubstituted positions of picryl chloride is faster than attack at substituted positions. Rate and absorbance data are interpreted according to the scheme below which allows for the slower attack of carbanion and methoxide to the



1-position of picryl chloride. Ionisation of adduct 5.50 is expected to be rapid. For kinetic measurements made under first order conditions, the relevant rate expression for the formation of adducts 5.50 and 5.51 is 5.55.

$$k_{fast} = k_3 [R_1R_2\bar{C}H] + \frac{k_{-3}}{1 + K[MeO^-]} \quad 5.55$$

The equilibrium constant for reaction of methoxide at the 3-position of picryl chloride has the low value⁴⁴ of 2.6 l mol^{-1} so that this process may be neglected at the low base concentrations used in the present work.

a) dimethylmalonate

Mixing solutions of picryl chloride and dimethylmalonate in methanol in the presence of methoxide produced a transient red colour which was attributed to the adduct 5.50 ($R_1=R_2=CO_2Me$). UV/visible spectra even at the highest dimethylmalonate concentration used showed at no stage the formation of the substituted products 5.52 and 5.53 but instead the formation of a stable σ -adduct with λ_{max} 414 nm (shoulder). This was taken to indicate the appearance of 5.54. The equilibrium constant for its direct formation from 2,4,6-trinitroanisole has the value⁴⁷ $17\,000 \text{ l mol}^{-1}$ and indeed, the spectra showed that the substrate was largely converted to this adduct at methoxide concentrations as low as $2.5 \times 10^{-3} \text{ M}$.

Kinetic measurements made by stopped flow spectrophotometry at 500 nm showed a rapid process followed by a much slower process, both colour forming. Data are shown in table 5.57. Values of K_{obs} derived from absorbances show no variation (within experimental error) with methoxide concentration. At *ca.* 0.01M methoxide the average value is 3500 l mol^{-1} . Plots of k_{fast} vs the concentration of dimethylmalonate anion at the two methoxide concentrations are linear with identical slopes and intercepts giving values of $k_3 = 21700 \text{ l mol}^{-1} \text{ s}^{-1}$ and $k_{-3} = 6.3 \text{ s}^{-1}$. Combination of these values give $K_3 = 3440 \text{ l mol}^{-1}$. Ionisation of the adduct 5.50 is not likely to be significant.

The rates of the slow reaction are also shown in the table. For a given methoxide concentration, increasing the concentration of dimethylmalonate anion leads to a decrease in the observed rate constant, evidence again that there is negligible formation of the substitution product 5.52 or 5.53. Since 2,4,6-trinitroanisole does not absorb at 500 nm the increase in absorbance is due to 5.54. The

rate constants for methoxide attack at the 1-positions of picryl chloride and 2,4,6-trinitroanisole are expected to be broadly similar. Thus the formation of 5.54 from picryl chloride will not be a simple single exponential process. Rate constants obtained by approximating the process to one are thus not very meaningful. However, if for the sake of argument, it is assumed that the observed rate constants, k_{slow} , correspond solely to the formation of 2,4,6-trinitroanisole, then the relevant rate expression would have the form;

$$k_{\text{slow}} = \frac{k_{\text{OMe}} [\text{OMe}^-]}{1 + K_3 [\text{DMM}^-]}$$

The expression explains the type of variation shown in the observed values of k_{slow} with $[\text{DMM}^-]$ and $[\text{OMe}^-]$.

The reaction of picryl chloride with dimethylmalonate has been previously studied⁴ by Kavalek *et al.* under similar conditions to those used here. Their results are of interest because, in contrast with this study, they were able to detect substitution by dimethylmalonate and therefore obtain a value for k_1 of $82 \text{ l mol}^{-1} \text{ s}^{-1}$

Also reported⁴ is a value for k_{OMe} of 17 l mol^{-1} . This is in poor agreement with Gan and Norris' value⁴⁴ of $27.4 \pm 2.0 \text{ l mol}^{-1} \text{ s}^{-1}$ which was obtained by monitoring the complex absorbance vs time dependence for production of 5.54 (the reactions producing 2,4,6-trinitroanisole and the adduct 5.54 are unseparable) and also in one instance by monitoring the rate of chloride ion release. The value of k_3 for methoxide addition to TNA, also obtained, was found⁴⁴ to be $14 \pm 1.2 \text{ l mol}^{-1} \text{ s}^{-1}$ in reasonable agreement with values^{47,48} ($17.3 \text{ l mol}^{-1} \text{ s}^{-1}$ $15.4 \text{ l mol}^{-1} \text{ s}^{-1}$) obtained in other studies.

The pK_a of the substituted product 5.52 ($\text{R}_1 = \text{R}_2 = \text{CO}_2\text{Me}$) has been reported⁴ as 8.5 ± 1 so the final product will exist in the ionised form. This latter has a λ_{max} of 510nm in methanol.

b) ethylcyanoacetate

The initial red colour obtained when solutions of picryl chloride and ethylcyanoacetate were mixed in the presence of methoxide faded to give UV/visible spectra with single maxima at 480 nm. These spectra were attributed to the substitution product 5.33 ($R_1 = \text{CN}$, $R_2 = \text{CO}_2\text{Et}$). When the concentration of ethylcyanoacetate was relatively small a proportion of the TNA-methoxide adduct 5.54 was produced as well. Kinetic and absorbance data are shown in table 5.58. The extinction coefficient for the adduct(s) of $1.45 \times 10^4 \text{ l mol}^{-1} \text{ cm}^{-1}$ at 500 nm was determined by using very large excesses of ethylcyanoacetate and methoxide. A plot of K_{Obs} vs equilibrium methoxide concentration according to expression 5.33 yields values of $K_3 = 270 \text{ l mol}^{-1}$ (intercept) and $KK_3 = 2.1 \times 10^5 \text{ l}^2 \text{ mol}^{-2}$ (slope).

Plots of k_{fast} vs carbanion concentration at various near constant methoxide concentrations are linear with gradients $9300 \text{ l mol}^{-1} \text{ s}^{-1}$. The intercepts are dependent on methoxide concentration. Experimental values of k_{fast} are in good accord, throughout the entire range of equilibrium carbanion and methoxide concentrations, with values k_{calc} calculated from expression 5.25 with $k_3 = 9300 \text{ l mol}^{-1} \text{ s}^{-1}$, $k_{-3} = 30 \text{ s}^{-1}$ and $K = 600 \text{ l mol}^{-1}$. Combination of rate constants gives a value of $K_3 = 310 \text{ l mol}^{-1}$. The value of KK_3 of $1.9 \times 10^5 \text{ l}^2 \text{ mol}^{-2}$ thus obtained is in good agreement with the value derived from absorbance data.

Since the UV/visible spectra indicated that methoxide and ethylcyanoacetate anion were competing for attack at the 1-position of picryl chloride, most of the data for k_{slow} (obtained at the λ_{max} of the substituted product) were obtained at relatively large concentration of ethylcyanoacetate anion.

Rate data are interpreted according to expression 5.56 which is derived in the appendix.

$$k_{\text{slow}} = \frac{k_1 [\text{ECA}^-]}{1 + K_3 [\text{ECA}^-] + KK_3 [\text{ECA}^-] [\text{MeO}^-]} \quad 5.56$$

Rate constants, k_{calc} , calculated with $K_3 = 310 \text{ l mol}^{-1}$, $K = 600 \text{ l mol}^{-1}$ and $k_1 = 290 \text{ l mol}^{-1} \text{ s}^{-1}$ are compared in the table with experimentally obtained values k_{slow} . Agreement between values is generally very good. However the values of k_{slow} obtained at relatively low concentrations of ethylcyanoacetate (notably at $1 \times 10^{-3} \text{ M}$ and $2 \times 10^{-3} \text{ M}$ $[\text{ECA}]_0$) show a marked deviation from k_{calc} . In these cases the competing process of methoxide attack at the 1-position of picryl chloride is likely to be important.

Data for dimethylmalonate and ethylcyanoacetate are summarised in table 5.69

c) phenylacetoneitriles

Stopped flow spectrophotometry showed that the observed adduct forming reactions were followed by a slower process which was not measured. With the low equilibrium concentrations of these carbanions generated in solution this slow process (always colour forming at 450 nm) is likely to involve predominantly methoxide attack at the 1-position of picryl chloride rather than carbanion attack at the 1-position.

4-nitrophenylacetoneitrile

In order to calculate values for K_{obs} a value of $\epsilon = 2.1 \times 10^4 \text{ l mol cm}^{-1}$ was used for the adduct 5.50. There is a fairly large error associated with the calculated values of K_{obs} which range from *ca.* $1 \times 10^4 \text{ l mol}^{-1}$ (0.0025M NaOMe) to $1.5 \times 10^4 \text{ l mol}^{-1}$ (0.010M NaOMe). Plots of k_{obs} vs $[\text{PNPA}^-]$ are linear with slopes of $1.75 \times 10^5 \text{ l mol}^{-1} \text{ s}^{-1}$. Values of the intercepts $k_{-3}/(1 + K[\text{OMe}^-])$ are 12.9 s^{-1} , 13.3 s^{-1} , 14.3 s^{-1} and *ca.* 15 s^{-1} for sodium methoxide concentrations 0.01M, $7.5 \times 10^{-3} \text{ M}$, $5 \times 10^{-3} \text{ M}$ and $2.5 \times 10^{-3} \text{ M}$ respectively. These values are in line with a value for K of about 40 l mol^{-1} and $k_{-3} \approx 17 \text{ s}^{-1}$. Combination of rate coefficients gives a value for $K_3 = 1 \times 10^4 \text{ l mol}^{-1}$. This value and the value of $K = 40 \text{ l mol}^{-1}$ are in reasonable agreement with values of K_{obs} . Data are given in table 5.59.

4-cyanophenylacetonitrile

The average value of K_3K_{CH} obtained from absorbances (table 5.60) is $8300 \text{ l}^2\text{mol}^{-2}$; kinetic data lead to values $K_3K_{\text{CH}} = 3.2 \times 10^4 \text{ l}^2\text{mol}^{-2}$ and $k_{-3} = 3.8 \text{ s}^{-1}$. Combination of rate coefficients gives a value of $K_3K_{\text{CH}} = 8400 \text{ l}^2\text{mol}^{-2}$.

2-cyanophenylacetonitrile

Absorbances obtained at 450 nm at the completion of the fast reaction give an average value of $K_3K_{\text{CH}} = 2500 \text{ l}^2\text{mol}^{-2}$ (table 5.61). Kinetic data lead to values $K_3K_{\text{CH}} = 3.0 \times 10^4 \text{ l}^2\text{mol}^{-2}$ and $k_{-3} = 12.1 \text{ s}^{-1}$.

Data for these three phenylacetonitriles are summarised in table 5.70

Table 5.57 Kinetic and absorbance data for the reaction of dimethylmalonate anion with picryl chloride in MeOH at 25°C. (Ionic strength maintained to 0.01M with NaCl)

[DMM] /M	10 ³ [NaOMe] /M	10 ⁴ [DMM] /M ^a	A ₅₀₀ ^{b,g}	A _{0Me} ^{b,c}	10 ⁻² K _{obs} l/mol ^d	k _{fast} ^e s	k _{slow} ^e s	10 ³ [NaOMe] _{eq} /M
0.01	7.5	0.34	0.16	0.03	33	7.0		
0.04	7.5	1.32	0.49	0.02	41	9.0		
0.08	7.5	2.60	0.73	0.02	44	11.8		
0.12	7.5	3.83	0.81	0.01	39	14.2		
0.16	7.5	5.02	0.94			17.2		
0.20	10.0	6.18	0.99			19.7		
0.01	10.0	0.45	0.19	0.04	29	7.2		
0.02	10.0	0.89	0.35	0.03	37	7.7		
0.04	10.0	1.76	0.51	0.02	33	9.9		
0.05	10.0	2.19					0.055	9.78
0.06	10.0	2.62	0.65	0.02	34	11.8		
0.075	10.0	3.25					0.033	9.68
0.08	10.0	3.46	0.80	0.02	41	13.7		
0.10	10.0	4.29	0.82	0.02	35	15.2	0.023	9.57
0.125	10.0	5.30					0.019	9.47
0.14	10.0	5.90	0.99			18.0		
0.15	10.0	6.30					0.017	9.37
0.18	10.0	7.46	1.01			21.1		
0.02	2.5	0.22					0.024	2.48
0.03	2.5	0.44					0.022	2.46
0.10	2.5	1.08					0.018	2.39
0.20	2.5	2.06					0.015	2.29
0.30	20.0		1.34					
0.40	20.0		1.35					
0.50	20.0		1.35					

a Concentration calculated using $K_{CH}=0.45$. b Absorbance corresponds to pathlength of 1cm and a picryl chloride concentration of $= 1 \times 10^{-4} M$
c Eqm. abs. due to methoxide adduct calculated using $K_{OMe}= 2.6 \text{ l mol}^{-1}$ and an $\epsilon=1.8 \times 10^4 \text{ l mol cm}^{-1}$ for the methoxide adduct.

d calculated as
$$\frac{A_{500}}{(1.35 - A_{500} - A_{0Me}) [DMM^-]}$$

e Data at 500nm measured by monitoring an increase in absorbance.

Table 5.58
Kinetic and Absorbance data for the reaction of
ethylcyanoacetate anion with picryl chloride in methanol
at 25°C
Ionic strength 0.01M (NaCl)

$10^3 [\text{NaOMe}]$ M	$10^3 [\text{ECA}]$ M	$10^4 [\text{ECA}]_{\text{eq}}$ M	$10^3 [\text{NaOMe}]_{\text{eq}}$ M	A_{500} b,c	A_{OMe^-} b,d	$10^{-1} K_{\text{obs}}$ e M ⁻¹	$k_{\text{fast}}^{500\text{nm}}$ s ⁻¹	k_{calc} f s ⁻¹	$k_{\text{slow}}^{480\text{nm}}$ g s ⁻¹	k_{calc} h s ⁻¹
10.0	0.25	0.48	9.95	0.141	0.041	159	5.1	4.8		
10.0	0.5	0.96	9.90	0.270	0.037	206	5.7	5.2		
10.0	1.0	1.91	9.81	0.503	0.029	262	6.3	6.1		
10.0	1.0	1.91	9.81	0.442	0.031	213	6.5	6.1		
10.0	2.0	3.75	9.62	0.763	0.019	289	9.0	7.9		
10.0	2.5	4.66	9.53	0.732	0.022	212	10.2	8.8		
10.0	5.0	8.97	9.10	0.936	0.015	200	14.2	13.0		
10.0	7.5	12.96	8.70						0.100	0.107
10.0	8.0	13.72	8.63	1.073	0.010	206	19.5	17.6		
10.0	10.0	16.67	8.33	1.144	0.008	223	21.3	20.5	0.117	0.118
10.0	15.0	23.32	7.67	1.213			27.4	27.0	0.138	0.134
10.0	20.0	29.09	7.09	1.213			34.4	32.8	0.147	0.147
10.0	25.0	34.13	6.59	1.313			37.0	37.8		
10.0	40.0	45.94	5.41	1.265			45.8	49.8		
10.0	40.0	45.94	5.41	1.213			51.5	49.8	0.203	0.189
7.5	0.25	0.38	7.46	0.131	0.031	102	6.2	5.8		
7.5	0.5	0.76	7.42	0.188	0.030	163	6.3	6.2		
7.5	0.5	0.76	7.42	0.176	0.030	151	6.5	6.2		
7.5	1.0	1.50	7.35	0.345	0.026	192	6.8	6.9		
7.5	1.5	2.23	7.28	0.468	0.023	203	7.8	7.7		
7.5	2.0	2.95	7.21	0.439	0.023	139	8.2	8.4		
7.5	3.0	4.35	7.07	0.693	0.017	205	10.2	9.8		
7.5	4.0	5.70	6.93	0.657	0.017	142	10.5	11.1		
7.5	6.0	8.28	6.67	0.939	0.011	219	15.3	13.7		

Table 5.58 continued

10^3 [NaOMe] M	10^3 [ECA] M	10^4 [ECA] eq M	10^3 [NaOMe] eq M	A_{500} b,c	A_{OMe^-} b,d	10^{-1} K_{obs} e M ⁻¹	k_{fast}^{500nm} s ⁻¹	k_{calc} f s ⁻¹	k_{slow}^{480nm} g s ⁻¹	k_{calc} h s ⁻¹
7.5	10.0	12.96	6.20	0.910	0.011	128	20.0	18.4	0.133	0.130
7.5	12.0	15.09	5.99	0.968	0.009	132	19.7	20.6		
7.5	15.0	18.04	5.70	0.977	0.009	113	21.9	23.6	0.152	0.151
7.5	20.0	22.41	5.26						0.178	0.167
7.5	25.0	26.21	4.88	1.092	0.006	116	31.4	32.0		
5.0	0.5	0.53	4.95	0.113	0.021	130	7.3	8.0		
5.0	1.0	1.05	4.89	0.206	0.019	143	8.1	8.6		
5.0	1.0	1.05	4.89	0.229	0.019	164	8.1	8.6	0.057	0.027
5.0	2.0	2.06	4.79	0.352	0.017	148	9.0	9.7		
5.0	2.0	2.06	4.79	0.392	0.016	173	9.1	9.7	0.061	0.048
5.0	4.0	3.98	4.60	0.493	0.014	126	11.5	11.7		
5.0	4.0	3.98	4.60	0.554	0.013	152	11.1	11.7	0.077	0.079
5.0	6.0	5.99	4.40	0.575	0.012	107	14.2	13.8		
5.0	8.0	7.42	4.26	0.763	0.009	148	14.5	15.3		
5.0	10.0	8.97	4.10	0.699	0.010	102	17.9	17.0	0.122	0.133
5.0	12.0	10.41	3.96	0.862	0.007	140	17.3	18.6		
5.0	20.0	15.35	3.46	0.939	0.006	119	21.9	24.0		
5.0	20.0	15.35	3.46	0.763	0.008	72	23.1	24.0	0.221	0.181
2.5	0.5	0.28	2.47				13.2	12.3		
2.5	1.0	0.55	2.44	0.079	0.010	92	12.7	12.7	0.035	0.015
2.5	2.0	1.09	2.39	0.136	0.010	88	13.8	13.3		
2.5	2.0	1.09	2.39	0.113	0.010	71	14.2	13.3		
2.5	4.0	2.09	2.29	0.211	0.009	78	14.6	14.6		
2.5	4.0	2.09	2.29	0.184	0.009	66	15.9	14.6		
2.5	8.0	3.86	2.11	0.263	0.008	56	17.4	16.8		
2.5	12.0	5.39	1.96	0.375	0.007	64	18.8	18.8		
2.0	1.5	0.67	1.93	0.062	0.009	57	14.6	14.5		
2.0	4.0	1.68	1.83	0.118	0.008	49	16.9	15.9		
40	0.02			1.45						
60	0.02			1.43						

Legend for table 5.58

- a. calculated with $K_{CH} = 24 \text{ l mol}^{-1}$
- b. normalised to a pathlength of 1cm and a picryl chloride concentration of $1 \times 10^{-4} \text{ M}$
- c. absorbance at completion of fast reaction
- d. equilibrium absorbance due to methoxide adduct
- e. calculated as
$$\frac{A_{500} - A_{OMe^-}}{(1.45 - A_{500}) [ECA^-]}$$
- f. calculated with $k_3 = 9300 \text{ l mol}^{-1} \text{ s}^{-1}$, $k_{-3} = 30 \text{ s}^{-1}$ and $K = 600 \text{ l mol}^{-1}$ according to expression 5.56
- g. colour forming at 480 nm.
- h. calculated with $k_3 = 310 \text{ l mol}^{-1} \text{ s}^{-1}$, $K = 600 \text{ l mol}^{-1}$ and $k_1 = 290 \text{ l mol}^{-1} \text{ s}^{-1}$ according to expression 5.56

Table 5.59
Kinetic and Equilibrium data for the reaction of 4-nitrophenylacetonitrile anion
with picryl chloride

10^2 [NaOMe]	10^3 [PNPA]	10^5 [picryl chloride]	10^5 [PNPA ⁻] ^a	A_{450} ^b	A_{PNPA^-} ^{b,c}	k_{obs} ^d	k_{calc} ^d	A_{450} ^{b,e}	A_{OMe^-} ^{b,f}	$10^{-3} K_{\text{obs}}$ ^g
M	M	M				s ⁻¹	s ⁻¹			l mol ⁻¹
2.5	2.04	10	0.59	0.297	0.106	15.9	16.5	0.191	0.010	—
2.5	4.08	6	1.18	0.395	0.229	16.3	17.5	0.277	0.010	12
2.5	6.12	4	1.77	0.464	—	17.0	18.6	0.276	0.010	8
5.0	1.36	8	0.79	0.305	0.157	15.4	15.5	0.185	0.020	11
5.0	2.72	6	1.58	0.490	0.309	16.5	16.9	0.302	0.019	10
5.0	4.08	4	2.35	0.594	0.444	17.3	18.3	0.375	0.018	9
5.0	5.44	3	3.14	0.768	0.609	18.7	19.7	0.530	0.016	10
7.5	0.68	10	0.59	0.293	—	15.2	14.1	0.175	0.030	13
7.5	1.36	8	1.18	0.443	0.217	16.0	15.1	0.283	0.028	12
7.5	2.72	6	2.35	0.713	0.455	17.5	17.2	0.430	0.026	10
7.5	4.08	4	3.71	0.942	0.696	19.4	19.6	0.615	0.023	11
7.5	5.44	3	4.70	1.178	—	21.2	21.3	0.822	0.020	13
7.5	6.80	3	5.87	1.380	1.118	23.2	23.3	0.873	0.018	12
7.5	8.16	3	7.03	1.728	1.402	25.3	25.4	1.087	0.015	13

Table 5.59 continued

10^2 [NaOMe] M	10^3 [PNPA] M	10^5 [picryl chloride] M	^a 10^5 [PNPA ⁻]	^b A_{450}	^{b,c} A_{PNPA^-}	^k _{obs} s ⁻¹	^d k_{calc} s ⁻¹	^{b,e} A_{450}	^{b,f} A_{OMe^-}	^g $10^{-3} K_{\text{obs}}$ lmol ⁻¹
10.0	0.29	10	0.31	0.168	0.064	15±2	12.7	0.104	0.041	10
10.0	0.58	10	0.66	0.273	—	14.7	13.3	0.148	0.040	8
10.0	0.72	8	0.84	0.324	0.169	14.8	13.6	0.194	0.039	10
10.0	1.44	5	1.66	0.516	0.339	15.7	15.0	0.354	0.036	9
10.0	2.16	4	2.49	0.663	0.488	17.1	16.5	0.438	0.034	10
10.0	2.88	4	3.32	0.909	0.625	18.6	18.0	0.710	0.029	15
10.0	4.32	3	4.96	1.187	0.973	20.6	20.8	0.713	0.028	10
10.0	5.76	3	6.60	1.629	1.327	24.4	23.7	1.007	0.022	14
10.0	7.20	3	8.23	—	—	26.7	26.5	—	—	—

^a calculated with $K_{\text{CH}} = 1.17 \text{ lmol}^{-1}$ ^b normalised to a pathlength of 1cm. ^c experimental absorbances due to PNPA⁻ anion

^d calculated with $k_3 = 1.75 \times 10^5 \text{ lmol}^{-1}$ $k_{-3} = 17 \text{ s}^{-1}$ and $K = 40 \text{ lmol}^{-1}$ according to expression 5.55

^e absorbance due to adducts 5.50, 5.51 and the methoxide adduct, normalised to $1 \times 10^{-4} \text{ M}$ picryl chloride.

^f equilibrium absorbance due to methoxide adduct calculated with $K_{\text{CH}} = 2.6 \text{ lmol}^{-1}$ and $\epsilon_{\text{OMe}^-} = 1.74 \times 10^4 \text{ lmol}^{-1} \text{ cm}^{-1}$

^g calculated as $\frac{A_{450} - A_{\text{OMe}^-}}{(2.7 - A_{450}) [\text{PNPA}^-]}$ assuming an extinction coefficient of $2.1 \times 10^4 \text{ lmol}^{-1} \text{ cm}^{-1}$ for the 1,3 adducts

Table 5.60

Kinetic and Equilibrium data for the reaction of
4-cyanophenylacetonitrile with picryl chloride in methanol at 25°C

I = 0.01M (NaCl)

10^3 [NaOMe] /M	10^3 [4-CN] /M	a A_{450}	b A_{0Me}	c $10^{-2} K_3 K_{CH}$	d k_{obs} s^{-1}	10^5 [picryl chloride] /M	e k_{calc} s^{-1}
5.0	2	0.17	0.02	74	4.1	15	4.1
5.0	4	0.32	0.02	80	4.4	6	4.5
5.0	6	—			4.7	3	4.8
7.5	1	0.14	0.03	71	4.0	5	4.0
7.5	1	0.14	0.03	71	4.0	10	4.0
7.5	2	0.25	0.03	75	4.2	6	4.3
7.5	4	0.49	0.03	90	4.5	3	4.8
7.5	6	0.66	0.02	92	5.0	3	5.2
10.0	2	0.32	0.04	74	4.5	10	4.4
10.0	4	0.61	0.03	91	5.0	4	5.1
10.0	6	0.79	0.03	90	5.7	3	5.7
10.0	8	1.02	0.02	106	6.2	2	6.4
10.0	10	—			7.0	2	7.0
10.0	12	—			7.8	2	7.6

a absorbance due to adduct normalised to a pathlength of 1cm and 1×10^{-4} M picryl chloride. the absorbance due to 4-cyanophenylacetonitrile has been subtracted.

b equilibrium absorbance due to methoxide adduct.

c calculated as
$$\frac{A_{450} - A_{0Me}}{(2.2 - A_{450}) [NaOMe] [4-CN]}$$

This assumes an extinction coefficient of $2.2 \times 10^4 \text{ l mol}^{-1} \text{ cm}^{-1}$ for the 1,3 adduct(s)

d Data at 450 nm.

e calculated with $k_3 K_{CH} = 32000 \text{ l}^2 \text{ mol}^{-2} \text{ s}^{-1}$ and $k_{-3} = 3.8 \text{ s}^{-1}$.

Table 5.61
Kinetic and Equilibrium data for the reaction of
2-cyanophenylacetonitrile with picryl chloride in methanol at 25°C

10^3 [NaOMe] /M	10^3 [4-CN] /M	10^5 [picryl chloride] /M	^a A_{450}	^b A_{OCN}	^a A_{450}	^b A_{OMe}	10^{-2} ^c K_3K_{CH}	^d k_{obs} s ⁻¹	^e k_{calc} s ⁻¹
10.0	2	20	0.411	0.086	0.16	0.04	31	13±1	12.7
10.0	3	10	0.356	—	0.23	0.04	34	13.2	13.0
10.0	4	6	0.290	0.169	0.20	0.04	21	13.3	13.3
10.0	6	6	0.444	0.262	0.30	0.04	24	14.0	13.9
10.0	8	5	0.515	0.333	0.36	0.04	23	14.6	14.5
10.0	10	5	0.617	0.421	0.39	0.0	21	15.1	15.1
10.0	12	4	0.649	0.481	0.42	0.03	19	15.7	15.7

a absorbance (normalised to a pathlength of 1cm) due to adducts and 2-cyanophenylacetonitrile

b absorbance due to 2-cyanophenylacetonitrile (the neutral molecule) normalised to a pathlength of 1 cm.

c absorbance due to adducts normalised to 1×10^{-4} M picryl chloride and a pathlength of 1 cm.

d equilibrium absorbance due to methoxide adduct

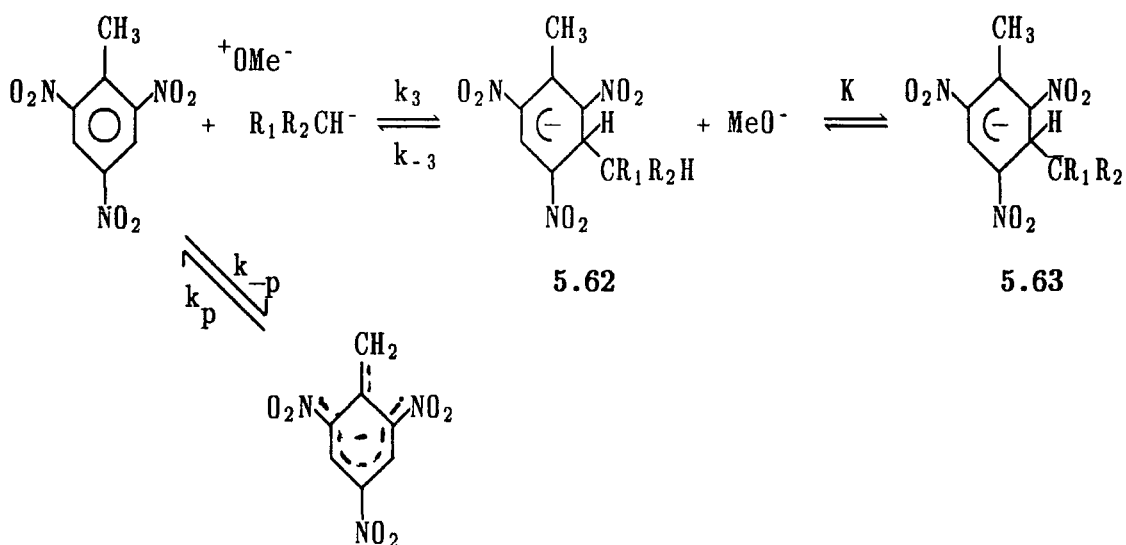
e calculated as
$$\frac{A_{450} - A_{OMe}}{(2.1 - A_{450}) [NaOMe] [2-CN]}$$

This assumes an extinction coefficient of 2.1×10^4 l mol⁻¹ cm⁻¹ for the adduct

d Calculated with $k_3K_{CH} = 3.00 \times 10^4$ l² mol² s⁻¹ and $k_{-3} = 12.1$ s⁻¹

v) Reactions with 2,4,6-trinitrotoluene (TNT)

There is good evidence^{41,49-51} that the major modes of interaction of TNT with bases are the formation of σ -adducts at unsubstituted ring positions and the formation of the TNT⁻ anion. Evidence for the latter includes the observation of a large primary deuterium isotope effect.⁵² With dilute solutions of TNT in methanolic sodium methoxide, formation of this anion is the major process, the equilibrium constant for direct addition of methoxide to the 3-position having the low value⁴⁹ of 0.07 l mol⁻¹. The TNT⁻ anion has a characteristic visible spectrum with λ_{max} at 370, 525 and 650 nm⁴⁹



Values of k_{-p} have been reported^{49,53} as 1.6 s⁻¹ and 1.1 s⁻¹ and K_p ($= k_p/k_{-p}$) as 12.4 l mol⁻¹. At the low concentrations of methoxide used ionisation of TNT is expected to be slow with respect to the formation of adducts. The rate expression for the fast process, measured under first order conditions, is 5.55.

a) Dimethylmalonate

Rate and absorbance data are shown in table 5.63. Because of the low value of the equilibrium constant K_3 it was necessary to work with solutions of TNT as concentrated as $1 \times 10^{-3} \text{M}$. Data are obtained at 460nm and a value for the extinction coefficient of $2.1 \times 10^4 \text{ l mol}^{-1} \text{ cm}^{-1}$ was used to calculate values of K_{obs} .

The obtained rate constants, all $65 \pm 10 \text{ s}^{-1}$, approximate to k_{-3} . The average value of K_3 obtained from absorbances is 30 l mol^{-1} . $k_3 (= k_{-3} K_3)$ is therefore $1950 \text{ l mol}^{-1} \text{ s}^{-1}$. The second slow process (ionisation of TNT) had a rate *ca.* 1.4 s^{-1} which approximates to k_{-p} . A third slower process was observed (presumably diadduct formation) but not measured.

b) ethylcyanoacetate

The reaction of TNT was studied at two different ionic strengths. Equilibrium and kinetic data are shown in table 5.64.

At 0.05M ionic strength the relatively slow rates of reaction meant that the second process (ionisation of TNT) was more interfering than before. Extrapolation of the linear portions of the rate curves was therefore necessary to obtain infinity and absorbance values. An extinction coefficient of $2.1 \times 10^4 \text{ l mol}^{-1} \text{ cm}^{-1}$ at 460 nm was again assumed in order to calculate equilibrium constants. A plot of K_{obs} vs methoxide concentration (for data at $I = 0.05\text{M}$) is linear with slope $KK_3 = 720 \text{ l}^2 \text{ mol}^{-2}$ and intercept $K_3 = 3 \text{ l mol}^{-1}$. However it was not possible to obtain a good fit of experimental rate constants with those calculated with eqn. 5.55 using $K_3 = 3 \text{ l mol}^{-1}$ and $K = 240 \text{ l mol}^{-1}$, for the entire range of values. Nevertheless a value for $k_{-3} < 170 \text{ s}^{-1}$ is indicated.

Since the equilibrium constant K applies to a reaction between two charged species, this value is expected to be rather lower than 240 l mol^{-1} at the ionic strength of 0.01M. Values of K_{obs} here show no correlation with residual

methoxide concentration. The value of K is probably less than 150 l mol^{-1} and $k_{-3} = 160 \pm 10 \text{ s}^{-1}$. With $K_3 = 2.9 \pm 0.1 \text{ l mol}^{-1}$ then $k_3 (=K_3.k_{-3})$ is $460 \pm 50 \text{ l mol}^{-1}\text{s}^{-1}$. Data for dimethylmalonate and ethylcyanoacetate are summarised in table 5.69.

c) 4-nitrophenylacetonitrile (Table 5.65)

The observed rate constants which approximate to $k_{-3}/(1 + K[\text{OMe}^-])$ are in accord with values for k_{-3} of 65 s^{-1} and a K of *ca* 30 l mol^{-1} . Values of K_{obs} are *ca* 24 l mol^{-1} ($5 \times 10^{-3} \text{ M}$ methoxide), 27 l mol^{-1} ($7.65 \times 10^{-3} \text{ M}$ methoxide) and 280 l mol^{-1} (0.01 M methoxide). Thus K_3 is *ca* 220 l mol^{-1} and $k_3 (K_3.k_{-3})$ $14300 \text{ l mol}^{-1}\text{s}^{-1}$.

d) 4-cyanophenylacetonitrile (Table 5.67)

Values of K_3K_{CH} determined from absorbances range from $150 \text{ l}^2\text{mol}^{-2}$ to $200 \text{ l}^2\text{mol}^{-2}$. These values are noticeably larger at 0.01 M sodium methoxide than at $5 \times 10^{-3} \text{ M}$ sodium methoxide. Absorbance values obtained at the lower concentration (where the ionisation of TNT is less interfering) required less extrapolation and are likely to be more accurate. The observed rate constants which correspond to k_{-3} also show much less variation at the lower concentration of sodium methoxide. The preferred values are $K_3K_{\text{CH}} = 160 \text{ l}^2\text{mol}^{-2}$ and $k_{-3} = 21 \text{ s}^{-1}$.

e) 2-cyanophenylacetonitrile (Table 5.68)

Absorbance values obtained at 450 nm at the completion of the fast reaction lead to a value of $K_3K_{\text{CH}} = 50 \pm 10 \text{ l}^2\text{mol}^{-2}$. With $k_{-3} = 53 \text{ s}^{-1}$, k_3K_{CH} is therefore $2650 \text{ l}^2\text{mol}^{-2}\text{s}^{-1}$. Data for these phenylacetonitriles are summarised in table 5.70.

f) Reactions with other phenylacetonitriles

For the 4-CF₃ derivative, the rate of production of the TNT⁻ anion (with observed rate constant 1.3 – 1.6 s⁻¹) was found to exceed the rate of σ -adduct formation which was barely detectable. For the remaining phenylacetonitriles values of k_{-3} are expected to become even smaller.

Table 5.63

Reaction of TNT with dimethylmalonate anion

in MeOH at 25°C I = 0.01M (NaCl)

$10^3 [\text{NaOMe}]$ /M	[DMM] /M	$10^4 [\text{DMM}]_{\text{eq}}$	$10^3 [\text{NaOMe}]_{\text{eq}}$ /M	A_{460}	K_{obs} l mol^{-1}	k_{fast} s^{-1}
10	0.1	0.1	4.29	0.026	29	65±10
10	0.2	0.2	7.40	0.048	32	65±10
10	0.2	0.2	7.40	0.049	32	"
10	0.4	0.4	15.21	0.090	29	"
10	0.4	0.4	15.21	0.084	27	"
10	0.6	0.6	21.20	0.142	34	"
10	0.6	0.6	21.20	0.126	30	"
5	0.4	0.4	7.61	0.040	26	"
5	0.6	0.6	10.62	0.067	31	"

- a Calculated with $K_{\text{CH}} = 0.45$
- b Absorbance at completion of fast reaction, normalise to a pathlength of 1 cm and a TNT concentration of $1 \times 10^4 \text{ M}$.
- c Calculated as
- $$\frac{A_{460}}{(2.1 - A_{460}) [\text{DMM}^-]}$$
- an extinction coefficient of $2.1 \times 10^4 \text{ l mol}^{-1} \text{ cm}^{-1}$ is assumed for the adduct.
- d data at 460nm.

Table 5.64

**Rate and Absorbance data for the reaction of TNT
with ethylcyanoacetate anion in MeOH**

I = 0.05M (NaCl)

[ECA] M	[NaOMe] M	^a 10 ³ [ECA ⁻] M	10 ³ [NaOMe] M	^b A _{460nm}	^c K _{obs} l mol ⁻¹	^d k _{obs} s ⁻¹
0.05	0.05	2.66	47.3	0.279	58	15.4
0.01	0.05	5.18	44.8	0.360	38	18.4
0.02	0.05	9.82	40.2	0.499	32	20.5
0.04	0.05	17.52	32.5	0.615	24	29.0
0.06	0.05	23.4	26.6	0.64	19	34.3
0.10	0.05	31.1	18.9	0.630	14	41.8
0.005	0.03	2.01	28.0	0.116	29	19.4
0.02	0.03	7.09	22.9	0.270	21	26.8
0.04	0.03	12.05	18.0	0.345	16	34.7
0.005	0.02	1.54	18.4	0.069	22	23.6
0.015	0.02	4.14	15.9	0.133	16	30.4
0.03	0.02	7.09	12.9	0.170	12	34.5
0.01	0.01	1.67	8.3	0.032	9	36.8
0.04	0.01	4.50	5.4	0.061	7	52.9

I = 0.01M (NaCl)

[ECA] M	[NaOMe] M	^a 10 ³ [ECA ⁻] M	10 ³ [NaOMe] M	^b A _{460nm}	^c K _{obs} l mol ⁻¹	^d k _{obs} s ⁻¹
0.06	5 x 10 ⁻³	2.89	2.11	0.022	3.7	150±20
0.20	5 x 10 ⁻³	4.12	0.88	0.027	3.2	130±20
0.40	5 x 10 ⁻³	4.52	0.48	0.029	3.1	140±20
0.10	0.01	6.91	3.09	0.044	3.1	150±20
0.20	0.01	8.22	1.78	0.051	3.0	110±20

a calculated with K_{CH} = 24 l mol⁻¹b absorbances at the end of the fast reaction. Normalised to a pathlength of 1 cm and a TNT concentration of 1 x 10⁻⁴ M.c calculated as $\frac{A_{460}}{(2.1 - A_{460}) [ECA^-]}$

d data at 460nm.

Table 5.65
Kinetic and Equilibrium data for the reaction of
4-nitrophenylacetonitrile anion
with 2,4,6 trinitrotoluene in methanol at 25°C
I = 0.01M (NaCl)

10^3 [NaOMe] M	10^3 [PNPA] M	10^4 [TNT] M	10^5 [PNPA ⁻] M	a b,c A_{450}	b,d A_{PNPA^-}	e k_{obs} s ⁻¹	f k_{calc} s ⁻¹	b,g A_{450}	h $10^{-1}K_{\text{obs}}$ l mol ⁻¹
2.5	4.29	18	1.24	0.374	0.229	56	61	0.0081	31
2.5	5.71	15	1.65	0.482	0.311	56	61	0.0114	33
2.5	8.57	8	2.47	0.595	0.567	61	61	0.0110	21
5.0	2.86	18	1.66	0.501	0.330	50	57	0.0095	27
5.0	4.29	10	2.47	0.618	0.497	54	57	0.0121	23
5.0	5.71	8	3.29	0.810	0.618	57	57	0.0240	35
5.0	7.19	8	4.11	0.990	0.842	59	57	0.0185	22
7.5	2.86	12	2.47	0.658	0.491	48	53	0.0139	27
7.5	4.29	10	3.70	0.892	0.738	53	54	0.0154	20
7.5	5.71	8	4.93	1.239	1.021	54	54	0.0273	27
7.5	7.14	4	6.16	1.365	1.233	56	54	0.0330	26
10.0	2.86	10	3.29	0.868	0.675	49	50	0.0193	28
10.0	4.29	8	4.92	1.281	1.030	52	51	0.0314	31
10.0	5.71	8	6.56	1.602	1.320	52	51	0.0353	26
10.0	7.14	8	8.19	2.051	1.707	54	51	0.0430	26

- a calculated with $K_{\text{CH}} = 1.17 \text{ l mol}^{-1}$
b absorbances correspond to a pathlength of 1cm.
c absorbance due to adducts 5.62, 5.63 and PNPA⁻
d absorbance due to PNPA⁻ anion
e data at 450nm.
f calculated with $k_3 = 13700 \text{ l mol}^{-1} \text{ s}^{-1}$, $k_{-3} = 65 \text{ s}^{-1}$ and k_3 (wot!) =
 $14300 \text{ l mol}^{-1} \text{ s}^{-1}$ according to expression 5.55
g absorbance due to adducts 5.62 and 5.63 normalised to $1 \times 10^{-4} \text{ M TNT}$
h calculated as

$$\frac{A_{450}}{(2.1 - A_{450}) [\text{PNPA}^-]}$$

assuming an extinction coefficient of $2.1 \times 10^4 \text{ l mol}^{-1} \text{ cm}^{-1}$

Table 5.67
Kinetic and Equilibrium data for the reaction of
4-cyanophenylacetonitrile with TNT in methanol at 25^oC

$10^3 [\text{NaOMe}]$ M	$10^3 [4\text{-CN}]$ M	$10^3 A_{450}$ ^a	$K_3 K_{\text{CH}}$ ^b $\text{l}^2 \text{mol}^{-2}$	k_{obs} ^c s^{-1}
10.0	2	8.3	198	19
10.0	4	14.6	175	15
10.0	8	28.0	169	18
10.0	12	48.8	198	20
5.0	6	10.9	174	20
5.0	8	13.1	157	21
5.0	12	18.9	151	21
5.0	16	24.2	146	22

a absorbance due to the adduct normalised to a pathlength of 1cm and a TNT concentration of 1×10^{-4} M.

b calculated as $\frac{A_{450}}{(2.1 - A_{450}) [4\text{-CN}] [\text{NaOMe}]}$

assuming an extinction coefficient of $2.4 \times 10^4 \text{ l mol}^{-1} \text{ cm}^{-1}$ for the adduct.

c data at 450nm.

Table 5.68
Kinetic and Equilibrium data for the reaction of
2-cyanophenylacetonitrile with TNT in methanol at 25^oC

10^3 [NaOMe] M	10^3 [2-CN] M	10^3 [TNT] M	A_{450} ^a	A_{0CN} ^b	$10^3 A_{450}$	$K_3 K_{CH}$ ^b $l^2 mol^{-2}$	k_{obs} s^{-1}
10	6	4	0.26	0.236	6.0	48	50
10	6	10	0.31	0.236	7.4	59	54
10	10	10	0.48	0.370	11.0	53	53
10	10	4	(0.39)	(0.359)	(7.8)	(37)	53
10	14	10	0.64	0.520	12.0	41	54

a measured absorbance at the completion of the fast reaction determined by stopped flow spectrophotometry. Normalised to a pathlength of 1 cm.

b absorbance due to 2-cyanophenylacetonitrile

c absorbance due to adduct normalised to 1×10^{-4} M TNT and pathlength of 1 cm.

d calculated as
$$\frac{A_{450}}{(2.1 - A_{450}) [2-CN] [NaOMe]}$$

v) Comparisons of data and determination of intrinsic rate constant

Data for dimethylmalonate and ethylcyanoacetate are summarised in table 5.69 along with the data from the literature for other carbanions. There is a general correlation between carbon basicities⁵⁴ (thermodynamic affinity for carbon) as measured by K_3 values and with proton basicities as measured by pK_a values. However there is some evidence that steric effects in the adducts with TNB may be important. Hence the high value of K_3 for nitromethane may reflect the linearity of the carbanion which minimises steric interactions, while the relatively low value for ethylmalononitrile may derive from unfavourable steric interactions in the adduct.

Values of K_3 for reaction with TNB are 3 to 12 times larger (2 to 8 times larger after statistical correction) than corresponding values for picryl chloride. The decrease in values of equilibrium constants derives entirely from a decrease in the forward rate constant, values of k_{-3} for picryl chloride always being smaller than the corresponding k_{-3} values for TNB. The decrease in value of K_3 may be attributed⁵⁵ to the steric effect of the chlorine substituent which disrupts the planarity of the nitro groups so that they cannot exert their maximum electron withdrawing influence. This effect overrides the electron withdrawing nature of the chlorine group.

Ratios of k_3/k_1 (not statistically corrected) for picryl chloride reacting with malononitrile ions and ethylcyanoacetate ions are 17 and 32 respectively. For dimethylmalonate (with picryl chloride and TNA) the ratios (366 and 343) are greater by more than an order of magnitude. These differences seem very large for carbanions of similar structure. However, the dimethylmalonate carbanion is somewhat bulkier than the ethylcyanoacetate carbanion so that steric effects in the transition state for attack at the 1-position of the substrates may be important.

Values of K_3 for TNT are much smaller than those for TNB, TNA or picryl chloride. The inductive effect of the CH_3 - substituent will be an important factor in

reducing adduct stability as well as the previously mentioned disruption in planarity of the nitro groups^{4,9}

A comparison of values of K for ionisation by methoxide of the ethylcyanoacetate adduct shows that these values increase in the order that the substituents (CH_3 , H , Cl) become increasingly electron withdrawing. Although the negative charge produced cannot be directly delocalised into the ring, the results nevertheless show that a large proportion of this charge must be situated there.

Data obtained for three phenylacetonitriles with TNB, picryl chloride and TNT, summarised in table 5.70, follow much the same pattern. The steric effect of the 2-cyano derivative in reducing adduct stability is shown in the values of K_3K_{CH} which are 3 to 5 times smaller than the corresponding values for the 4-cyano and 4-nitro derivatives.

The logarithmic plots of rate coefficient against equilibrium constant (figures 5.71 to 5.75) allow the determination of intrinsic rate constants (k_0) which are summarised in table 5.71

Table 5.71

Intrinsic rate constants k_0 for carbanion addition to unsubstituted positions of trinitroactivated aromatics in methanol

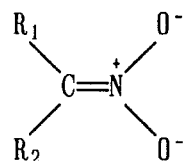
Carbon acid	k_0
nitromethane ^a	0.18
nitroethane ^a	0.22
dimethylmalonate	200
ethylcyanoacetate	200
4-nitrophenylacetonitrile	280
4-cyanophenylacetonitrile	10^3
2-cyanophenylacetonitrile	10^3
malononitrile ^b	2.5×10^4

a data from reference 2

b data from reference 10,2

The results are best understood in terms of structural / electronic / solvational reorganisation during the reaction:^{5,6}

In methanol the nitroalkanes may be represented by the structure below in which the negative charge is largely on the oxygen atoms and is strongly solvated. Reaction through carbon therefore requires the transfer of charge resulting in



considerable structural / electronic reorganisation and accompanying solvent reorganisation:^{5,6} Hence the low value of k_0 . By way of contrast, the observed value for malononitrile is 10^5 times larger. There is evidence^{5,7} that in nitrile anions the negative charge is not strongly delocalised onto the nitrogens giving them more the character of a true carbanion. Thus much less structural / electronic reorganisation is involved and k_0 is consequently large

In the case of dimethylmalonate and ethylcyanoacetate anions some of the negative charge will be delocalised onto the oxygens of the ester functions. The carbanions thus formed will have a character intermediate between the two extremes of the nitroalkanes and nitriles. They are also more likely to be more strongly solvated relative to malononitrile, so the accompanying solvational reorganisation will also be larger.

The predominant factor in causing the decrease of k_0 for 4-nitrophenylacetonitrile relative to the 2-cyano and 4-cyano derivatives is likely to be enhanced solvational reorganisation. In support of this, Bernasconi³¹ has found that the value of k_0 for proton transfer of 2,4-dinitrophenylacetonitrile is about 10-fold lower than that for 4-nitrophenylacetonitrile. The main reason for the decrease is an enhanced solvational reorganisation in the reaction of the dinitro compound as there are two nitro groups which need to be solvated in the anion. Since the nitro

group in 4-nitrophenylacetonitrile is known to be specifically solvated in water;^{20,21} the fact that k_0 for proton transfer decreases markedly on going from 50/50 (v/v) DMSO/H₂O to water³¹ adds further to this argument.

Comparisons of the values of k_0 for addition to trinitroactivated aromatics (table 5.71) with corresponding values^{5,8} obtained for proton transfer reactions in 50/50 (v/v) DMSO/H₂O (malononitrile $\log k_0 \approx 7.0$; 4-nitrophenylacetonitrile $\log k_0 = 3.95$; nitromethane $\log k_0 = 0.73$) reveals a similar trend, though the values for proton transfer are spread over a greater range. Ratios of k_0 for malononitrile / 4-nitrophenylacetonitrile are *ca* 10^3 for proton transfer and *ca* 10^2 for addition to ring carbon.

Table 5.69 Rate and Equilibrium data for carbanion addition to 1-X-2,4,6-trinitrobenzenes in methanol at 25°C

carbon acid	sub-strate	pK _a	K ₃ l mol ⁻¹	k ₃ l mol ⁻¹ s ⁻¹	k ₋₃ s ⁻¹	k ₁ l mol ⁻¹ s ⁻¹	K l mol ⁻¹	ref
2-nitro-propane	TNB	<13.9	4	0.36	0.09			2
malono-nitrile	"	14.14	40	3x10 ⁵	6500		2x10 ⁴	10
nitro-ethane	"	14.22	380	34	0.09			2
methyl-cyano-acetate	"	15.19	1660	1.3x10 ⁵	62		670	3
ECA	"	15.54	2330	9.3x10 ⁴	40		230	†
nitro-methane	"	15.15	7x10 ⁴	800	0.011			2
ethyl-malono-nitrile	"	15.60	33	—	—			10
DMM	"	17.22	12,200	2.5x10 ⁵	20.5			3
DMM	"	17.27	10,000	2.4x10 ⁵	24		small	†
malono-nitrile	picryl chloride	14.14	7	3x10 ⁴	4400	1.75x10 ³	*	10
methyl-cyano-acetate	"	15.19	140	5200	37		*	3
ECA	"	15.54	310	9300	30	290	600	†
DMM	"	17.22	3500	3.0x10 ⁴	8.6	82		4
DMM	"	17.27	3440	2.17x10 ⁴	6.3		small	†
methyl-cyano-acetate	TNA	15.19	106	7600	72		*	6
DMM	"	17.22	2090	2.95x10 ⁴	14.2	86		7
malono-nitrile	TNT	14.14	0.05	3.5x10 ³	7x10 ⁴			10
nitro-ethane	"	14.22	0.63	0.16	0.25			2
ECA	"	15.54	2.9	460	160		<150	†
nitro-methane	"	15.58	62	4.3	0.07			2
DMM	"	17.27	30	1950	65			†

* assumed the same value as the for TNB adduct

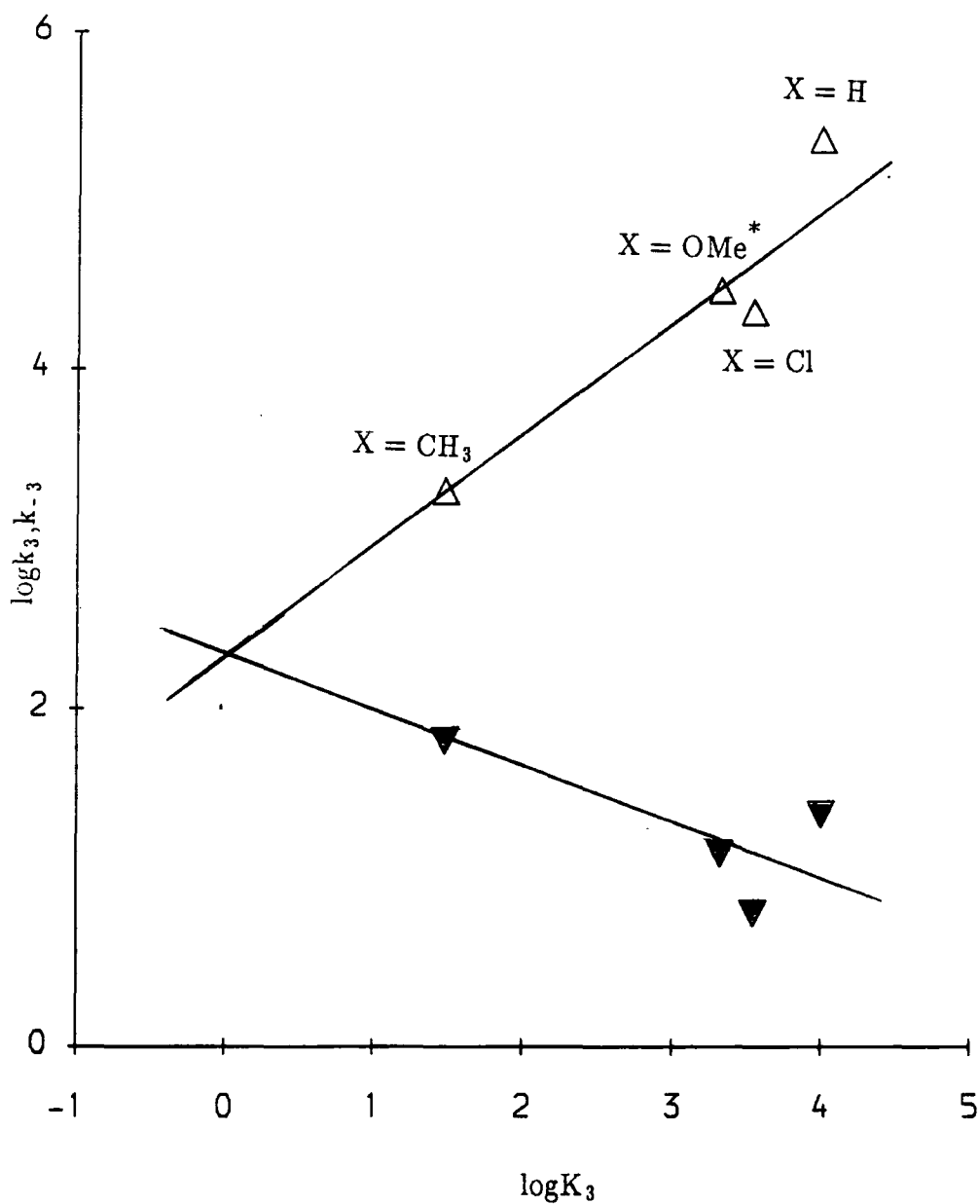
† this study

Table 5.70
Rate and Equilibrium data for substituted phenylacetonitriles
in methanol at 25°C

subst- ituent	subs- trate	K_{CH} $l\text{mol}^{-1}$	K_3K_{CH} $l^2\text{mol}^{-2}$	k_3K_{CH} $l^2\text{mol}^{-2}$	k_{-3} s^{-1}	k_3 $l\text{mol}^{-1}s^{-1}$	K_3 $l\text{mol}^{-1}$
4-NO ₂	TNB	1.17	6.2x10 ⁴		18	9.6x10 ⁵	5.3x10 ⁴
4-CN	TNB	2.5x10 ⁻⁴	5.4x10 ⁴	2.2x10 ⁵	4.1	8.8x10 ⁸	2.1x10 ⁸
2-CN	TNB	3.5x10 ⁻⁴	1.8x10 ⁴	2.7x10 ⁵	15	7.7x10 ⁸	5.1x10 ⁷
4-NO ₂	PicCl	1.17	1.2x10 ⁴		17	1.75x10 ⁵	1.0x10 ⁴
4-CN	PicCl	2.5x10 ⁻⁴	8420	3.2x10 ⁴	3.8	1.3x10 ⁸	3.4x10 ⁷
2-CN	PicCl	3.5x10 ⁻⁴	2500	3.0x10 ⁴	12	8.6x10 ⁷	7.1x10 ⁶
4-NO ₂	TNT	1.17	245		65	1.4x10 ⁴	210
4-CN	TNT	2.5x10 ⁻⁴	160	3360	21	1.3x10 ⁷	6.4x10 ⁵
2-CN	TNT	3.5x10 ⁻⁴	50	2650	53	7.6x10 ⁶	1.4x10 ⁵

Figure 5.71

Determination of intrinsic reactivities: Reactions of dimethylmalonate ions at unsubstituted ring positions of 1-X-2,4,6-trinitrobenzenes. * Data from ref. 7



$\nabla = k_{-3}$
 $\Delta = k_3$

Figure 5.72

Determination of intrinsic reactivities: Reactions of ethylcyanoacetate ions at unsubstituted ring positions of 1-X-2,4,6-trinitrobenzenes.

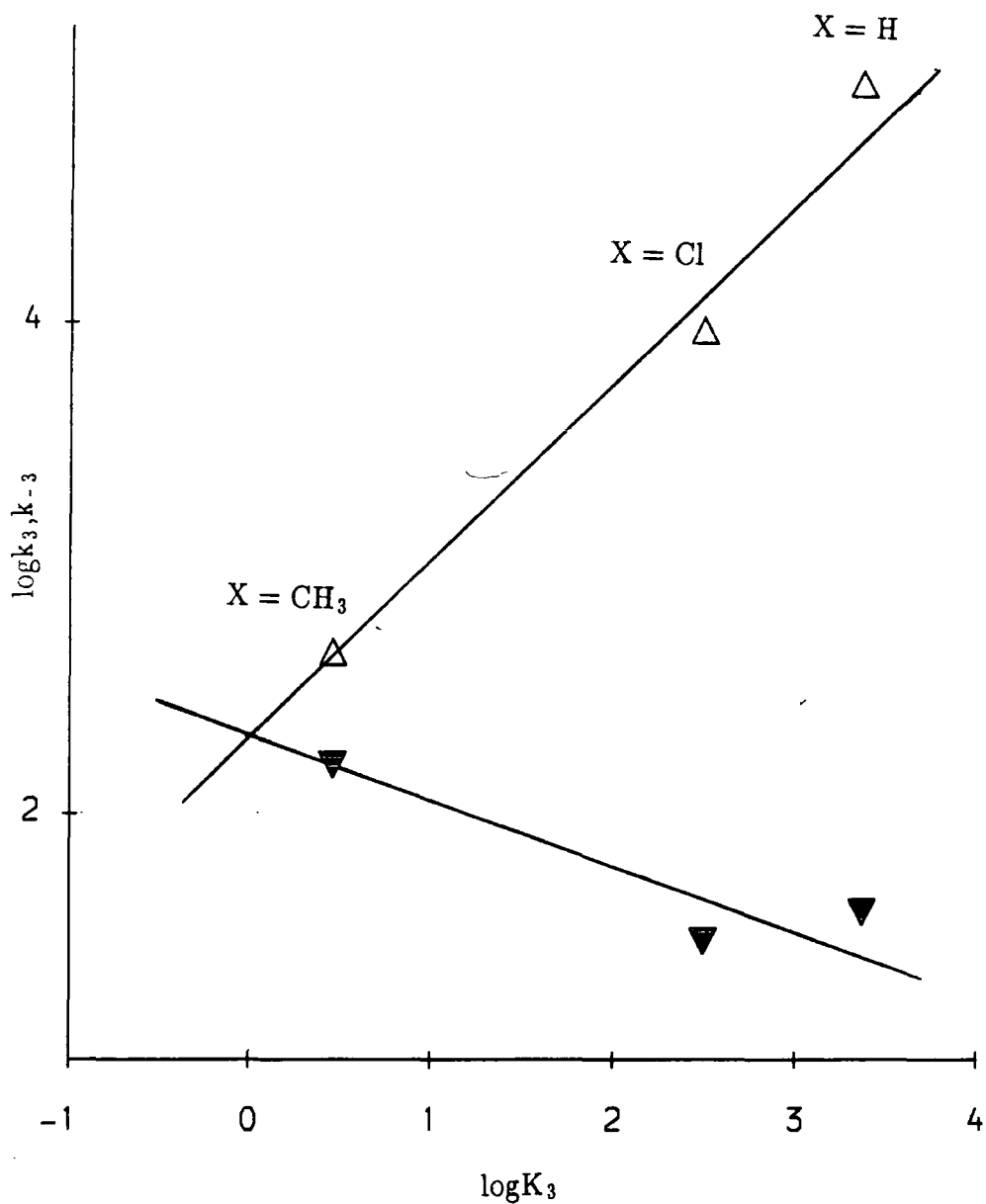
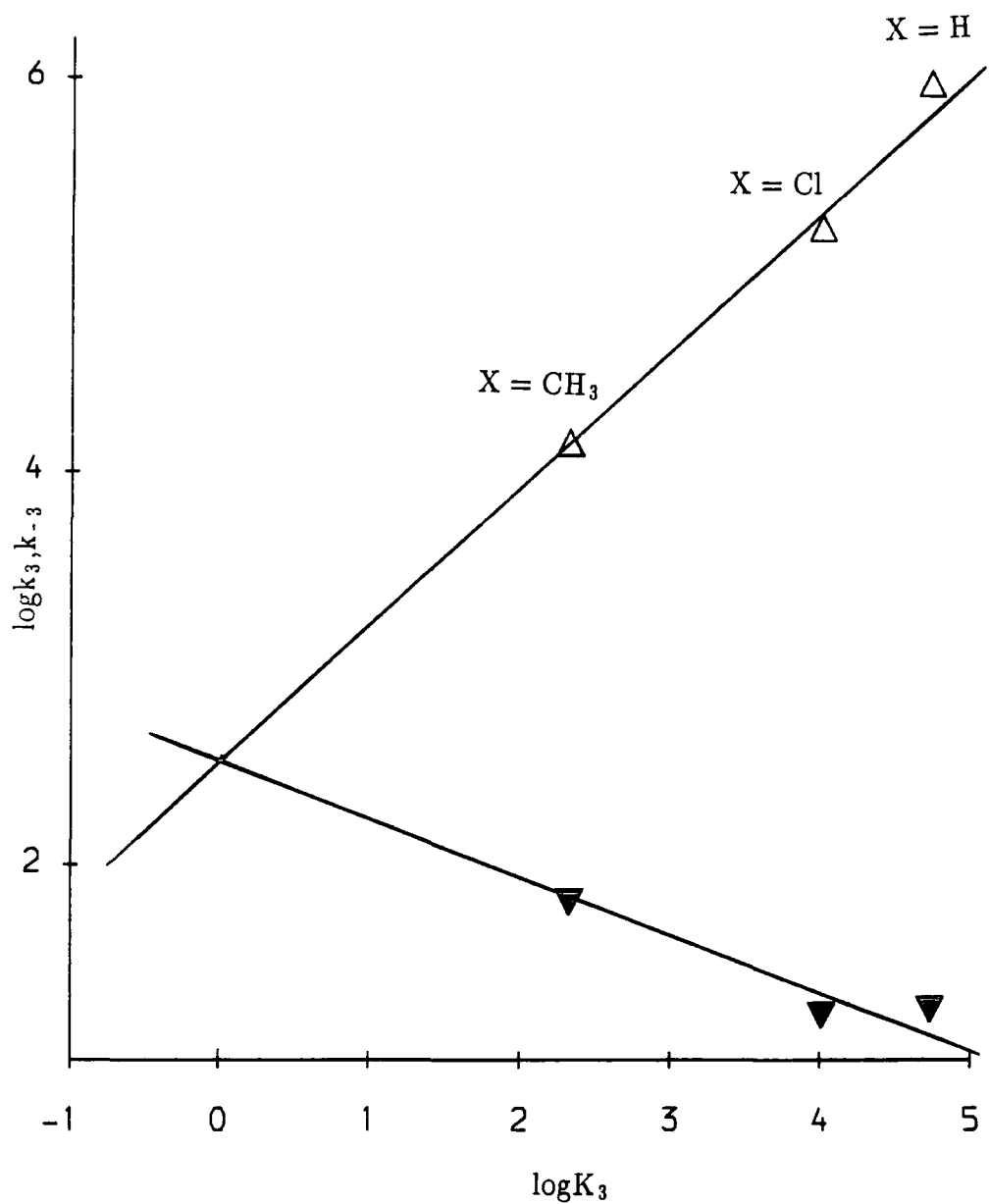


Figure 5.73

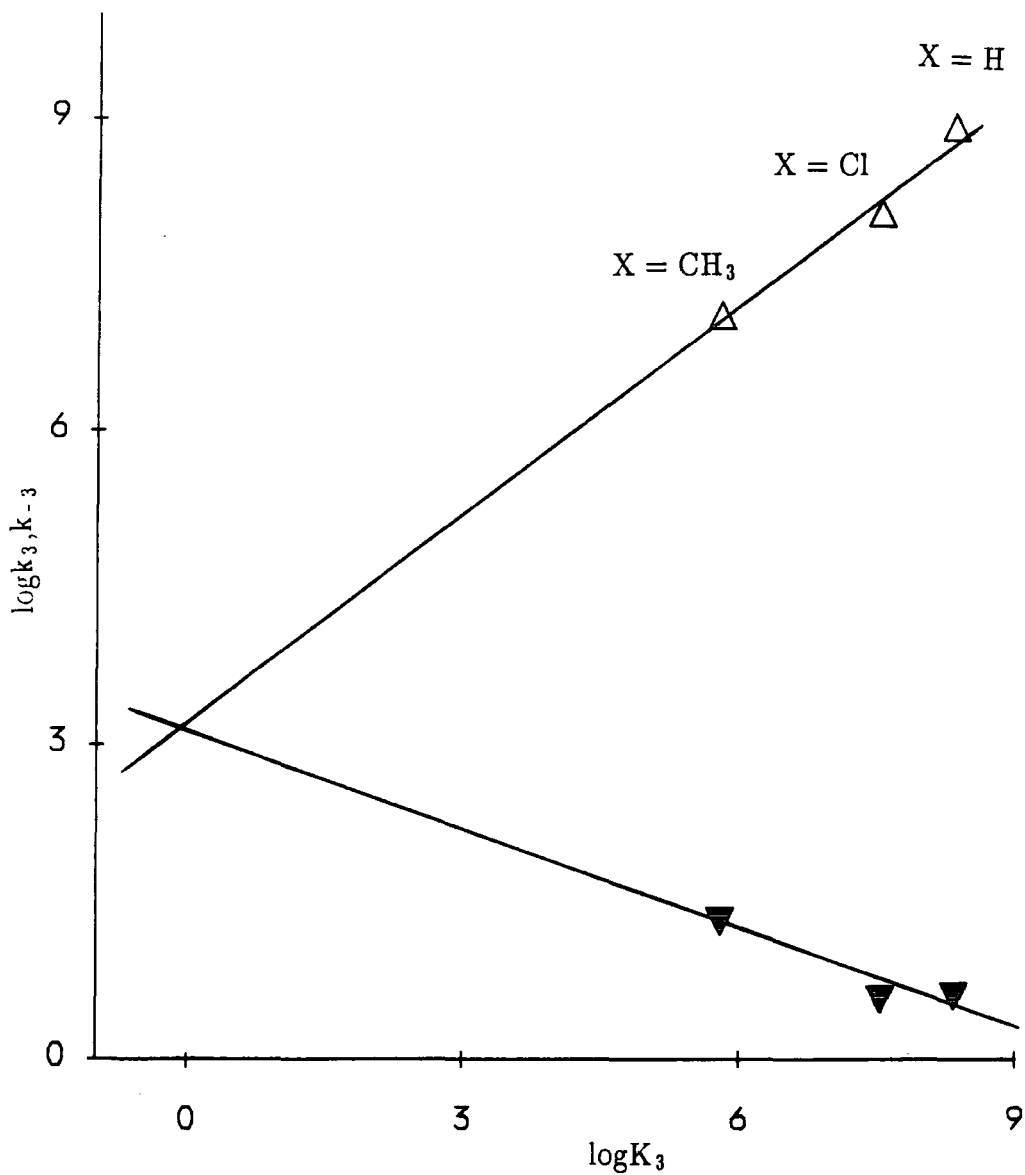
Determination of intrinsic reactivities: Reactions of 4-nitrophenylacetonitrile ions at unsubstituted ring positions of 1-X-2,4,6-trinitrobenzenes.



▼ = k_{-3}
△ = k_3

Figure 5.74

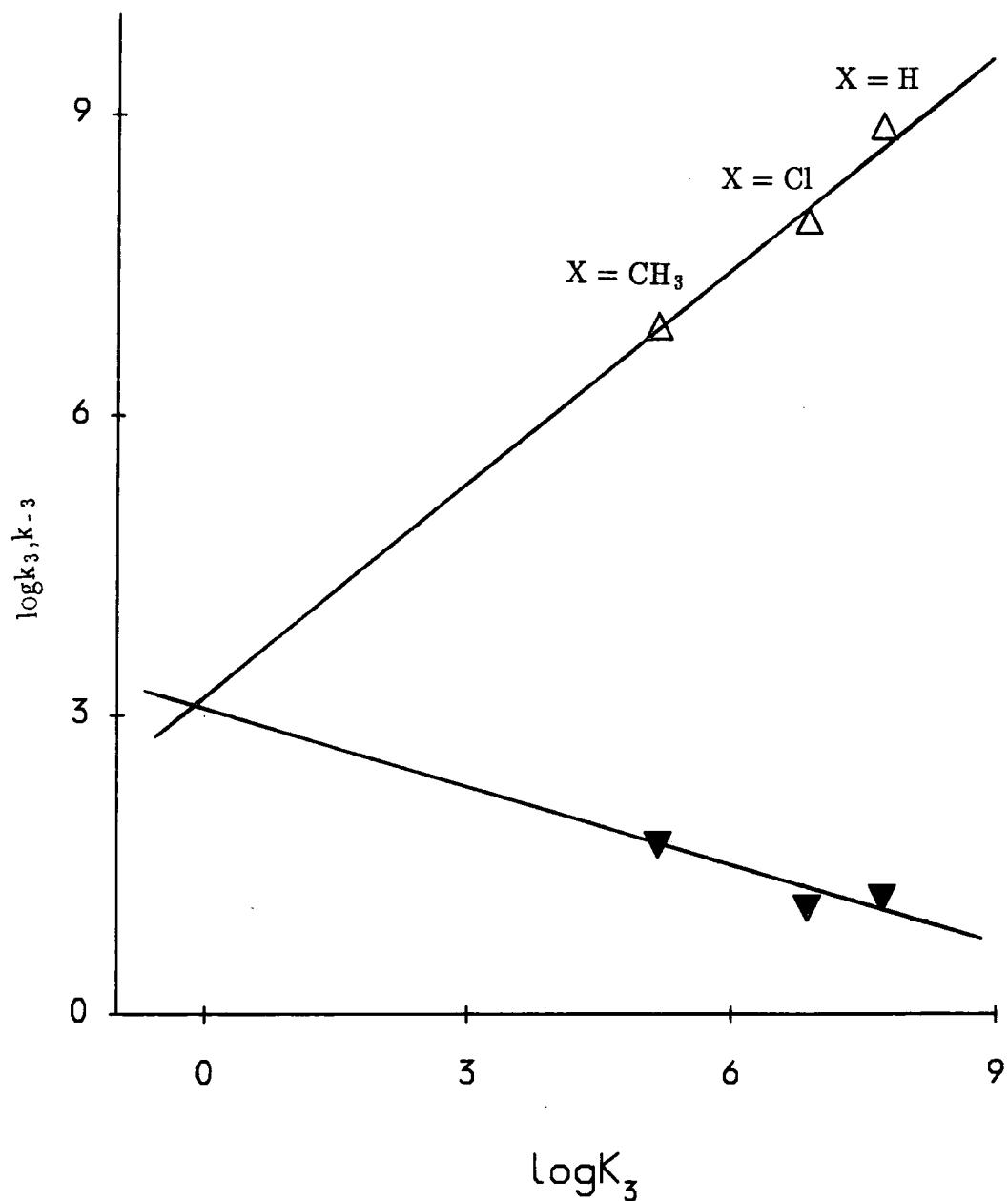
Determination of intrinsic reactivities: Reactions of 4-cyanophenylacetonitrile anions at unsubstituted ring positions of 1-X-2,4,6-trinitrobenzenes.



▼ = k_{-3}
△ = k_3

Figure 5.75

Determination of intrinsic reactivities: Reactions of 2-cyanophenylacetonitrile ions at unsubstituted ring positions of 1-X-2,4,6-trinitrobenzenes.

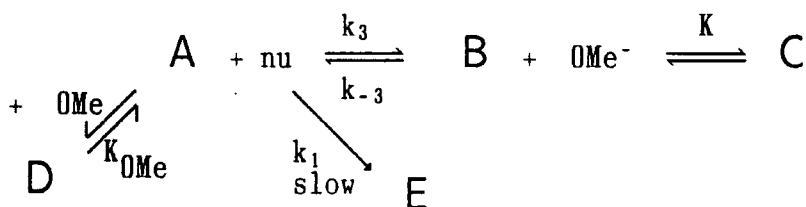
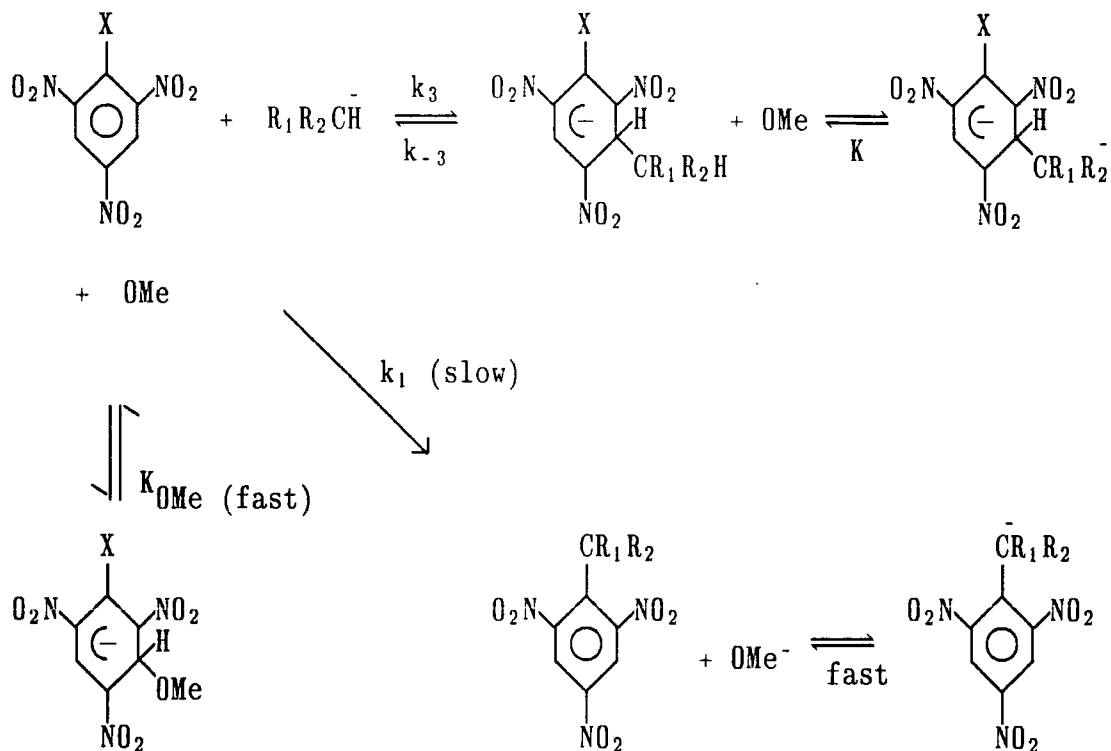


▽ = k_{-3}

△ = k_3

Appendix

i) Derivation of rate equations



a) derivation of k_{obs} for the fast process. With $X = \text{CH}_3, \text{Cl}$ formation of E may be neglected. For ($X=\text{Cl}$), formation of E is slow

$$-\frac{d[\text{A}]}{dt} = k_3 [\text{A}] [\text{nu}] - k_{-3} [\text{B}] \quad 5.76$$

The stoichiometric concentration of A, $[A]_0$ is given by

$$[A]_0 = [A] + [B] + [C] \quad 5.77$$

$$K \text{ is defined as } K = \frac{[C]}{[B][O\text{Me}^-]} \quad 5.78$$

$[B]$ may be eliminated from 5.76 by using 5.77 and 5.88. Thus,

$$\frac{-d[A]}{dt} = k_3 [A] [\text{nu}] + \frac{k_3 ([A] - [A]_0)}{1 + K [O\text{Me}^-]} \quad 5.79$$

at equilibrium

$$\frac{-d[A]}{dt}_{\text{eq}} = 0 = k_3 [A]_{\text{eq}} [\text{nu}] + \frac{k_3 ([A]_{\text{eq}} - [A]_0)}{1 + K [O\text{Me}^-]} \quad 5.80$$

The concentration of methoxide and carbanion (nu) are kept in large excess of $[A]$ and thus remain effectively constant. Subtracting 5.80 from 5.79 yields

$$\frac{-d[A]}{dt} = ([A] - [A]_{\text{eq}}) \left[k_3 [\text{nu}] + \frac{k_{-3}}{1 + K [O\text{Me}^-]} \right] \quad 5.81$$

Thus

$$k_{\text{obs}} = \frac{-1}{[A] - [A]_{\text{eq}}} \frac{d[A]}{dt} = k_3 [\text{nu}] + \frac{k_{-3}}{1 + K [O\text{Me}^-]} \quad (5.55)$$

In the case of trinitrobenzene ($X = \text{H}$), the rapid pre-equilibrium with methoxide reduces $[A]$ by a factor

$$\frac{1}{1 + K [O\text{Me}^-]}$$

Thus

$$\frac{-d[A]}{dt} = \frac{k_3 [A] [\text{nu}]}{1 + K_{O\text{Me}} [O\text{Me}^-]} + \frac{k_{-3} ([A] - [A]_{\text{eq}})}{1 + K [O\text{Me}^-]} \quad 5.82$$

which may be treated in the same way to arrive at

$$k_{\text{obs}} = \frac{k_3 [\text{nu}]}{1 + K_{\text{OMe}} [\text{OMe}^-]} + \frac{k_{-3}}{1 + K [\text{OMe}^-]} \quad (5.31)$$

b) Derivation of k_{slow}

$$\frac{d[\text{E}]}{dt} = k_1 [\text{A}] [\text{nu}] \quad 5.83$$

The stoichiometric concentration of A, $[\text{A}]_0$ is given by

$$[\text{A}]_0 = [\text{A}] + [\text{B}] + [\text{C}] + [\text{E}] \quad 5.84$$

(negligible D for X=Cl)

The equilibrium constant K_3 is

$$K_3 = \frac{[\text{B}]}{[\text{A}] [\text{nu}]} \quad 5.85$$

Equations 5.84, 5.85 and 5.78 are used to obtain $[\text{A}]$ in terms of $[\text{E}]$

$$[\text{A}] = \frac{[\text{A}]_0 - [\text{E}]}{1 + K_3 [\text{nu}] + K K_3 [\text{MeO}^-] [\text{nu}]} \quad 5.86$$

Hence

$$\frac{d[\text{E}]}{dt} = \frac{k_1 ([\text{A}]_0 - [\text{E}]) [\text{nu}]}{1 + K_3 [\text{nu}] + K K_3 [\text{MeO}^-] [\text{nu}]} \quad 5.87$$

Thus

$$\frac{1}{[\text{A}]_0 - [\text{E}]} \frac{d[\text{E}]}{dt} = k_{\text{obs}} = \frac{k_1 [\text{nu}]}{1 + K_3 [\text{nu}] + K K_3 [\text{MeO}^-] [\text{nu}]} \quad 5.56$$

ii) Sample kinetic runs

Reaction of TNB with 3-chlorophenylacetonitrile

[3-chlorophenylacetonitrile] = 1.5×10^{-3} M, [TNB] = 8×10^{-5} M, [NaOMe] = 0.01 M

t s	A _{450nm}	k _{obs} s ⁻¹	A _{450nm}	k _{obs} s ⁻¹
0	0.529		0.532	
10	0.623	0.022	0.616	0.020
20	0.693	0.020	0.685	0.020
30	0.752	0.021	0.742	0.020
40	0.800	0.021	0.791	0.021
50	0.838	0.021	0.829	0.020
60	0.868	0.020	0.858	0.019
70	0.893	0.020	0.886	0.022
80	0.914	0.021	0.909	0.023
90	0.931	0.021	0.924	0.018
100	0.945	0.021	0.938	0.021
110			0.949	0.020
∞	1.005		0.998	
Average		0.021	0.020	

Reaction of TNB with 4-chlorophenylacetonitrile

[4-chlorophenylacetonitrile] = 1.5×10^{-3} M, [TNB] = 1×10^{-4} M, [NaOMe] = 0.01M

t s	A _{450nm} ^a	10 ³ k _{obs} s ⁻¹	A _{450nm}	10 ³ k _{obs} s ⁻¹
0	0.536		0.532	
40	0.640	4.7	0.616	4.6
80	0.732	5.0	0.685	4.6
120	0.804	4.7	0.742	5.1
160	0.868	5.1	0.791	4.9
200	0.920	5.1	0.829	4.9
240	0.964	5.3	0.858	5.2
260	0.996	4.7	0.886	5.5
300	1.028	5.7	0.909	5.6
340	1.052	5.4	1.924	4.6
380	1.068	4.4	1.938	5.6
420			1.949	4.6
∞	1.152		1.136	
Average		5.0		5.0

a absorbance corresponds to 1cm cells.

Reaction of TNB with 3-methylphenylacetonitrile

[3-methylphenylacetonitrile] = 4×10^{-3} M, [NaOMe] = 5×10^{-3} M

t s	a		b	
	$A_{450\text{nm}}$	$10^4 k_{\text{obs}}$ s ⁻¹	$A_{450\text{nm}}$	$10^4 k_{\text{obs}}$ s ⁻¹
0	0.204		0.240	
150	0.269	6.9	0.318	7.0
300	0.330	7.2	0.391	7.3
450	0.384	7.1	0.458	7.4
600	0.434	7.3	0.526	8.5
750	0.480	7.5	0.576	7.0
900	0.522	7.7	0.624	7.5
1050	0.560	7.9	0.666	7.4
1200	0.592	7.4	0.707	8.1
1350	0.618	6.7	0.742	7.7
1500	0.644	7.4	0.774	7.4
1650	0.670	8.4	0.802	8.4
1800	0.690	7.3	0.827	7.9
1950	0.708	7.3	0.850	8.2
2100	0.726	8.2	0.869	7.6
2250	0.742	8.2	0.886	7.6
2400	0.756	8.1	0.901	7.6
2550			0.914	7.3
2700			0.926	7.6
∞	0.864		1.026	
Average		7.5		7.6

a [TNB] = 7.5×10^{-5} M pathlength is 1cm.

b [TNB] = 8×10^{-5} M pathlength is 1cm.

References

- 1 CA Fyfe, *Can. J. Chem.*, 1968, 46, 3047
- 2 JPL Cox, MR Crampton, P Wight, *J. Chem. Soc. Perkin Trans. II*, 1988, 25
- 3 J Kolb, V Machacek, V Sterba, *Collect. Czech. Chem. Commun.*, 1976, 41, 1914
- 4 J Kavalek, M Pastrnek, V Sterba *ibid.*, 1978, 43, 1401
- 5 V Machacek, V Sterba, A Lycka *ibid.*, 1987, 52, 132
- 6 J Kavalek, V Machacek, A Lycka *ibid.*, 1979, 44, 1453
- 7 J Kavalek, V Machacek, M Pastrnek, V Sterba *ibid.*, 1977, 42, 2928
- 8 KT Leffek, AE Matinopoulos-Scordou, *Can. J. Chem.*, 1977, 55, 2656
- 9 KT Leffek, PH Tremaine *ibid.*, 1973, 51, 1659
- 10 MR Crampton, TP Kee, JR Wilcock *ibid.*, 1986, 64, 1714
- 11 GA Artamkina, MP Egorov, IP Beletskaya, *Chem. Rev.*, 1982, 82, 427
- 12 Heller, *Annalen*, 1908, 358, 357
- 13 Mellinghof, *Berichte*, 1889, 22, 3209
- 14 N Kornblum, *Org. React.*, 1962, 12, 101
- 15 CH Rochester, B Rossall, *J. Chem. Soc. Perkin Trans. II*, 1967
- 16 OA Peutov, IP Beletskaya, KP Butin, "*C-H acids*", Pergamon Press, Oxford, 1978
- 17 MR Crampton, *J. Chem. Soc.(B)*, 1967, 85
- 18 Silverstein, Bassler and Mornill, "*Spectrometric Identification of Organic Compounds*". Wiley
- 19 RA More O'Ferrall, JH Ridd, *J. Chem. Soc.*, 1963, 5030
- 20 EA Walters, *J. Phys. Chem.*, 1977, 81, 1995
- 21 EA Walters *ibid.*, 1978, 82, 1219
- 22 MA Paul, F Long, *Chem. Rev.*, 1957, 57, 1
- 23 DJ Kroeger, R Stewart, *Can. J. Chem.*, 1967, 45, 2163
- 24 K Bowden, *Chem. Rev.*, 1966, 66, 119
- 25 R Stewart, JP O'Donnell, DJ Cram, B Rickborn, *Tetrahedron*, 1962, 18, 917

- 26 K Bowden, R Stewart, *Tetrahedron*, 1965,21,261
- 27 TH Lowry, KS Richardson, "*Mechanism and Theory in Organic Chemistry*", Harper and Row, New York
- 28 Tseng Kuang-Chih, *Acta Chim. Sinica*, 1966,32,107
- 29 O Exner, *Prog. Phys. Org. Chem.*, 1973,10,1, Chapter 10
- 30 Stewart and O'Donnell, *J. Am. Chem. Soc.*,1962,84,493
- 31 CF Bernasconi, SA Hibdon, *J. Am. Chem. Soc.*, 1983,105,4343
- 32 FG Bordwell, *Acc. Chem. Res.*, 1988,21,456
- 33 FG Bordwell *et al.*, *J. Org. Chem.*, 1977,42, 2 321
- 34 CF Bernasconi, DAV Kliner, AS Mullin, JX Ni, *J. Org. Chem.*, 1988,53,3342
- 35 FG Bordwell, *Pure and Appl. Chem.*, 49,963
- 36 CF Bernasconi, *J. Am. Chem. Soc.*,1970,92,4682
- 37 MR Crampton, HA Khan, *J. Chem. Soc. Perkin Trans. II*,1973,710
- 38 FC Schaefer, GA Peters, *J. Org. Chem.*, 1961,26,412
- 39 MR Crampton, *J. Chem. Soc.(B)*, 1971, 2112
- 40 E Buncel, JGK Webb, *Can. J. Chem.*, 1974,52,630
- 41 E Buncel, MR Crampton, MJ Strauss, F Terrier, "*Electron Deficient Aromatic and Heteroaromatic Base Interactions*", Elsevier, 1984
- 42 MR Crampton, MA El Ghariani, HA Khan, *Tetrahedron*, 1972,28,3294
- 43 B Gibson, MR Crampton, *J. Chem. Soc. Perkin Trans. II*, 1979,648
- 44 LH Gan, AR Norris, *Can. J. Chem.*, 1974,52,18
- 45 V Gold, CH Rochester, *J. Chem. Soc.*,1964, 1687
- 46 MR Crampton, V Gold, *J. Chem. Soc.*,1964, 4293
- 47 JH Fendler, EJ Fendler, CE Griffin, *J. Org. Chem.*, 1969,34,689
- 48 M Sasaki, N Takisawa, F Amita, *J. Am. Chem. Soc.*, 1980,102,7268
- 49 DN Brooke, MR Crampton, *J. Chem. Res.*, 1980,(S) 340; (M) 4401
- 50 CA Fyfe, CD Malkiewich, SWH Damji, AR Norris, *J. Am. Chem. Soc.*, 1976,98,6983
- 51 F Terrier, *Chem. Rev.*

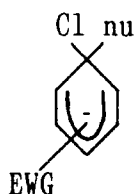
- 52 E Bunce, KE Russell, J Wood, *Chem. Commun.*, 1968, 252
- 53 CF Bernasconi, *J. Org. Chem.*, 1971,36,12,1671
- 54 J Hine, RD Weimar, *J. Am. Chem. Soc.*,1965,87,3387
- 55 MR Crampton, C Greenhalgh, *J. Chem. Soc. Perkin Trans. II*,
- 56 CF Bernasconi, *Pure and Appl. Chem.*, 1982,54,12,2335
- 57 J Hine, *Adv. Phys. Org. Chem.*, 1977,15,1
- 58 CF Bernasconi, *Acc. Chem. Res.*, 1987,20,301

Chapter 6

Reactions of 1-X-2,4-dinitrobenzenes with hydroxide ions.

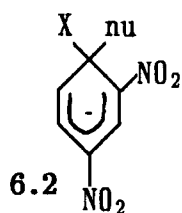
Comparison of relative rates of nucleophilic attack at substituted and unsubstituted ring-positions.

There have been several reports of the observation of σ -adducts during nucleophilic substitutions of ring-activated chlorobenzenes!¹⁻⁵ Spectroscopic and kinetic studies of these reactions have shown⁶⁻¹⁰ that the observed adducts result from nucleophilic addition to unsubstituted ring positions rather than at the chloro-substituted position. The intermediates 6.1 are not observed due to the rapid expulsion of chloride. Nucleophilic attack at unsubstituted ring positions of activated chlorobenzenes is found to be more rapid than attack at substituted ring positions!^{7,12,13}

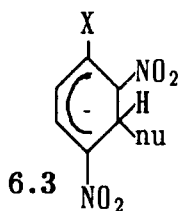


6.1

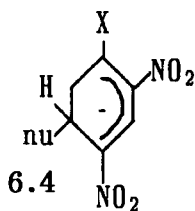
In the reactions of 1-X-2,4-dinitrobenzenes with nucleophiles there is the possibility of attack at 1-, 3- or 5-positions, giving rise to the adducts 6.2, 6.3 and 6.4. Abe and Hasegawa^{4,5} have used rapid scan recording techniques to observe the visible spectra at various times after mixing of a series of 1-X-2,4-dinitrobenzenes with hydroxide ions in DMSO/H₂O. Two species were found to be present in the initial stages of the reactions, the first with a λ_{\max} 565-650 nm attributable to 6.3 (nu = OH) and the second with λ_{\max} 480-550 nm consistent with 6.4 (nu = OH) where addition has occurred *para* to a nitro-group!^{4,5} Except for X = H, the final product was 2,4-dinitrophenolate. The intermediates 6.2 (nu = OH, X \neq H) are expected to be unstable with respect to loss of hydroxide and were not observed.



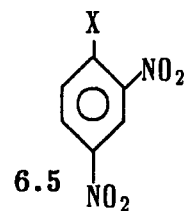
6.2



6.3



6.4



6.5

Similarly, addition of methoxide in MeOH/DMSO to 6.5 (X = OMe) was observed^{14,15} to give both 6.3 (X = OMe, nu = OMe) and 6.4 (X = OMe, nu = OMe) which preceded formation of the thermodynamically more stable adduct 6.2 (X = OMe, nu = OMe). As a consequence of the large stabilising effect of a nitro-group *para* to the site of addition the 1,5-adducts 6.4 typically have much greater stabilities than the 1,3-adducts 6.3. In the case of sulphite, addition to the 3-position of 1-chloro-2,4-dinitrobenzene could not be observed by ¹H nmr¹⁰ or spectrophotometric methods!² Acetate ions react with 1-X-2,4-dinitrobenzenes to yield a mixture of the isomeric adducts in which 6.4 (nu = CH₂COCH₃) prevails for X = OMe, CO₂Me!^{6,17} F, Cl, Br, I!⁸ Me, Et, *i*-Pr, *t*-Bu!¹⁷ but 6.3 (nu = CH₂COCH₃) for X = SEt and SCN!⁶ The effect of the sulphur containing substituents has been attributed to the high electron accepting capacity of the sulphur atom with its unoccupied d-orbitals!⁶

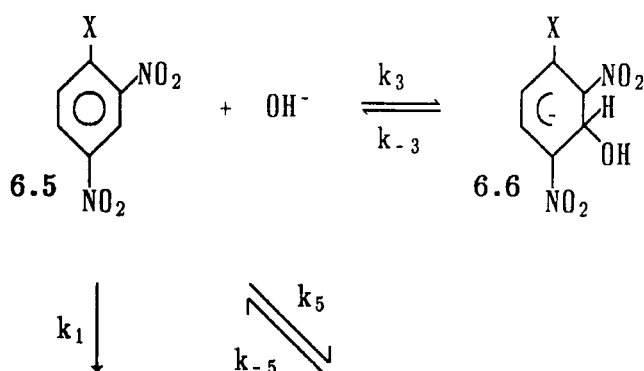
This work reports kinetic and equilibrium data for the reactions of hydroxide ions with 1-bromo- and 1-fluoro-2,4-dinitrobenzenes and compares the results with those obtained for other 1-X-2,4-dinitrobenzenes. The results provide evidence for two kinds of steric interaction (i) between the 1-substituent and the *ortho*-nitro-group and (ii) between entering and leaving groups.

Experimental

Kinetic and equilibrium measurements were made by stopped flow spectrophotometry. One syringe contained a solution of the nitrocompound and the other a solution of the base. All measurements refer to 80/20 (v/v) DMSO/H₂O unless otherwise stated and it was found convenient to have solutions of identical DMSO content in both syringes. Solutions of the 1-X-2,4-dinitrobenzenes (particularly for X = F) were found to be unstable due to hydrolysis and were used rapidly. Rate constants at 25⁰C were measured under first order conditions with the base in large excess of the nitrocompound and are the average of at least five determinations. Stock solutions of the nitrocompounds in dioxan were also unstable due to hydrolysis and were freshly prepared. After dilution the solvent contained < 1% of the organic component. Tetramethylammonium hydroxide was a commercial sample (2.8M) in water; due account of the water content of the base was taken when making up solutions.

Results and Discussion

Measurements were made in 80/20 (v/v) dimethylsulphoxide/water where there was evidence for the processes shown in scheme 6.9

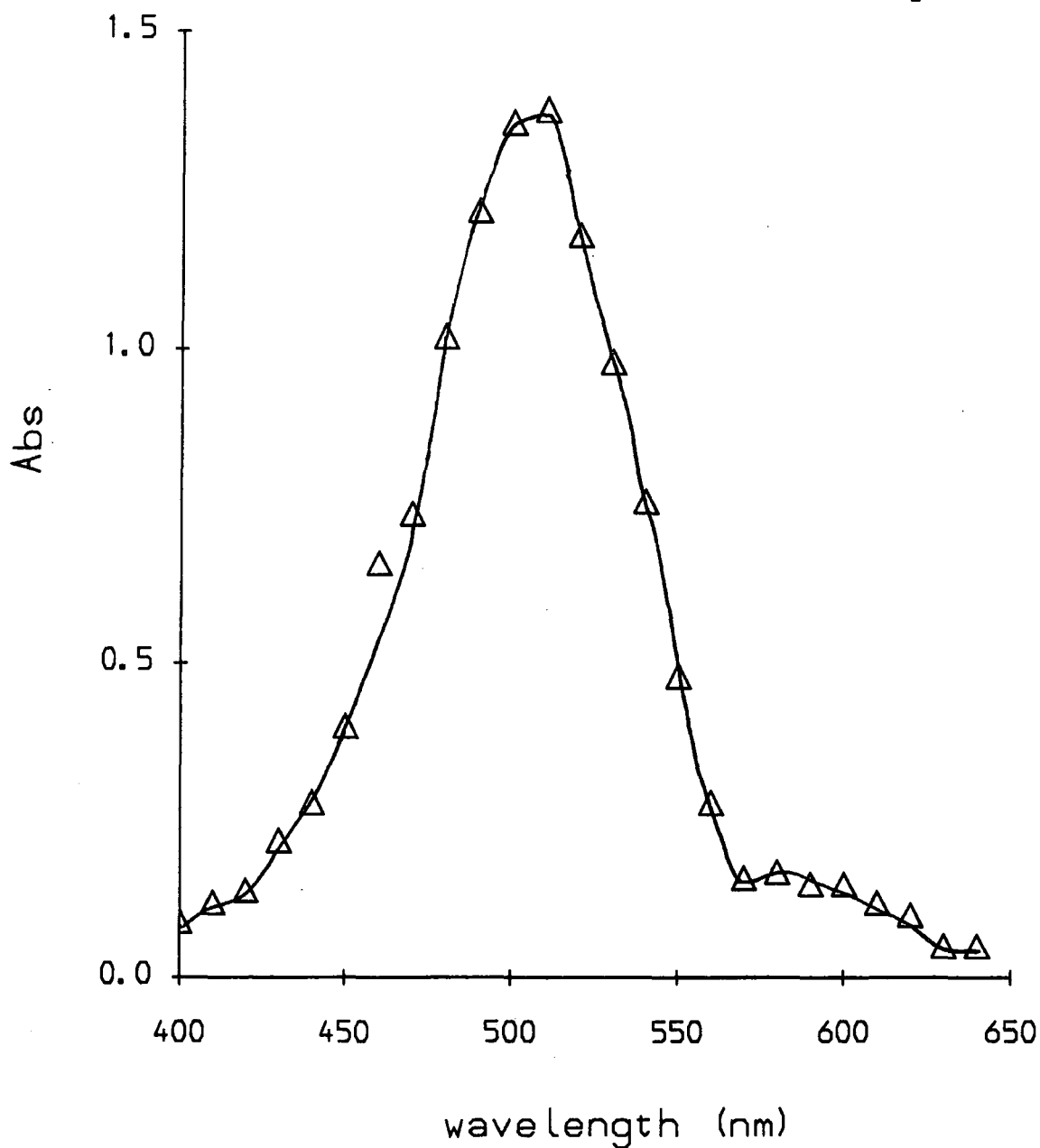


Scheme 6.9 X = F, Br

The 1,3-hydroxy adducts 6.6 were found to have absorption maxima at longer wavelength (λ_{max} 560-580 nm) than the 1,5 adducts 6.7 (λ_{max} ca 510 nm) where addition occurs para to a strongly electron withdrawing nitro group.¹¹ There was eventually complete conversion into 2,4-dinitrophenolate ions 6.8 with λ_{max} 360 nm, 420 nm. Absorbance data obtained by stopped flow spectrophotometry at various wavelengths immediately after the adduct forming processes are given in table 6.12. The spectra for 1-bromo-2,4-dinitrobenzene (figure 6.12) and 1-fluoro-2,4-dinitrobenzene show clearly the λ_{max} attributed to the two isomeric adducts. In the case of the fluoro-compound the spectrum also shows substantial conversion to 2,4-dinitrophenolate ions. There is strong evidence¹¹⁻¹³ that, though DMSO has good ability to solvate delocalised negative charges it is much inferior to water in the solvation of localised negative charges. Thus no evidence was found for the ionisation of added hydroxy groups in adducts 6.6 and 6.7 to form di-anions.

Figure 6.12

Visible spectrum of adducts formed from
1-bromo-2,4-dinitrobenzene ($1 \times 10^{-4}M$)
and NMe_4OH (0.08M) in 80/20 (v/v) DMSO/ H_2O



252A

a) 1-bromo-2,4-dinitrobenzene

There were two major processes observed on the stopped flow timescale, namely the rapid formation of the 1,5-adduct (with associated rate constants k_{fast}) and the much slower conversion of 1-bromo-2,4-dinitrobenzene into diphenolate with associated rate constants k_{slow} . The relevant rate expressions are given by 6.10 and 6.11. Kinetic and equilibrium data are given in table 6.13. Absorbances measured at 510 nm at completion of the adduct forming reaction were used to determine a value of $K_5 = 16 \text{ l mol}^{-1}$. A linear plot of k_{fast} according to equation 6.10 gave values $k_5 = 11.2 \text{ l mol}^{-1} \text{ s}^{-1}$ and $k_{-5} = 0.7 \text{ s}^{-1}$. Combination of rate coefficients leads to $K_5 = 16 \text{ l mol}^{-1}$. The formation of 6.8 was monitored at 422 nm. A linear plot of $1/k_{\text{slow}}$ against $1/[\text{OH}^-]$ (expression 6.11) yielded values $k_1 = 0.38 \text{ l mol s}^{-1}$ ($= 1/\text{slope}$) and $K_5 = 16 \text{ l mol}^{-1}$ ($= \text{intercept} / \text{slope}$).

The formation of the 1,3-adduct 6.6 ($X = \text{Br}$) was a third observable process at relatively large concentrations of hydroxide and had a very low amplitude. Absorbance measurements at 580 nm at the completion of the adduct forming reaction lead to a value for K_3 of *ca* 0.8 l mol^{-1} , assuming an extinction coefficient for 6.6 ($X = \text{Br}$) of $2.2 \times 10^4 \text{ l mol}^{-1} \text{ cm}^{-1}$ as obtained for the isomeric adduct 6.7 ($X = \text{Br}$). Kinetic data lead to values $k_3 = 9 \text{ l mol}^{-1} \text{ s}^{-1}$ and $k_{-3} = 11 \text{ s}^{-1}$

$$k_{\text{fast}} = k_5 [\text{OH}^-] + k_{-5} \quad 6.10$$

$$k_{\text{slow}} = \frac{k_1 [\text{OH}^-]}{1 + K_5 [\text{OH}^-]} \quad 6.11$$

b) 1-fluoro-2,4-dinitrobenzene

1-fluoro-2,4-dinitrobenzene was much more reactive than the corresponding bromo-compound and analysis of the kinetic data was much more complicated. Values of k_1 (table 6.14) were obtained in DMSO/H₂O mixtures containing 50, 60 and 70% DMSO by volume where formation of the dinitrophenolate ion was the only major reaction (though rapid reactions involving formation of the 6.6 and 6.7 (X = F) were observable). Linear extrapolation^{11-13,19} of this data (a plot of $\log k_1$ vs. mol% DMSO) gave a value of $k_1 = 500 \pm 20 \text{ l mol}^{-1} \text{ s}^{-1}$. In 80/20 (v/v) DMSO/H₂O the equilibration of parent and 6.6 was observed as a process with low amplitude at 560-580 nm. Extrapolation to zero base concentration of kinetic data obtained at 570 nm gave $k_{-3} = 9 \pm 2 \text{ s}^{-1}$. The λ_{max} of 6.6 and 6.7 are well separated so there was minimal interference from the reaction forming 6.7 (X = F) at 570 nm. Using initial absorbances obtained at this wavelength with an assumed value of ϵ of $2 \times 10^4 \text{ l mol}^{-1} \text{ cm}^{-1}$ typical for such adducts the value $K_3 = 5 \pm 1 \text{ l mol}^{-1} \text{ s}^{-1}$ was obtained. Hence $k_3 (= K_3 \cdot k_{-3})$ has the value $45 \pm 20 \text{ l mol}^{-1} \text{ s}^{-1}$. The reaction forming the 1,3-adduct was a minor process and in the range of concentrations (<0.012M) of hydroxide used, 6.6 (X = F) accounted for <10% of the parent. Data are given in table 6.15.

At 510 nm, the λ_{max} of the 1,5-adduct, two reactions were observed – a colour forming process, k_{fast} , and a slower fading reaction k_{slow} . Since these latter reactions are strongly coupled the following equations (see appendix) will apply!⁹

$$k_{\text{fast}} + k_{\text{slow}} = (k_1 + k_5) [\text{OH}^-] + k_{-5} \quad 6.16$$

$$k_{\text{fast}} \cdot k_{\text{slow}} = k_1 \cdot k_{-5} [\text{OH}^-] \quad 6.17$$

The experiment at 510 nm was performed on two occasions and both sets of data are give in table 6.15. Linear plots (figures 6.14 and 6.15 for data from set A)

according 6.16 and 6.17 yield values $k_1+k_5 = 710 \text{ l mol}^{-1}\text{s}^{-1}$, $k_{-5} = 1.1 \text{ s}^{-1}$, $k_1k_{-5} = 570 \text{ l mol}^{-1}\text{s}^{-2}$ (set A) and $k_1+k_5 = 810 \text{ l mol}^{-1}\text{s}^{-1}$, $k_{-5} = 0.6 \text{ s}^{-1}$, $k_1k_{-5} = 590 \text{ l mol}^{-1}\text{s}^{-2}$ (set B). Since k_1 has the value of $500 \pm 20 \text{ l mol}^{-1}\text{s}^{-1}$, k_{-5} (obtained from the product k_1k_{-5}) is therefore $1.15 \pm 0.1 \text{ s}^{-1}$ and k_5 $250 \pm 70 \text{ l mol}^{-1}\text{s}^{-1}$. Thus $K_5 (= k_5/k_{-5})$ has the value 220 l mol^{-1} .

Table 6.12
Absorbance data for the reactions of
1-X,2,4-dinitrobenzenes with hydroxide ions

λ nm	a, b		λ nm	a, b	
	A (X=F)	A (X=Br)		A (X=F)	A (X=Br)
350	1.12		500	0.20	1.36
360	1.28		510	0.22	1.38
370	1.30		520	0.18	1.18
380	1.32		530		0.98
390	1.06	0.07	540	0.18	0.76
400	1.04	0.09	550		0.48
410	1.34	0.12	560	0.22	0.28
420	1.48	0.14	570	0.19	0.16
430	0.86	0.22	580	0.15	0.17
440	0.86	0.28	590	0.06	0.15
450	0.38	0.40	600	0.05	0.15
460	0.22	0.66	610		0.12
470	0.19	0.74	620		0.10
480	0.18	1.02	630		0.05
490		1.22	640		0.05

- a** measured by stopped flow spectrophotometry at the completion of the rapid adduct forming processes. Normalised to $1 \times 10^{-4} \text{ M}$ of nitro-compound and a pathlength of 1 cm.
- b** $[\text{NMe}_4\text{OH}] = 0.10 \text{ M}$
- c** $[\text{NMe}_4\text{OH}] = 0.08 \text{ M}$

Table 6.13 Kinetic and equilibrium data for the reactions of 1-bromo-2,4-dinitrobenzene^a with hydroxide ions in 80/20 (v/v) DMSO/H₂O at 25°C

[NMe ₄ OH] M	^b k _{fast} s ⁻¹	^c k _{calc} s ⁻¹	^d A _{510nm}	^e K ₅ lmol ⁻¹	^f k _{fast} s ⁻¹	^g A _{580nm}	^h K ₃ lmol ⁻¹	ⁱ k _{slow} lmol ⁻¹ s ⁻¹	^j k _{calc} lmol ⁻¹ s ⁻¹
0.01	0.76	0.81	0.30	16		—	—	0.0034	0.0034
0.015	—	—	—	—		—	—	0.0047	0.0048
0.02	0.91	0.92	0.52	15		0.033	0.8	0.0066	0.0064
0.04	1.10	1.15	0.84	15		0.044	0.5	0.0083	0.0097
0.06	1.38	1.37	0.94	12	12±1	0.093	0.7	0.010	0.012
0.08	1.62	1.60	1.22	16	12±1	0.139	0.8	0.013	0.014
0.10	1.75	1.82	1.40	18	13±1	0.194	1.0	0.015	0.015

^a concentration is 1x10⁴M. ^b measured by stopped-flow spectrophotometry at 510nm. ^c calculated from expression 6.10 with values k₅ = 11.2 lmol⁻¹s⁻¹ and k₋₅ = 0.7 s⁻¹. ^d measured at the completion of the reaction forming the 1,5-adduct and normalised to a pathlength of 1 cm. ^e calculated as A_{510nm} / (2.2 - A_{510nm}) [NMe₄OH]. A Benesi-Hildebrand plot gave ε = 2.2x10⁴ lmol⁻¹cm⁻¹ for the 1,5-adduct at 510nm. ^f measured by stopped-flow spectrophotometry at 580nm. ^g measured at the completion of the reaction forming the 1,3-adduct and normalised to a pathlength of 1 cm. ^h calculated as A_{580nm} / (2.2 - A_{580nm}) [NMe₄OH]. ⁱ data at 422nm. ^j calculated from equation 6.11 with k₁ = 0.4 lmol⁻¹s⁻¹ and K₅ = 16 lmol⁻¹.

Table 6.14

Rate constants (k_1) for the reaction of 1-fluoro-2,4-dinitrobenzene with hydroxide ions with varying solvent composition

DMSO/H ₂ O (v/v)	mol% DMSO	k_1 l mol ⁻¹ s ⁻¹	log k_1
50/50	20.2	3.0	0.48
60/40	27.6	10.1	1.00
70/30	37.2	55.1	1.74
80/20	50.3	510*	2.17*

* values by extrapolation of log k_1 vs mol% DMSO

Table 6.15

Kinetic and equilibrium data for the reaction of 1-fluoro-2,4-dinitrobenzene with hydroxide in 80/20 DMSO/water at 25°C

[NMe ₄ OH]	Set A: 510nm		Set B: 510nm		570nm		A _{570nm}	K ₃ l mol ⁻¹
	a k _{fast} s ⁻¹	b k _{slow} s ⁻¹	a k _{fast} s ⁻¹	b k _{slow} s ⁻¹	c k _{fast} s ⁻¹	d k _{slow} s ⁻¹		
0.001	1.28	0.27	–	–	9.2	0.25	0.012	6
0.002	–	–	1.8	0.38	10.9	0.64	0.021	5
0.003	2.97	0.56	–	–	13.9	0.79	0.029	5
0.004	–	–	3.2	0.67	–	–		
0.005	4.09	0.71	–	–	15.9	1.22	0.034	4
0.006	–	–	4.3	0.74	–	–		
0.007	5.08	0.74	–	–	17.7	1.60		
0.008	–	–	6.4	0.78	–	–		
0.010	7.37	0.77	7.9	0.80	20.6	2.15		
0.012			8.2	0.84				

a colour forming at 510 nm.

b fading at 510 nm.

c colour forming at 570 nm.

d fading at 570 nm.

e Absorbance at completion of reaction forming 1,3-adduct

Figure 6.14 (set A)

Plot of kinetic data at 510nm for the reaction of hydroxide ions with 1-fluoro-2,4-dinitrobenzene in 80/20 (v/v) DMSO/H₂O

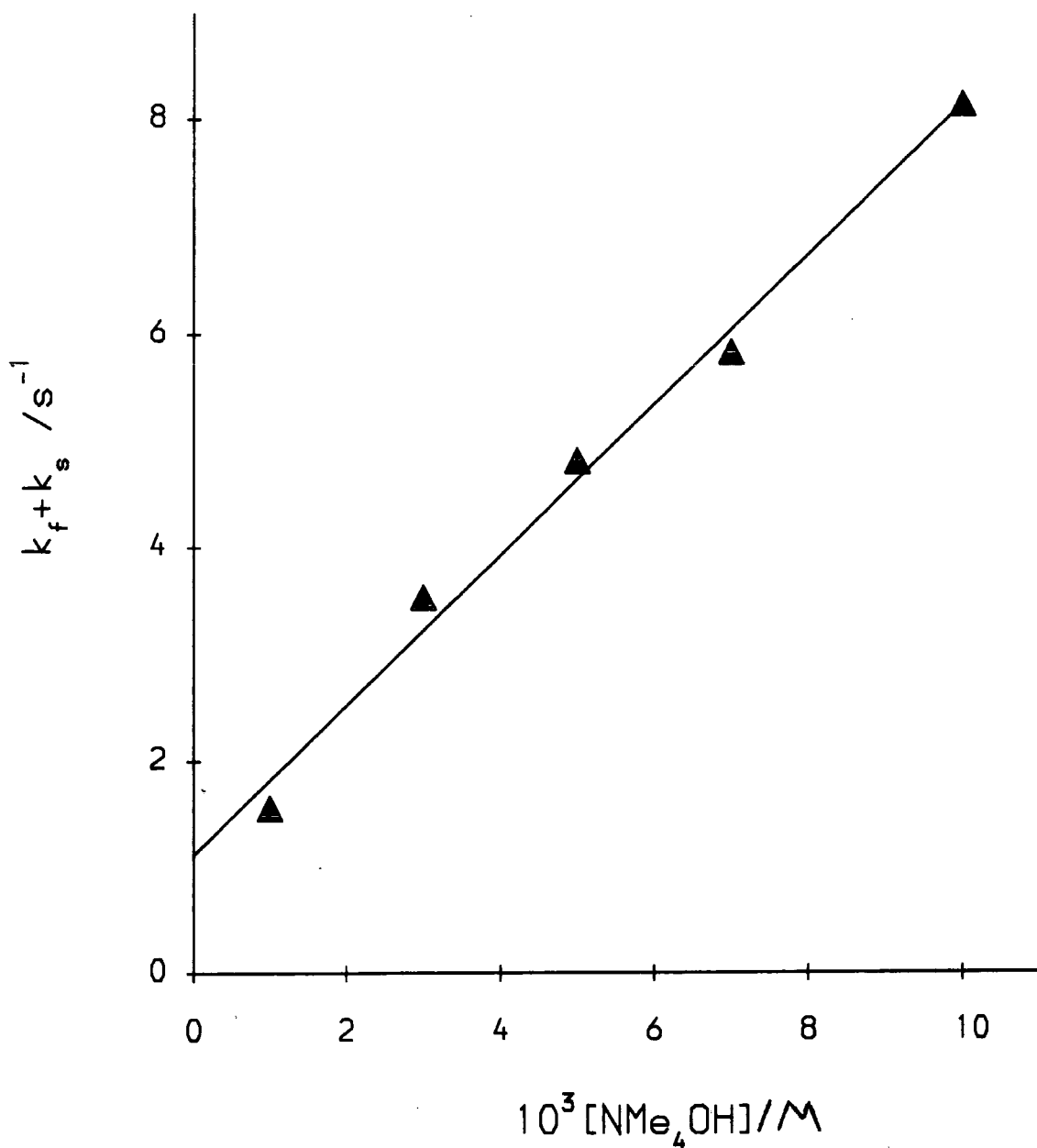
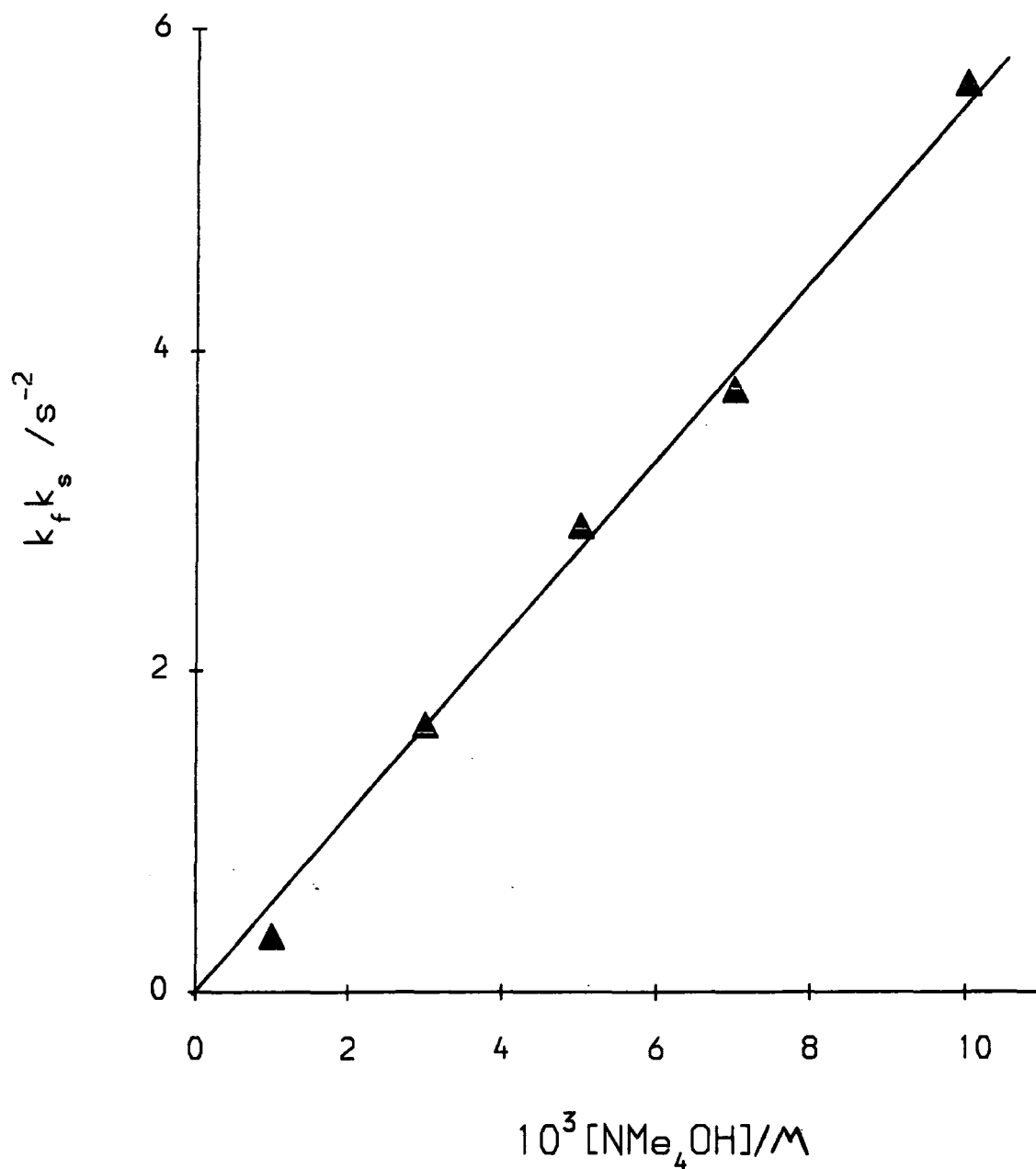


Figure 6.15 (set A)

Plot of kinetic data at 510nm for the reaction of hydroxide ions with 1-fluoro-2,4-dinitrobenzene in 80/20 (v/v) DMSO/H₂O



Comparisons of data

Data for addition to 1-X-2,4-dinitrobenzenes are summarised in table 6.18. Values of K_5 (statistically corrected) are larger for the halogen substituted compound ($X = \text{I, Br, Cl, F}$) than for *meta*-dinitrobenzene ($X = \text{H}$) as a consequence of the electron withdrawing effect of the halogens. However, the polar effect at the 5- (or 3-) position of the halogen substituents should be similar since σ_m values²⁰ are in the narrow range 0.34 – 0.39 for the four halogens. The observed decrease in values of K_5 is in the order of increasing size of the 1-substituent ($\text{F} > \text{Cl} > \text{Br} > \text{I}$) and provides evidence for steric interactions between the *ortho* nitro-group and the halogen. The larger the halogen, the more the *ortho* nitro-group will be rotated from the ring plane and the less reactive the ring will become towards nucleophiles. Since addition to the 5-position of the substrate occurs *para* to the *ortho* nitro-group it is conceivable that values of K_5 will be more strongly affected by this kind of steric effect than will values of K_3 . Accordingly, ratios of K_5/K_3 are found to be higher for the fluoro-compound (44) than for the bromo-compound (20). Values of k_{-5} (and k_{-3}) are relatively insensitive to the nature of the 1-substituent. This may indicate that the transition states for hydroxide attack are relatively advanced and resemble the hydroxy-adducts.

Hydroxide attack at the 1-position results in the formation of 2,4-dinitrophenolate ions. Values of k_1 decrease in the order of increasing halogen size ($\text{F} > \text{Cl} > \text{Br} > \text{I}$) in agreement with the generally accepted mechanism¹¹ ($\text{S}_{\text{N}}\text{A}_{\text{r}}$) for activated aromatic nucleophilic substitution which involves rate limiting formation of a σ -adduct intermediate. Ratios of k_1/k_5 are shown in the final column of table 6.18. The slower attack of hydroxide by a factor of *ca.* 20 (for $X = \text{I, Br, Cl}$) at halogen substituted positions than at the unsubstituted 5-position can be attributed to the steric and electrostatic repulsions between the entering and

leaving groups^{3,3} For X = I, Br, Cl the values are fairly constant and this may indicate that increasing steric repulsion in the series (Cl, Br, I) is balanced by decreasing electrostatic repulsion. The value of k_1/k_5 of ca. 2 for X = F can be attributed to the very small size of the fluorine atom together with its high electronegativity which will result in a high positive charge at the reaction centre.

Table 6.18

Comparison of statistically corrected values^a of rate and equilibrium constants for hydroxide attack at the 5- and 1-positions of 1-X-2,4-dinitrobenzenes in 80/20 (v/v) DMSO/H₂O at 25^oC

X	k_5 l mol ⁻¹ s ⁻¹	k_{-5} s ⁻¹	K_5 l mol ⁻¹	k_1 l mol ⁻¹ s ⁻¹	k_1/k_5
I ^b	6	0.7	8	0.35	0.058
Br ^c	11.2	0.7	16	0.40	0.036
Cl ^b	17	0.7	24	1.0	0.059
F ^d	250	1.15	220	500	2.0
H ^e	3.5	2.5	1.4	3.5	1

a values of k_5 and K_5 for *meta*-DNB have been divided by 2.

b data obtained by A.B. Davis, C. Greenhalgh

c also obtained $k_3 = 9$ l mol⁻¹ s⁻¹, $k_{-3} = 11$ s⁻¹

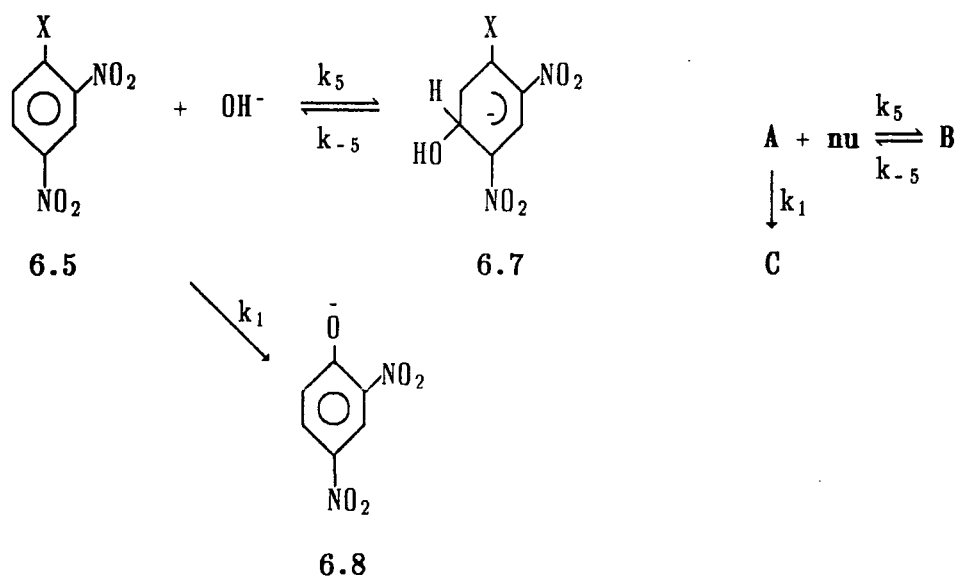
d also obtained $k_3 = 45$ l mol⁻¹ s⁻¹, $k_{-3} = 9$ s⁻¹

e data from reference 13.

Appendix

i) Derivation of rate expressions

In the reaction of 1-X-2,4-dinitrobenzenes with hydroxide ions the reaction producing the 1,3-adduct 6.6 is of minor importance



a) In the case of the 6.5 (X = Br) equilibration of A and B was found to be rapid with respect to the formation of C

$$\frac{d[\text{C}]}{dt} = k_1 [\text{A}] [\text{nu}] \quad 6.19$$

$$[\text{A}]_0 = [\text{A}] + [\text{B}] + [\text{C}] \quad 6.20$$

$$K_5 = \frac{[\text{B}]}{[\text{A}] [\text{nu}]} \quad 6.21$$

$[A]_0$ is the stoichiometric concentration of A. 6.20 and 6.21 are used to obtain $[A]$ in terms of $[C]$. 6.19 becomes

$$\frac{d[C]}{dt} = \frac{k_1 ([A]_0 - [C]) \nu}{1 + K_5 \nu} \quad 6.23$$

Thus

$$\frac{1}{[A]_0 - [C]} \frac{d[C]}{dt} = \frac{k_1 \nu}{1 + K_5 \nu} = k_{\text{obs}} \quad [6.11]$$

b) In the reaction of 6.5 ($X = F$) with hydroxide the rates of formation of B and C are similar and there is strong mutual coupling between the two processes

$$-\frac{d[A]}{dt} = (k_1 + k_5) [A] [\nu] - k_{-5} [B] \quad 6.24$$

$$\frac{d[B]}{dt} = k_5 [A] [\nu] - k_{-5} [B] \quad 6.25$$

Equations 6.24 and 6.25 are of the general form

$$\frac{dx_1}{dt} + a_{11}x_1 + a_{12}x_2 = 0 \quad 6.26$$

$$\frac{dx_2}{dt} + a_{21}x_1 + a_{22}x_2 \quad 6.27$$

with

$$x_1 = [A], \quad a_{11} = (k_1 + k_5) [\nu], \quad a_{12} = -k_{-5}$$

$$x_2 = [B], \quad a_{21} = -k_5 [\nu], \quad a_{22} = k_{-5}$$

for which particular solutions are

$$x_1 = x_1^0 \exp(-t/\tau) \quad 6.28$$

$$x_2 = x_2^0 \exp(-t/\tau) \quad 6.29$$

It follows that $\frac{dx_1}{dt} = -\frac{1}{\tau} x_1^0 \exp(-t/\tau) = -\frac{1}{\tau} x_1$ 6.30

$$\frac{dx_2}{dt} = -\frac{1}{\tau} x_2^0 \exp(-t/\tau) = -\frac{1}{\tau} x_2 \quad 6.31$$

Substituting into 6.26 and 6.27

$$(a_{11} - \frac{1}{\tau})x_1 + a_{12}x_2 = 0 \quad 6.32$$

$$a_{21}x_1 + (a_{22} - \frac{1}{\tau})x_2 = 0 \quad 6.33$$

These simultaneous equations can be solved for τ^{-1} by eliminating x_1 and x_2 .

This can be done by solving the determinantal equation 6.34

$$\begin{vmatrix} a_{11} - \frac{1}{\tau} & a_{12} \\ a_{21} & a_{22} - \frac{1}{\tau} \end{vmatrix} = 0 \quad 6.34$$

6.34 is equivalent to a quadratic equation with roots $\frac{1}{\tau_1}, \frac{1}{\tau_2}$.

It can be shown that $\frac{1}{\tau_1} + \frac{1}{\tau_2} = a_{11} + a_{22}$ 6.35

and $\left(\frac{1}{\tau_1}\right) \cdot \left(\frac{1}{\tau_2}\right) = a_{11}a_{22} - a_{12}a_{21}$ 6.36

For equations 6.25 and 6.26, the roots are $k_{\text{slow}} (= \frac{1}{\tau_1})$ and $k_{\text{fast}} (= \frac{1}{\tau_2})$.

Thus $k_{\text{slow}} + k_{\text{fast}} = (k_5 + k_1) [\text{nu}] + k_{-5}$ [6.16]

$$\begin{aligned} k_{\text{slow}} \cdot k_{\text{fast}} &= k_{-5}(k_5 + k_1) [\text{nu}] - k_{-5}k_5 [\text{nu}] \\ &= k_{-5}k_1 [\text{nu}] \end{aligned} \quad [6.17]$$

ii) Sample kinetic runs

1-bromo-2,4-dinitrobenzene ($8 \times 10^{-5} \text{ M}$ and NMe_4OH (0.01M)

Phenol forming reaction in 80/20 (v/v) DMSO/ H_2O at 422nm

t s	Absorbance (arbitrary units)	t	Absorbance (arbitrary units)	$10^3 k_{\text{obs}}^a$ s ⁻¹
0	6.6	600	82.1	—
30	14.4	630	83.4	3.0
60	21.6	660	84.4	3.1
90	28.2	690	85.1	3.3
120	34.0	720	85.6	3.3
150	39.3	750	86.0	3.3
180	44.3	780	86.5	3.4
210	48.9	810	86.9	3.5
240	53.0	840	87.2	3.5
270	56.9	870	87.5	3.7
300	60.4	900	87.9	3.4
330	63.6	930	88.2	3.7

average value	3.4
---------------	-----

a calculated by the Guggenheim method

1-bromo-2,4-dinitrobenzene ($8 \times 10^{-5} \text{M}$ and NMe_4OH (0.02M)
 Phenol forming reaction in 80/20 (v/v) DMSO/ H_2O at 422nm

t s	Absorbance (arbitrary units)	$10^3 k_{\text{obs}}$ s^{-1}
0	6.5	-
20	15.2	6.3
40	23.3	6.7
60	30.2	6.5
80	36.7	6.9
100	42.3	6.9
120	46.4	5.7
140	50.3	6.1
160	54.1	6.8
180	57.5	7.0
200	60.4	6.8
220	62.8	6.8
240	65.0	6.8
260	66.8	6.3
280	68.3	5.9
300	69.8	6.7
320	71.0	6.1
340	72.2	7.0
ω	80.2	av. 6.6

References

- 1 R Gaboriaud, R Schaal, P Letellier, *Bull. Soc. Chim. France*, 1969,**8**,2683
- 2 M Gisler, H Zollinger, *Angew. Chem., Int. Ed. Engl.*, 1981,**20**,203
- 3 F Terrier, *Chem. Rev.*, 1982,**82**,77
MJ Strauss *ibid.*,1970,**70**,667
- 4 Y Hasegawa, T Abe, *Chem. Lett.*, 1972,985; *Bull. Chem. Soc. Jpn.*, 1973,**46**,
2756
- 5 Y Hasegawa, *Bull. Chem. Soc. Jpn.*, 1974,**47**,2186
- 6 MR Crampton, MA Al-Ghariani, HA Khan, *Tetrahedron*, 1972,**28**,3299
- 7 MR Crampton, B Gibson, *J. Chem. Soc. Perkin Trans. II*, 1979,648
- 8 K Bowden, RS Cook, *J. Chem. Soc. B*, 1971,1771
- 9 K Bowden, NS Nadri, *J. Chem. Soc. Perkin Trans. II*, 1987,189
- 10 JF Bunnett, M Gisler, H Zollinger, *Helv. Chim. Acta*, 1982,**65**,63
- 11 E Buncel, MR Crampton, MJ Strauss, F Terrier, "*Electron Deficient Aromatic and Heteroaromatic - Base Interactions*", Elsevier, Amsterdam, 1984
- 12 MR Crampton, C Greenhalgh, *J. Chem. Soc. Perkin Trans. II*, 1985,599
- 13 MR Crampton, C Greenhalgh, *ibid.*, 1986, 187,873
- 14 F Millot, F Terrier, *Bull. Soc. Chim. France*, 1969,2692
- 15 F Terrier, F Millot, *ibid.*, 1970,1743
- 16 SS Gitis, A Ya Kaminsky, EA Bronstein, EA Gol'teuzen, Yu D Grudtsyn, *Zh. Org. Khim.*, 1975,**9**,2091
- 17 SS Gitis *et al.*, *Teor. Exp. Khim.*, 1972,**8**,261
- 18 SS Gitis *et al.*, *Zh. Org. Khim.*, 1975,**11**,2106
- 19 CF Bernasconi, "*Relaxation Kinetics*", Academic Press, NY, 1976
- 20 GB Barlin, DD Perrin, *Q. Rev. (London)*, 1966,**20**,75
- 21 G Bartoli, PE Todesco, *Acc. Chem. Res.*, 1977,**10**,125

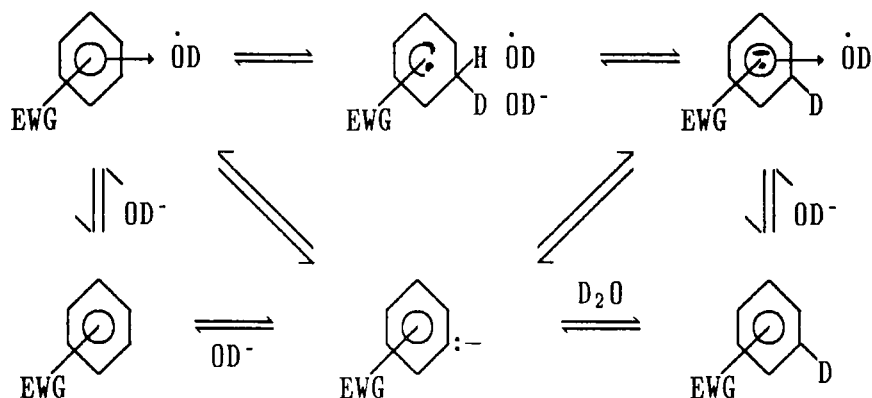
Chapter 7
Hydrogen Exchange in 1-fluoro-2,4-dinitrobenzene.
Evidence for intermediates on the pathway to
 σ -adduct formation ?

Radical anions are accepted intermediates in $S_{RN}1$ substitutions¹ and there is now evidence for single electron transfer in many organic reactions which have hitherto been considered solely as two electron transfer processes. These include electrophilic aromatic substitution², S_N2 reactions^{3,4} and addition of organometallic reagents^{5,6}. Nitroaromatic compounds are often efficient electron acceptors in basic solution and several radical anions formed by such compounds have been characterised by spin resonance techniques^{7,8}. These are known to absorb strongly between 250 and 350nm, and at 400 – 500nm⁹. However, in more activated nitrocompounds, the formation of anionic σ -adducts becomes favoured at equilibrium relative to the formation of radical anions⁷. The presence of free radicals was not detected in solutions of 1,3,5-trinitrobenzene (TNB) or 2,4,6-trinitroanisole in methanolic sodium methoxide or in ethanolic sodium ethoxide¹⁰ and only a low concentration of radical anion was detected in solutions of TNB in *t*-butyl alcohol containing *t*-butoxide⁶.

The reactions of aromatic nitrocompounds with bases may yield π -complexes^{11,12} and these are possible intermediates in aromatic nucleophilic addition and substitution. However, their formation is not favoured in polar solvents. The rapidly formed products in the reactions of 2,4,6-trinitroanisole, TNB and 2,4,6-trinitrotoluene with ethoxide in ethanol, initially thought to be π -complexes¹³, were later shown¹⁴ to be σ -adducts produced by ethoxide attack to unsubstituted positions of the aromatic ring.

In recent investigations¹⁵ by stopped flow spectrophotometry of the reactions of some 1-X-2,4,6-trinitrobenzenes ($X = Cl, H, SO_3^-$) with hydroxide ions in water or 50/50 DMSO/H₂O (v/v), Bacaloglu *et al.* reported that two intermediates were observable on the pathway to σ -adduct formation. These intermediates were postulated to be π or charge transfer complexes 7.1 absorbing at *ca.* 500nm and radical pairs 7.2 absorbing at *ca.* 260nm¹⁵.

Scheme I shows the situation for the production of a 1:1 adduct with TNB.



Scheme II

In order to attempt to verify these claims, the reaction of TNB with hydroxide ions in 50/50 (v/v) DMSO/H₂O was re-examined briefly and hydrogen exchange experiments with 1-fluoro-2,4-dinitrobenzene were carried out. In contrast with Bacaloglu's observations, no spectrophotometric evidence was obtained for the formation of intermediates 7.1 or 7.2 in the reaction of TNB with hydroxide ions in the aqueous solvent. Instead the results showed direct conversion of TNB to σ -adduct. The results for hydrogen exchange showed that the product (2,4-dinitrophenolate ions) was more exchanged than the starting material. However, there was also evidence for hydrogen exchange in the product when OD⁻ was added to 7.4 (X = OH)₁.

Experimental

Stopped flow measurements were made under first-order conditions with $[\text{OH}^-] \gg [\text{nitrocompound}]$. One syringe contained a solution of hydroxide in 50/50 (v/v) DMSO/H₂O and the other contained a solution of the nitrocompound in 50/50 (v/v) DMSO/H₂O. TNB was a stock solution in dioxan. When diluted the solvent contained < 1% of the organic component. The mixing time of the apparatus has been shown to be < 2ms!⁹

¹H nmr measurements were made in 68.5/31.5 (v/v) [²H₆]-DMSO/D₂O corresponding to a solvent containing 70% [²H₆]-DMSO by weight. NaOD was prepared by reaction of sodium metal in D₂O. Solutions of nitrocompound and solutions of OD⁻ (both in 68.5/31.5 (v/v) [²H₆]-DMSO/D₂O) were mixed slowly by micropipette or more rapidly by simultaneous and dropwise addition of equimolar solutions of OD⁻ and nitrocompound into a small beaker containing a magnetic stirrer. Spectra were taken as soon as possible after mixing the reagents. All measurements refer to internal tetramethylsilane.

Results and Discussion

i) Reaction of TNB with hydroxide in 50/50 (v/v) DMSO/H₂O

At $[\text{OH}^-] = 0.05$ and 0.10M , stopped flow spectrophotometry showed just one process due to the formation of a σ -adduct, colour forming at 500nm and fading at 258nm. This latter wavelength is near the λ_{max} of TNB (*ca.* 250nm) in this solvent. The most rapid oscilloscope sweep gave near straight lines with no signs of any previous forming or fading reactions. At $[\text{OH}^-] = 0.05\text{M}$ the observed rate constant was $32 \pm 2 \text{ s}^{-1}$. At this concentration, Bacaloglu *et al.* reported two observed rate constants, one (*ca.* 450 s^{-1}) for the conversion of 7.1 to 7.2 and the other (20 s^{-1}) for the formation of the σ -adduct.

ii) Hydrogen exchange in 1-fluoro-2,4-dinitrobenzene

Nmr data for 7.74 ($X = F$), the phenol 7.4 ($X = OH$) and the substituted product 7.4 ($X = O^-$) are given in table III. The results show that the bands due to the hydrogens at the 5-position of 7.4 ($X = F$) and the 3-position of 7.4 ($X = O^-$) are similarly positioned and in spectra containing both product and starting material these bands overlap. The relative intensities of the hydrogens were obtained from integrated peak area. Replacement of 1H by D will result in a decrease in intensity of the bands. In order to split the integral due to H_5 (F) and H_3 (O^-) it was assumed that exchange occurred only at the 3-position in 7.4 ($X = F$) so that the intensity due to H_5 (F) is equal to that for H_6 (F). In the product, integrated peak areas due to H_5 and H_6 were found to be equal.

The data in table IV show that, in agreement with Bacaloglu's work, the product is consistently more exchanged than the starting material. In addition, there was also found to be hydrogen exchange (at the 3-position) of 7.4 ($X = O^-$) when *ca.* 1 equivalent of OD^- was added to the phenol. The fact that exchange was found to occur here when the excess concentration of hydroxide was at most very small, shows that 7.4 ($X = O^-$) can also be expected to be reactive with respect to exchange. Hence the observation of greater hydrogen exchange in 7.4 ($X = O^-$) than in 7.4 ($X = F$) does not necessarily require the formation of a reactive intermediate on the pathway to σ -adduct formation. Previous work has shown that the rate of hydrogen exchange is slow compared with the rate of σ -adduct formation and that these processes compete with each other, the σ -adduct being an unreactive form of substrate!⁸ In the reaction of 1-fluoro-2,4-dinitrobenzene with OD^- the most rapid reaction will be attack of OD^- at the 1-position of the substrate to give 7.4 ($X = OD^-$) which is subsequently ionised by base. The rate of OD^- attack is expected to be fast given the relatively large concentrations of reagent used so that the base will be rapidly neutralised. A possibility worth considering is that, although care was taken to mix the reagents as rapidly as

possible, the rapidity of this reaction may make it impossible to achieve a homogeneous solution of base and nitrocompound. This would have the effect of increasing the amount of hydrogen exchange in 7.4 ($X = O^-$) relative to 7.4 ($X = F$) as only a small proportion of the base would "see" the unreacted compound.

Using the same solvent system Bacalogli *et al.* obtained almost twice as much hydrogen exchange in the product than in unreacted 1-fluoro-2,4-dinitrobenzene!⁷ In all the other compounds which were studied, the amount of hydrogen exchange in product and unreacted substrate were at least comparable and in several cases the unreacted substrate was found to be more exchanged than the product.

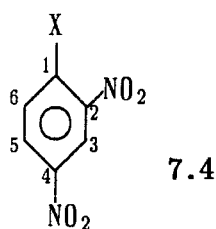


Table III

Nmr data for 1-X-2,4-dinitrobenzenes in 68.5/31.5 (v/v) [²H₆]-DMSO/D₂O

X	ring proton resonances			measured coupling constants
	H ₃	H ₅	H ₆	
F	8.89	8.65 (multiplets)	7.80	$\left\{ \begin{array}{l} J_{H_6F} = 9\text{Hz}, J_{H_5H_6} = 9\text{Hz}, J_{H_3F} = 6\text{Hz} \\ J_{H_3H_5} = 3\text{Hz}, J_{H_5F} = 3\text{Hz} \end{array} \right.$
O ⁻	8.62(d)	7.92(dd)	6.54(d)	$J_{H_5H_6} = 9.6\text{Hz}, J_{H_3H_5} = 3.2\text{Hz}$
OH	8.55(d)	8.34(dd)	7.17(d)	$J_{H_5H_6} = 9.4\text{Hz}, J_{H_3H_5} = 2.7\text{Hz}$

Table IV
Hydrogen exchange of 1-fluoro-2,4-dinitrobenzene in 68.5/31.5 (v/v) DMSO/D₂O

X	[sub- trate] M	[OD ⁻] M	relative intensities in starting material			% exchange in starting material	relative intensities in product			% exchange in product	% ^d conversion into product
			H ₃	H ₅	H ₆		H ₃	H ₅	H ₆		
F	ca 0.2	ca 0.2	45±2	61±3 ^b	61±3	26	27±7 ^c	45±2	45±2	40	42
F [*]	0.133	0.067	32±2	40±2 ^b	40±2	20	13±4 ^c	18±2	18±2	28	31
F ^{**}	0.216	0.216	55±3	68±3 ^b	68±3	19	32±8 ^c	45±2	45±2	29	40
OH	ca 0.2	ca 0.2	—	—	—	—	28±2 ^c	32±2	32±2	13	100

a at 3-position

b assumed the same as for H₆

c obtained by difference from total intensity due to H₅ (starting material) and H₃ (product)

d calculated on the basis of signal intensities at the 6-position.

* mixed with micropipettes

** mixed dropwise with rapid stirring.

References

- 1 JF Bunnett, *Acc. Chem. Res.*, 1978,11,413
- 2 CL Perrin, *J. Am. Chem. Soc.*, 1977,99,5516
L Ebersson, F Radner, *Acc. Chem. Res.*, 1987,20,53
S Sankararaman, AW Haney, JK Kochi, *J. Am. Chem. Soc.*, 1987,109,5235
- 3 A Pross, *Acc. Chem. Res.*, 1985,109,5235
- 4 GA Russell, WC Daren, *J. Am. Chem. Soc.*, 1966,88,5663; 1968,90,347
GA Russell, *Pure Appl. Chem.*, 1971,4,67
N Kornblum, *Angew. Chem., Int. Ed. Engl.* 1975,14,734
RW Bowman, CR Symons, *J. Chem. Soc. Perkin Trans. II*,1983,25
FG Bordwell, CA Wilson, *J. Am. Chem. Soc.*,1987,109,5470
- 5 JK Kochi, "*Organometallic Mechanism and Catalysis*", Academic Press, New York, 1978
- 6 GA Russell, EG Janzen, ET Strom, *J. Am. Chem. Soc.*, 1964,86,1807
- 7 E Buncl, AR Norris, KE Russell, *Q. Rev. Chem. Soc.*, 1986,22,123
- 8 GA Russell, EG Janzen, *J. Am. Chem. Soc.*, 1962,84,4153; 1967,89,300
- 9 D Behar, PJ Neta, *J. Phys. Chem.*, 1981,85,690
- 10 V Gold, CH Rochester, *J. Chem. Soc.*, 1964, 1692
- 11 EM Kosower, *Prog. Phys. Org. Chem.*, 1963,3,81
RE Miller, WFK Wynne-Jones, *J. Chem. Soc.*,1959,2375; 1961,4886
- 12 J Hayami, S Otani, F Yamaguchi, Y Nishikawa, *Chem. Lett.*, 1987,739
RI Cattana, JO Singh, JD Annunziata, JJ Silber, *J. Chem. Soc. Perkin Trans. II*, 1987,79
- 13 JB Ainscough, EF Caldin, *J. Chem. Soc.*, 1956, 2528,2540,2546
- 14 F Terrier, *Chem. Rev.*, 1982,82,77
- 15 R Bacaloglu, CA Bunton, G Cerichelli, *J. Am. Chem. Soc.*, 1987,109,621;
1988,110,3505
- 16 MR Crampton, B Gibson, *J. Chem. Soc. Perkin Trans. II*, 1979, 648
MR Crampton, *J. Chem. Soc. Perkin Trans. II*,1978, 343
- 17 R Bacaloglu, CA Bunton, G Cerichelli, F Ortega, *J. Am. Chem. Soc.*,
1988,110,3495
- 18 E Buncl, EA Symons, *J. Org. Chem.*, 1973,38,1201
MR Crampton, V Gold, *J. Chem. Soc. (B)*, 1966, 498
- 19 MR Crampton, C Greenhalgh – unpublished observations

Appendix
Lectures, Colloquia and
Conferences

- a) Lectures and Colloquia organised by Durham University Chemical Society
(Those attended marked*).

1ST AUGUST 1987 to 31st JULY 1988

- * BIRCHALL, Prof. D. (I.C.I. Advanced Materials) 25th April 1988
Environmental Chemistry of Aluminium
- BORER, Dr. K. (University of Durham Industrial Research Labs.) 18th February 1988
The Brighton Bomb - A Forensic Science View
- BOSSONS, L. (Durham Chemistry Teachers' Centre) 16th March 1988
GCSE Practical Assessment
- BUTLER, Dr. A.R. (University of St. Andrews) 5th November 1987
Chinese Alchemy
- CAIRNS-SMITH, Dr. A. (Glasgow University) 28th January 1988
Clay Minerals and the Origin of Life
- DAVIDSON, Dr. J. (Herriot-Watt University) November 1987
Metal Promoted Oligomerisation Reactions of Alkynes
- * GRADUATE CHEMISTS (Northeast Polytechnics and Universities) 19th April 1988
R.S.C. Graduate Symposium
- GRAHAM, Prof. W.A.G. (University of Alberta, Canada) 3rd March 1988
Rhodium and Iridium Complexes in the Activation of Carbon-Hydrogen Bonds
- * GRAY, Prof. G.W. (University of Hull) 22nd October 1987
Liquid Crystals and their Applications
- HARTSHORN, Prof. M.P. (University of Canterbury, New Zealand) 7th April 1988
Aspects of Ipso-Nitration
- HOWARD, Dr. J. (I.C.I. Wilton) 3rd December 1987
Chemistry of Non-Equilibrium Processes
- JONES, Dr. M.E. (Durham Chemistry Teachers' Centre) 29th June 1988
GCSE Chemistry Post-mortem
- JONES, Dr. M.E. (Durham Chemistry Teachers' Centre) 6th July 1988
GCE Chemistry A Level Post-mortem
- KOCH, Prof. H.F. (Ithaca College, U.S.A.) 7th March 1988
Does the E2 Mechanism Occur in Solution?
- LACEY, Mr. (Durham Chemistry Teachers' Centre) 9th February 1988
Double Award Science
- * OLAH, Prof. G.A. (University of Southern California) 29th June, 1988
New Aspects of Hydrocarbon Chemistry)
- * PALMER, Dr. F. (University of Nottingham) 21st January 1988
Luminescence (Demonstration Lecture)

- * PINES, Prof. A. (University of California, Berkeley, U.S.A.) 28th April 1988
Some Magnetic Moments
- * RICHARDSON, Dr. R. (University of Bristol) 27th April 1988
X-Ray Diffraction from Spread Monolayers
- ROBERTS, Mrs. E. (SATRO Officer for Sunderland) 13th April 1988
Talk - Durham Chemistry Teachers' Centre - "Links
Between Industry and Schools"
- ROBINSON, Dr. J.A. (University of Southampton) 27th April 1988
Aspects of Antibiotic Biosynthesis
- ROSE van Mrs. S. (Geological Museum) 29th October 1987
Chemistry of Volcanoes
- SAMMES, Prof. P.G. (Smith, Kline and French) 19th December 1987
Chemical Aspects of Drug Development
- * SEEBACH, Prof. D. (E.T.H. Zurich) 12th November 1987
From Synthetic Methods to Mechanistic Insight
- SODEAU, Dr. J. (University of East Anglia) 11th May 1988
Durham Chemistry Teachers' Centre Lecture: "Spray
Cans, Smog and Society"
- SWART, Mr. R.M. (I.C.I.) 16th December 1987
The Interaction of Chemicals with Lipid Bilayers
- * TURNER, Prof. J.J. (University of Nottingham) 11th February 1988
Catching Organometallic Intermediates
- UNDERHILL, Prof. A. (University of Bangor) 25th February 1988
Molecular Electronics
- WILLIAMS, Dr. D.H. (University of Cambridge) 26th November 1987
Molecular Recognition
- * WINTER, Dr. M.J. (University of Sheffield) 15th October 1987
Pyrotechnics (Demonstration Lecture)
- 1ST AUGUST 1988 to 31st JULY 1989
- ASHMAN, Mr. A. (Durham Chemistry Teachers' Centre) 3rd May, 1989
The Chemical Aspects of the National Curriculum
- * AVEYARD, Dr. R. (University of Hull) 15th March, 1989
Surfactants at your Surface
- AYLETT, Prof. B.J. (Queen Mary College, London) 16th February, 1989
Silicon-Based Chips:- The Chemist's Contribution
- * BALDWIN, Prof. J.E. (Oxford University) 9th February, 1989
Recent Advances in the Bioorganic Chemistry of
Penicillin Biosynthesis
- * BALDWIN & WALKER, Drs. R.R. & R.W. (Hull University) 24th November, 1988
Combustion: Some Burning Problems
- BOLLEN, Mr. F. (Durham Chemistry Teachers' Centre) 18th October, 1988
Lecture about the use of SATIS in the classroom
- * BUTLER, Dr. A.R. (St. Andrews University) 15th February, 1989
Cancer in Linxiam: The Chemical Dimension

- *CADOGAN, Prof. J.I.G. (British Petroleum) 10th November, 1988
From Pure Science to Profit
- CASEY, Dr. M. (University of Salford) 20th April, 1989
Sulphoxides in Stereoselective Synthesis
- CRESSEY & WATERS, Mr. D. & T. (Durham Chemistry Teachers' Centre) 1st February, 1989
GCSE Chemistry 1988: "A Coroner's Report"
- CRICH, Dr. D. (University College London) 27th April, 1989
Some Novel Uses of Free Radicals in Organic Synthesis
- DINGWALL, Dr. J. (Ciba Geigy) 18th October, 1988
Phosphorus-containing Amino Acids: Biologically Active Natural and Unnatural Products
- ERRINGTON, Dr. R.J. (University of Newcastle-upon-Tyne) 1st March, 1989
Polymetalate Assembly in Organic Solvents
- FREY, Dr. J. (Southampton University) 11th May, 1989
Spectroscopy of the Reaction Path: Photodissociation Raman Spectra of NOCl
- *GRADUATE CHEMISTS, (Polytechs and Universities in North East England) 12th April, 1989
R.S.C. Symposium for presentation of papers by postgraduate students
- *HALL, Prof. L.D. (Addenbrooke's Hospital, Cambridge) 2nd February, 1989
NMR - A Window to the Human Body
- *HARDGROVE, Dr. G. (St. Olaf College, U.S.A.) December, 1988
Polymers in the Physical Chemistry Laboratory
- HARWOOD, Dr. L. (Oxford University) 25th January, 1988
Synthetic Approaches to Phorbols Via Intramolecular Furan Diels-Alder Reactions: Chemistry under Pressure
- JÄGER, Dr. C. (Friedrich-Schiller University GDR) 9th December, 1988
NMR Investigations of Fast Ion Conductors of the NASICON Type
- JENNINGS, Prof. R.R. (Warwick University) 26th January, 1989
Chemistry of the Masses
- JOHNSON, Dr. B.F.G. (Cambridge University) 23rd February, 1989
The Binary Carbonyls
- JONES, Dr. M.E. (Durham Chemistry Teachers' Centre) 14th June, 1989
Discussion Session on the National Curriculum
- JONES, Dr. M.E. (Durham Chemistry Teachers' Centre) 28th June, 1989
GCSE and A Level Chemistry 1989
- *LUDMAN, Dr. C.J. (Durham University) 18th October, 1988
The Energetics of Explosives
- MACDOUGALL, Dr. G. (Edinburgh University) 22nd February, 1989
Vibrational Spectroscopy of Model Catalytic Systems
- *MARKO, Dr. I. (Sheffield University) 9th March, 1989
Catalytic Asymmetric Osmylation of Olefins
- McLAUHLAN, Dr. K.A. (University of Oxford) 16th November, 1988
The Effect of Magnetic Fields on Chemical Reactions

- *MOODY, Dr. C.J. (Imperial College) 17th May, 1989
Reactive Intermediates in Heterocyclic Synthesis
- MORTIMER, Dr. C. (Durham Chemistry Teachers' Centre) 14th December, 1988
The Hindenberg Disaster - an Excuse for Some Experiments
- NICHOLLS, Dr. D. (Durham Chemistry Teachers' Centre) 11th July, 1989
Demo. "Liquid Air"
- *PAETZOLD, Prof. P. (Aachen) 23rd May, 1989
Iminoboranes $\text{XB}\equiv\text{NR}$: Inorganic Acetylenes?
- PAGE, Dr. P.C.B. (University of Liverpool) 3rd May, 1989
Stereocontrol of Organic Reactions Using 1,3-dithiane-1-oxides
- POLA, Prof. J. (Czechoslovak Academy of Sciences) 15th June, 1989
Carbon Dioxide Laser Induced Chemical Reactions - New Pathways in Gas-Phase Chemistry
- *REES, Prof. C.W. (Imperial College London) 27th October, 1988
Some Very Heterocyclic Compounds
- REVELL, Mr. P. (Durham Chemistry Teachers' Centre) 14th March, 1989
Implementing Broad and Balanced Science 11-16
- SCHMUTZLER, Prof. R. (Technische Universität Braunschweig) 6th October, 1988
Fluorophosphines Revisited - New Contributions to an Old Theme
- *SCHROCK, Prof. R.R. (M.I.T.) 13th February, 1989
Recent Advances in Living Metathesis
- SINGH, Dr. G. (Teesside Polytechnic) 9th November, 1988
Towards Third Generation Anti-Leukaemics
- SNAITH, Dr. R. (Cambridge University) 1st December, 1988
Egyptian Mummies: What, Where, Why and How?
- STIBER, Dr. R. (Czechoslovak Academy of Sciences) 16th May, 1989
Recent Developments in the Chemistry of Intermediate-Sited Carboranes
- VON RAGUE SCHLEYER, Prof. P. (Universität Erlangen Nürnberg) 21st October, 1988
The Fruitful Interplay Between Computational and Experimental Chemistry
- *WELLS, Prof. P.B. (Hull University) 10th May, 1989
Catalyst Characterisation and Activity

1ST AUGUST 1989 TO 31ST JULY 1990

- ASHMAN, Mr. A. (Durham Chemistry Teachers' Centre) 11th October, 1989
The National Curriculum - an update
- *BADYAL, Dr. J.P.S. (Durham University) 1st November, 1989
Breakthroughs in Heterogeneous Catalysis
- BECHER, Dr. J. (Odense University) 13th November, 1989
Synthesis of New Macrocylic Systems using Heterocyclic Building Blocks
- *BERCAW, Prof. J.E. (California Institute of Technology) 10th November, 1989
Synthetic and Mechanistic Approaches to Ziegler-natta Polymerization of Olefins

- BLEASDALE, Dr. C. (Newcastle University) 21st February, 1990
The Mode of Action of some Anti-tumour Agents
- BOLLEN, Mr. F. (Formerly Science Advisor, Newcastle LEA) 27th March, 1990
Whats's New in Satis, 16-19
- *BOWMAN, Prof. J.M. (Emory University) 23rd March, 1990
Fitting Experiment with Theory in Ar-OH
- *BUTLER, Dr. A. (St. Andrews University) 7th December, 1989
The Discovery of Penicillin: Facts and Fancies
- CAMPBELL, Mr. W.A. (Durham Chemistry Teachers' Centre) 12th September, 1989
Industrial catalysis - some ideas for the
National Curriculum
- CHADWICK, Dr. P. (Dept. of Physics, Durham University) 24th January, 1990
Recent Theories of the Universe (with Reference
to National Curriculum Attainment Target 16)
- *CHEETHAM, Dr. A.K. (Oxford University) 8th March, 1990
Chemistry of Zeolite Cages
- *CLARK, Prof. D.T. (ICI Wilton) 22nd February, 1990
Spatially Resolved Chemistry (using Natures's
Paradigm in the Advanced Materials Arena)
- COLE-HAMILTON, Prof. D.J. (St. Andrews University) 29th November, 1989
New Polymers from Homogeneous Catalysis
- *CROMBIE, Prof. L. (Nottingham University) 15th February, 1990
The Chemistry of Cannabis and Khat
- *DYER, Dr. U. (Glaxo) 31st January, 1990
Synthesis and Conformation of C-Glycosides
- FLORIANI, Prof. C. (University of Lausanne,
Switzerland) 25th October, 1989
Molecular Aggregates - A Bridge between
homogeneous and Heterogeneous Systems
- GERMAN, Prof. L.S. (USSR Academy of Sciences -
Moscow) 9th July, 1990
New Syntheses in Fluoroaliphatic Chemistry:
Recent Advances in the Chemistry of Fluorinated
Oxiranes
- GRAHAM, Dr. D. (B.P. Reserch Centre) 4th December, 1989
How Proteins Absorb to Interfaces
- *GREENWOOD, Prof. N.N. (University of Leeds) 9th November, 1989
Novel Cluster Geometries in Metalloborane
Chemistry
- *HOLLOWAY, Prof. J.H. (University of Leicester) 1st February, 1990
Noble Gas Chemistry
- HUGHES, Dr. M.N. (King's College, London) 30th November, 1989
A Bug's Eye View of the Periodic Table
- *HUISGEN, Prof. R. (Universität München) 15th December, 1989
Recent Mechanistic Studies of [2+2] Additions
- IDDON, Dr. B. (Univeristy of Salford) 15th December, 1989
Schools' Christmas Lecture - The Magic of
Chemistry

- JONES, Dr. M.E. (Durham Chemistry Teachers' Centre) 3rd July, 1990
The Chemistry A Level 1990
- JONES, Dr. M.E. (Durham Chemistry Teachers' Centre) 21st November 1989
GCSE and Dual Award Science as a starting point
for A level Chemistry - how suitable are they?
- JOHNSON, Dr. G.A.L. (Durham Chemistry Teachers' Centre) 8th February, 1990
Some aspects of local Geology in the National
Science Curriculum (attainment target 9)
- *KLINOWSKI, Dr. J. (Cambridge University) 13th December 1989
Solid State NMR Studies of Zeolite Catalysts
- *LANCASTER, Rev. R. (Kimbolton Fireworks) 8th February, 1990
Fireworks - Principles and Practice
- *LUNAZZI, Prof. L. (University of Bologna) 12th February, 1990
Application of Dynamic NMR to the Study of
Conformational Enantiomerism
- PALMER, Dr. F. (Nottingham University) 17th October, 1989
Thunder and Lightning
- *PARKER, Dr. D. (Durham University) 16th November, 1989
Macrocycles, Drugs and Rock 'n' roll
- *PERUTZ, Dr. R.N. (York University) 24th January, 1990
Plotting the Course of C-H Activations with
Organometallics
- PLATONOV, Prof. V.E. (USSR Academy of Sciences - 9th July, 1990
Novosibirsk)
Polyfluoroindanes: Synthesis and Transformation
- POWELL, Dr. R.L. (ICI) 6th December, 1989
The Development of CFC Replacements
- POWIS, Dr. I. (Nottingham University) 21st March, 1990
Spinning off in a huff: Photodissociation of
Methyl Iodide
- RICHARDS, Mr. C. (Health and Safety Executive, 28th February, 1990
Newcastle)
Safety in School Science Laboratories and COSHH
- ROZHKOVA, Prof. I.N. (USSR Academy of Sciences - 9th July, 1990
Moscow)
Reactivity of Perfluoroalkyl Bromides
- *STODDART, Dr. J.F. (Sheffield University) 1st March, 1990
Molecular Lego
- SUTTON, Prof. D. (Simon Fraser University, 14th February, 1990
Vancouver B.C.)
Synthesis and Applications of Dinitrogen and Diazo
Compounds of Rhenium and Iridium
- THOMAS, Dr. R.K. (Oxford University) 28th February, 1990
Neutron Reflectometry from Surfaces
- *THOMPSON, Dr. D.P. (Newcastle University) 7th February, 1990
The role of Nitrogen in Extending Silicate
Crystal Chemistry

b) Conferences attended.

European Symposium on Organic Reactivity II, University of Padova, Italy,
27th August – 1st September 1989.

Fast Reactions and Reactive Intermediates, University of York, 18 – 19
December 1989.

Organic Reaction Mechanisms Group, ICI Blakely, 1st October 1990

c) First Year Induction Course, October 1987

This course consisted of one hour lectures on the services available in the
Department.

- i) Departmental Organisation
- ii) Safety Matters
- iii) Electrical Appliances and Infrared Spectroscopy.
- iv) Chromatography and Microanalysis.
- v) Atomic Absorptiometry and Inorganic Analysis.
- vi) Library Facilities.
- vii) Mass Spectroscopy.
- viii) Nuclear Magnetic Resonance Spectroscopy.
- ix) Glassblowing Technique.

